PHASE DIAGRAMS OF NUCLEAR REACTOR MATERIALS

R. E. Thoma, Editor

OAK RIDGE NATIONAL LABORATORY
operated by
UNION CARBIDE CORPORATION
for the
U.S. ATOMIC ENERGY COMMISSION

Contract No. W-7405-eng-26

REACTOR CHEMISTRY DIVISION
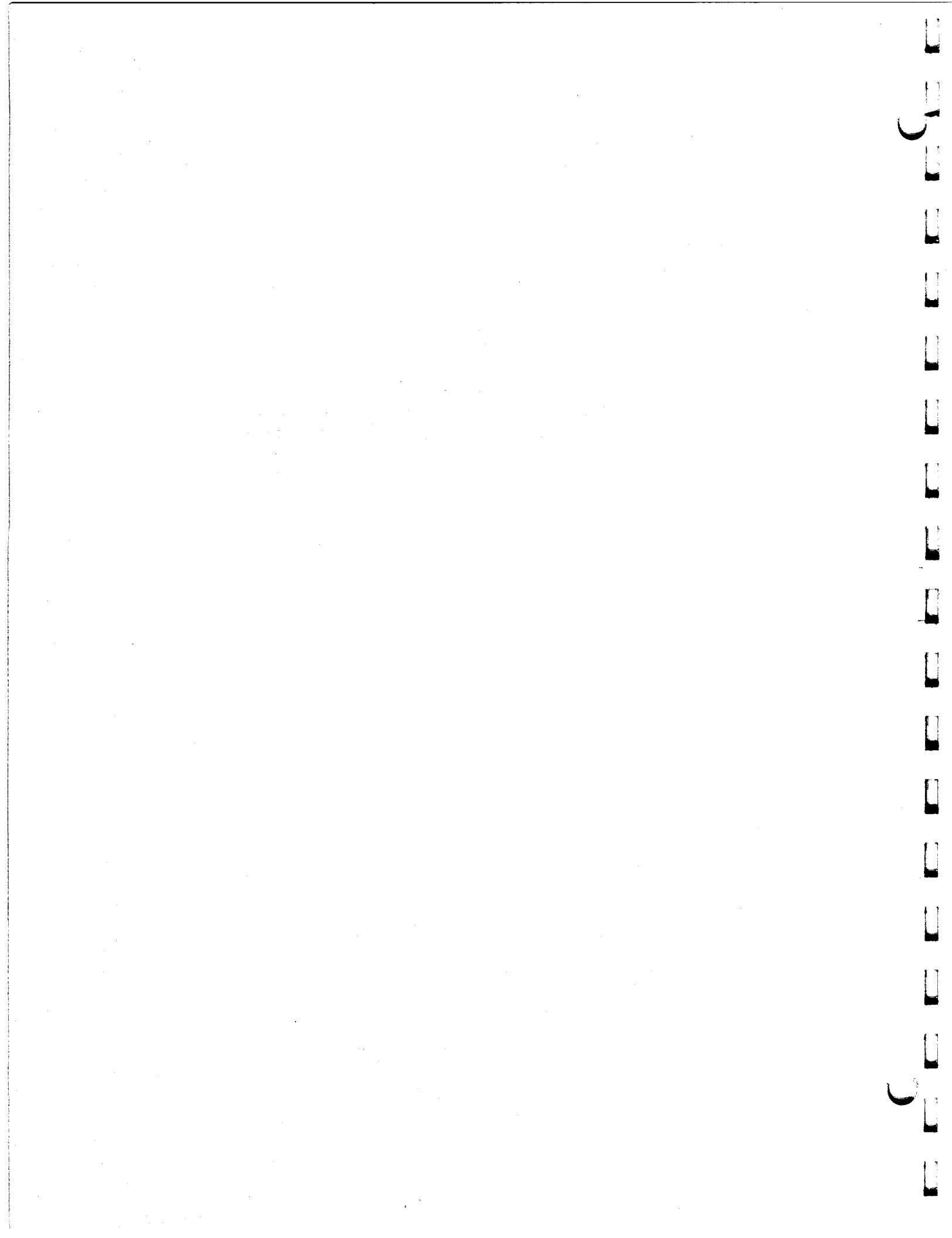
PHASE DIAGRAMS OF NUCLEAR REACTOR MATERIALS

R. E. Thoma, Editor

DATE ISSUED

NOV 20 1959

CONTENTS

PHASE DIAGRAMS OF NUCLEAR REACTOR MATERIALS

INTRODUCTION

This compilation presents the phase diagrams for possible materials for nuclear reactors developed at the Oak Ridge National Laboratory over the period 1950–59. It represents the efforts of certain personnel in what are now the Chemical Technology, Metallurgy, Chemistry, and Reactor Chemistry Divisions of ORNL. This document also contains diagrams originated by other installations under contract to ORNL during that interval. In addition, a few diagrams from the unclassified literature have been included when they form part of completed systems sequences.

No general discussion of the principles of heterogeneous phase equilibrium has been included since excellent discussions are available in many well-known publications. Equilibria in several of the fused-salt systems presented below have been described in some detail in a recent publication by Ricci.[1] Nor has any attempt been made to assemble the phase equilibrium data on reactor materials available from many other sources. For such information the reader is referred to other recently published compilations of phase diagrams[2-6] and to the several new works dealing specifically with nuclear reactor materials.[7-9]

While some of the diagrams presented below are the result of fundamental researches, most were obtained in support of the ORNL programs in development of fluid-fueled reactors. Others have been developed as a consequence of ORNL interests in reprocessing of nuclear fuels, reactor metallurgy, production of uranium and thorium from raw materials, and studies of mechanisms of corrosion.

Much of the research effort was devoted to searches for systems of direct use as fluid fuels or blanket materials; unpromising systems were often given only casual attention. The diagrams in this collection, accordingly, vary widely in the degree of completeness of examination. A brief description of the status of the work is presented in each case; in a few cases, where no detailed description of the system has been published, the available data have been included with the diagram.

[1] J. E. Ricci, *Guide to the Phase Diagrams of the Fluoride Systems*, ORNL-2396 (Nov. 19, 1958).

[2] J. F. Hogerton and R. C. Grass (eds.), *The Reactor Handbook*, vol 2, AECD-3646 (May 1955).

[3] T. Lyman (ed.), *Metals Handbook*, American Society for Metals, Cleveland, Ohio, 1948.

[4] F. A. Rough and A. A. Bauer (eds.), *Constitution of Uranium and Thorium Alloys*, BMI-1300 (June 2, 1958).

[5] E. M. Levin, H. F. McMurdie, and F. P. Hall, *Phase Diagrams for Ceramists*, The American Ceramic Society, Columbus, Ohio, 1956.

[6] E. M. Levin, H. F. McMurdie, and F. P. Hall, *Supplement to Phase Diagrams for Ceramists*, The American Ceramic Society, Columbus, Ohio, 1959.

[7] B. Yates, *Materials for Use in Nuclear Reactors. Information Bibliography*, IGRL-IB/R-15 (2nd ed.), 1958.

[8] H. H. Hausner and S. B. Roboff, *Materials for Nuclear Power Reactors*, Reinhold Publishing Corp., New York, 1955.

[9] B. Kopelman (ed.), *Materials for Nuclear Reactors*, McGraw-Hill Book Co., New York, 1959.

1. METAL SYSTEMS

1.1. The System Silver–Zirconium

J. O. Betterton, Jr., and D. S. Easton, "The Silver–Zirconium System," *Trans. Met. Soc. AIME* **212**, 470–75 (1958).

A detailed investigation was made of the phase diagram of silver–zirconium, particularly in the region 0 to 36 at. % Ag. The system was found to be characterized by two intermediate phases, Zr_2Ag and $ZrAg$, and a eutectoid reaction in which the β-zirconium solid solution decomposes into α-zirconium and Zr_2Ag. It was found that impurities in the range 0.05% from the iodide-type zirconium were sufficient to introduce deviations from binary behavior; with partial removal of these impurities an increase in the α-phase solid solubility limit from 0.1 to 1.1 at. % Ag was observed.
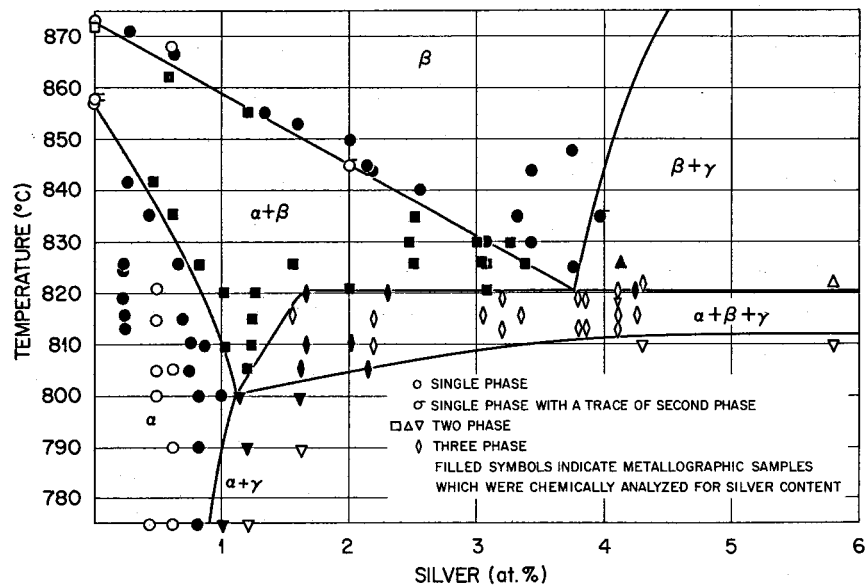
Fig. 1.1*a*. The System Silver–Zirconium in the Eutectoid Region (0–6 at. % Ag).
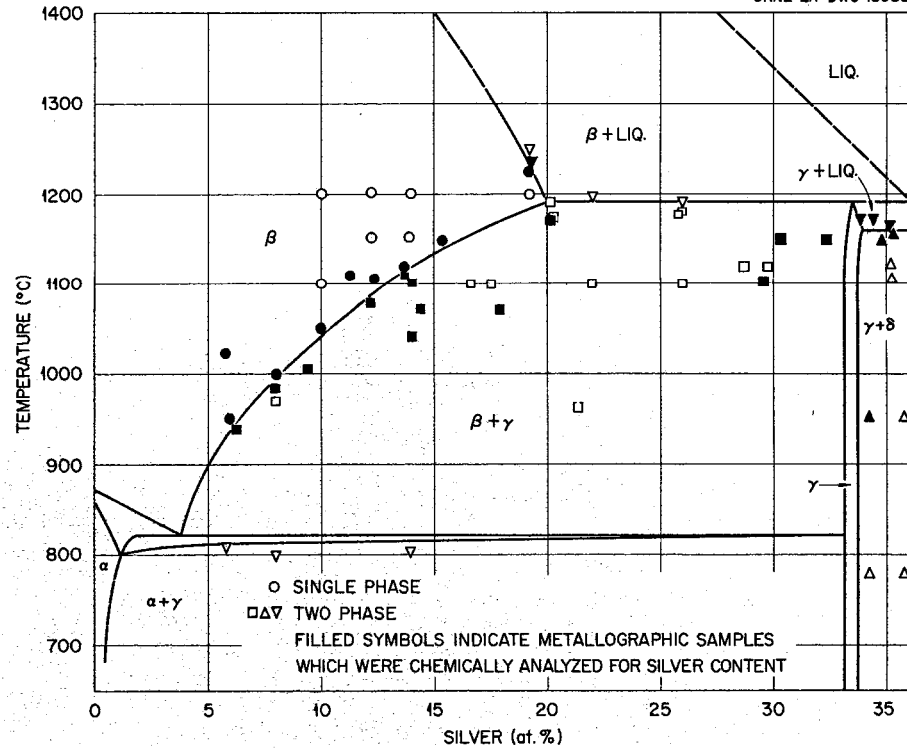
Fig. 1.1*b*. The System Silver–Zirconium in the Region 0–36 at. % Ag.

3

1.2. The System Indium–Zirconium

J. O. Betterton, Jr., and W. K. Noyce, "The Equilibrium Diagram of Indium–Zirconium in the Region 0–26 at. pct In," *Trans. Met. Soc. AIME* **212**, 340–42 (1958).

The zirconium-rich portion of the indium–zirconium phase diagram was determined as a study of the effect of alloying a trivalent B-subgroup element, indium, with zirconium in group IVA. The temperature of the allotropic transition was found to rise with indium, terminating in a peritectoid reaction, $\beta(9.3\% \text{ In}) + \gamma(22.4\% \text{ In}) \rightleftharpoons \alpha(10.1\% \text{ In})$ at 1003°C. In this respect the effect of indium is analogous to that of aluminum in zirconium and titanium alloys.
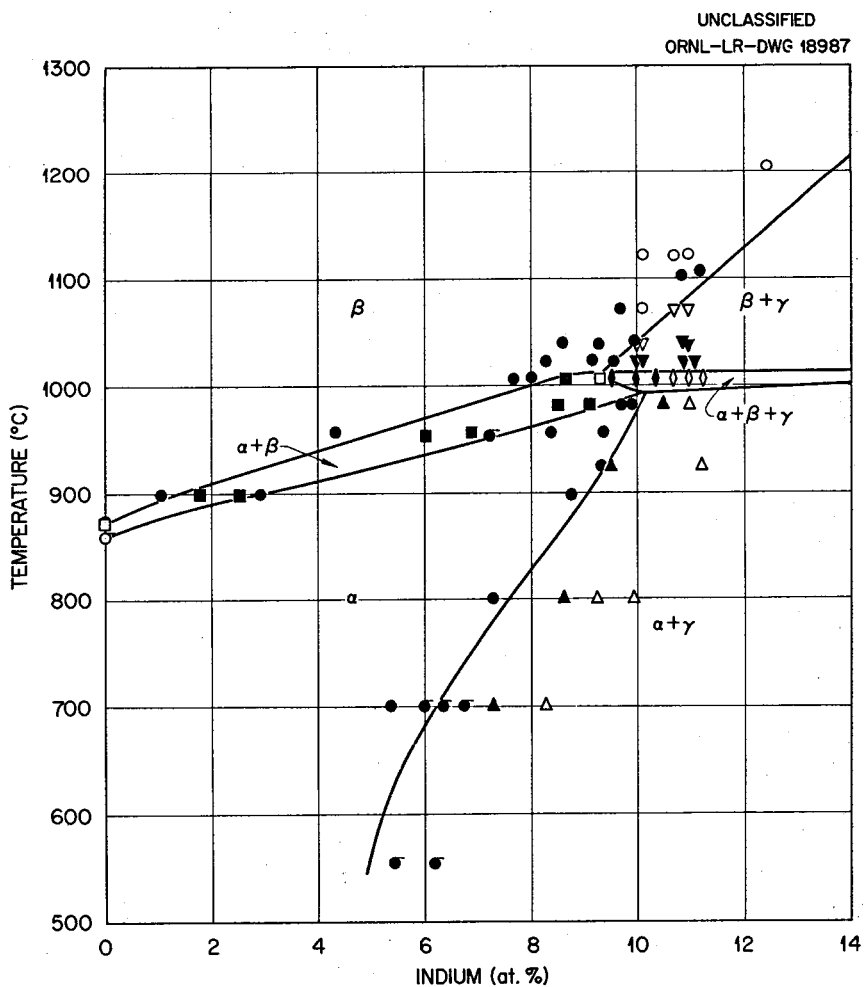
Fig. 1.2a. The System Indium–Zirconium in the Peritectoid Region (0–13 at. % In).
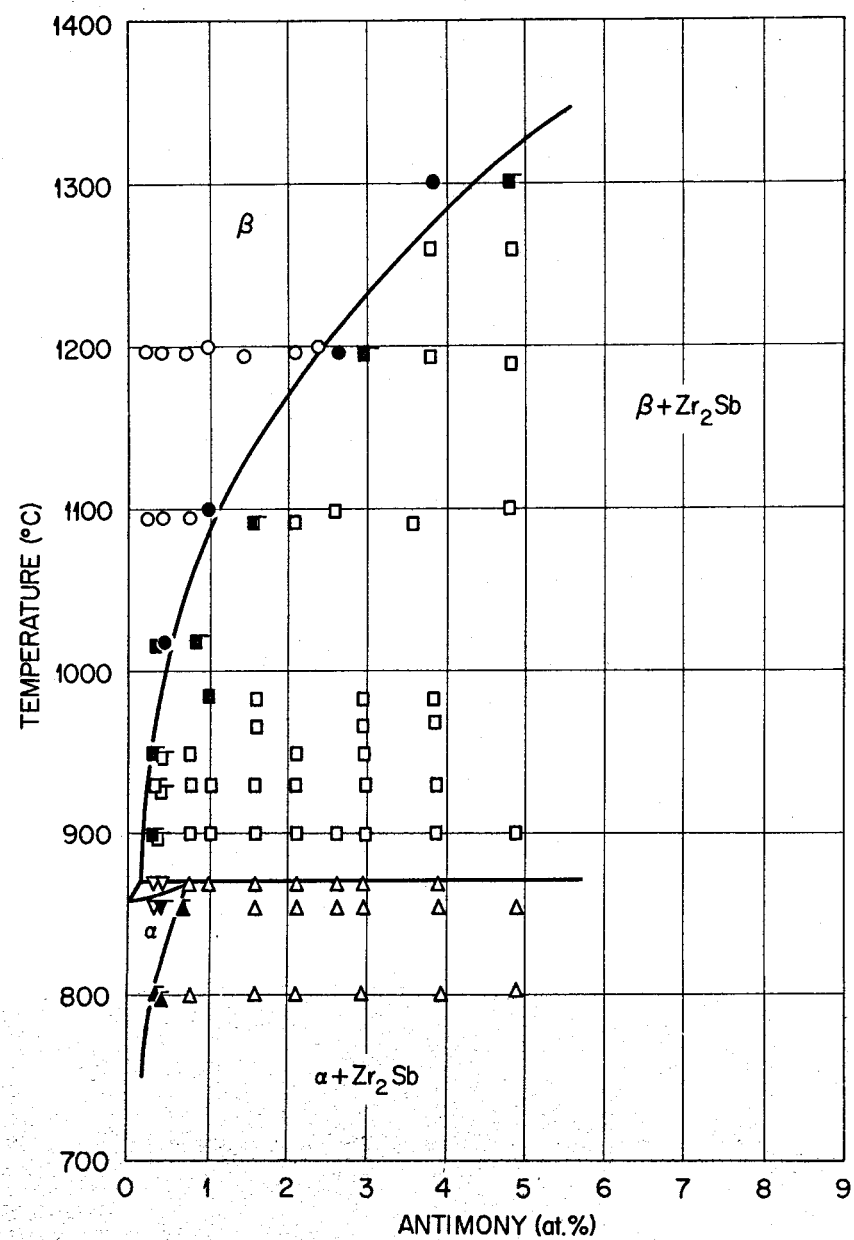
Fig. 1.3b. The System Antimony–Zirconium in the Peritectoid Region (0–6 at. % Sb).

1.4. The System Lead–Zirconium

G. D. Kneip, Jr., and J. O. Betterton, Jr., cited by E. T. Hayes and W. L. O'Brien, "Zirconium Equilibrium Diagrams," p 443–83 in *The Metallurgy of Zirconium*, ed. by B. Lustman and F. Kerze, Jr., McGraw-Hill Book Co., New York, 1955.
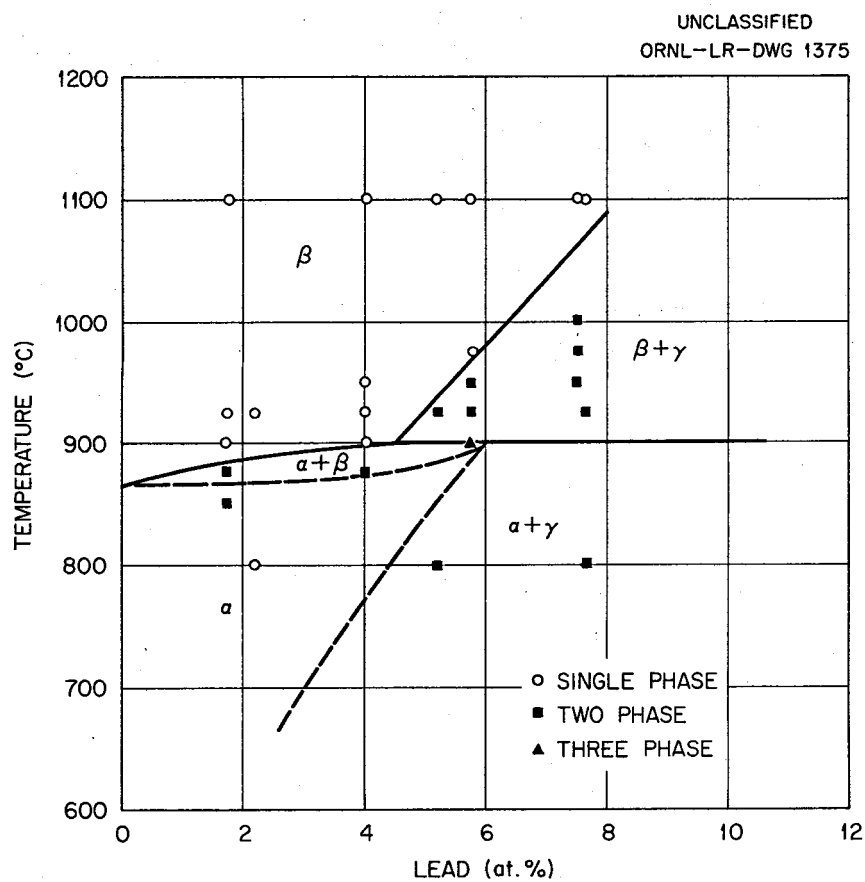
Fig. 1.4 The System Lead–Zirconium in the Peritectoid Region (0–12 at. % Pb).

2. METAL–FUSED-SALT SYSTEMS

2.1. The Sodium Metal–Sodium Halide Systems

M. A. Bredig and J. E. Sutherland, "High-Temperature Region of the Sodium–Sodium Halide Systems," *Chem. Ann. Prog. Rep. June 20, 1957*, ORNL-2386, p 119. Subsequent report on these systems to be published.
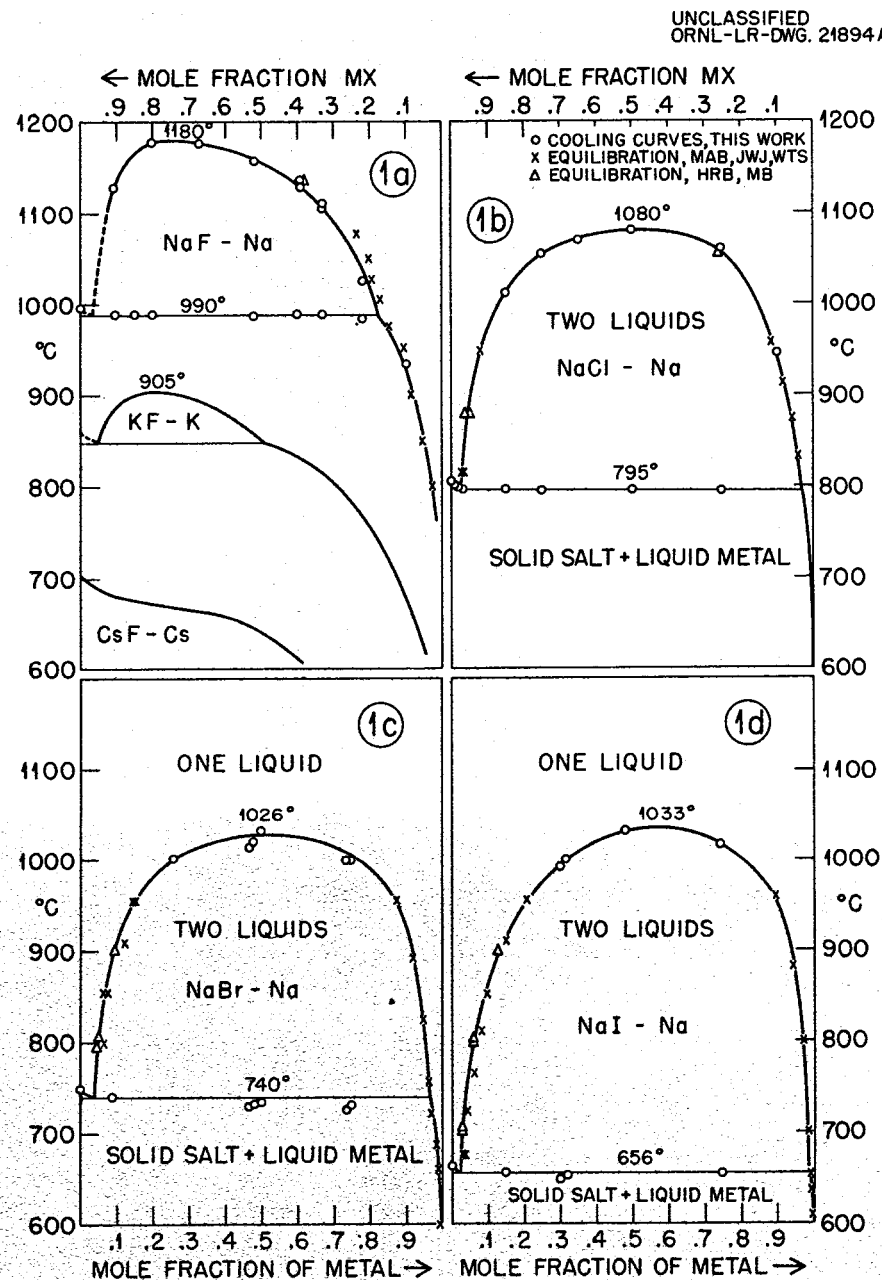
Fig. 2.1. The Sodium Metal–Sodium Halide Systems.

2.2. The Potassium Metal–Potassium Halide Systems

J. W. Johnson and M. A. Bredig, "Miscibility of Metals with Salts in the Molten State. III. The Potassium–Potassium Halide Systems," *J. Phys. Chem.* 62, 604 (1958).

Complete miscibility of metal and salt exists in the KX–K systems, X = F, Cl, Br, and I, at and above 904, 790, 727, and 717°C, that is, as close as +47, +18, −7, and +22°, respectively, to the melting points of the salts. The asymmetry of the liquid-liquid coexistence areas, especially of the fluoride and chloride systems, as indicated by the consolute compositions (20, 39, 44, and 50 mole % metal, respectively), is largely explained by the difference in molar volumes of salt and metal. At the monotectic temperature, the solubility of the solid salts in the liquid metal, as well as of the metal in the liquid salt phase, is much larger than in the case of the sodium systems.
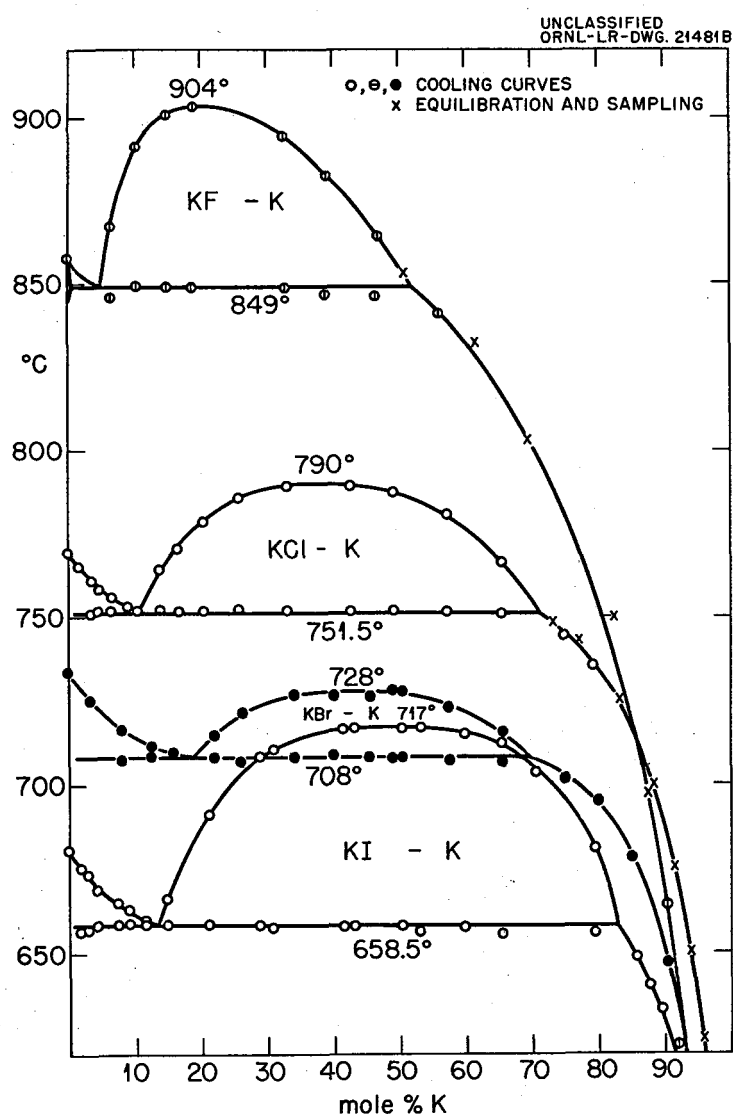
Fig. 2.2. The Potassium Metal–Potassium Halide Systems.

2.3. The Rubidium Metal—Rubidium Halide Systems

M. A. Bredig and J. W. Johnson, "Rubidium—Rubidium Halide Systems," *Chem. Ann. Prog. Rep. June 20, 1957*, ORNL-2386, p 122; M. A. Bredig, J. E. Sutherland, and A. S. Dworkin, "Molten Salt—Metal Solutions. Phase Equilibria," *Chem. Ann. Prog. Rep. June 20, 1958*, ORNL-2584, p 73. Subsequent report on these systems to be published.
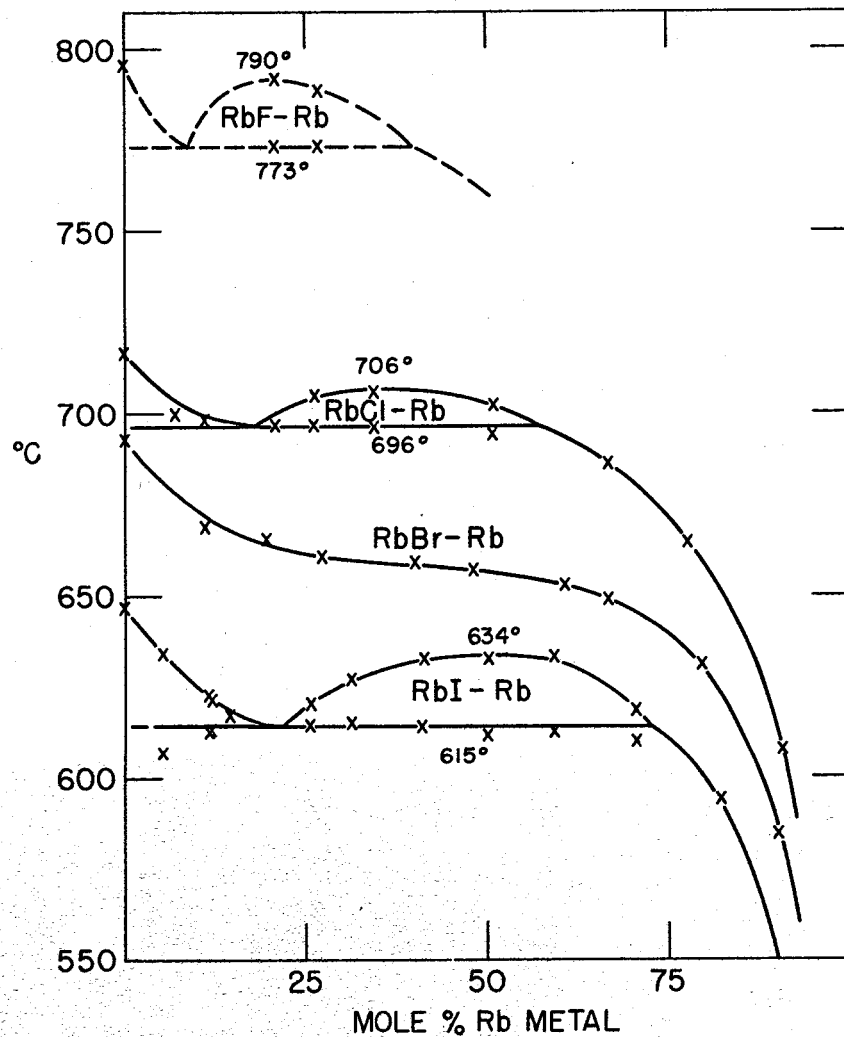
Fig. 2.3. The Rubidium Metal—Rubidium Halide Systems.

2.4. The Cesium Metal–Cesium Halide Systems

M. A. Bredig, H. R. Bronstein, and W. T. Smith, Jr., "Miscibility of Liquid Metals with Salts. II. The Potassium–Potassium Fluoride and Cesium–Cesium Halide Systems," *J. Am. Chem. Soc.* **77**, 1454 (1955).

Miscibility in all proportions of cesium metal with cesium halides at and above the melting points of the pure salts, and of potassium metal with potassium fluoride 50° above the melting point of the salt, occurs. The temperature-concentration range of coexistence of two liquid phases decreases in going from sodium to potassium systems and disappears altogether for the cesium systems. The solubility of the solid halides in the corresponding liquid alkali metals, at a given temperature, increases greatly with increase of atomic number of the metal.

UNCLASSIFIED
ORNL-LR-DWG. 37011
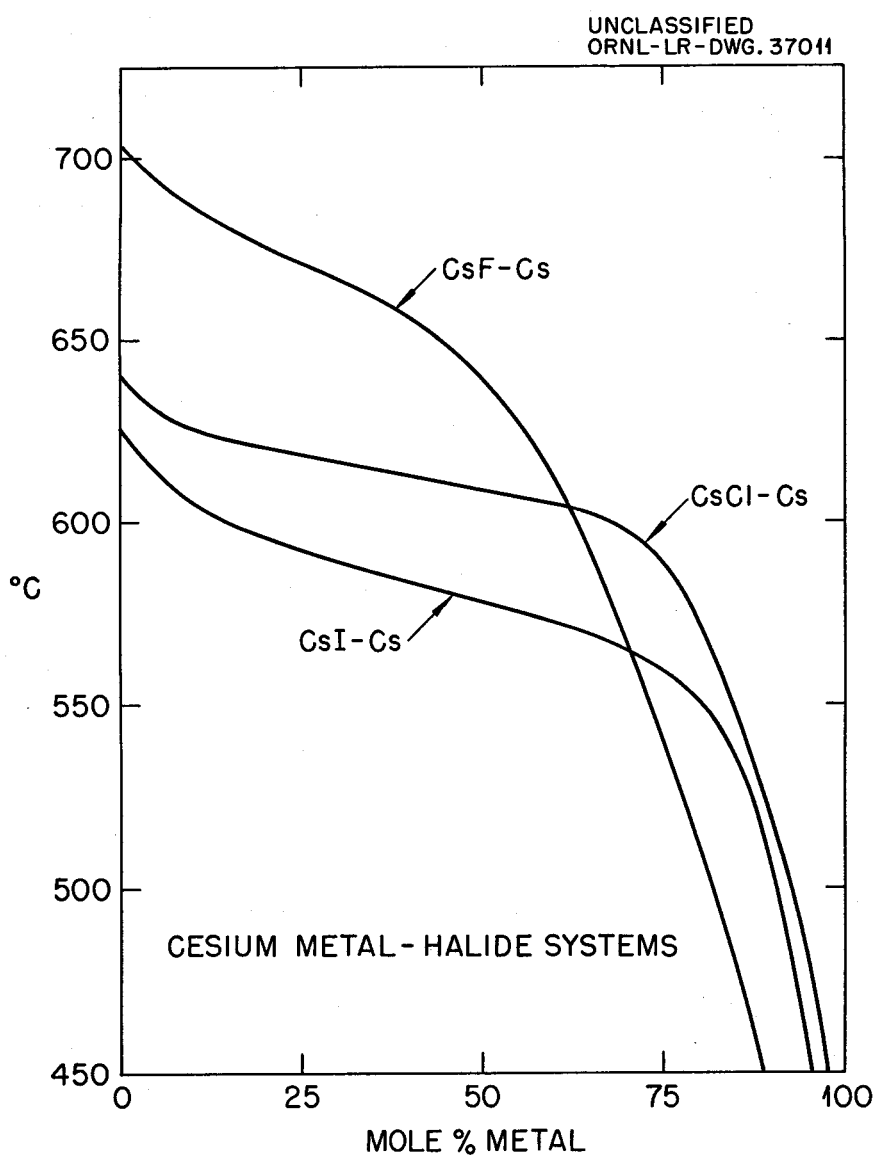
Fig. 2.4. The Cesium Metal–Cesium Halide Systems.

2.5. The Alkali Metal–Alkali Metal Fluoride Systems

M. A. Bredig, J. E. Sutherland, and A. S. Dworkin, "Molten Salt–Metal Solutions. Phase Equilibria," *Chem. Ann. Prog. Rep. June 20, 1958*, ORNL-2584, p 73.
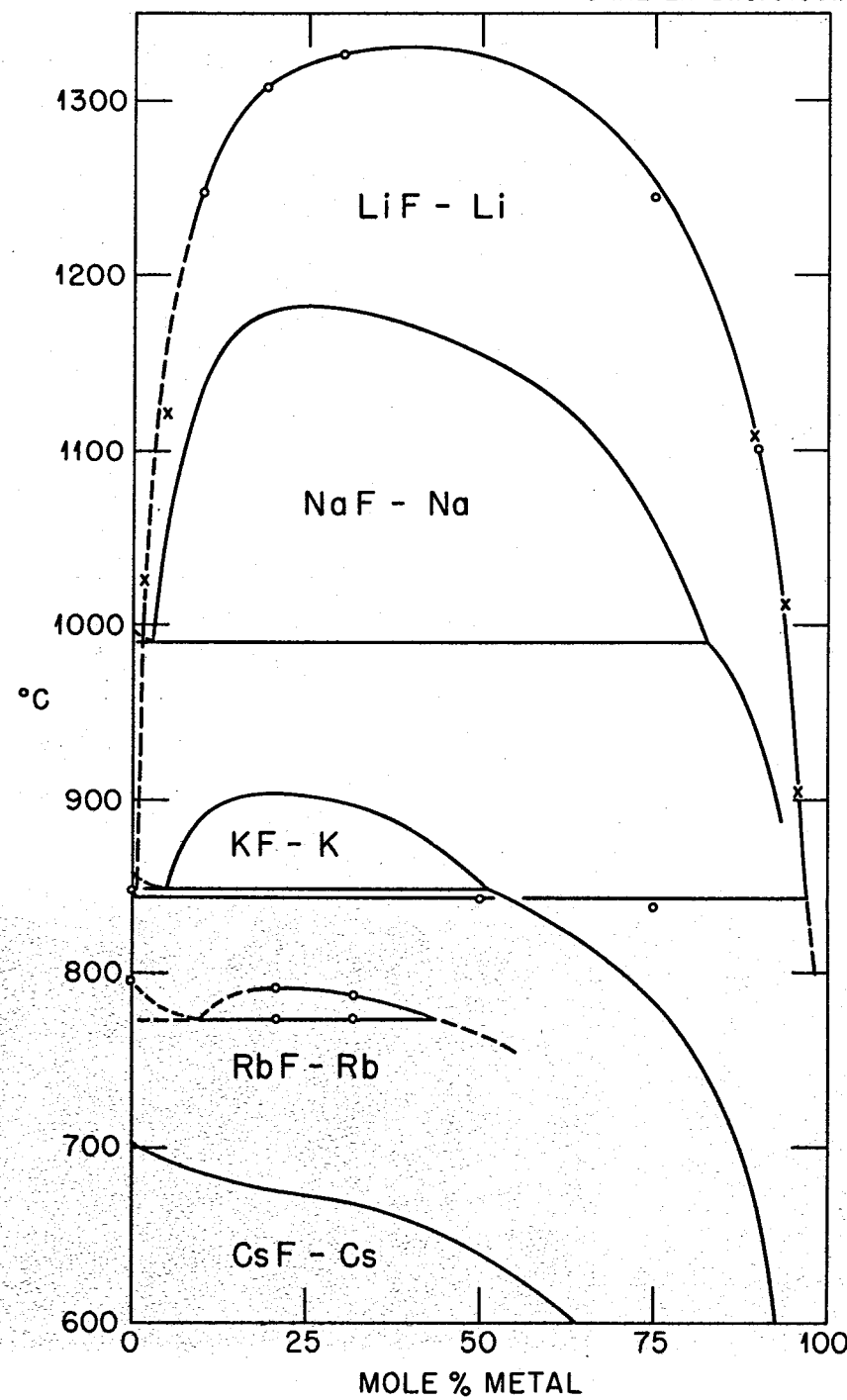
Fig. 2.5. The Alkali Metal–Alkali Metal Fluoride Systems.

3. FUSED-SALT SYSTEMS

3.1. The System LiF–NaF

A. G. Bergman and E. P. Dergunov, "Fusion Diagram of LiF–KF–NaF," *Compt. rend. acad. sci. U.R.S.S.* **31,** 753–54 (1941).

The system LiF–NaF contains a single eutectic at 60 LiF–40 NaF (mole %), m.p. 652°C.
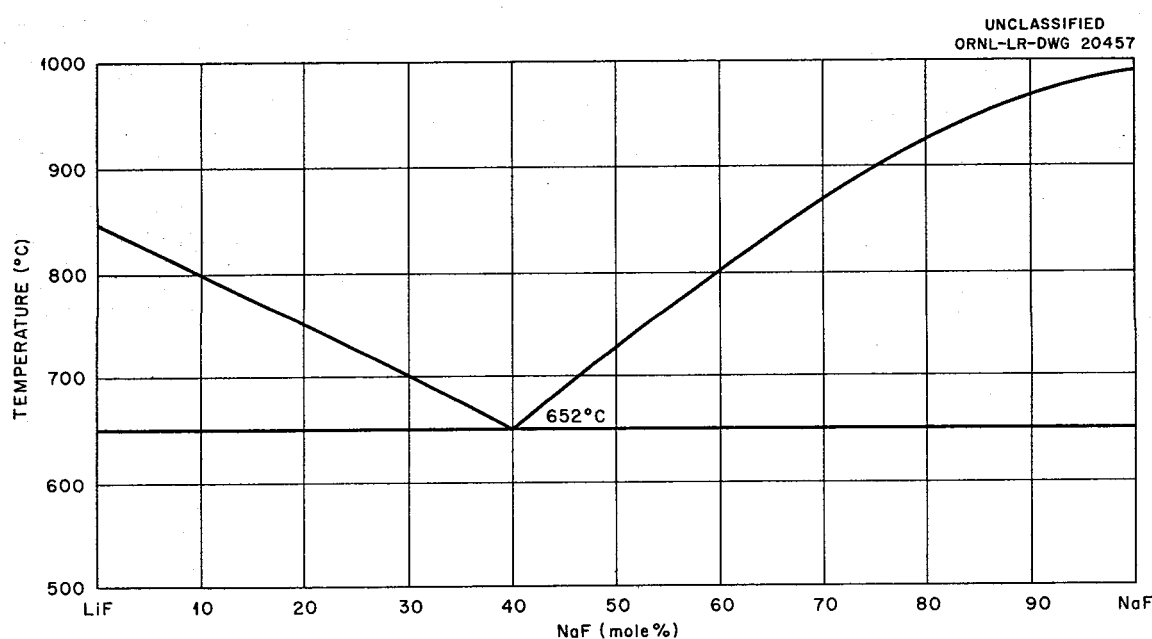
Fig. 3.1. The System LiF–NaF.

3.2. The System LiF—KF

A. G. Bergman and E. P. Dergunov, "Fusion Diagram of LiF—KF—NaF," *Compt. rend. acad. sci. U.R.S.S.* **31,** 753–54 (1941).

The system LiF—KF contains a single eutectic at 50 LiF—50 KF (mole %), m.p. 492°C.
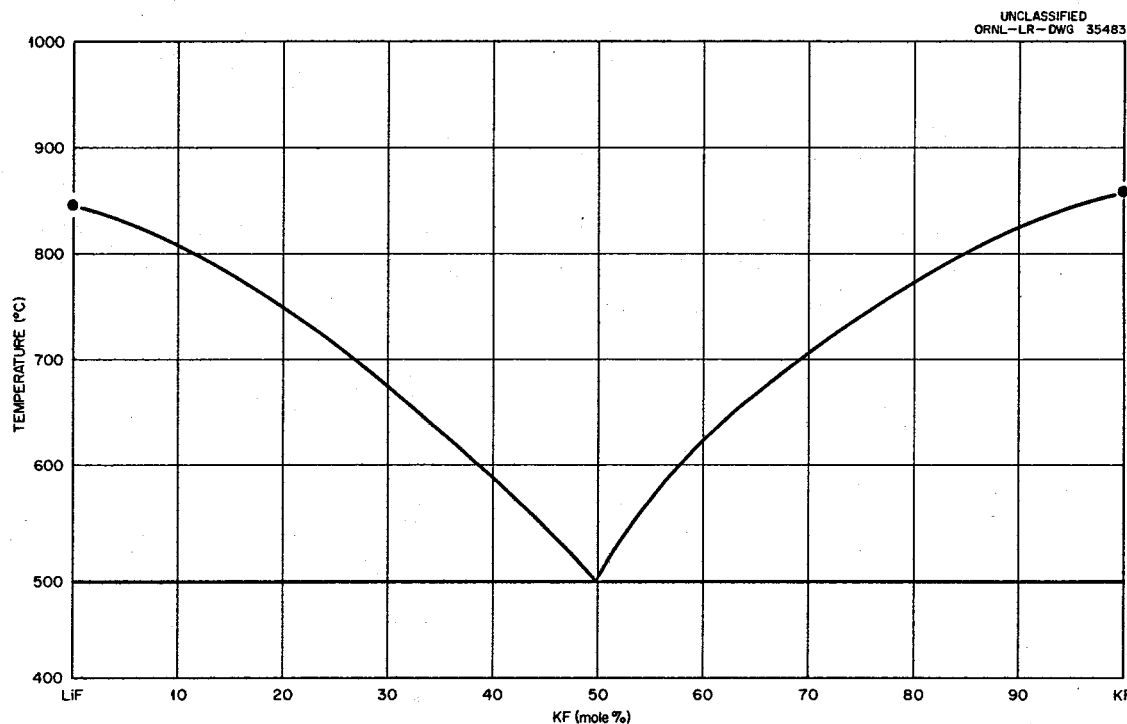
Fig. 3.2. The System LiF—KF.

3.3. The System LiF–RbF

C. J. Barton, T. N. McVay, L. M. Bratcher, and W. R. Grimes, unpublished work performed at the Oak Ridge National Laboratory, 1951–54.

Preliminary diagram.

Invariant Equilibria

Mole % LiF in Liquid	Invariant Temperature (°C)	Type of Equilibrium	Phase Reaction at Invariant Temperature
44	470	Eutectic	$L \rightleftharpoons RbF + LiF \cdot RbF$
47	475	Peritectic	$L + LiF \rightleftharpoons LiF \cdot RbF$

General characteristics of the system have been reported by E. P. Dergunov, "Fusion Diagrams of the Ternary Systems of the Fluorides of Lithium, Sodium, Potassium, and Rubidium," *Doklady Akad. Nauk S.S.S.R.* **58**, 1369–72 (1947).
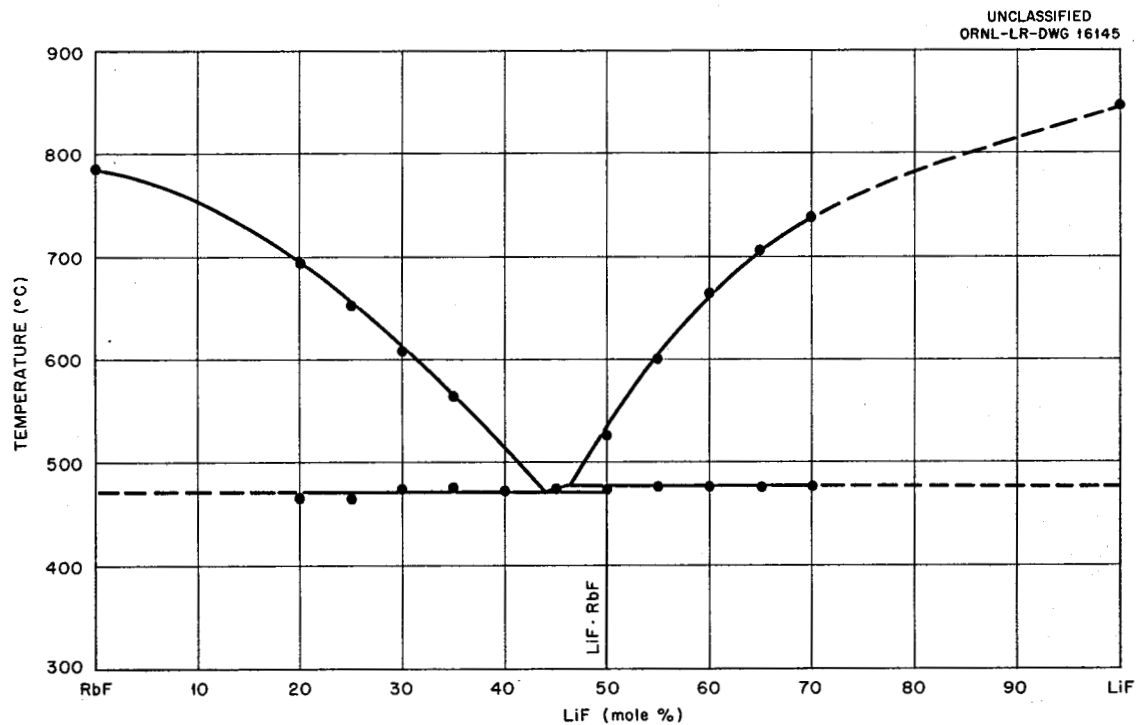
Fig. 3.3. The System LiF–RbF.

3.4. The System LiF–CsF

C. J. Barton, L. M. Bratcher, T. N. McVay, and W. R. Grimes, unpublished work performed at the Oak Ridge National Laboratory, 1952–54.

Preliminary diagram.

<div align="center">Invariant Equilibria</div>

Mole % CsF in Liquid	Invariant Temperature (°C)	Type of Equilibrium	Phase Reaction at Invariant Temperature
55	495 ± 5	Peritectic	$LiF + L \rightleftharpoons LiF \cdot CsF$
63	475 ± 5	Eutectic	$L \rightleftharpoons LiF \cdot CsF + CsF$
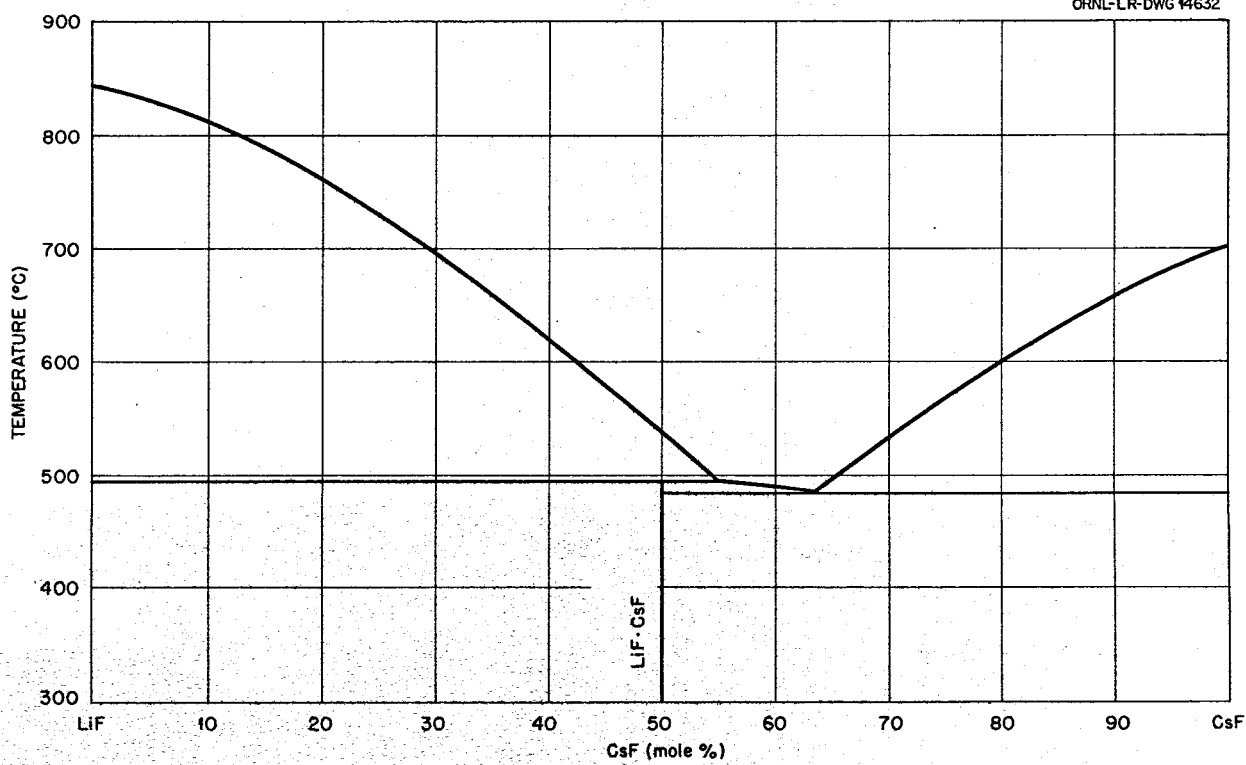
Fig. 3.4. The System LiF–CsF.

3.5. The System NaF–KF

A. G. Bergman and E. P. Dergunov, "Fusion Diagram of LiF–KF–NaF," *Compt. rend. acad. sci. U.R.S.S.* **31**, 753–54 (1941).

The system NaF–KF contains a single eutectic at 40 NaF–60 KF (mole %), m.p. 710°C.
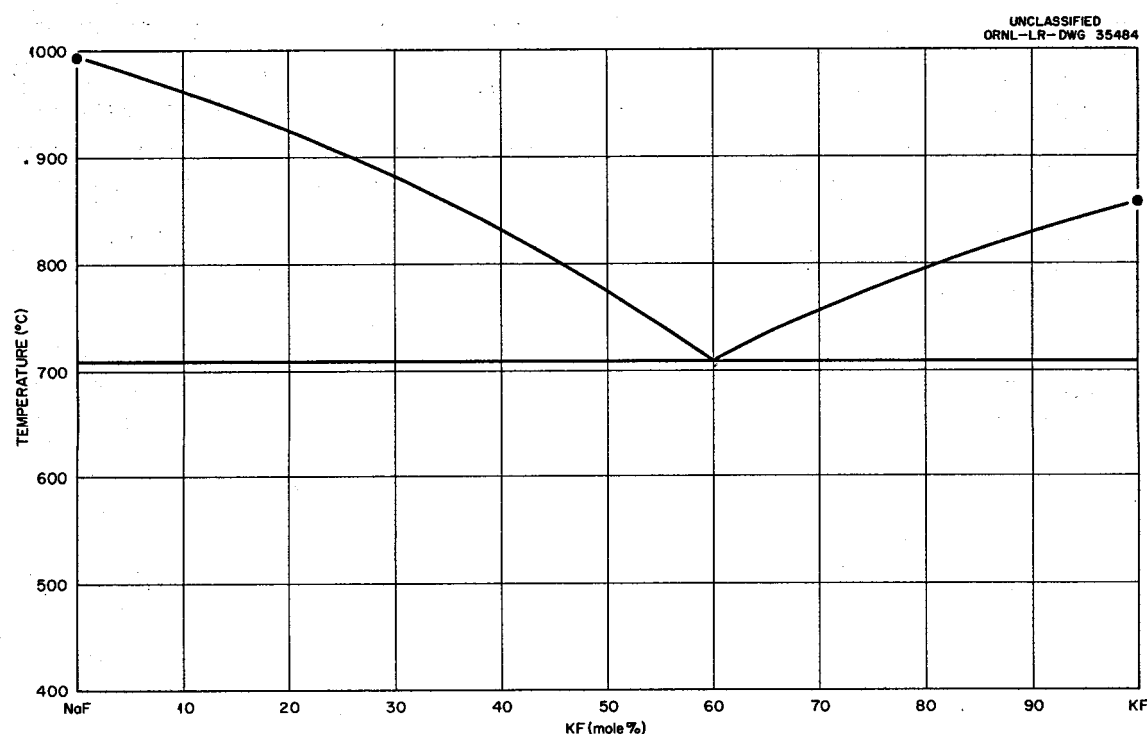
Fig. 3.5. The System NaF–KF.

3.6. The System NaF–RbF

C. J. Barton, J. P. Blakely, L. M. Bratcher, and W. R. Grimes, unpublished work performed at the Oak Ridge National Laboratory, 1951.

Preliminary diagram. The system NaF–RbF contains a single eutectic at 27 NaF–73 RbF (mole %), m.p. 675 ± 10°C.

General characteristics of the system have been reported by E. P. Dergunov, "Fusion Diagrams of the Ternary Systems of the Fluorides of Lithium, Sodium, Potassium, and Rubidium," *Doklady Akad. Nauk S.S.S.R.* **58**, 1369–72 (1947).
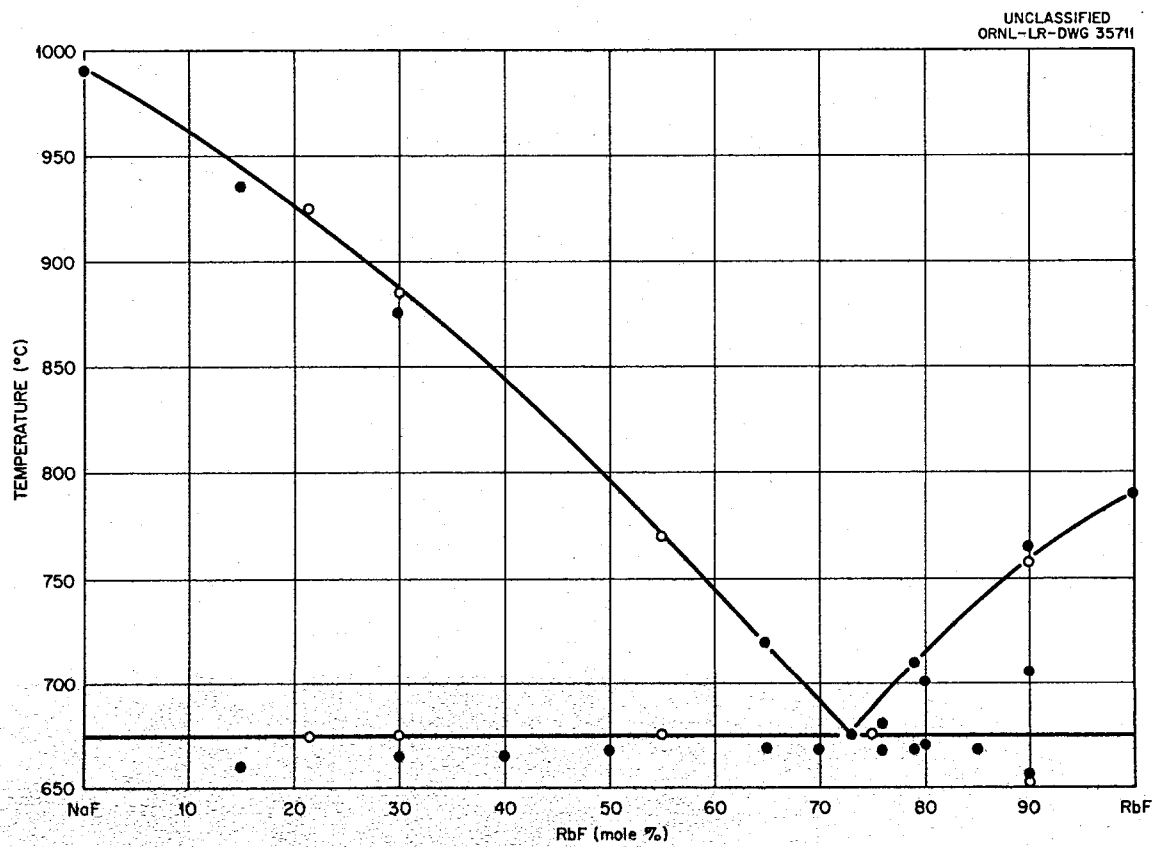
Fig. 3.6. The System NaF–RbF.

3.7. The System KF-RbF

C. J. Barton, J. P. Blakely, L. M. Bratcher, and W. R. Grimes, unpublished work performed at the Oak Ridge National Laboratory, 1951.

Preliminary diagram. The system KF-RbF contains a solid solution minimum at 28 KF-72 RbF (mole %), m.p. 770 ± 10°C.
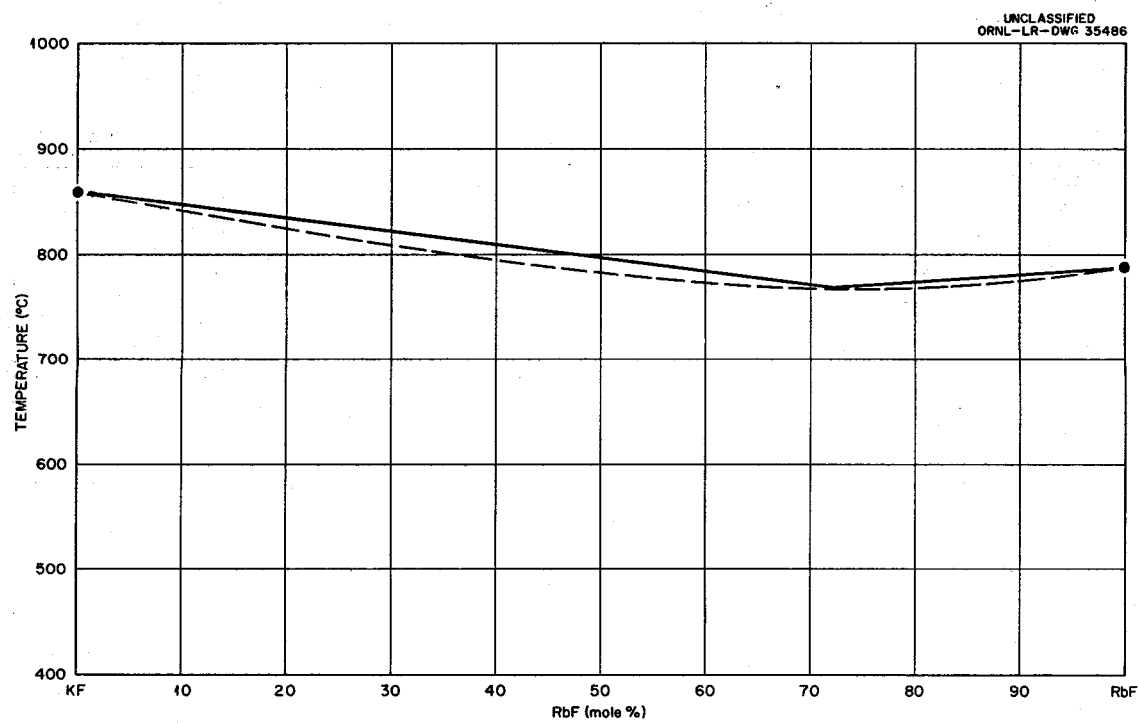
Fig. 3.7. The System KF-RbF.

3.8. The System LiF–NaF–KF

A. G. Bergman and E. P. Dergunov, "Fusion Diagram of LiF–KF–NaF," *Compt. rend. acad. sci. U.R.S.S.* **31**, 753–54 (1941).

The system LiF–NaF–KF contains a single eutectic at 46.5 LiF–11.5 NaF–42.0 KF (mole %), m.p. 454°C.
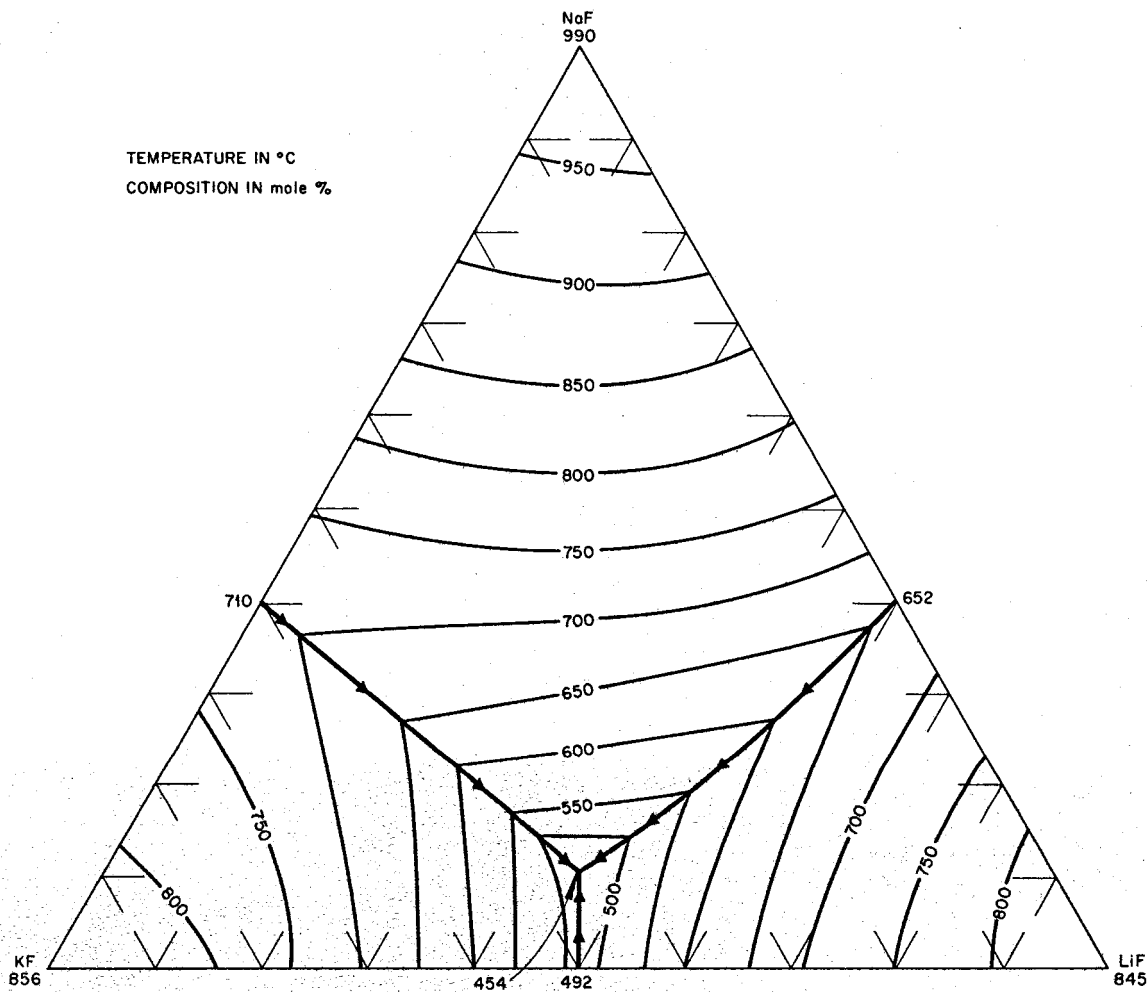
Fig. 3.8. The System LiF–NaF–KF.

3.9. The System LiF–NaF–RbF

C. J. Barton, L. M. Bratcher, J. P. Blakely, and W. R. Grimes, unpublished work performed at the Oak Ridge National Laboratory, 1951.

Preliminary diagram. The system LiF–NaF–RbF contains a single eutectic at 42 LiF–6 NaF–52 RbF (mole %), m.p. 430 ± 10°C. The composition and temperature of the ternary peritectic point have not yet been determined.

General characteristics of the system have been reported by E. P. Dergunov, "Fusion Diagrams of the Ternary systems of the Fluorides of Lithium, Sodium, Potassium, and Rubidium," *Doklady Akad. Nauk S.S.S.R.* **58**, 1369–72 (1947). Dergunov lists the composition and temperature of the ternary eutectic as 46.5 LiF–6.5 NaF–47 RbF (mole %), m.p. 426°C.
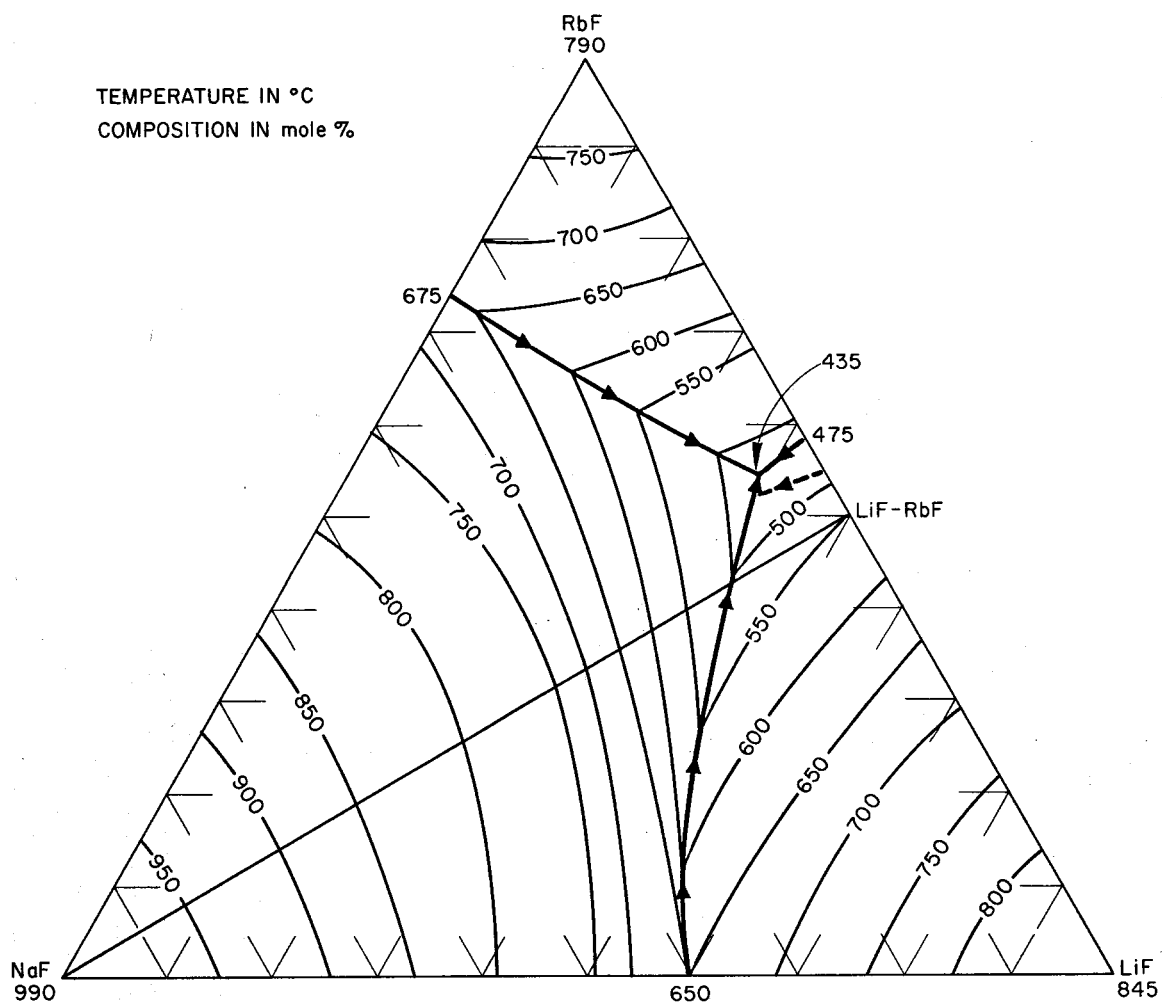
Fig. 3.9. The System LiF–NaF–RbF.

3.10. The System LiF-KF-RbF

C. J. Barton, J. P. Blakely, L. M. Bratcher, and W. R. Grimes, unpublished work performed at the Oak Ridge National Laboratory, 1951.

Preliminary diagram. The system LiF-KF-RbF contains a single eutectic at 40 LiF-32.5 KF-27.5 RbF (mole %), m.p. 440 ± 10°C.

General characteristics of the system have been reported by E. P. Dergunov, "Fusion Diagrams of the Ternary Systems of the Fluorides of Lithium, Sodium, Potassium, and Rubidium," *Doklady Akad. Nauk S.S.S.R.* **58**, 1369–72 (1947).
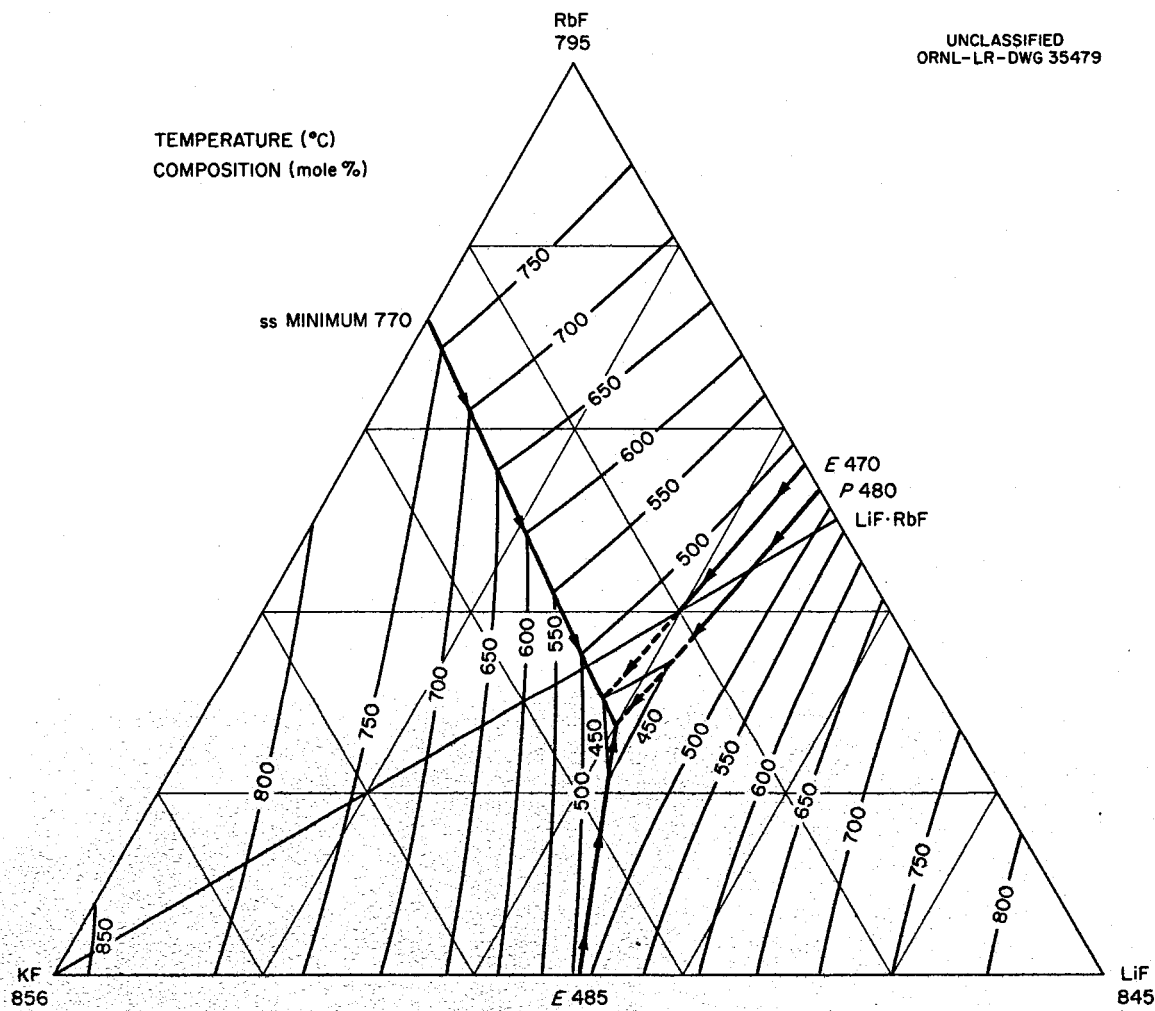
Fig. 3.10. The System LiF-KF-RbF.

3.11. The System NaF–KF–RbF

C. J. Barton, L. M. Bratcher, J. P. Blakely, and W. R. Grimes, unpublished work performed at the Oak Ridge National Laboratory, 1951.

Preliminary diagram. The system NaF–KF–RbF contains a single eutectic at 21 NaF–5 KF–74 RbF (mole %), m.p. 621 ± 10°C.
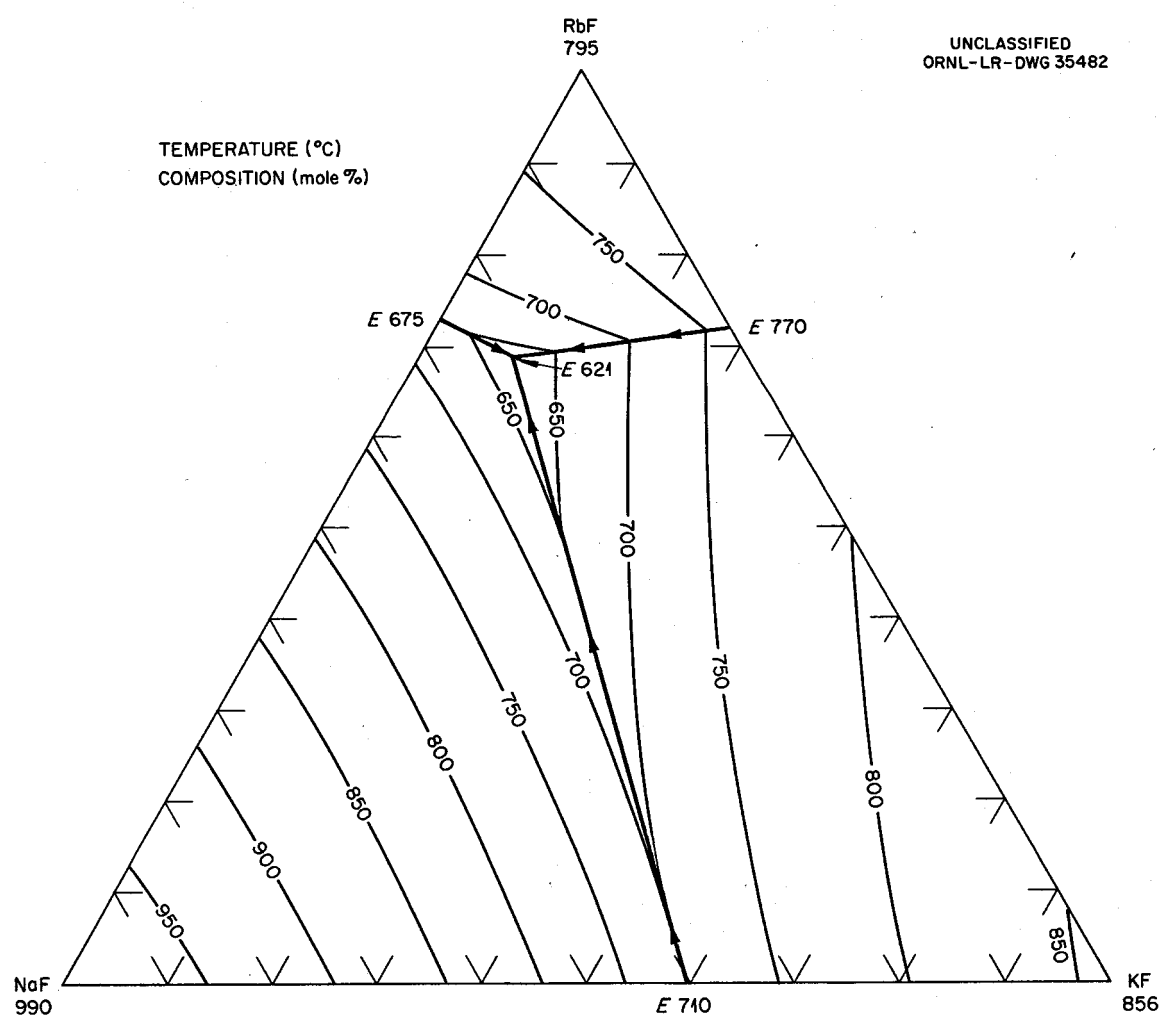
Fig. 3.11. The System NaF–KF–RbF.

3.12. The System NaBF$_4$-KBF$_4$

R. E. Moore, J. G. Surak, and W. R. Grimes, unpublished work performed at the Oak Ridge National Laboratory, 1957.

Preliminary diagram. The system NaBF$_4$-KBF$_4$ contains a single eutectic at 88 NaBF$_4$-12 KBF$_4$ (mole %), m.p. 355°C. The dotted line was obtained from thermal effects representing incompletely understood solid-phase transformations of KBF$_4$ and NaBF$_4$.
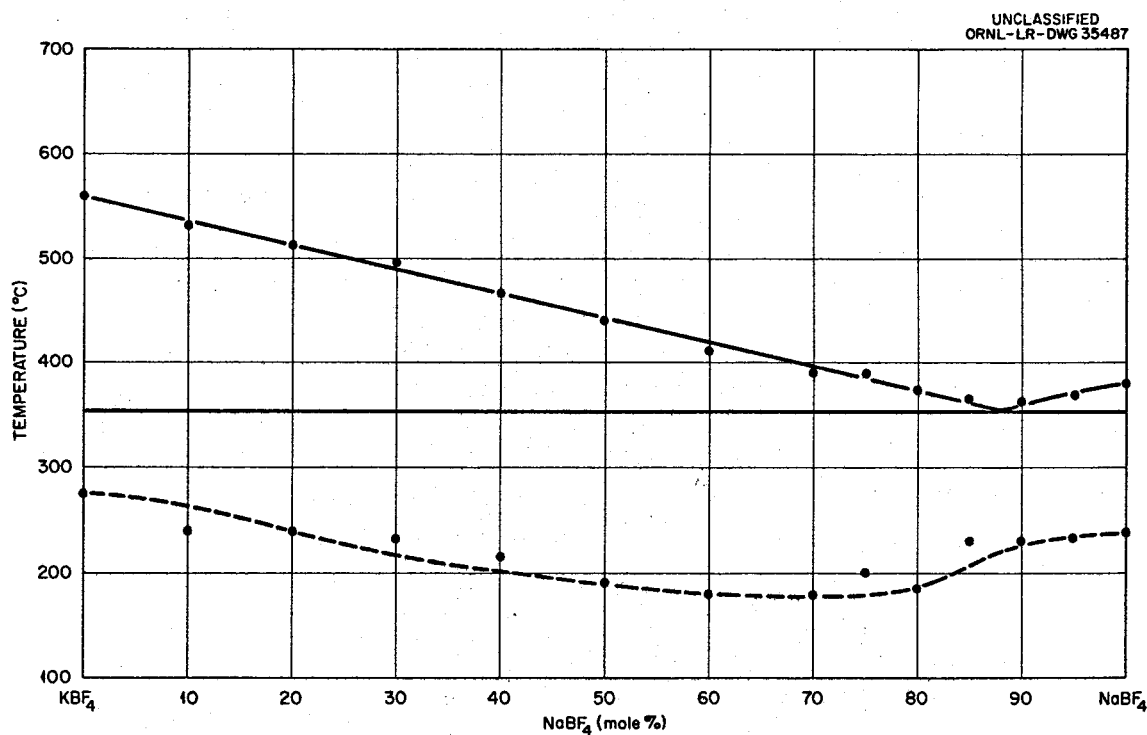
Fig. 3.12 The System NaBF$_4$-KBF$_4$.

3.13. The System NaF–FeF$_2$

R. E. Thoma, H. A. Friedman, B. S. Landau, and W. R. Grimes, unpublished work performed at the Oak Ridge National Laboratory, 1957.

Preliminary diagram.

Invariant Equilibria

Mole % FeF$_2$ in Liquid	Invariant Temperature (°C)	Type of Equilibrium	Phase Reaction at Invariant Temperature
30	680	Eutectic	$L \rightleftharpoons NaF + NaF \cdot FeF_2$
50	783	Congruent melting point	$L \rightleftharpoons NaF \cdot FeF_2$
63	745	Eutectic	$L \rightleftharpoons NaF \cdot FeF_2 + FeF_2$
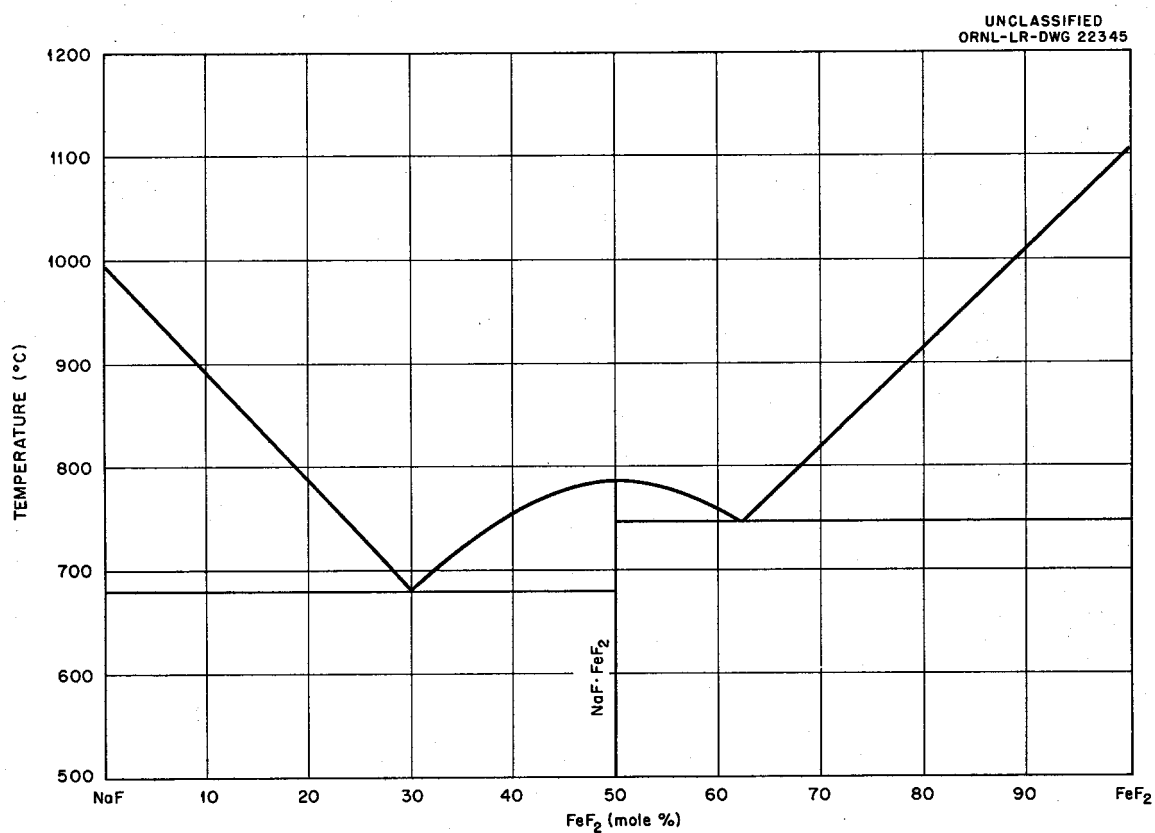
Fig. 3.13. The System NaF–FeF$_2$.

3.14. The System $NaF-NiF_2$

R. E. Thoma, H. A. Friedman, B. S. Landau, and W. R. Grimes, unpublished work performed at the Oak Ridge National Laboratory, 1957.

Preliminary diagram.

Invariant Equilibria

Mole % NiF_2 in Liquid	Invariant Temperature (°C)	Type of Equilibrium	Phase Reaction at Invariant Temperature
23	795	Eutectic	$L \rightleftharpoons NaF + NaF \cdot NiF_2$
50	1045	Congruent melting point	$L \rightleftharpoons NaF \cdot NiF_2$
57	1040	Eutectic	$L \rightleftharpoons NaF \cdot NiF_2 + NiF_2$
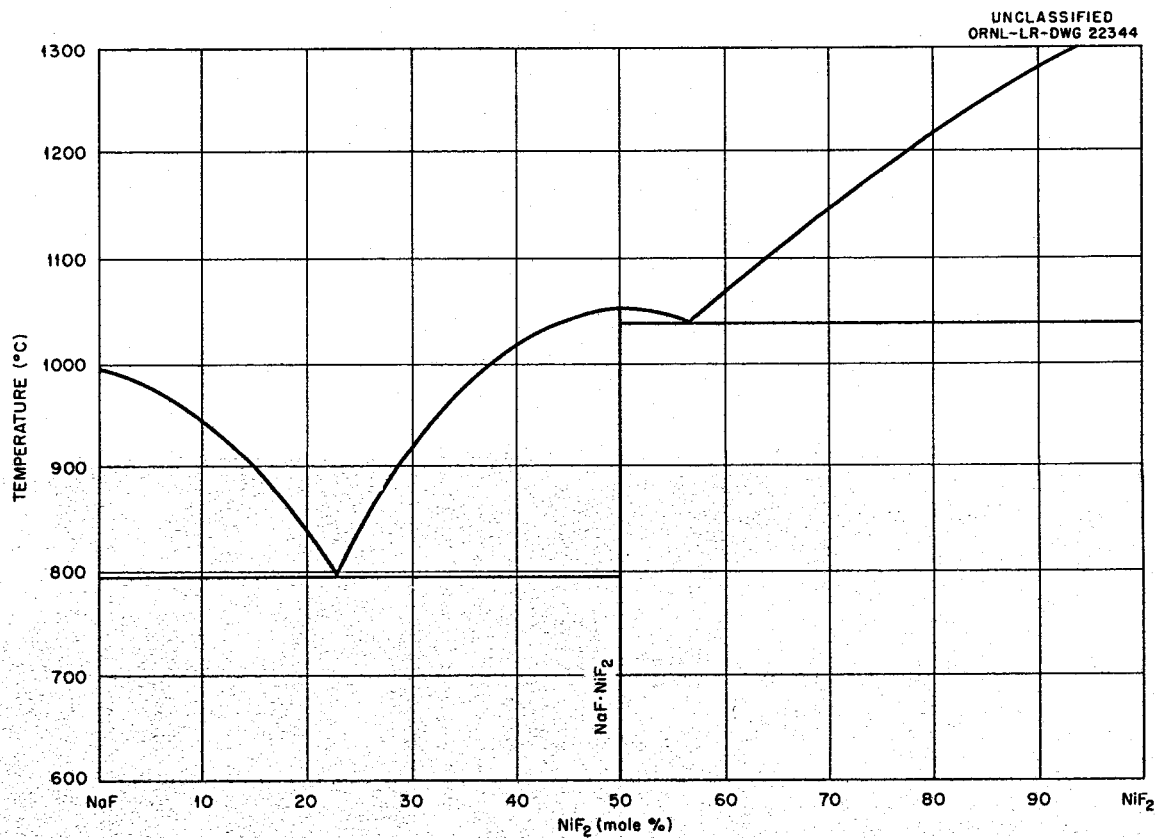
Fig. 3.14. The System $NaF-NiF_2$

3.15. The System RbF–CaF$_2$

C. J. Barton, L. M. Bratcher, R. J. Sheil, and W. R. Grimes, unpublished work performed at the Oak Ridge National Laboratory, 1956.

Preliminary diagram.

Invariant Equilibria

Mole % CaF$_2$ in Liquid	Invariant Temperature (°C)	Type of Equilibrium	Phase Reaction at Invariant Temperature
9	760	Eutectic	$L \rightleftharpoons RbF + RbF \cdot CaF_2$
50	1110	Congruent melting point	$L \rightleftharpoons RbF \cdot CaF_2$
57	1090	Eutectic	$L \rightleftharpoons RbF \cdot CaF_2 + CaF_2$
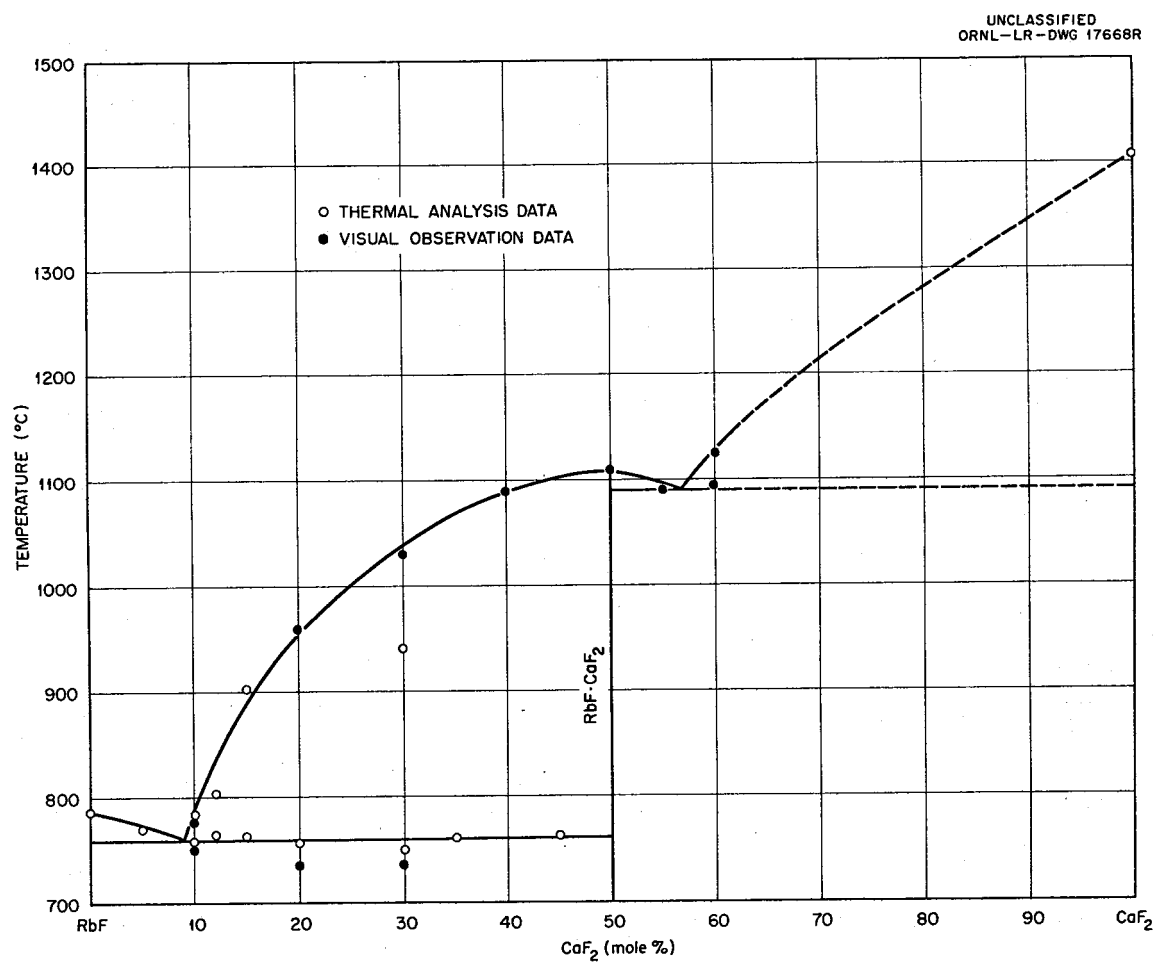
Fig. 3.15. The System RbF–CaF$_2$.

3.16. The System LiF–NaF–CaF$_2$

C. J. Barton, L. M. Bratcher, and W. R. Grimes, unpublished work performed at the Oak Ridge National Laboratory, 1955–56.

Preliminary diagram. The system LiF–NaF–CaF$_2$ contains a single eutectic at 53 LiF– 36 NaF–11 CaF$_2$ (mole %), m.p. 616°C.

Fig. 3.16. The System LiF–NaF–CaF$_2$

TEMPERATURES ARE IN °C
COMPOSITION IN mole %
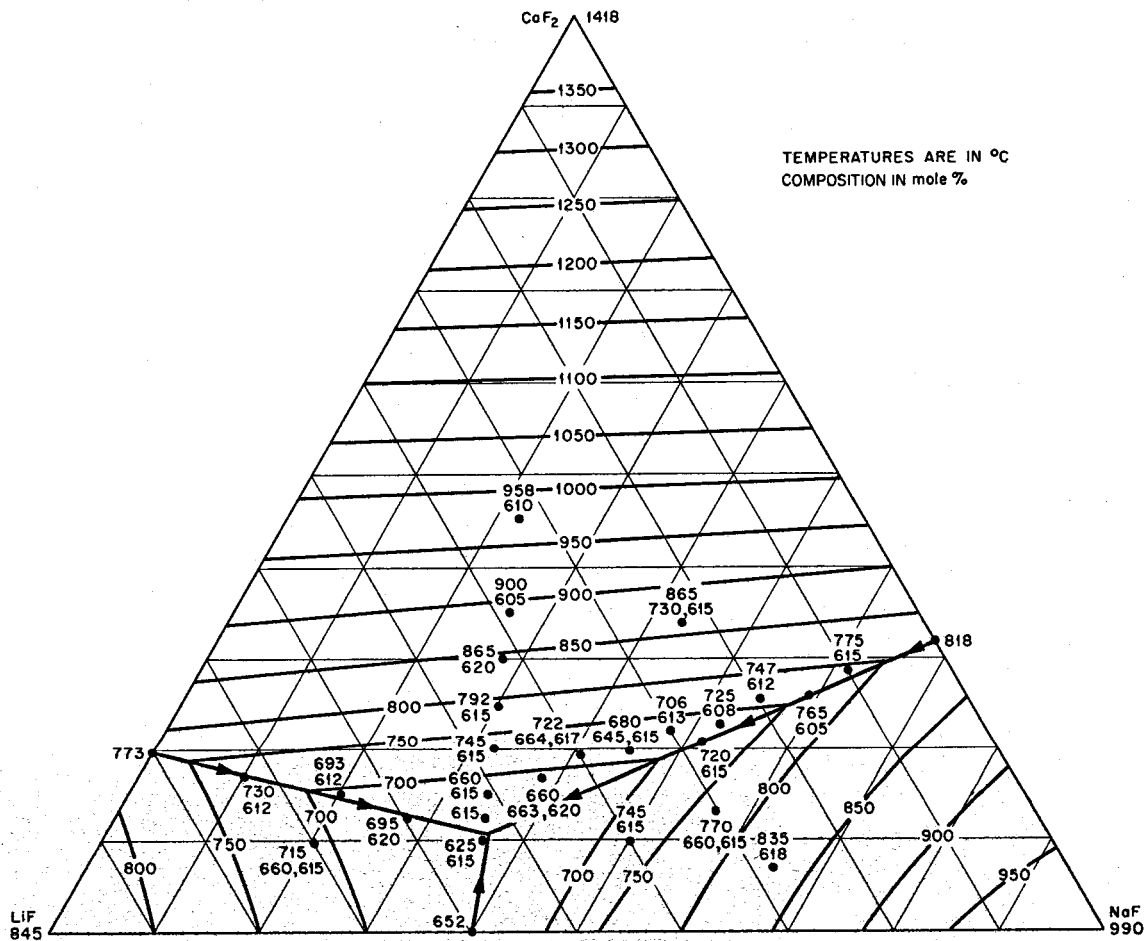
3.17. The System NaF–MgF$_2$–CaF$_2$

C. J. Barton, L. M. Bratcher, J. P. Blakely, and W. R. Grimes, unpublished work performed at the Oak Ridge National Laboratory, 1955–56.

Preliminary diagram.

Invariant Equilibria

Composition of Liquid (mole %)			Temperature (°C)	Type of Equilibrium	Solids Present at Invariant Temperature
NaF	CaF$_2$	MgF$_2$			
65	23	12	745	Eutectic	NaF, NaF·MgF$_2$, and CaF$_2$
35	28	37	905	Eutectic	CaF$_2$, MgF$_2$, and NaF·MgF$_2$

COMPOSITION IN mole %
TEMPERATURE IN °C
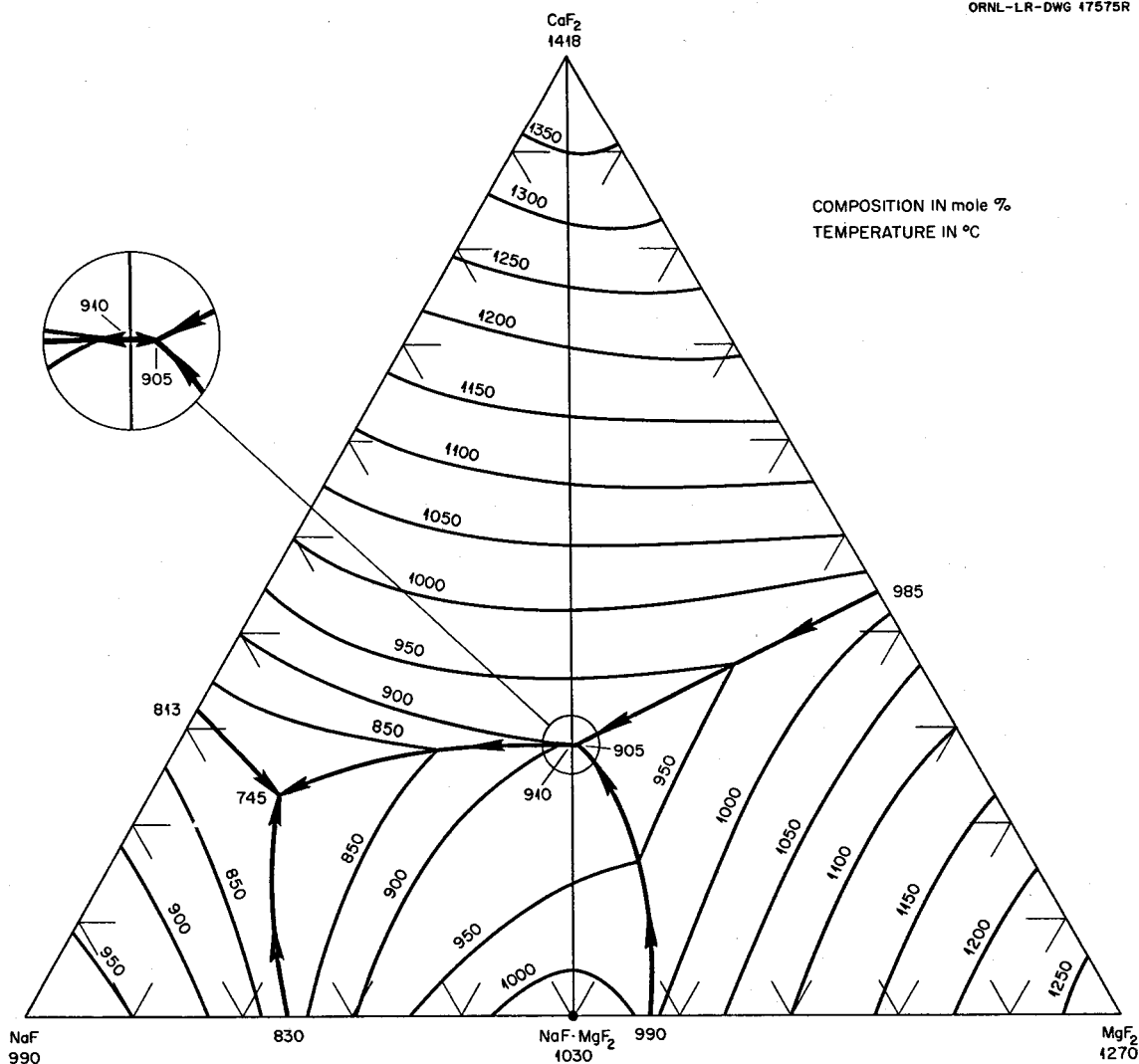
Fig. 3.17a. The System NaF–MgF$_2$–CaF$_2$

The minimum temperature along the quasi-binary section $NaF \cdot MgF_2 - CaF_2$ occurs at the composition 36 NaF–36 MgF_2–28 CaF_2 (mole %), at 910°C.

The existence of the compound $NaF \cdot MgF_2$ was previously reported by A. G. Bergman and E. P. Dergunov, *Compt. rend. acad. sci. U.R.S.S.* **31**, 755 (1941).

Ternary systems of alkali fluorides with MgF_2 have been reported by Bergman *et al.* as follows: the system $LiF–NaF–MgF_2$ by A. G. Bergman and E. P. Dergunov, *Compt. rend. acad. sci. U.R.S.S.* **31**, 755 (1941); the system $LiF–KF–MgF_2$ by A. G. Bergman and S. P. Parlenko, *Compt. rend. acad. sci. U.R.S.S.* **31**, 818–19 (1941); the system $NaF–KF–MgF_2$ by A. G. Bergman and E. P. Dergunov, *Compt. rend. acad. sci. U.R.S.S.* **48**, 330 (1945).
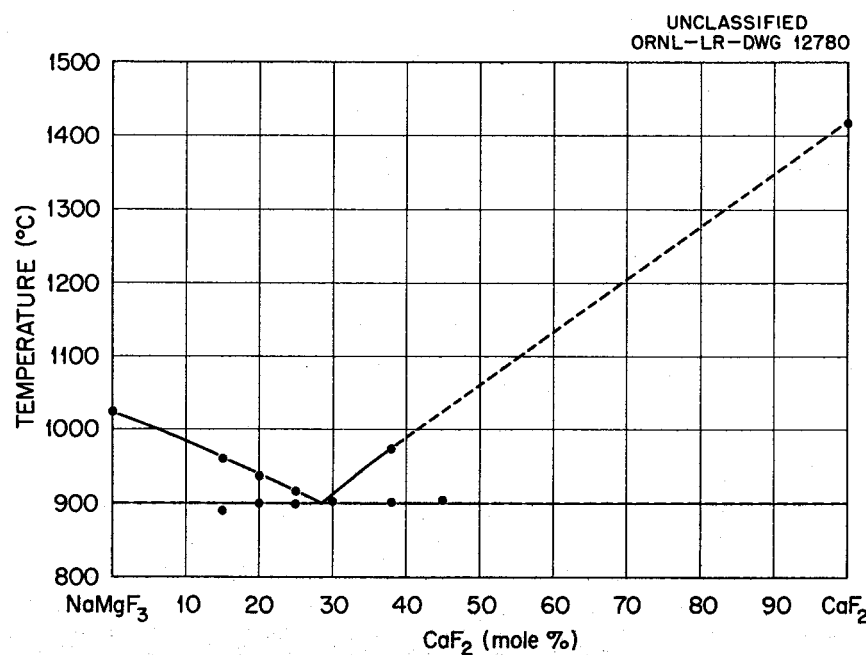
Fig. 3.17b. The Subsystem $NaF \cdot MgF_2 - CaF_2$.

3.18. The System NaF–KF–AlF₃

C. J. Barton, L. M. Bratcher, and W. R. Grimes, unpublished work performed at the Oak Ridge National Laboratory, 1951–52.

Preliminary diagram. No study has been made at the Oak Ridge National Laboratory of the phase relationships occurring within the system $NaF–KF–AlF_3$. Phase diagrams have been reported for the AlF_3 binary systems, $NaF–AlF_3$ [P. P. Fediotieff and W. P. Iljinsky, *Z. anorg. Chem.* **80**, 121 (1913); also N. A. Pushin and A. V. Baskow, *ibid.* **81**, 350 (1913)] and $KF–AlF_3$ [P. P. Fediotieff and K. Timofeef, *Z. anorg. u. allgem. Chem.* **206**, 265 (1932)].
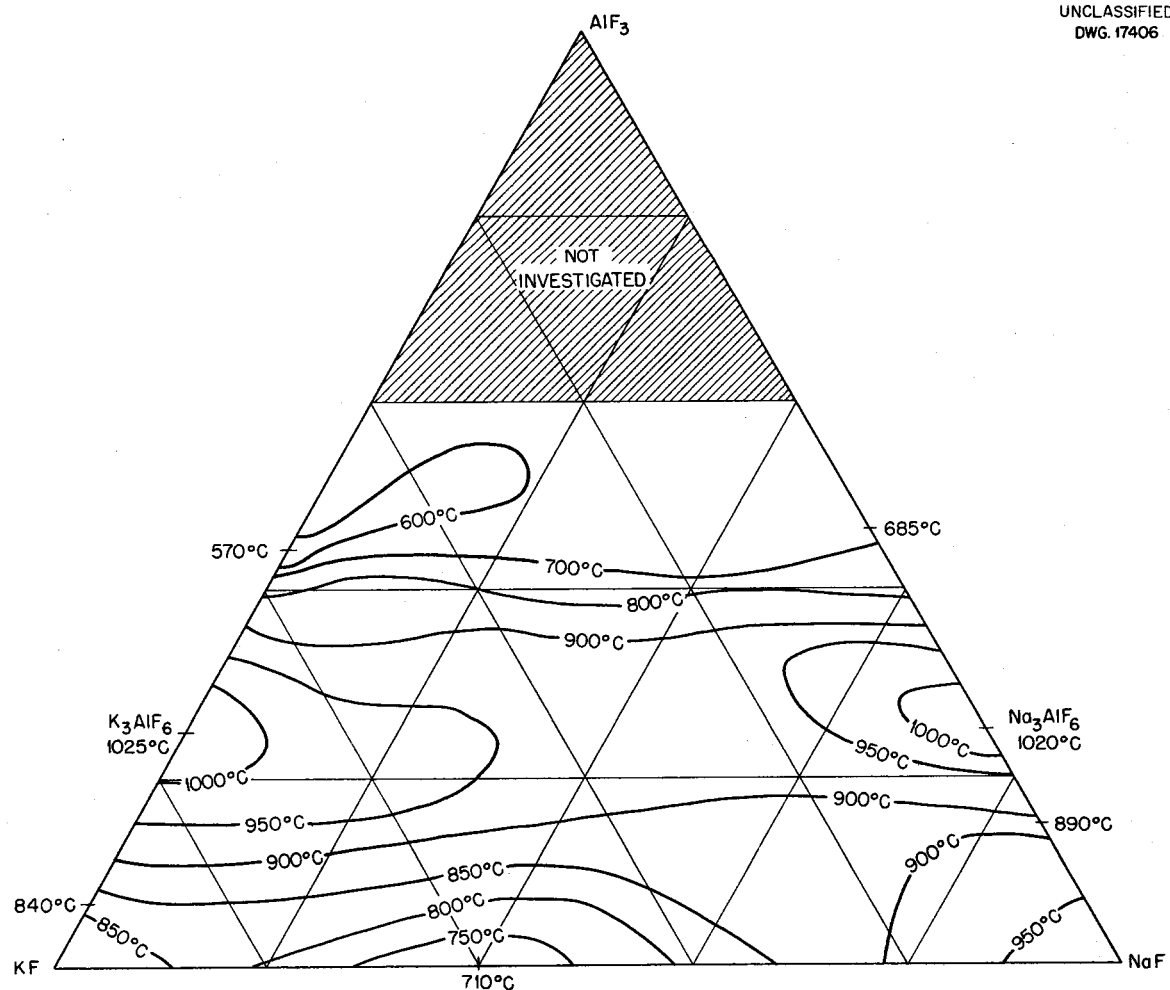
Fig. 3.18. The System $NaF–KF–AlF_3$.

3.19. The System LiF–BeF$_2$

This phase diagram is a composite from several published sources[1-3] and from unpublished data derived at the Oak Ridge National Laboratory (R. E. Moore, C. J. Barton, R. E. Thoma, and T. N. McVay) and at the Mound Laboratory (J. F. Eichelberger, C. R. Hudgens, L. V. Jones, and T. B. Rhinehammer). Thermal gradient quenching data (ORNL) and differential thermal analysis data (Mound Laboratory) have served to corroborate this composite diagram.

Invariant Equilibria

Mole % BeF$_2$ in Liquid	Invariant Temperature (°C)	Type of Equilibrium	Phase Reaction at Invariant Temperature
33.5*	454	Peritectic	$L + LiF \rightleftharpoons 2LiF \cdot BeF_2$
52	355	Eutectic	$L \rightleftharpoons 2LiF \cdot BeF_2 + BeF_2$
–	280	Upper temperature of stability for LiF·BeF$_2$	$2LiF \cdot BeF_2 + BeF_2 \rightleftharpoons LiF \cdot BeF_2$

*Ref 3.

Roy, Roy, and Osborn have reported the presence of the compound LiF·2BeF$_2$ in the system LiF–BeF$_2$ although neither the Mound Laboratory nor the ORNL data have indicated the existence of this compound.

[1]D. M. Roy, R. Roy, and E. F. Osborn, *J. Am. Ceram. Soc.* 37, 300 (1954).

[2]A. V. Novoselova, Yu. P. Simanov, and E. I. Yarembash, *J. Phys. Chem. (U.S.S.R.)* 26, 1244 (1952).

[3]John L. Speirs, *The Binary and Ternary Systems Formed by Calcium Fluoride, Lithium Fluoride, and Beryllium Fluoride: Phase Diagrams and Electrolytic Studies*, Ph.D. thesis, University of Michigan, May 29, 1952.
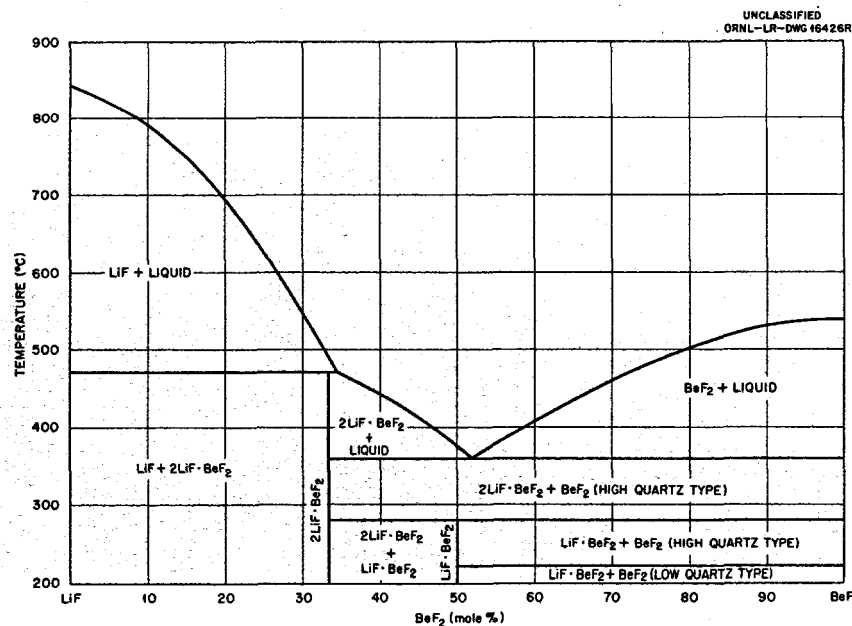
Fig. 3.19. The System LiF–BeF$_2$.

3.20. The System NaF–BeF$_2$

D. M. Roy, R. Roy, and E. F. Osborn, "Fluoride Model Systems: III. The System NaF–BeF$_2$ and the Polymorphism of Na$_2$BeF$_4$ and BeF$_2$," *J. Am. Ceram. Soc.* **36**, 185 (1953).

Invariant Equilibria*

Mole % BeF$_2$ in Liquid	Invariant Temperature (°C)	Type of Equilibrium	Phase Reaction at Invariant Temperature
31	570	Eutectic	$L \rightleftharpoons NaF + \alpha\text{-}2NaF\cdot BeF_2$
33.3	600	Congruent melting point	$L \rightleftharpoons \alpha\text{-}2NaF\cdot BeF_2$
—	320	Inversion	$\alpha\text{-}2NaF\cdot BeF_2 \rightleftharpoons \alpha'\text{-}2NaF\cdot BeF_2$
—	225	Inversion	$\alpha'\text{-}2NaF\cdot BeF_2 \rightleftharpoons \gamma\text{-}2NaF\cdot BeF_2$
43	340	Eutectic	$L \rightleftharpoons \alpha\text{-}2NaF\cdot BeF_2 + \beta\text{-}NaF\cdot BeF_2$
50	376 ± 5	Congruent melting point	$L \rightleftharpoons \beta'\text{-}NaF\cdot BeF_2$
55	365	Eutectic	$L \rightleftharpoons \beta'\text{-}NaF\cdot BeF_2 + BeF_2$

*Roy, Roy, and Osborn did not list invariant equilibria; those shown are estimates made from the reported work and from experiments performed at the Oak Ridge National Laboratory.
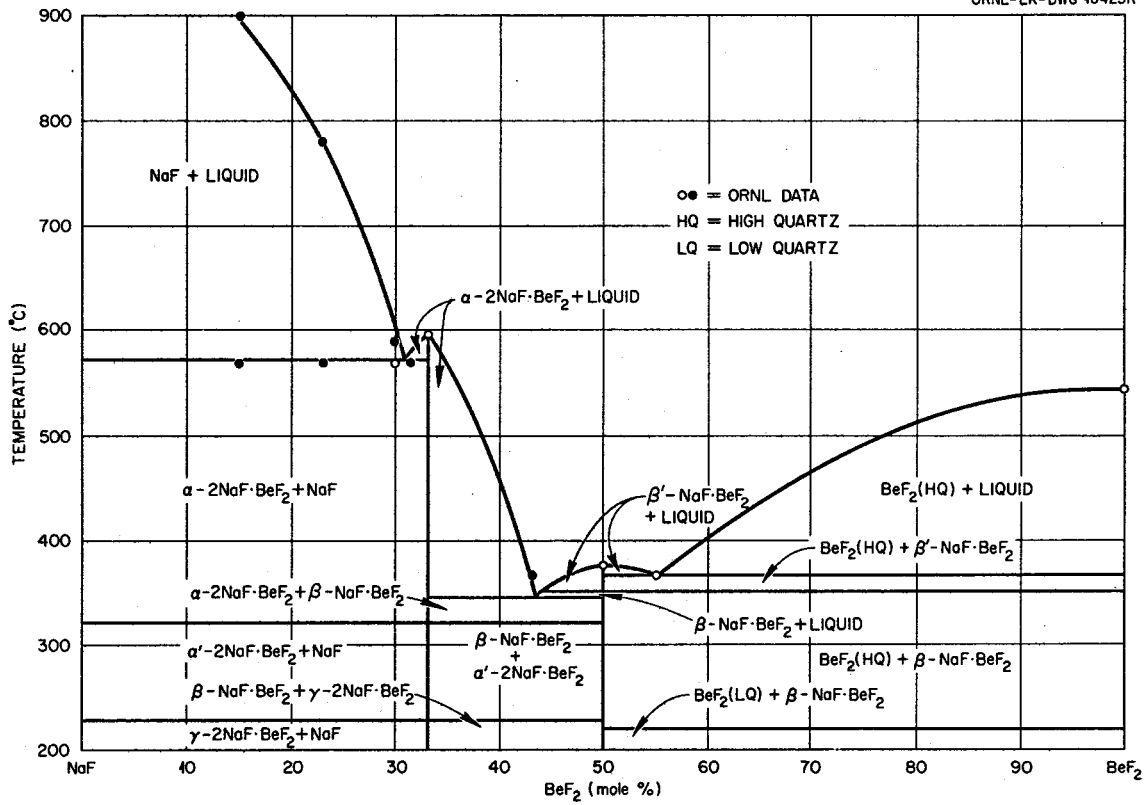
Fig. 3.20. The System NaF—BeF$_2$.

3.21. The System KF–BeF$_2$

R. E. Moore, C. J. Barton, L. M. Bratcher, T. N. McVay, G. D. White, R. J. Sheil, W. R. Grimes, R. E. Meadows, and L. A. Harris, unpublished work performed at the Oak Ridge National Laboratory, 1955–56.

Preliminary diagram.

Invariant Equilibria

Mole % BeF$_2$ In Liquid	Invariant Temperature (°C)	Type of Equilibrium	Phase Reaction at Invariant Temperature
19	720	Eutectic	$L \rightleftharpoons KF + 3KF \cdot BeF_2$
25	740	Congruent melting point	$L \rightleftharpoons 3KF \cdot BeF_2$
27	730	Eutectic	$L \rightleftharpoons 3KF \cdot BeF_2 + \alpha\text{-}2KF \cdot BeF_2$
33.3	787	Congruent melting point	$L \rightleftharpoons \alpha\text{-}2KF \cdot BeF_2$
–	685	Inversion	$\alpha\text{-}2KF \cdot BeF_2 \rightleftharpoons \beta\text{-}2KF \cdot BeF_2$
52	390	Peritectic	$\beta\text{-}2KF \cdot BeF_2 + L \rightleftharpoons KF \cdot BeF_2$
59	330	Eutectic	$L \rightleftharpoons KF \cdot BeF_2 + \beta\text{-}KF \cdot 2BeF_2$
66.7	358	Congruent melting point	$L \rightleftharpoons \alpha\text{-}KF \cdot 2BeF_2$
–	334	Inversion	$\alpha\text{-}KF \cdot 2BeF_2 \rightleftharpoons \beta\text{-}KF \cdot 2BeF_2$
72.5	323	Eutectic	$L \rightleftharpoons \beta\text{-}KF \cdot 2BeF_2 + BeF_2$

This system has been reported by M. P. Borzenkova, A. V. Novoselova, Yu. P. Simanov, V. I. Chernikh, and E. I. Yarembash, "Thermal and X-Ray Analysis of the KF–BeF$_2$ System," *Zhur. Neorg. Khim.* **1**, 2071–82 (1956).
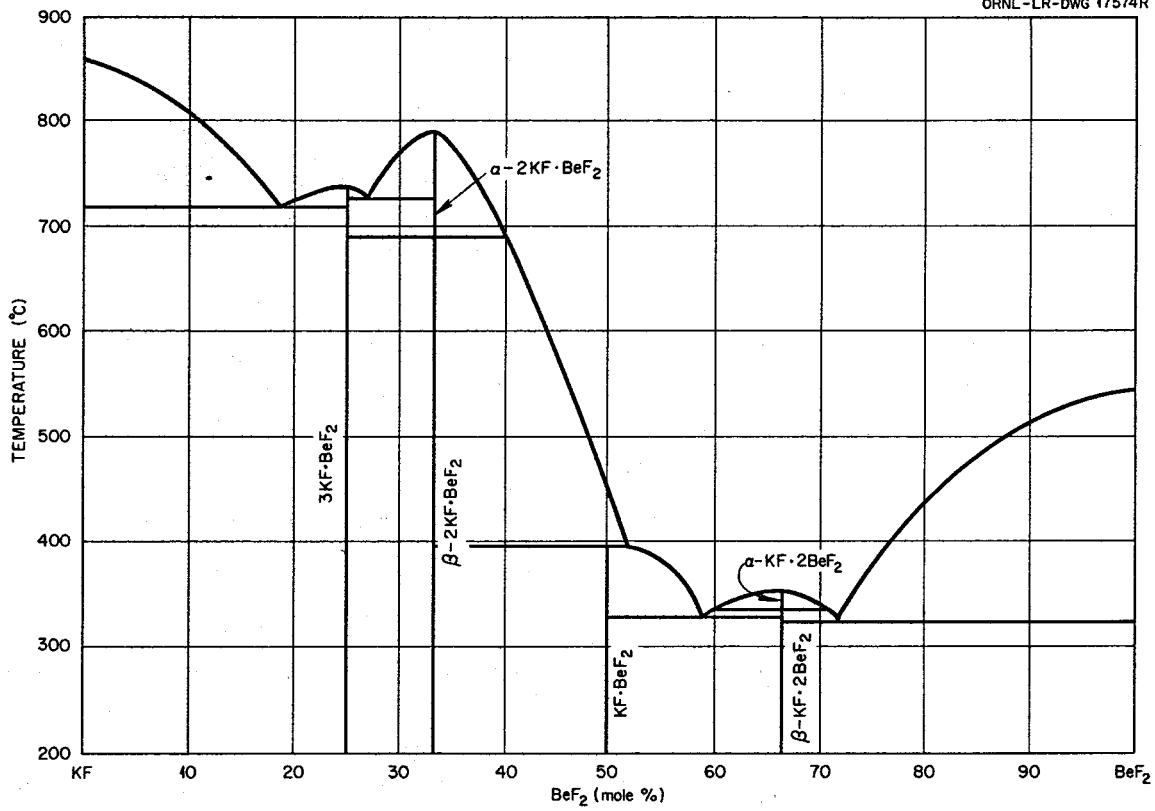
Fig. 3.21. The System KF–BeF$_2$.

3.22. The System RbF–BeF$_2$
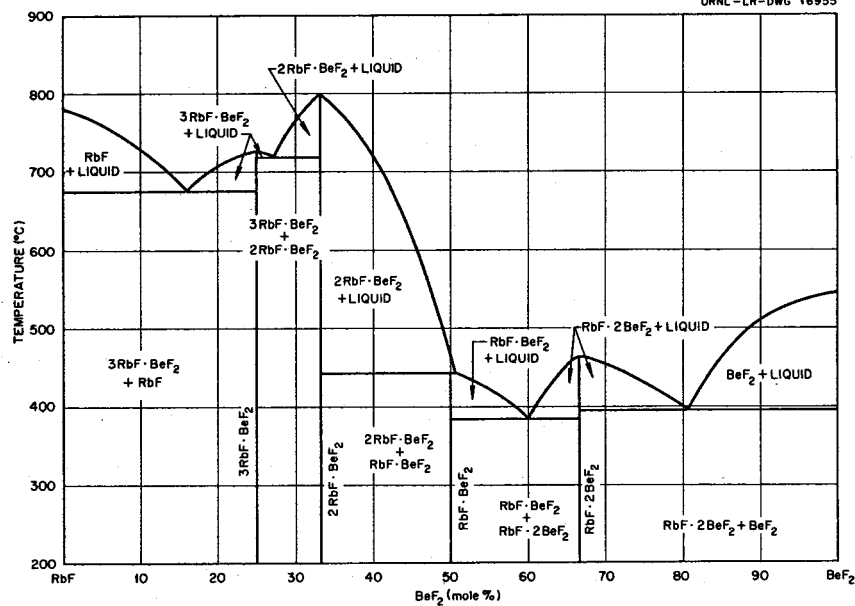
R. E. Moore, C. J. Barton, L. M. Bratcher, T. N. McVay, G. D. White, R. J. Sheil, W. R. Grimes, and R. E. Meadows, unpublished work performed at the Oak Ridge National Laboratory, 1955–56.

Preliminary diagram.

Invariant Equilibria

Mole % BeF$_2$ in Liquid	Invariant Temperature (°C)	Type of Equilibrium	Phase Reaction at Invariant Temperature
16	675	Eutectic	$L \rightleftharpoons RbF + 3RbF \cdot BeF_2$
25	725	Congruent melting point	$L \rightleftharpoons 3RbF \cdot BeF_2$
27	720	Eutectic	$L \rightleftharpoons 3RbF \cdot BeF_2 + 2RbF \cdot BeF_2$
33.3	800	Congruent melting point	$L \rightleftharpoons 2RbF \cdot BeF_2$
50.5	442	Peritectic	$L + 2RbF \cdot BeF_2 \rightleftharpoons RbF \cdot BeF_2$
61	383	Eutectic	$L \rightleftharpoons RbF \cdot BeF_2 + RbF \cdot 2BeF_2$
66.7	464	Congruent melting point	$L \rightleftharpoons RbF \cdot 2BeF_2$
81	397	Eutectic	$L \rightleftharpoons RbF \cdot 2BeF_2 + BeF_2$

This system has also been reported by R. G. Grebenshchikov, "Investigation of the Phase Diagram of the RbF–BeF$_2$ System and of Its Relationship to the BaO–SiO$_2$ System," *Doklady Akad. Nauk S.S.S.R.* **114,** 316 (1957).

Fig. 3.22. The System RbF—BeF$_2$.

3.23. The System CsF–BeF$_2$

O. N. Breusov, A. V. Novoselova, and Yu. P. Simanov, "Thermal and X-Ray Phase Analysis of the System CsF–BeF$_2$ and Its Interrelationships with MeF and BeF$_2$ Systems," *Doklady Akad. Nauk S.S.S.R.* **118**, 935–37 (1958).

Invariant Equilibria

Mole % BeF$_2$ in Liquid	Invariant Temperature (°C)	Type of Equilibrium	Phase Reaction at Invariant Temperature
14	598	Eutectic	$L \rightleftharpoons CsF + \beta\text{-}3CsF\cdot BeF_2$
23.5	659	Peritectic	$\alpha\text{-}2CsF\cdot BeF_2 + L \rightleftharpoons \alpha\text{-}3CsF\cdot BeF_2$
–	617	Inversion	$\alpha\text{-}3CsF\cdot BeF_2 \rightleftharpoons \beta\text{-}3CsF\cdot BeF_2$
33.3	793	Congruent melting point	$L \rightleftharpoons \alpha\text{-}2CsF\cdot BeF_2$
–	404	Inversion	$\alpha\text{-}2CsF\cdot BeF_2 \rightleftharpoons \beta\text{-}2CsF\cdot BeF_2$
48	449	Eutectic	$L \rightleftharpoons \alpha\text{-}2CsF\cdot BeF_2 + \alpha\text{-}CsF\cdot BeF_2$
50	475	Congruent melting point	$L \rightleftharpoons \alpha\text{-}CsF\cdot BeF_2$
–	360	Inversion	$\alpha\text{-}CsF\cdot BeF_2 \rightleftharpoons \beta\text{-}CsF\cdot BeF_2$
–	140	Inversion	$\beta\text{-}CsF\cdot BeF_2 \rightleftharpoons \gamma\text{-}CsF\cdot BeF_2$
58.4	393	Eutectic	$L \rightleftharpoons \alpha\text{-}CsF\cdot BeF_2 + \beta\text{-}CsF\cdot 2BeF_2$
66.7	480	Congruent melting point	$L \rightleftharpoons \alpha\text{-}CsF\cdot 2BeF_2$
–	450	Inversion	$\alpha\text{-}CsF\cdot 2BeF_2 \rightleftharpoons \beta\text{-}CsF\cdot 2BeF_2$
77.5	367	Eutectic	$L \rightleftharpoons \beta\text{-}CsF\cdot 2BeF_2 + BeF_2$
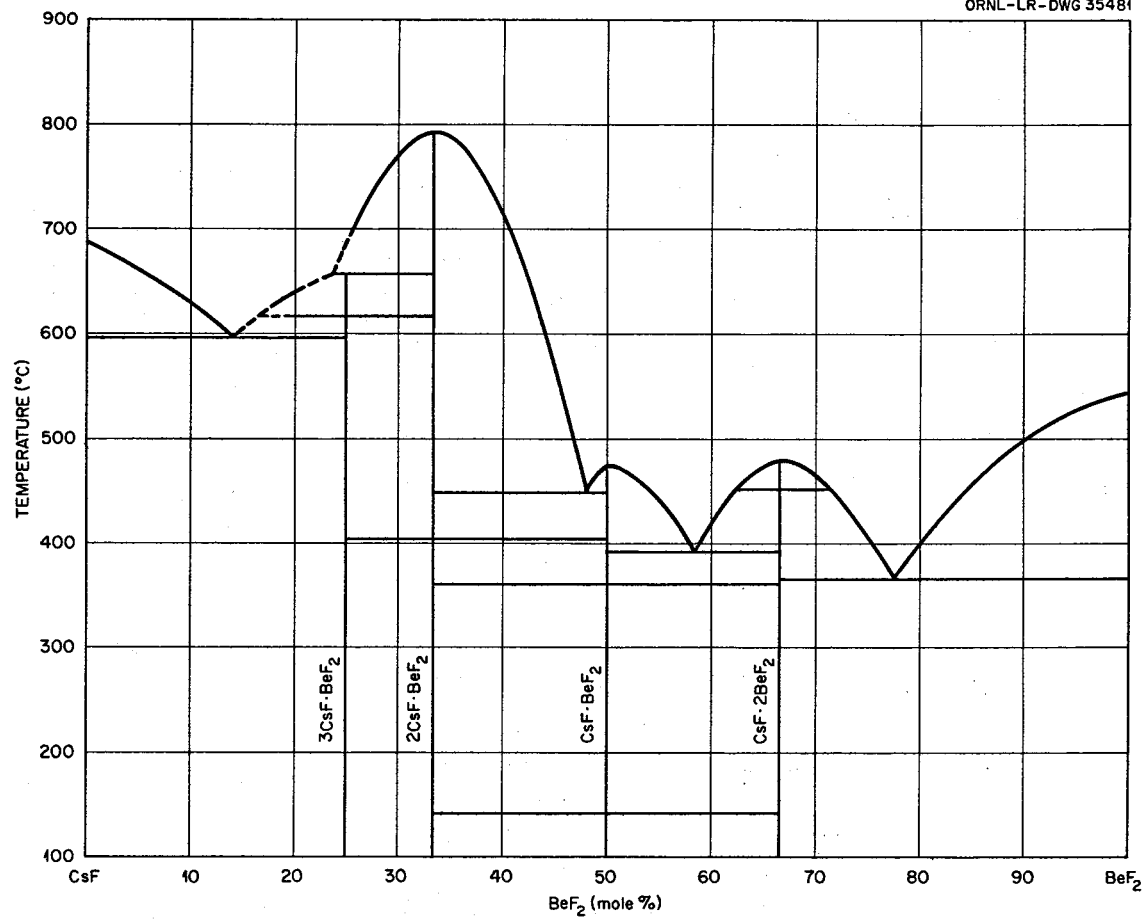
Fig. 3.23. The System CsF–BeF$_2$

3.24. The System LiF–NaF–BeF$_2$

R. E. Moore, C. J. Barton, W. R. Grimes, R. E. Meadows, L. M. Bratcher, G. D. White, T. N. McVay, and L. A. Harris, unpublished work performed at the Oak Ridge National Laboratory, 1951–58.

Preliminary diagram.

Invariant Equilibria*

Composition of Liquid (mole %)			Invariant Temperature (°C)	Type of Equilibrium	Solids Present at Invariant Point
LiF	NaF	BeF$_2$			
15	58	27	480	Eutectic	NaF, LiF, and 2NaF·BeF$_2$
23	41	36	328	Eutectic	LiF, 2NaF·BeF$_2$, and 2NaF·LiF·2BeF$_2$
20	40	40	355	Congruent melting point	2NaF·LiF·2BeF$_2$
5	53	42	318	Eutectic	NaF·BeF$_2$, 2NaF·BeF$_2$, and 2NaF·LiF·2BeF$_2$
31.5	31	37.5	315	Eutectic	2LiF·BeF$_2$, LiF, and 2NaF·LiF·2BeF$_2$

*Invariant equilibria shown in the phase diagram by the intersections of dotted-line boundary curves have not been determined with sufficient precision to be listed in the table.

Minimum Temperature on Alkemade Lines

Composition of Liquid (mole %)			Temperature (°C)	Alkemade Line
LiF	NaF	BeF$_2$		
16	56	28	485	2NaF·BeF$_2$–LiF
26	37	37	340	2NaF·LiF·2BeF$_2$–LiF
11	44	45	332	NaF·BeF$_2$–2NaF·LiF·2BeF$_2$
16	45	39	343	2NaF·BeF$_2$–2NaF·LiF·2BeF$_2$
30.5	31	38.5	316	2LiF·BeF$_2$–2NaF·LiF·2BeF$_2$

Phase relationships of two of the ternary compounds in this system have been reported by W. Jahn ["Silicate Models. V. NaLi(BeF$_4$), a Model Substance for Monticellite, CaMg(SiO$_4$);" Z. anorg. u. allgem. Chem. **276**, 113–27 (1954); "Silicate Models. VI. Na$_3$Li(BeF$_4$)$_2$, a New Compound in the Ternary System NaF–LiF–BeF$_2$, and Its Relation to Merwinite, Ca$_3$Mg(SiO$_4$)$_2$," Z. anorg. u. allgem. Chem. **277**, 274–86 (1954)].
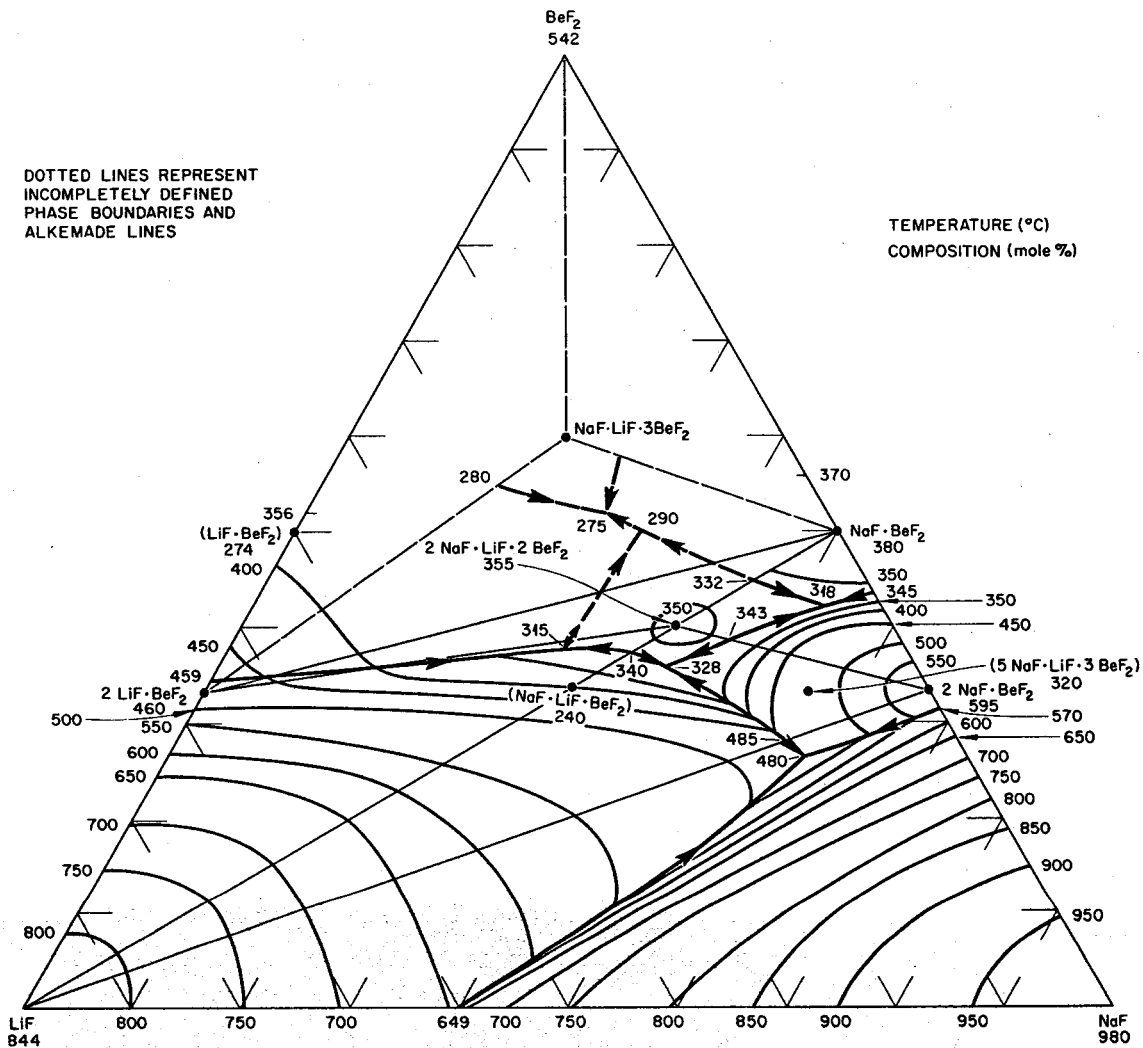
Fig. 3.24. The System LiF–NaF–BeF$_2$

43

3.25. The System LiF–RbF–BeF$_2$

T. B. Rhinehammer, D. E. Etter, C. R. Hudgens, N. E. Rogers, and P. A. Tucker, unpublished work performed at the Mound Laboratory.

Preliminary diagram.

Invariant Equilibria and Singular Points

Composition of Liquid (mole %)			Temperature (°C)	Type of Equilibrium	Solid Phases Present
LiF	RbF	BeF$_2$			
40.0	20.0	40.0	485 ± 5	Congruent melting point	2LiF·RbF·2BeF$_2$
33.3	33.3	33.3	544 ± 5	Incongruent melting point of LiF·RbF·BeF$_2$	
33.0	8.0	59.0	295 ± 5	Eutectic	2LiF·BeF$_2$, 2LiF·RbF·2BeF$_2$, and BeF$_2$
26.0	12.0	62.0	305–320	Peritectic	2LiF·RbF·2BeF$_2$, RbF·2BeF$_2$, and BeF$_2$
12.0	29.0	59.0	334 ± 5	Quasi-binary eutectic	2LiF·RbF·2BeF$_2$ and RbF·2BeF$_2$
11.0	34.0	55.0	300 ± 5	Eutectic	2LiF·RbF·2BeF$_2$, RbF·BeF$_2$, and RbF·2BeF$_2$
11.5	35.5	53.0	335 ± 5	Peritectic	2LiF·RbF·2BeF$_2$, LiF·RbF·BeF$_2$, and RbF·BeF$_2$
9.0	40.0	51.0	380 ± 5	Peritectic	LiF·RbF·BeF$_2$, 2RbF·BeF$_2$, and RbF·BeF$_2$
50.0	8.0	42.0	426 ± 5	Peritectic	LiF, 2LiF·RbF·2BeF$_2$, and 2LiF·BeF$_2$
41.5	19.5	39.0	473 ± 5	Quasi-binary eutectic	LiF and 2LiF·RbF·2BeF$_2$
35.0	25.5	39.5	470 ± 5	Peritectic	LiF, 2LiF·RbF·2BeF$_2$, and LiF·RbF·BeF$_2$
23.0	40.0	37.0	530 ± 5	Peritectic	LiF, 2RbF·BeF$_2$, and LiF·RbF·BeF$_2$
30.0	35.0	35.0	544 ± 5	Maximum on the boundary	LiF and LiF·RbF·BeF$_2$
41.0	39.5	19.5	640 ± 5	Quasi-binary eutectic	LiF and 2RbF·BeF$_2$
43.0	50.0	7.0	527 ± 5	Peritectic	LiF, 3RbF·BeF$_2$, and 2RbF·BeF$_2$
43.0	54.0	3.0	470 ± 5	Peritectic	LiF, LiF·RbF, and 3RbF·BeF$_2$
43.0	55.0	2.0	462 ± 5	Eutectic	LiF·RbF, RbF, and 3RbF·BeF$_2$
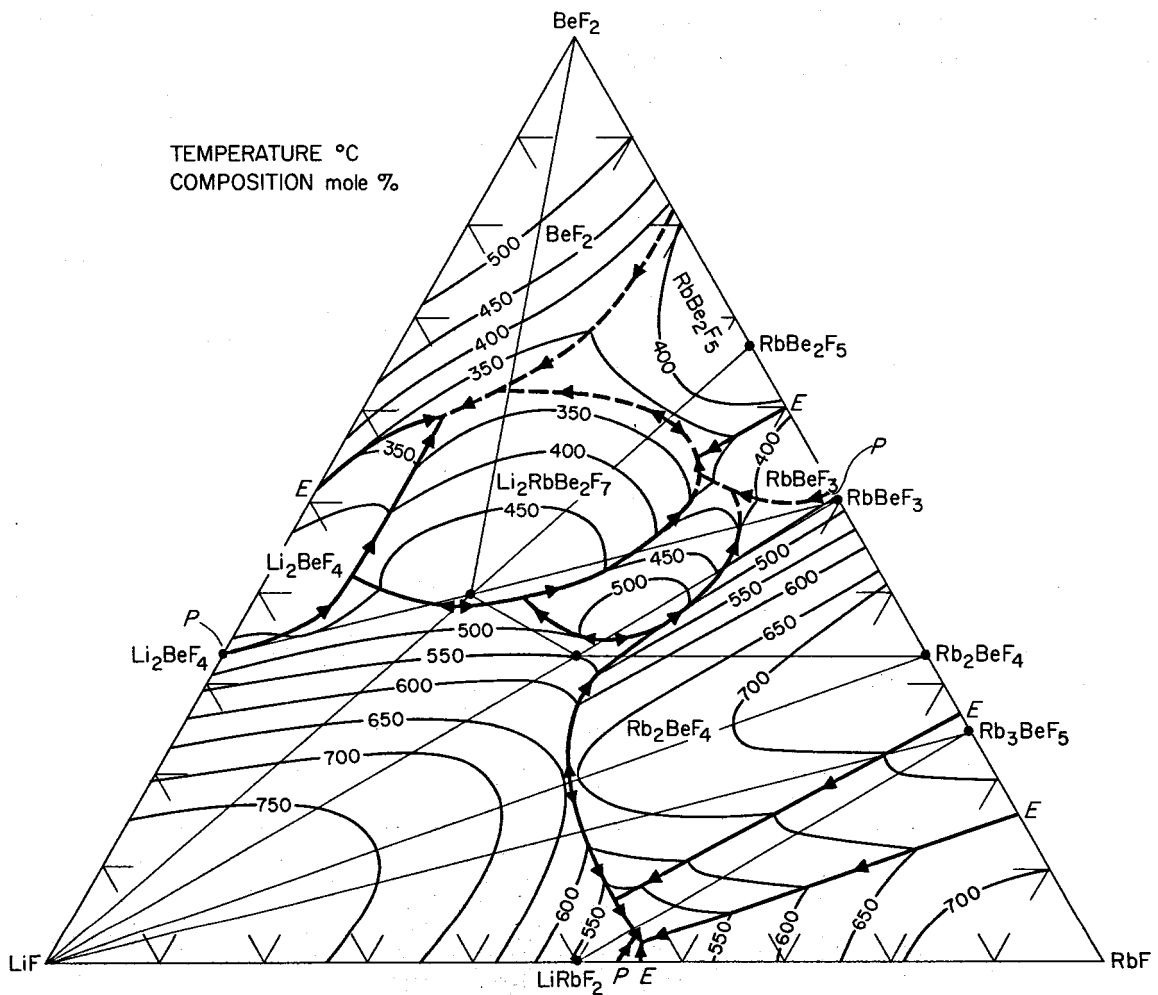
Fig. 3.25. The System LiF–RbF–BeF₂.

3.26. The System NaF–KF–BeF$_2$

R. E. Moore, C. J. Barton, L. M. Bratcher, T. N. McVay, and W. R. Grimes, unpublished work performed at the Oak Ridge National Laboratory, 1952–55.

Preliminary diagram. Phase relationships within the system NaF–KF–BeF$_2$ have not yet become so well defined at the Oak Ridge National Laboratory that the compositions and temperatures of the invariant points may be listed.
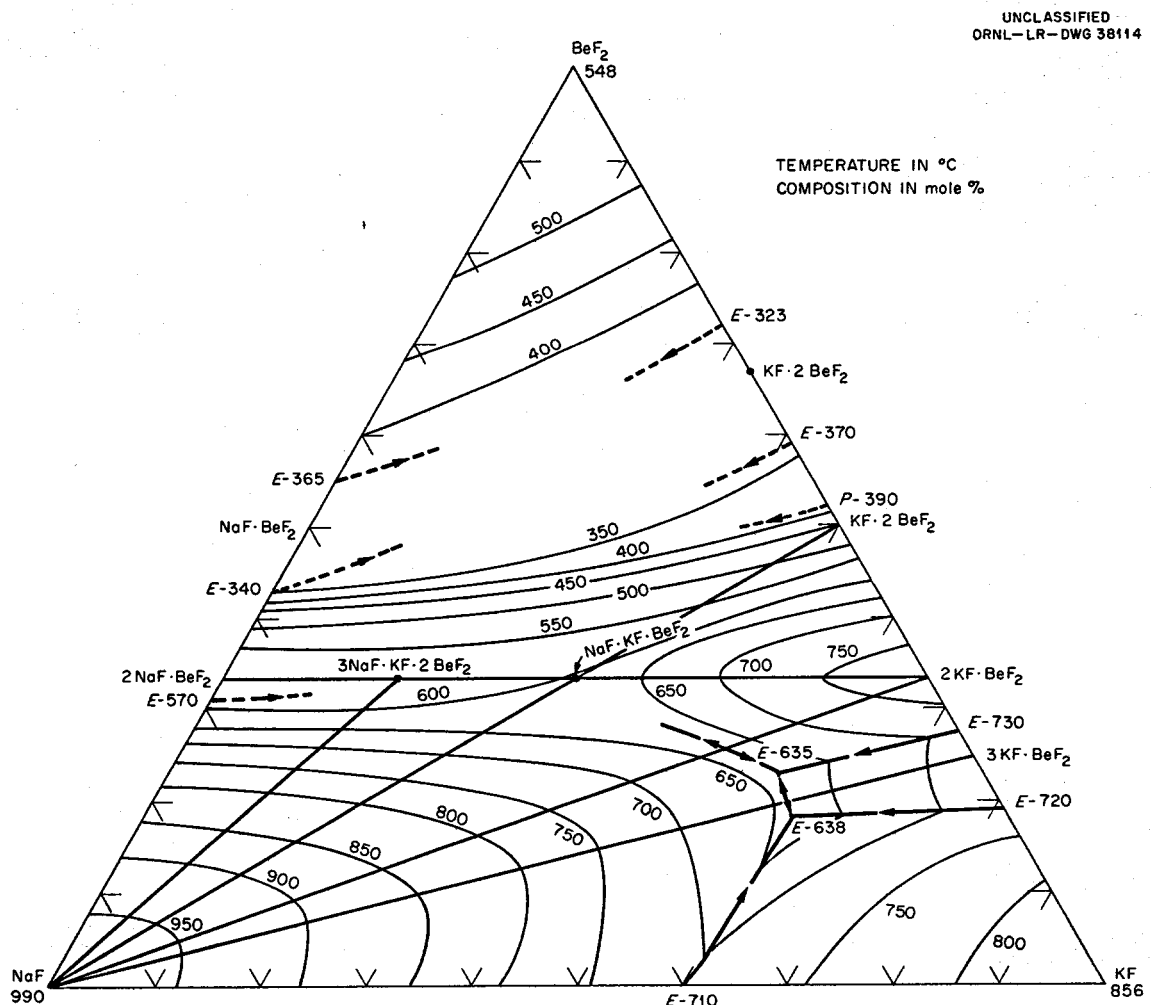
Fig. 3.26. The System NaF–KF–BeF$_2$.

3.27. The System NaF-RbF-BeF$_2$

R. E. Moore, C. J. Barton, L. M. Bratcher, and W. R. Grimes, unpublished work performed at the Oak Ridge National Laboratory, 1954-57.

Preliminary diagram.

Invariant Equilibria and Singular Points

Composition of Liquid (mole %)			Temperature (°C)	Type of Equilibrium	Solids Present at Invariant Temperature
NaF	RbF	BeF$_2$			
20.5	68.5	11.0	610	Eutectic	RbF, NaF, and 3RbF·BeF$_2$
50	37.5	12.5	640	Quasi-binary eutectic	3RbF·BeF$_2$ and NaF
46	38	16	635	Eutectic	3RbF·BeF$_2$, 2RbF·BeF$_2$, and NaF
45	37	18	650	Quasi-binary eutectic	2RbF·BeF$_2$ and NaF
37	33	30	570	Peritectic	2RbF·BeF$_2$, NaF, and 2NaF·4RbF·3BeF$_2$
52	15	33	477	Eutectic	2NaF·4RbF·3BeF$_2$, NaF, and 2NaF·BeF$_2$
33	33.7	33.3	580	Peritectic	2RbF·BeF$_2$ and 2NaF·4RbF·3BeF$_2$
51.7	15	33.3	480	Quasi-binary eutectic	2NaF·4RbF·3BeF$_2$ and 2NaF·BeF$_2$

UNCLASSIFIED
ORNL-LR-DWG 22343R2

BE BINARY EUTECTIC
BP BINARY PERITECTIC
CM CONGRUENT MELTING POINT
IM INCONGRUENT MELTING POINT
TE TERNARY EUTECTIC
TP TERNARY PERITECTIC
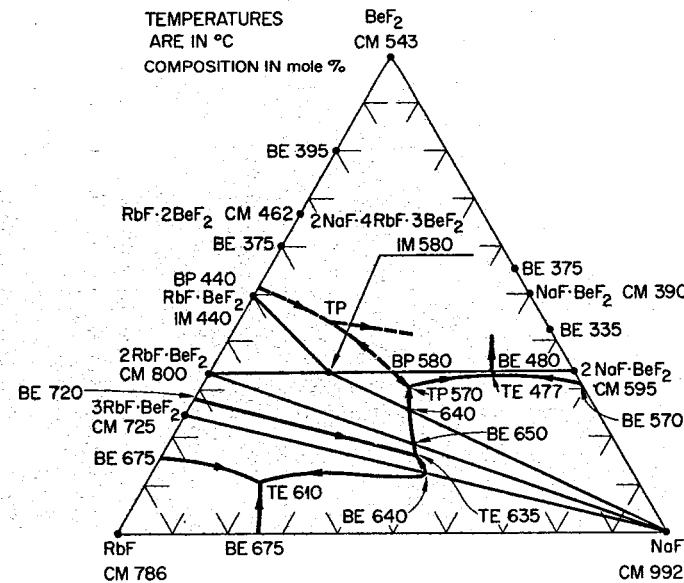
Fig. 3.27. The System NaF-RbF-BeF$_2$.

3.28. The System NaF–ZnF$_2$

C. J. Barton, L. M. Bratcher, and W. R. Grimes, unpublished work performed at the Oak Ridge National Laboratory, 1952.

Preliminary diagram.

Invariant Equilibria

Mole % ZnF$_2$ in Liquid	Invariant Temperature (°C)	Type of Equilibrium	Phase Reaction at Invariant Temperature
33	635	Eutectic	$L \rightleftharpoons NaF + NaF \cdot ZnF_2$
50	748 ± 10	Congruent melting point	$L \rightleftharpoons NaF \cdot ZnF_2$
69	685	Eutectic	$L \rightleftharpoons NaF \cdot ZnF_2 + ZnF_2$

UNCLASSIFIED
DWG 14627 R
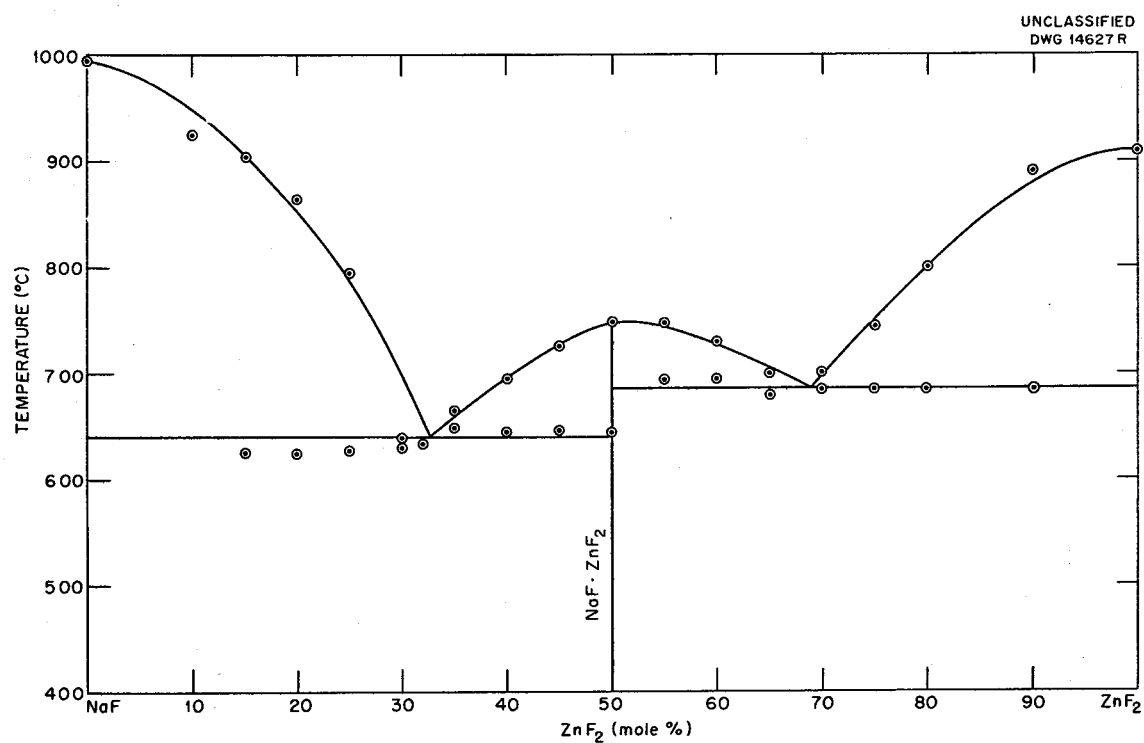
Fig. 3.28. The System NaF–ZnF$_2$.

48

3.29. The System KF–ZnF$_2$

C. J. Barton, L. M. Bratcher, and W. R. Grimes, unpublished work performed at the Oak Ridge National Laboratory, 1952.

Preliminary diagram.

Invariant Equilibria

Mole % ZnF$_2$ in Liquid	Invariant Temperature (°C)	Type of Equilibrium	Phase Reaction at Invariant Temperature
21	670	Eutectic	$L \rightleftharpoons KF + 2KF \cdot ZnF_2$
30	720 ± 10	Peritectic	$L + KF \cdot ZnF_2 \rightleftharpoons 2KF \cdot ZnF_2$
50	850 ± 10	Congruent melting point	$L \rightleftharpoons KF \cdot ZnF_2$
80	740 ± 5	Eutectic	$L \rightleftharpoons KF \cdot ZnF_2 + ZnF_2$
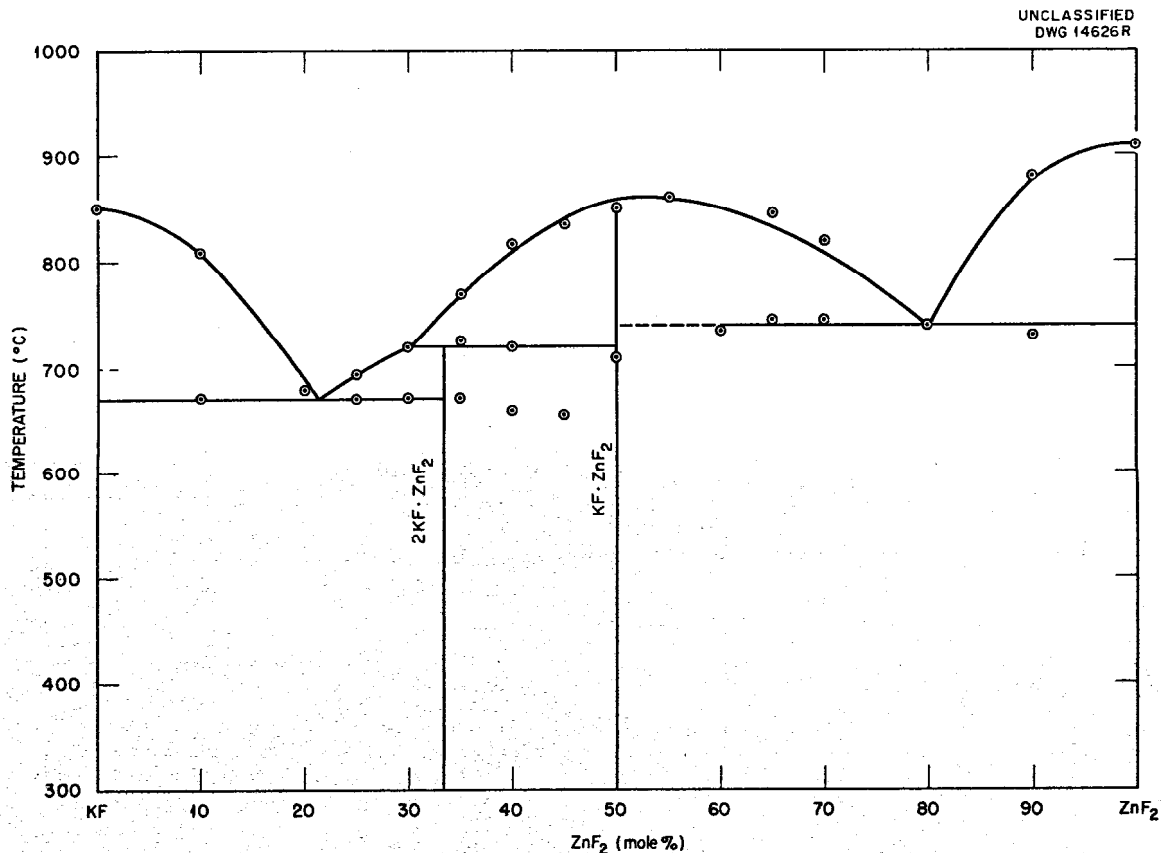
Fig. 3.29. The System KF–ZnF$_2$.

3.30. The System RbF–ZnF$_2$

C. J. Barton, L. M. Bratcher, and W. R. Grimes, unpublished work performed at the Oak Ridge National Laboratory, 1952.

Preliminary diagram.

Invariant Equilibria

Mole % ZnF$_2$ in Liquid	Invariant Temperature (°C)	Type of Equilibrium	Phase Reaction at Invariant Temperature
21	595 ± 10	Eutectic	$L \rightleftharpoons RbF + 2RbF \cdot ZnF_2$
32	620 ± 10	Peritectic	$L + RbF \cdot ZnF_2 \rightleftharpoons 2RbF \cdot ZnF_2$
50	730 ± 10	Congruent melting point	$L \rightleftharpoons RbF \cdot ZnF_2$
70	650	Eutectic	$L \rightleftharpoons RbF \cdot ZnF_2 + ZnF_2$
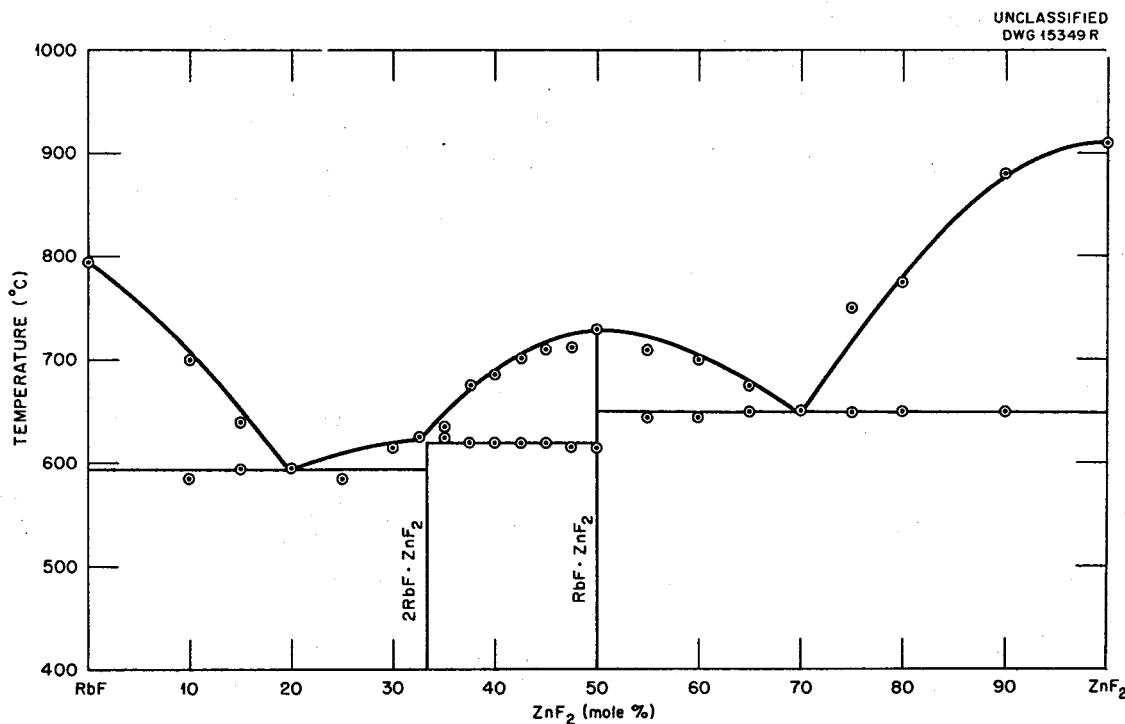
Fig. 3.30. The System RbF–ZnF$_2$

3.31. The System LiF–YF₃

R. E. Thoma, C. F. Weaver, and H. A. Friedman, unpublished work performed at the Oak Ridge National Laboratory, 1958–59.

Preliminary diagram.

Invariant Equilibria

Mole % YF_3 in Liquid	Invariant Temperature (°C)	Type of Equilibrium	Phase Reaction at Invariant Temperature
19	695	Eutectic	$L \rightleftharpoons LiF + LiF \cdot YF_3$
49	815	Peritectic	$L + YF_3 \rightleftharpoons LiF \cdot YF_3$
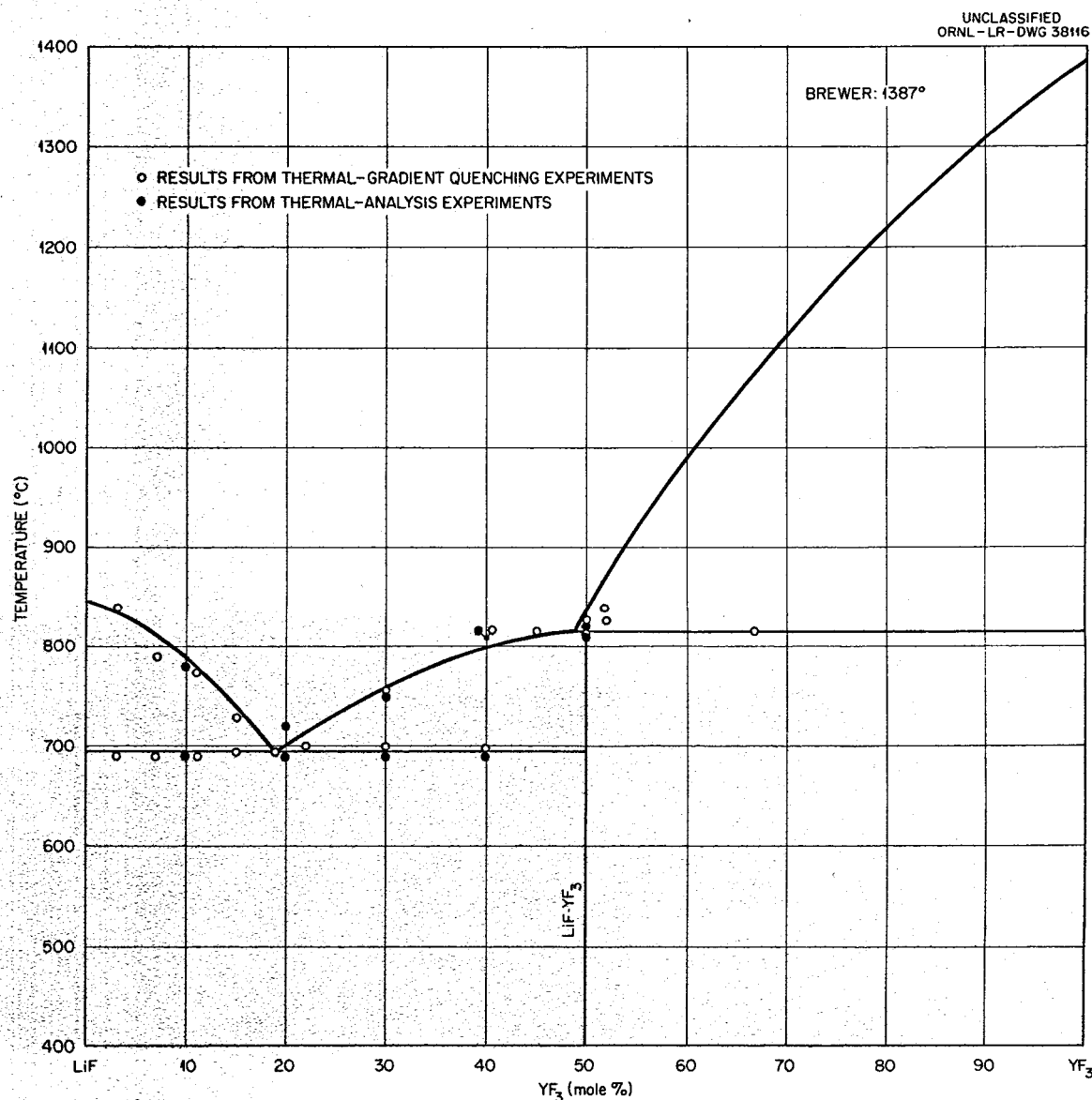
Fig. 3.31. The System LiF–YF₃.

3.32. The System LiF–ZrF$_4$

R. E. Moore, F. F. Blankenship, W. R. Grimes, H. A. Friedman, C. J. Barton, R. E. Thoma, and H. Insley, unpublished work performed at the Oak Ridge National Laboratory, 1951–56. Preliminary diagram.

Invariant Equilibria

Mole % ZrF$_4$ in Liquid	Invariant Temperature (°C)	Type of Equilibrium	Phase Reaction at Invariant Temperature
21	598	Eutectic	$L \rightleftharpoons \text{LiF} + \alpha\text{-3LiF·ZrF}_4$
25	662	Congruent melting point	$L \rightleftharpoons \alpha\text{-3LiF·ZrF}_4$
–	475	Inversion	$\alpha\text{-3LiF·ZrF}_4 \rightleftharpoons \beta\text{-3LiF·ZrF}_4$
–	470	Decomposition	$\beta\text{-3LiF·ZrF}_4 \rightleftharpoons \text{LiF} + 2\text{LiF·ZrF}_4$
29.5	570	Eutectic	$L \rightleftharpoons \alpha\text{-3LiF·ZrF}_4 + 2\text{LiF·ZrF}_4$
33.3	596	Congruent melting point	$L \rightleftharpoons 2\text{LiF·ZrF}_4$
49	507	Eutectic	$L \rightleftharpoons 2\text{LiF·ZrF}_4 + 3\text{LiF·4ZrF}_4$
51.5	520	Peritectic	$L + \text{ZrF}_4 \rightleftharpoons 3\text{LiF·4ZrF}_4$
–	466	Decomposition	$3\text{LiF·4ZrF}_4 \rightleftharpoons 2\text{LiF·ZrF}_4 + \text{ZrF}_4$
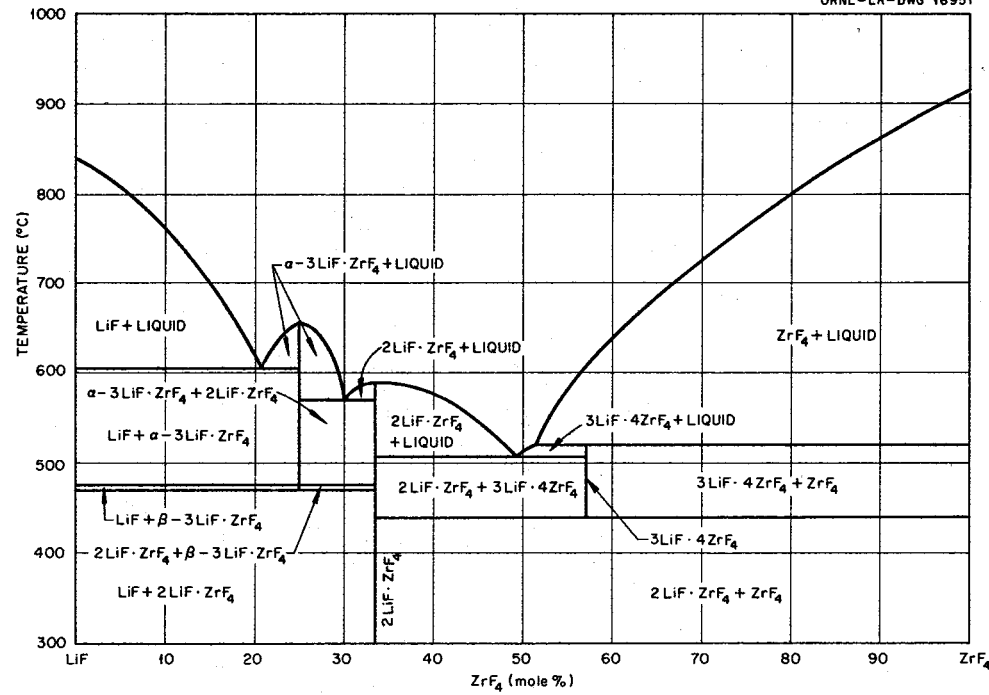
Fig. 3.32. The System LiF–ZrF$_4$.

3.33. The System NaF–ZrF$_4$

C. J. Barton, W. R. Grimes, H. Insley, R. E. Moore, and R. E. Thoma, "Phase Equilibria in the Systems NaF–ZrF$_4$, UF$_4$–ZrF$_4$, and NaF–ZrF$_4$–UF$_4$," *J. Phys. Chem.* **62**, 665–76 (1958).

Invariant Equilibria

Mole % ZrF$_4$ in Liquid	Invariant Temperature (°C)	Type of Equilibrium	Phase Reaction at Invariant Temperature
20	747	Eutectic	$L \rightleftharpoons NaF + 3NaF \cdot ZrF_4$
25	850	Congruent melting point	$L \rightleftharpoons 3NaF \cdot ZrF_4$*
–	523	Inversion	$\alpha\text{-}5NaF \cdot 2ZrF_4 \rightleftharpoons \beta\text{-}5NaF \cdot 2ZrF_4$
30.5	500	Eutectoid	$\alpha\text{-}5NaF \cdot 2ZrF_4 ss \rightleftharpoons \beta\text{-}5NaF \cdot 2ZrF_4 + \gamma\text{-}2NaF \cdot ZrF_4$
34	640	Peritectic	$L + 3NaF \cdot ZrF_4 (ss, ca.\ 27.5\ mole\ \%\ ZrF_4) \rightleftharpoons \alpha\text{-}5NaF \cdot 2ZrF_4$
39.5	544	Peritectic	$L + \alpha\text{-}5NaF \cdot 2ZrF_4 (ss, 30\ mole\ \%\ ZrF_4) \rightleftharpoons \alpha\text{-}2NaF \cdot ZrF_4$
–	533	Inversion	$\alpha\text{-}2NaF \cdot ZrF_4 \rightleftharpoons \beta\text{-}2NaF \cdot ZrF_4$
–	505	Inversion	$\beta\text{-}2NaF \cdot ZrF_4 \rightleftharpoons \gamma\text{-}2NaF \cdot ZrF_4$
40.5	500	Eutectic	$L \rightleftharpoons \gamma\text{-}2NaF \cdot ZrF_4 + 7NaF \cdot 6ZrF_4 ss$
46.2	525	Congruent melting point	$L \rightleftharpoons 7NaF \cdot 6ZrF_4$
49.5	512	Eutectic	$L \rightleftharpoons 7NaF \cdot 6ZrF_4 + 3NaF \cdot 4ZrF_4$
56.5	537	Peritectic	$L + ZrF_4 \rightleftharpoons 3NaF \cdot 4ZrF_4$

*A determination of the crystal structure of 3NaF·ZrF$_4$ has been reported by L. A. Harris, "The Crystal Structures of Na$_3$ZrF$_7$ and Na$_3$HfF$_7$," *Acta Cryst.* **12**, 172 (1959).
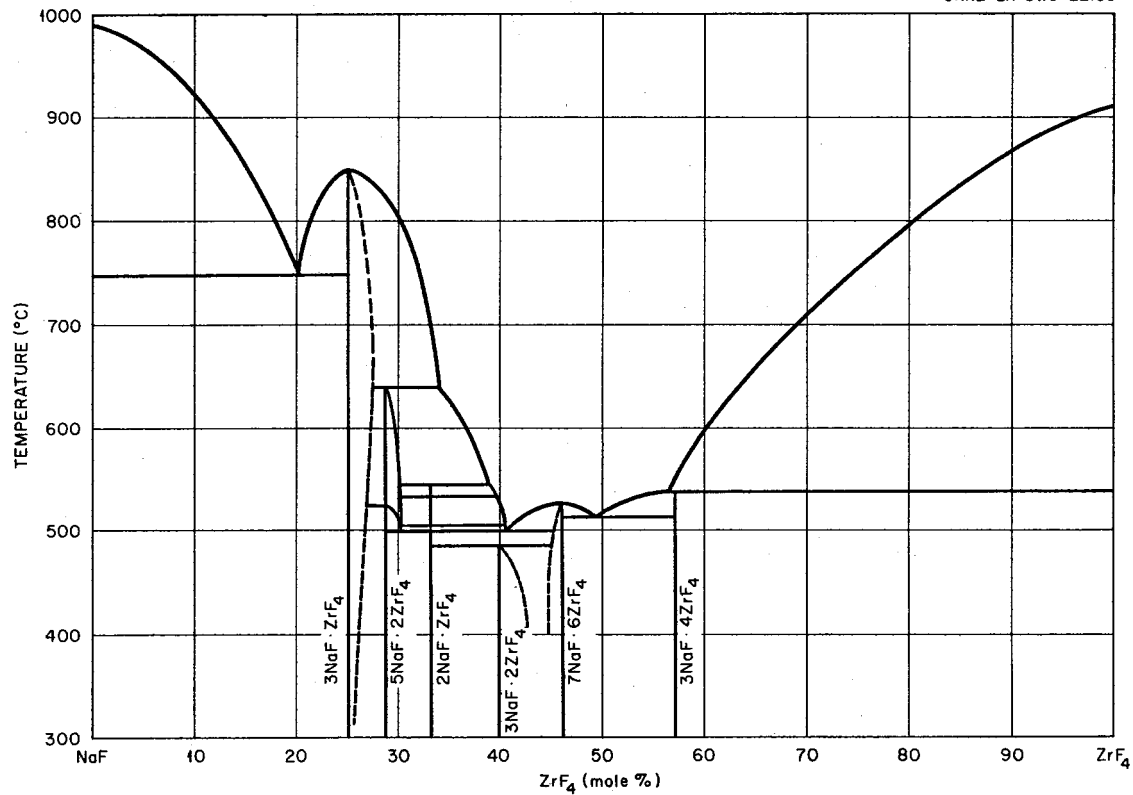
Fig. 3.33. The System NaF-ZrF₄.

3.34. The System KF–ZrF$_4$

C. J. Barton, H. Insley, R. P. Metcalf, R. E. Thoma, and W. R. Grimes, unpublished work performed at the Oak Ridge National Laboratory, 1951–55.

Preliminary diagram.

Invariant Equilibria

Mole % ZrF$_4$ in Liquid	Invariant Temperature (°C)	Type of Equilibrium	Phase Reaction at Invariant Temperature
14	765	Eutectic	$L \rightleftharpoons KF + 3KF \cdot ZrF_4$
25	910	Congruent melting point	$L \rightleftharpoons 3KF \cdot ZrF_4$
36	590	Peritectic	$3KF \cdot ZrF_4 + L \rightleftharpoons 2KF \cdot ZrF_4$
40.5	412	Peritectic	$2KF \cdot ZrF_4 + L \rightleftharpoons 3KF \cdot 2ZrF_4$
42	390	Eutectic	$L \rightleftharpoons 3KF \cdot 2ZrF_4 + KF \cdot ZrF_4$
50	475	Congruent melting point	$L \rightleftharpoons KF \cdot ZrF_4$
55	440	Eutectic	$L \rightleftharpoons KF \cdot ZrF_4 + ZrF_4$

UNCLASSIFIED
ORNL–LR–DWG 18965
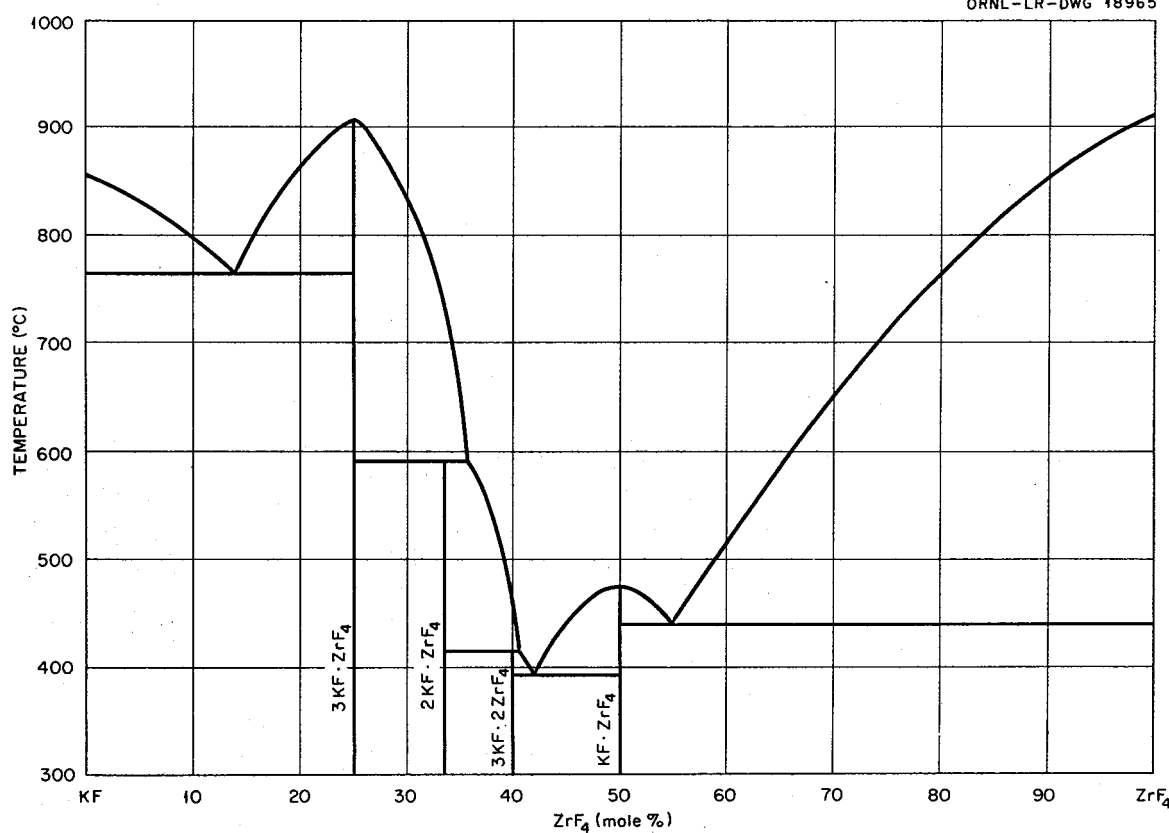
Fig. 3.34. The System KF–ZrF$_4$.

3.35. The System RbF–ZrF$_4$

R. E. Moore, R. E. Thoma, C. J. Barton, W. R. Grimes, H. Insley, B. S. Landau, and H. A. Friedman, unpublished work performed at the Oak Ridge National Laboratory, 1955–56.

Preliminary diagram.

Invariant Equilibria

Mole % ZrF$_4$ in Liquid	Invariant Temperature (°C)	Type of Equilibrium	Phase Reaction at Invariant Temperature
10	710	Eutectic	$L \rightleftharpoons RbF + 3RbF \cdot ZrF_4$
25	897	Congruent melting point	$L \rightleftharpoons 3RbF \cdot ZrF_4$
34	620	Peritectic	$L + 3RbF \cdot ZrF_4 ss \rightleftharpoons \alpha\text{-}2RbF \cdot ZrF_4$
–	460	Inversion	$\alpha\text{-}2RbF \cdot ZrF_4 \rightleftharpoons \beta\text{-}2RbF \cdot ZrF_4$
–	370	Lowered inversion and decomposition	$\alpha\text{-}2RbF \cdot ZrF_4 ss \rightleftharpoons \beta\text{-}2RbF \cdot ZrF_4 ss$
42	410	Eutectic	$L \rightleftharpoons \alpha\text{-}2RbF \cdot ZrF_4 ss + 5RbF \cdot 4ZrF_4$
44.4	445	Congruent melting point	$L \rightleftharpoons 5RbF \cdot 4ZrF_4$
48	390	Eutectic	$L \rightleftharpoons 5RbF \cdot 4ZrF_4 + \beta\text{-}RbF \cdot ZrF_4$
50	423	Congruent melting point	$L \rightleftharpoons \alpha\text{-}RbF \cdot ZrF_4$
–	391	Inversion	$\alpha\text{-}RbF \cdot ZrF_4 \rightleftharpoons \beta\text{-}RbF \cdot ZrF_4$
54	400	Eutectic	$L \rightleftharpoons \alpha\text{-}RbF \cdot ZrF_4 + RbF \cdot 2ZrF_4$
57	447	Peritectic	$L + ZrF_4 \rightleftharpoons RbF \cdot 2ZrF_4$
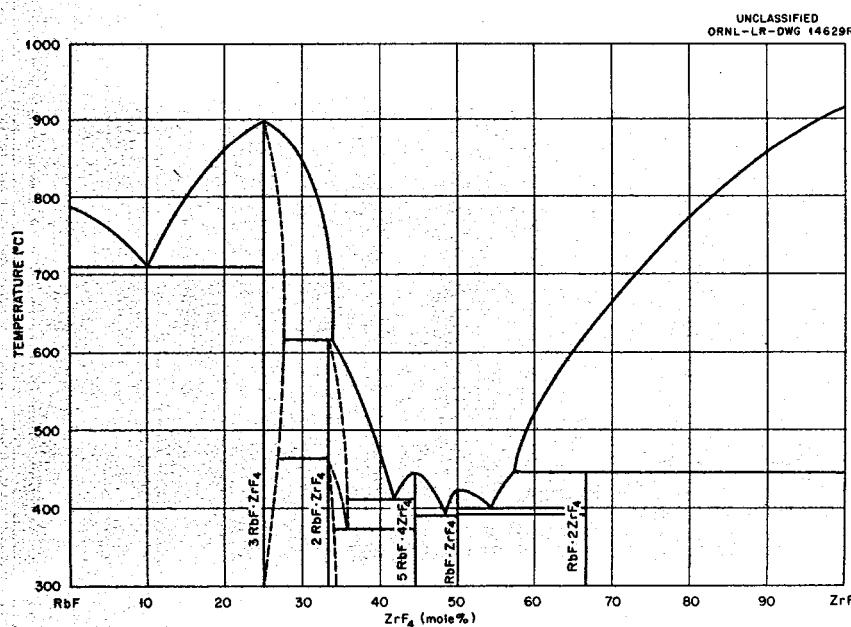
Fig. 3.35. The System RbF–ZrF$_4$.

3.36. The System $CsF-ZrF_4$

C. J. Barton, L. M. Bratcher, and W. R. Grimes, unpublished work performed at the Oak Ridge National Laboratory, 1952–53.

Preliminary diagram.

Invariant Equilibria

Mole % ZrF_4 in Liquid	Invariant Temperature (°C)	Type of Equilibrium	Phase Reaction at Invariant Temperature
9	640	Eutectic	$L \rightleftharpoons CsF + 3CsF \cdot ZrF_4$
25	775	Congruent melting point	$L \rightleftharpoons 3CsF \cdot ZrF_4$
35	520	Peritectic	$L + 3CsF \cdot ZrF_4 \rightleftharpoons 2CsF \cdot ZrF_4$
40	420	Eutectic	$L \rightleftharpoons 2CsF \cdot ZrF_4 + \alpha\text{-}CsF \cdot ZrF_4$
50	515	Congruent melting point	$L \rightleftharpoons \alpha\text{-}CsF \cdot ZrF_4$
–	320	Inversion	$\alpha\text{-}CsF \cdot ZrF_4 \rightleftharpoons \beta\text{-}CsF \cdot ZrF_4$
59	470	Eutectic	$L \rightleftharpoons \alpha\text{-}CsF \cdot ZrF_4 + ZrF_4$

Fig. 3.36. The System CsF–ZrF$_4$.

3.37. The System LiF–NaF–ZrF$_4$

F. F. Blankenship, H. A. Friedman, H. Insley, R. E. Thoma, and W. R. Grimes, unpublished work performed at the Oak Ridge National Laboratory, 1953–59.

Preliminary diagram.

Invariant Equilibria

Composition of Liquid (mole %)			Temperature (°C)	Type of Invariant	Solids Present at Invariant Temperature
LiF	NaF	ZrF$_4$			
37	52	11	604	Eutectic	NaF, LiF, and 3NaF·ZrF$_4$
55	22	23	590	Eutectic	α-3LiF·ZrF$_4$, 3NaF·ZrF$_4$ss, and LiF
32	36	32	450	Peritectic	β-3LiF·ZrF$_4$, 3NaF·ZrF$_4$ss, and 2LiF·ZrF$_4$
31	35	34	448	Peritectic	3NaF·ZrF$_4$, α-5NaF·2ZrF$_4$ss, and 2LiF·ZrF$_4$
31	34.5	34.5	445	Peritectic	2NaF·ZrF$_4$, α-5NaF·2ZrF$_4$ss, and 2LiF·ZrF$_4$
26	37	37	425	Eutectic	2NaF·ZrF$_4$, 7NaF·6ZrF$_4$, and 2LiF·ZrF$_4$
29	25.5	45.5	449	Eutectic	7NaF·6ZrF$_4$, 3NaF·4ZrF$_4$ss, and 2LiF·ZrF$_4$
29	24.5	46.5	453	Peritectic	3NaF·4ZrF$_4$ss, 3LiF·4ZrF$_4$ss, and 2LiF·ZrF$_4$
28	24	48	475	Peritectic	3NaF·4ZrF$_4$ss, 3LiF·4ZrF$_4$ss, and ZrF$_4$
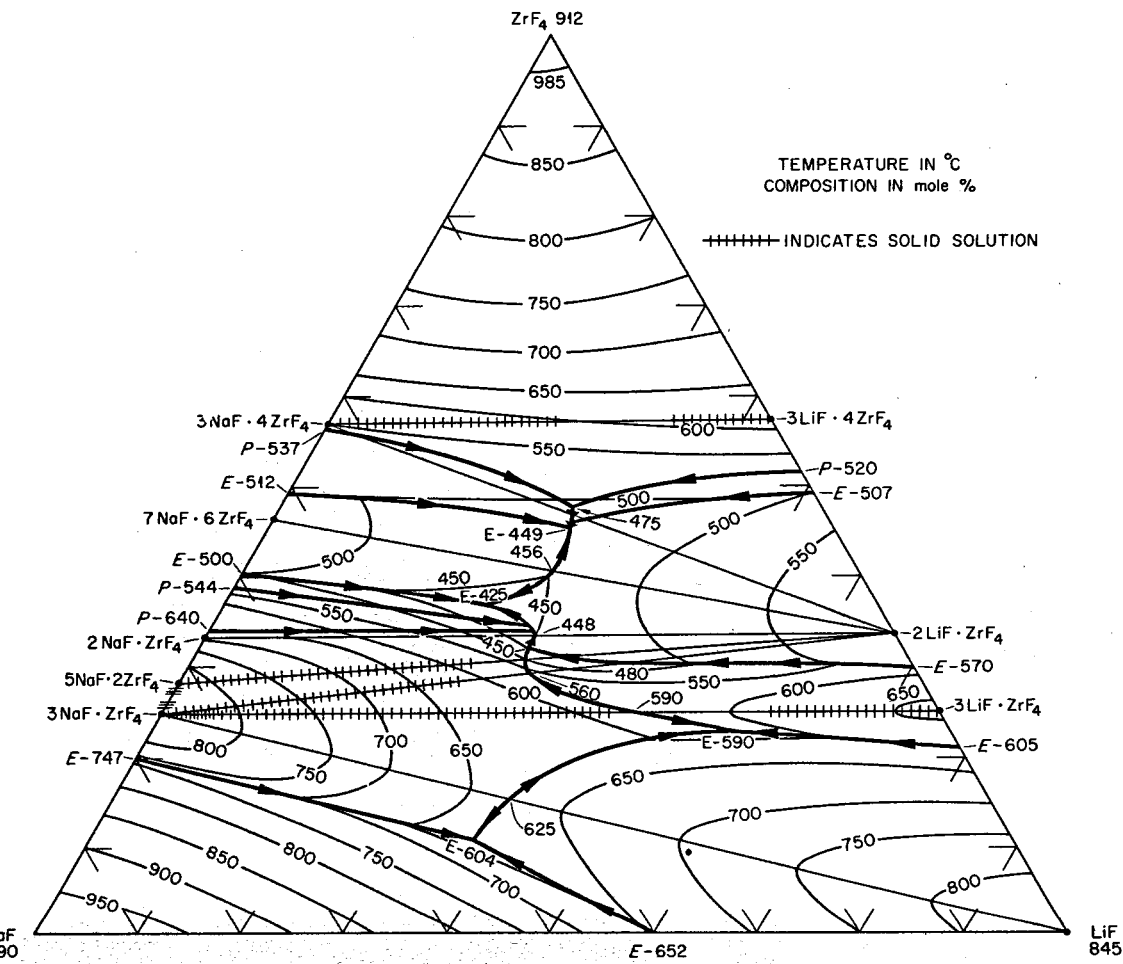
Fig. 3.37. The System LiF–NaF–ZrF₄.

3.38. The System NaF-KF-ZrF$_4$

R. E. Thoma, C. J. Barton, H. Insley, H. A. Friedman, and W. R. Grimes, unpublished work performed at the Oak Ridge National Laboratory, 1951–55.

Preliminary diagram.

Invariant Equilibria*

Composition of Liquid (mole %)**			Invariant Temperature (°C)	Type of Equilibrium	Solids Present at Invariant Point
NaF	KF	ZrF$_4$			
34	58	8	695	Eutectic	NaF, KF, and 3KF·ZrF$_4$
45	38	17	720	Eutectic	NaF, 3KF·ZrF$_4$, and 3NaF·3KF·2ZrF$_4$
61	19	20	710	Eutectic	NaF, 3NaF·ZrF$_4$, and 3NaF·3KF·2ZrF$_4$
52	17	31		Peritectic	3NaF·ZrF$_4$, 3NaF·3KF·2ZrF$_4$, and NaF·KF·ZrF$_4$
48	18	34		Peritectic	3NaF·ZrF$_4$, NaF·KF·ZrF$_4$, and 5NaF·2ZrF$_4$
33	32	35		Peritectic	3NaF·3KF·2ZrF$_4$, 3KF·ZrF$_4$, and NaF·KF·ZrF$_4$
12	51	37		Peritectic	3KF·ZrF$_4$, 2KF·ZrF$_4$, and NaF·KF·ZrF$_4$
40	21	39		Peritectic	5NaF·2ZrF$_4$, 2NaF·ZrF$_4$, and NaF·KF·ZrF$_4$
39	21	40		Peritectic	2NaF·ZrF$_4$, 7NaF·6ZrF$_4$, and NaF·KF·ZrF$_4$
11	49	40		Peritectic	2KF·ZrF$_4$, 3KF·2ZrF$_4$, and NaF·KF·ZrF$_4$
10	48	42	385	Eutectic	3KF·2ZrF$_4$, KF·ZrF$_4$, and NaF·KF·ZrF$_4$
15	40	45		Eutectic	KF·ZrF$_4$, NaF·KF·ZrF$_4$, and 2NaF·3KF·5ZrF$_4$
22	33	45		Peritectic	NaF·KF·ZrF$_4$, 7NaF·6ZrF$_4$, and 2NaF·3KF·5ZrF$_4$
25	25	50		Eutectic	7NaF·6ZrF$_4$, 3NaF·4ZrF$_4$, and 2NaF·3KF·5ZrF$_4$
21	29	51		Eutectic	3NaF·4ZrF$_4$, ZrF$_4$, and 2NaF·3KF·5ZrF$_4$
20	30	50	432	Congruent melting point	2NaF·3KF·5ZrF$_4$

*Three solid phases have been observed routinely in the composition region 30–50 mole % ZrF$_4$ which have not been identified as to composition. Whether these exhibit primary phases at the liquidus surface has not yet been determined.

**Compositions of invariant points shown by the intersection of dotted boundary curves are approximate.
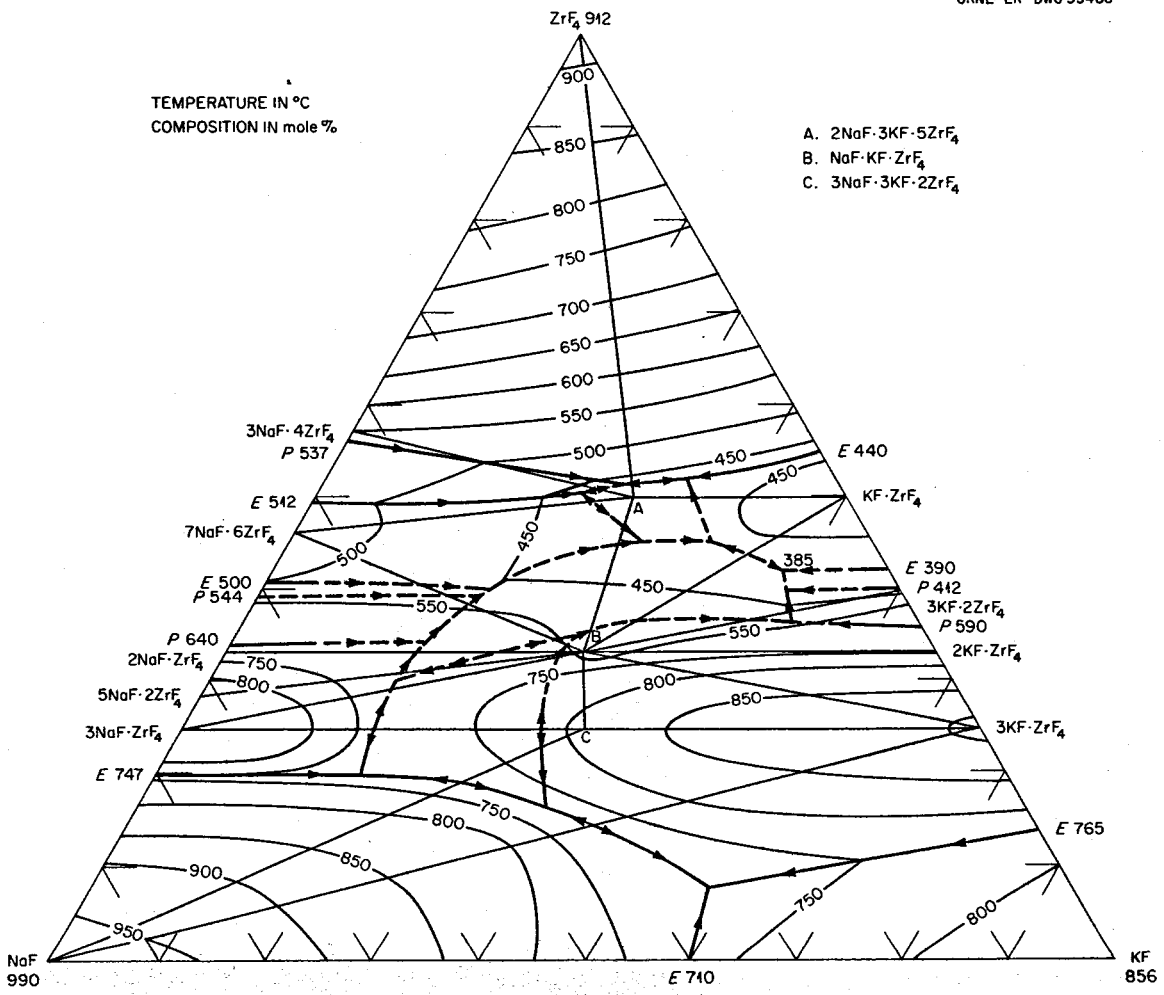
Fig. 3.38. The System NaF−KF−ZrF$_4$. The isotherms for the temperatures 600, 650, and 700°C between the 30 and 40 mole % ZrF$_4$ compositions have been omitted in order not to obscure the phase relationships in this polythermal projection.

3.39. The System NaF–RbF–ZrF$_4$

R. E. Thoma, H. Insley, H. A. Friedman, and W. R. Grimes, unpublished work performed at the Oak Ridge National Laboratory, 1951–56.

Preliminary diagram.

Invariant Equilibria

Composition of Liquid (mole %)			Invariant Temperature (°C)	Type of Equilibrium	Solids Present at Invariant Point
NaF	RbF	ZrF$_4$			
23	72	5	643	Eutectic	NaF, RbF, and 3RbF·ZrF$_4$
50	27	23	720	Eutectic	NaF, 3RbF·ZrF$_4$, and 3NaF·ZrF$_4$
37	32	31	605	Eutectic	3NaF·ZrF$_4$, 3RbF·ZrF$_4$, and NaF·RbF·ZrF$_4$
39	26	35	545	Peritectic	3NaF·ZrF$_4$, 5NaF·2ZrF$_4$, and NaF·RbF·ZrF$_4$
36.3	24.2	39.5	427	Peritectic	5NaF·2ZrF$_4$, 2NaF·ZrF$_4$, and NaF·RbF·ZrF$_4$
34.5	24	41.5	424	Peritectic	2NaF·ZrF$_4$, NaF·RbF·ZrF$_4$, and 3NaF·3RbF·4ZrF$_4$
34	23.5	42.5	422	Peritectic	2NaF·ZrF$_4$, 7NaF·6ZrF$_4$, and 3NaF·3RbF·4ZrF$_4$
33	23.5	43.5	420	Eutectic	7NaF·6ZrF$_4$, 3NaF·3RbF·4ZrF$_4$, and NaF·RbF·2ZrF$_4$
28.5	21.5	50	443	Eutectic	3NaF·4ZrF$_4$, 7NaF·6ZrF$_4$, and NaF·RbF·2ZrF$_4$
28	21.5	50.5	446	Peritectic	3NaF·4ZrF$_4$, ZrF$_4$, and NaF·RbF·2ZrF$_4$
23.5	39.5	37	470	Peritectic	NaF·RbF·ZrF$_4$, 2RbF·ZrF$_4$, and 3RbF·ZrF$_4$
21	40	39	438	Peritectic	NaF·RbF·ZrF$_4$, 2RbF·ZrF$_4$, and 3NaF·3RbF·4ZrF$_4$
8	50	42	400	Eutectic	3NaF·3RbF·4ZrF$_4$, 2RbF·ZrF$_4$, and 5RbF·4ZrF$_4$
8.5	47	44.5	395	Eutectic	3NaF·3RbF·4ZrF$_4$, 5RbF·ZrF$_4$, and NaF·RbF·2ZrF$_4$
6.2	45.8	48	380	Eutectic	NaF·RbF·2ZrF$_4$, 5RbF·4ZrF$_4$, and RbF·ZrF$_4$
5	42	53	398	Eutectic	NaF·RbF·2ZrF$_4$, RbF·ZrF$_4$, and RbF·2ZrF$_4$
6.5	39	54.5	423	Peritectic	ZrF$_4$, NaF·RbF·2ZrF$_4$, and RbF·2ZrF$_4$
33.3	33.3	33.3	642	Congruent melting point	NaF·RbF·ZrF$_4$
25	25	50	462	Congruent melting point	NaF·RbF·2ZrF$_4$

Composition of Liquid (mole %)			Temperature (°C)	Alkemade Line
NaF	RbF	ZrF$_4$		
24.75	24.75	51.5	455	NaF·RbF·2ZrF$_4$–ZrF$_4$
6	44	50	402	NaF·RbF·2ZrF$_4$–RbF·ZrF$_4$
7.5	46.5	46	405	NaF·RbF·2ZrF$_4$–5RbF·4ZrF$_4$
8.5	48.5	43	405	3NaF·RbF·4ZrF$_4$–5RbF·4ZrF$_4$
28	28	44	435	3NaF·RbF·4ZrF$_4$–NaF·RbF·2ZrF$_4$
22	40	38	442	3NaF·3RbF·4ZrF$_4$–2RbF·ZrF$_4$
29	41.5	49.5	450	NaF·RbF·2ZrF$_4$–7NaF·6ZrF$_4$
37	24.5	38.5	610	NaF·RbF·ZrF$_4$–3NaF·ZrF$_4$
47	28	25	732	3NaF·ZrF$_4$–3RbF·ZrF$_4$
36	48	16	777	NaF–3RbF·ZrF$_4$
30	36.7	33.3	598	NaF·RbF·ZrF$_4$–3RbF·ZrF$_4$
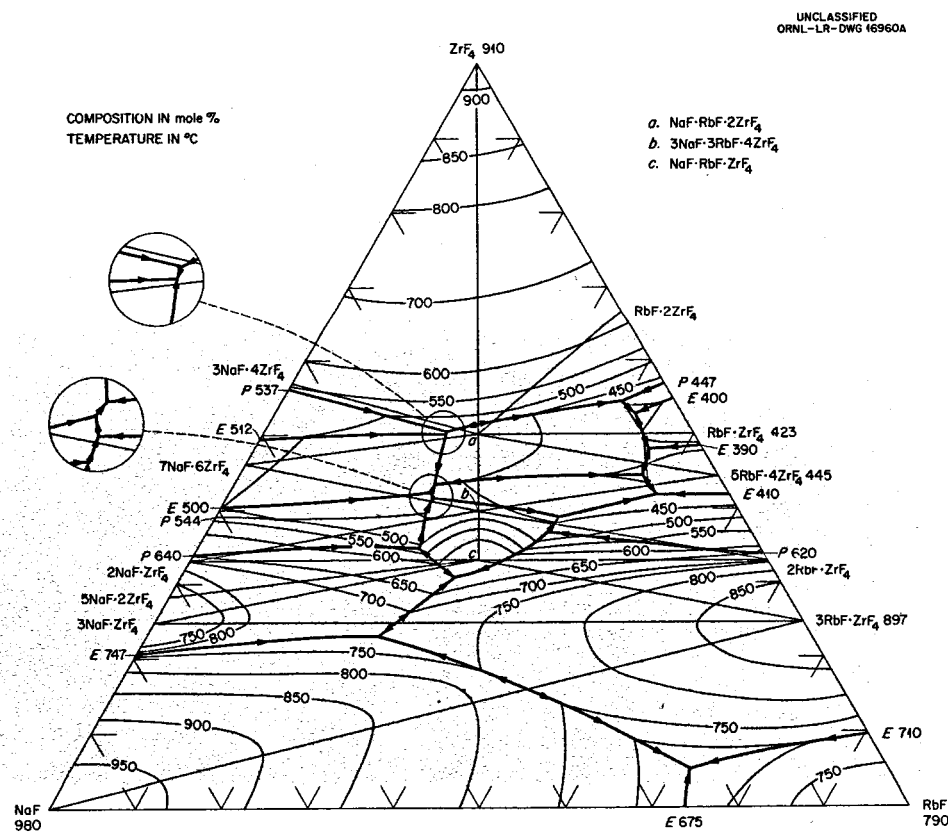
Fig. 3.39. The System NaF–RbF–ZrF$_4$.

3.40. The System NaF$-$CrF$_2-$ZrF$_4$: The Section NaF$\cdot$CrF$_2$ $-$ ZrF$_4$

R. E. Thoma, H. A. Friedman, B. S. Landau, and W. R. Grimes, unpublished work performed at the Oak Ridge National Laboratory, 1956–57.

Preliminary diagram. No invariant equilibria occur for compositions lying on the section NaF$\cdot$CrF$_2-$ZrF$_4$.
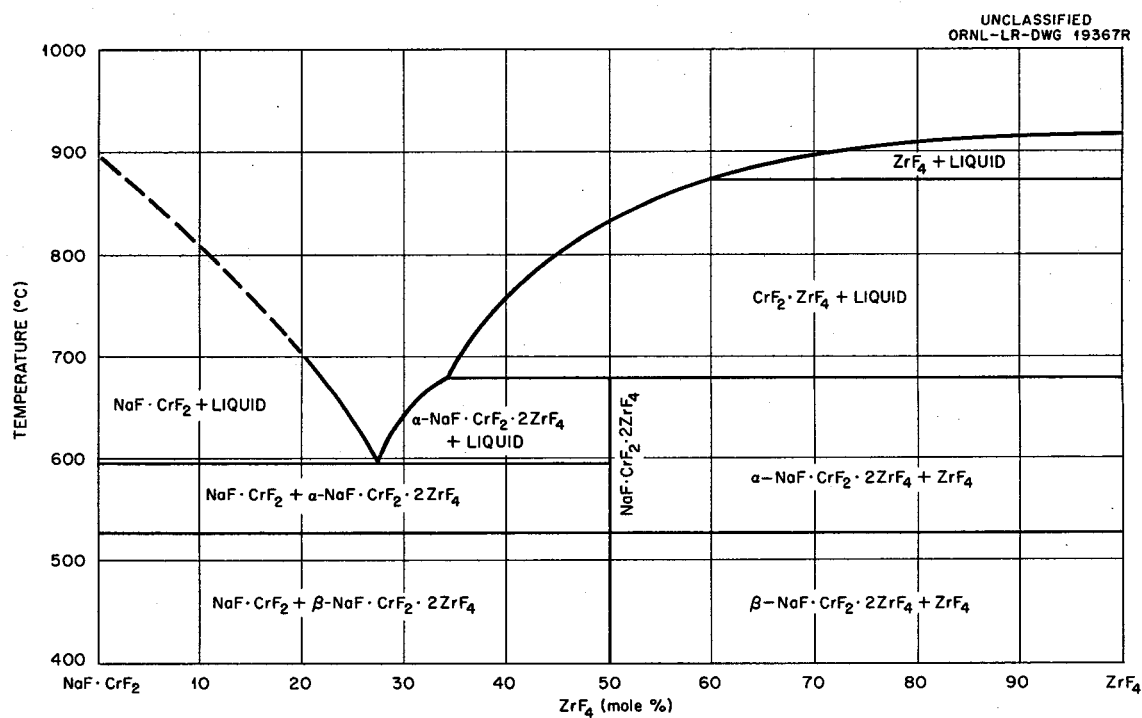
Fig. 3.40. The Section NaF$\cdot$CrF$_2-$ZrF$_4$.

3.41. The System NaF–CeF₃–ZrF₄

W. T. Ward, R. A. Strehlow, W. R. Grimes, and G. M. Watson, "Solubility Relationships of Rare Earth Fluorides and Yttrium Fluoride in Various Molten NaF–ZrF₄ and NaF–ZrF₄–UF₄ Solvents," *J. Chem. Eng. Data* (in press).
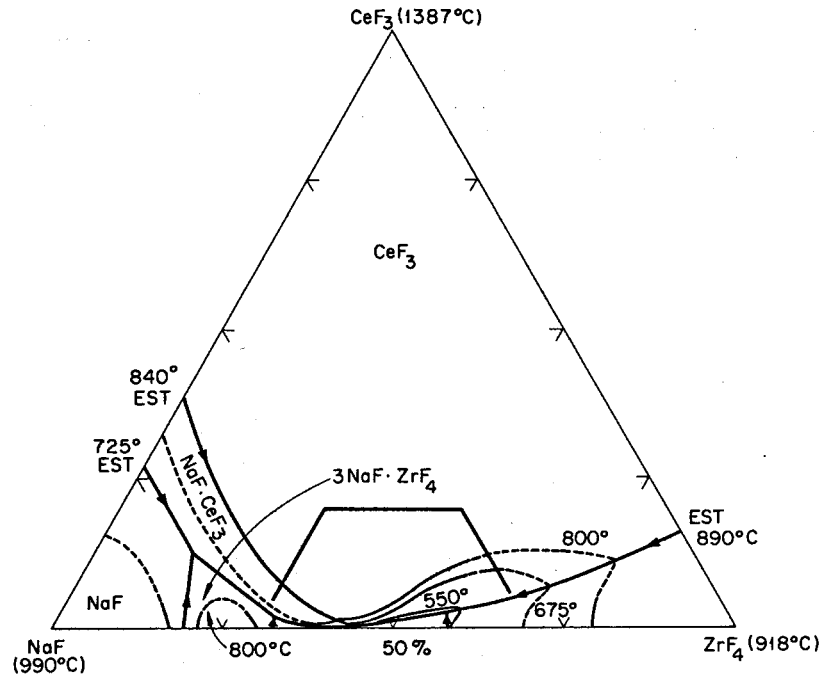
Fig. 3.41a. The System NaF–CeF₃–ZrF₄.

PROBABLE NaF·ZrF₄ PRIMARY PHASE FIELDS

A ZrF₄   D 2NaF·ZrF₄
B 3NaF·4ZrF₄   E 5NaF·2ZrF₄
C 7NaF·6ZrF₄   F 3NaF·ZrF₄
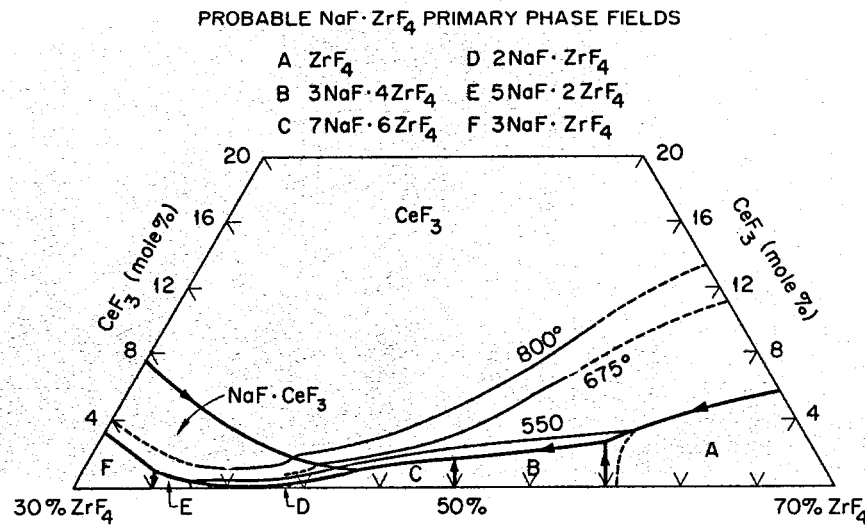
Fig. 3.41b. The System NaF–CeF₃–ZrF₄ in the Region 30–70 Mole % NaF, 0–20 Mole % CeF₃, 30–70 Mole % ZrF₄.

67

3.42. The System LiF–CeF$_3$

C. J. Barton, L. M. Bratcher, R. J. Sheil, and W. R. Grimes, unpublished work performed at the Oak Ridge National Laboratory, 1956–57.

Preliminary diagram. The system LiF–CeF$_3$ contains a single eutectic at 81 LiF–19 CeF$_3$ (mole %), m.p. 755 ± 5°C.
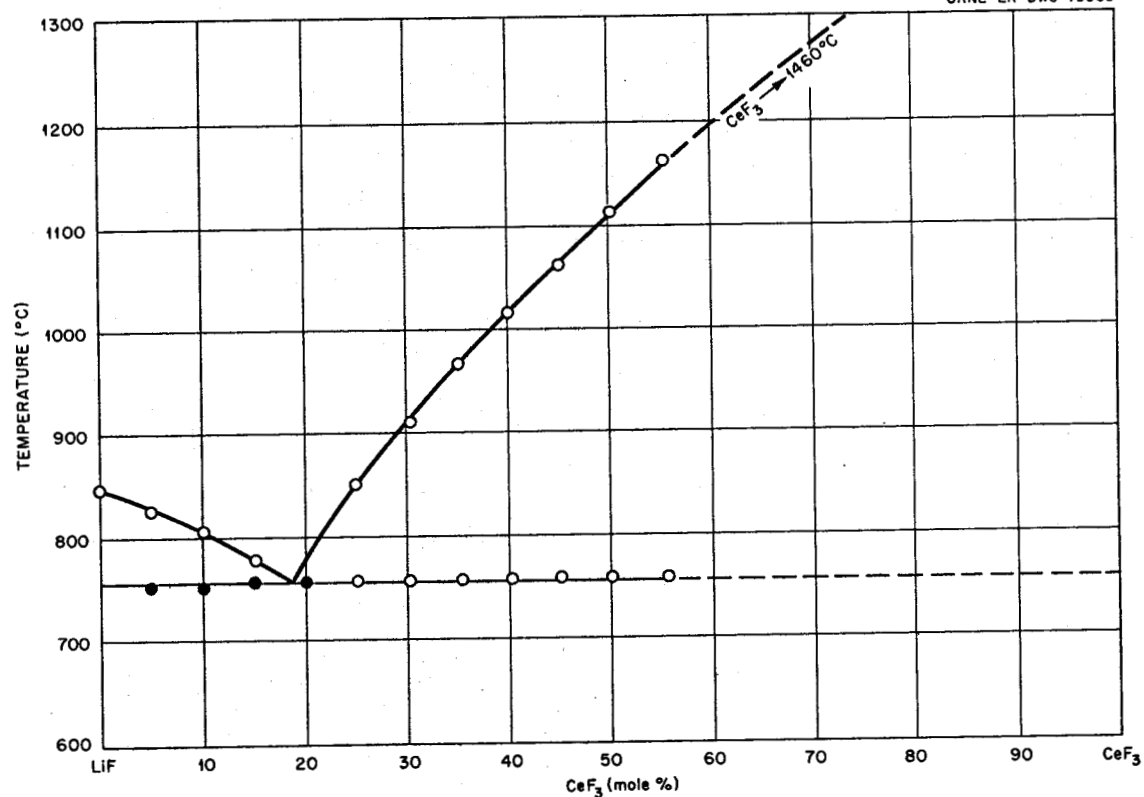
Fig. 3.42. The System LiF–CeF₃.

3.43. The System NaF–HfF$_4$

R. E. Thoma, C. F. Weaver, T. N. McVay, H. A. Friedman, and W. R. Grimes, unpublished work performed at the Oak Ridge National Laboratory, 1956–58.

Preliminary diagram.

Invariant Equilibria

Mole % HfF$_4$ in Liquid	Invariant Temperature (°C)	Type of Equilibrium	Phase Reaction at Invariant Temperature
18.5	695	Eutectic	$L \rightleftharpoons NaF + 3NaF{\cdot}HfF_4$
25	863	Congruent melting point	$L \rightleftharpoons 3NaF{\cdot}HfF_4$*
34	606	Peritectic	$L + 3NaF{\cdot}HfF_4 \rightleftharpoons \alpha\text{-}5NaF{\cdot}2HfF_4$
–	535	Inversion	$\alpha\text{-}5NaF{\cdot}2HfF_4 \rightleftharpoons \beta\text{-}5NaF{\cdot}2HfF_4$
35	586	Peritectic	$L + \alpha\text{-}5NaF{\cdot}2HfF_4 \rightleftharpoons \beta\text{-}2NaF{\cdot}HfF_4$
–	Below 350	Inversion	$\beta\text{-}2NaF{\cdot}HfF_4 \rightleftharpoons \gamma\text{-}2NaF{\cdot}HfF_4$
–	Below 350	Inversion	$\gamma\text{-}2NaF{\cdot}HfF_4 \rightleftharpoons \delta\text{-}2NaF{\cdot}HfF_4$
43	510	Eutectic	$L \rightleftharpoons \beta\text{-}2NaF{\cdot}HfF_4 + 7NaF{\cdot}6HfF_4$
45	531	Peritectic	$L + NaF{\cdot}HfF_4 \rightleftharpoons 7NaF{\cdot}6HfF_4$
50	557	Congruent melting point	$L \rightleftharpoons NaF{\cdot}HfF_4$
53	535	Eutectic	$L \rightleftharpoons NaF{\cdot}HfF_4 + HfF_4$

*A determination of the crystal structure of 3NaF·HfF$_4$ has been reported by L. A. Harris, "The Crystal Structures of Na$_3$ZrF$_7$ and Na$_3$HfF$_7$," *Acta Cryst.* **12**, 172 (1959).
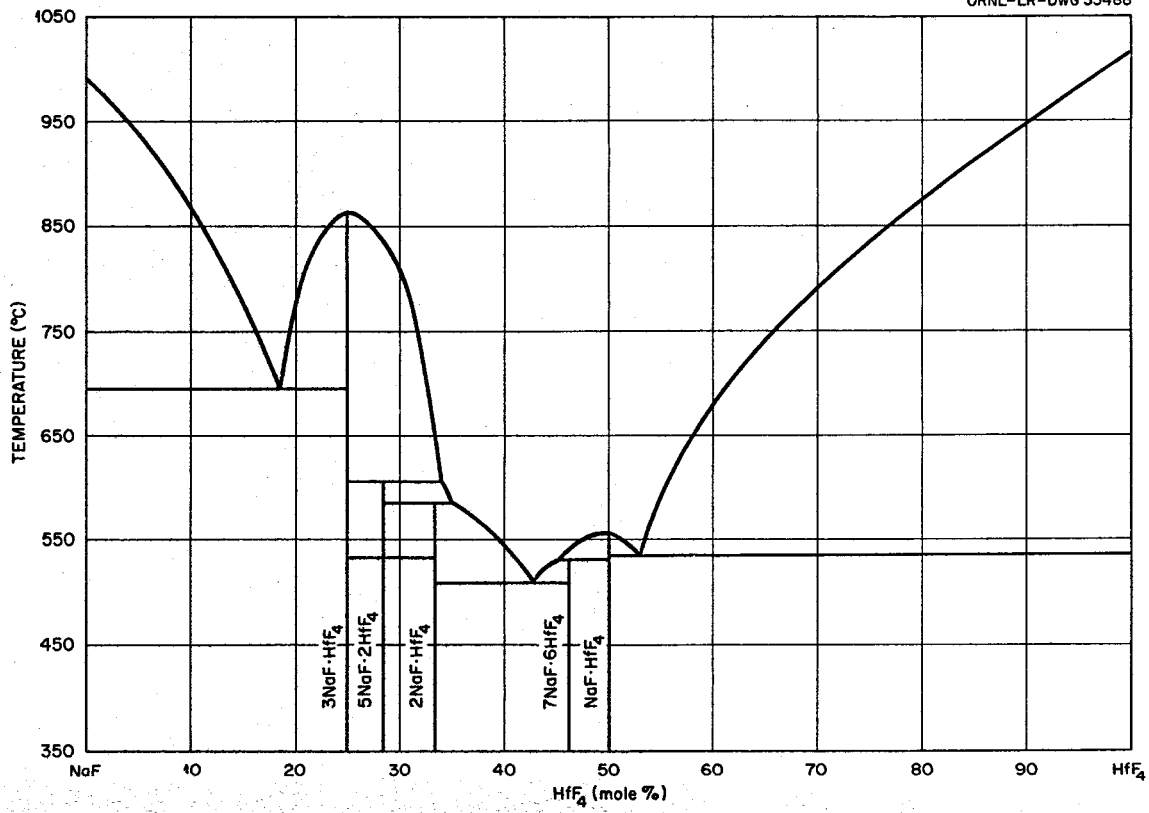
Fig. 3.43. The System NaF–HfF$_4$.

3.44. The System LiF–ThF$_4$

R. E. Thoma, H. Insley, B. S. Landau, H. A. Friedman, and W. R. Grimes, "Phase Equilibria in the Fused Salt Systems LiF–ThF$_4$ and NaF–ThF$_4$," *J. Phys. Chem.* **63**, 1266–74 (1959).

Invariant Equilibria

Mole % ThF$_4$ in Liquid	Invariant Temperature (°C)	Type of Equilibrium	Phase Reaction at Invariant Temperature
23	568	Eutectic	$L \rightleftharpoons \text{LiF} + 3\text{LiF·ThF}_4$
25	573	Congruent melting point	$L \rightleftharpoons 3\text{LiF·ThF}_4$
29	565	Eutectic	$L \rightleftharpoons 3\text{LiF·ThF}_4 + 7\text{LiF·6ThF}_4$
30.5	597	Peritectic	$\text{LiF·2ThF}_4 + L \rightleftharpoons 7\text{LiF·6ThF}_4$
42	762	Peritectic	$\text{LiF·4ThF}_4 + L \rightleftharpoons \text{LiF·2ThF}_4$
62	897	Peritectic	$\text{ThF}_4 + L \rightleftharpoons \text{LiF·4ThF}_4$

UNCLASSIFIED
ORNL–LR–DWG 26535A
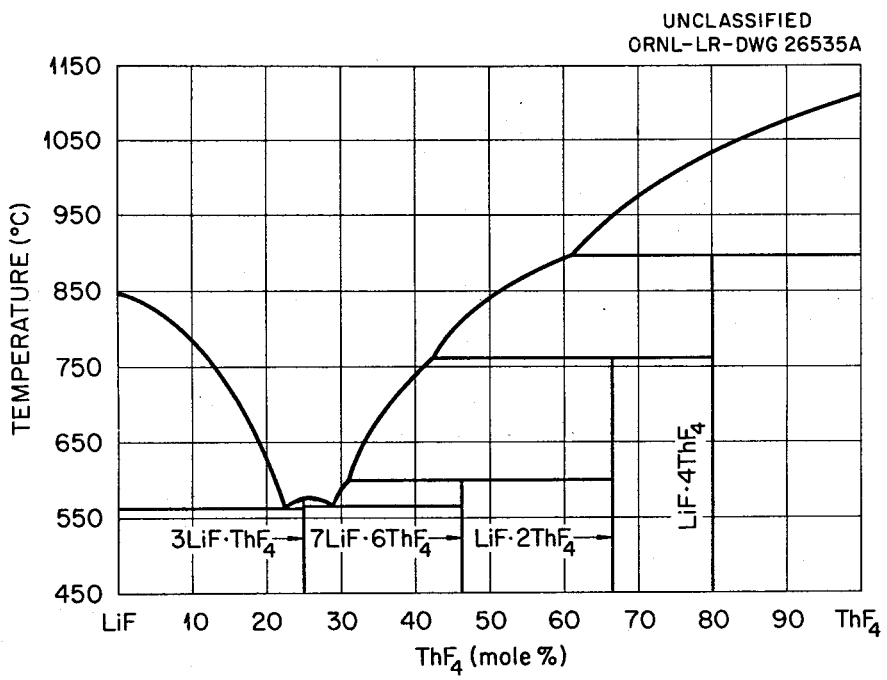
Fig. 3.44. The System LiF–ThF$_4$.

3.45. The System NaF–ThF$_4$

R. E. Thoma, H. Insley, B. S. Landau, H. A. Friedman, and W. R. Grimes, "Phase Equilibria in the Fused Salt Systems LiF–ThF$_4$ and NaF–ThF$_4$," *J. Phys. Chem.* **63**, 1266–74 (1959).

Invariant Equilibria

Mole % ThF$_4$ in Liquid	Invariant Temperature (°C)	Type of Equilibrium	Phase Reaction at Invariant Temperature
21.5	645	Peritectic	$NaF + L \rightleftharpoons \alpha\text{-}4NaF \cdot ThF_4$
22.5	618	Eutectic	$L \rightleftharpoons \alpha\text{-}4NaF \cdot ThF_4 + 2NaF \cdot ThF_4$
–	604	Inversion	$\alpha\text{-}4NaF \cdot ThF_4 \rightleftharpoons \beta\text{-}4NaF \cdot ThF_4$
–	558	Decomposition	$\beta\text{-}4NaF \cdot ThF_4 \rightleftharpoons NaF + 2NaF \cdot ThF_4$
33.3	705	Congruent melting point	$L \rightleftharpoons 2NaF \cdot ThF_4$
37	690	Eutectic	$L \rightleftharpoons 2NaF \cdot ThF_4 + 3NaF \cdot 2ThF_4$
40	712	Congruent melting point	$L \rightleftharpoons 3NaF \cdot 2ThF_4$
41	705	Eutectic	$L \rightleftharpoons 3NaF \cdot 2ThF_4 + \alpha\text{-}NaF \cdot ThF_4$
–	683	Decomposition	$3NaF \cdot 2ThF_4 \rightleftharpoons 2NaF \cdot ThF_4 + \alpha\text{-}NaF \cdot ThF_4$
45.5	730	Peritectic	$NaF \cdot 2ThF_4 + L \rightleftharpoons \alpha\text{-}NaF \cdot ThF_4$
58	831	Peritectic	$ThF_4 + L \rightleftharpoons NaF \cdot 2ThF_4$
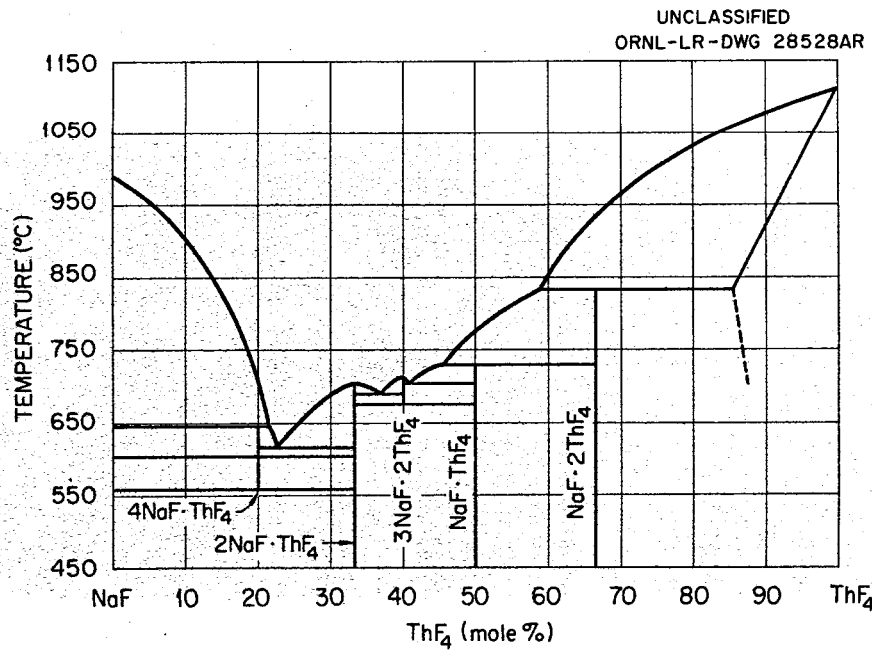
Fig. 3.45. The System NaF–ThF$_4$.

3.46. The System KF–ThF$_4$

W. J. Asker, E. R. Segnit, and A. W. Wylie, "The Potassium Thorium Fluorides," *J. Chem. Soc.* **1952**, 4470–79.

This system has also been reported by A. G. Bergman and E. P. Dergunov, *Doklady Akad. Nauk S.S.S.R.* **53**, 753 (1941) and by V. S. Emelyanov and A. J. Evstyukhin, "An Investigation of Fused-Salt Systems Based on Thorium Fluoride – II. NaF–KF–ThF$_4$, NaF–ThF$_4$, and KF–ThF$_4$," *J. Nuclear Energy* **5**, 108–14 (1957).

Invariant Equilibria

Mole % ThF$_4$ in Liquid	Invariant Temperature (°C)	Type of Equilibrium	Phase Reaction at Invariant Temperature
14	694	Eutectic	$L \rightleftharpoons KF + \beta\text{-}5KF{\cdot}ThF_4$
–	635	Inversion	$\alpha\text{-}5KF{\cdot}ThF_4 \rightleftharpoons \beta\text{-}5KF{\cdot}ThF_4$
–	712	Peritectic	$L + 3KF{\cdot}ThF_4 \rightleftharpoons \alpha\text{-}5KF{\cdot}ThF_4$
25	865	Congruent melting point	$L \rightleftharpoons 3KF{\cdot}ThF_4$
–	570	Decomposition	$3KF{\cdot}ThF_4 \rightleftharpoons \beta\text{-}5KF{\cdot}ThF_4 + \beta\text{-}2KF{\cdot}ThF_4$
31	691	Eutectic	$L \rightleftharpoons 3KF{\cdot}ThF_4 + \alpha\text{-}2KF{\cdot}ThF_4$
–	747	Peritectic	$L + KF{\cdot}ThF_4 \rightleftharpoons \alpha\text{-}2KF{\cdot}ThF_4$
–	645	Inversion	$\alpha\text{-}2KF{\cdot}ThF_4 \rightleftharpoons \beta\text{-}2KF{\cdot}ThF_4$
50*	905	Congruent melting point	$L \rightleftharpoons KF{\cdot}ThF_4$
56	875	Eutectic	$L \rightleftharpoons KF{\cdot}ThF_4 + KF{\cdot}2ThF_4$
66	930	Peritectic	$L + KF{\cdot}3ThF_4 \rightleftharpoons KF{\cdot}2ThF_4$
75	990	Congruent melting point	$L \rightleftharpoons KF{\cdot}3ThF_4$
78	980	Eutectic	$L \rightleftharpoons KF{\cdot}3ThF_4 + ThF_4 ss$

*It has been shown that the compound labeled by Asker *et al.* has the actual formula 7KF·6ThF$_4$; cf. R. E. Thoma, *Crystal Structures of Some Compounds of UF$_4$ and ThF$_4$ with Alkali Fluorides*, ORNL CF-58-12-40 (December 11, 1958).
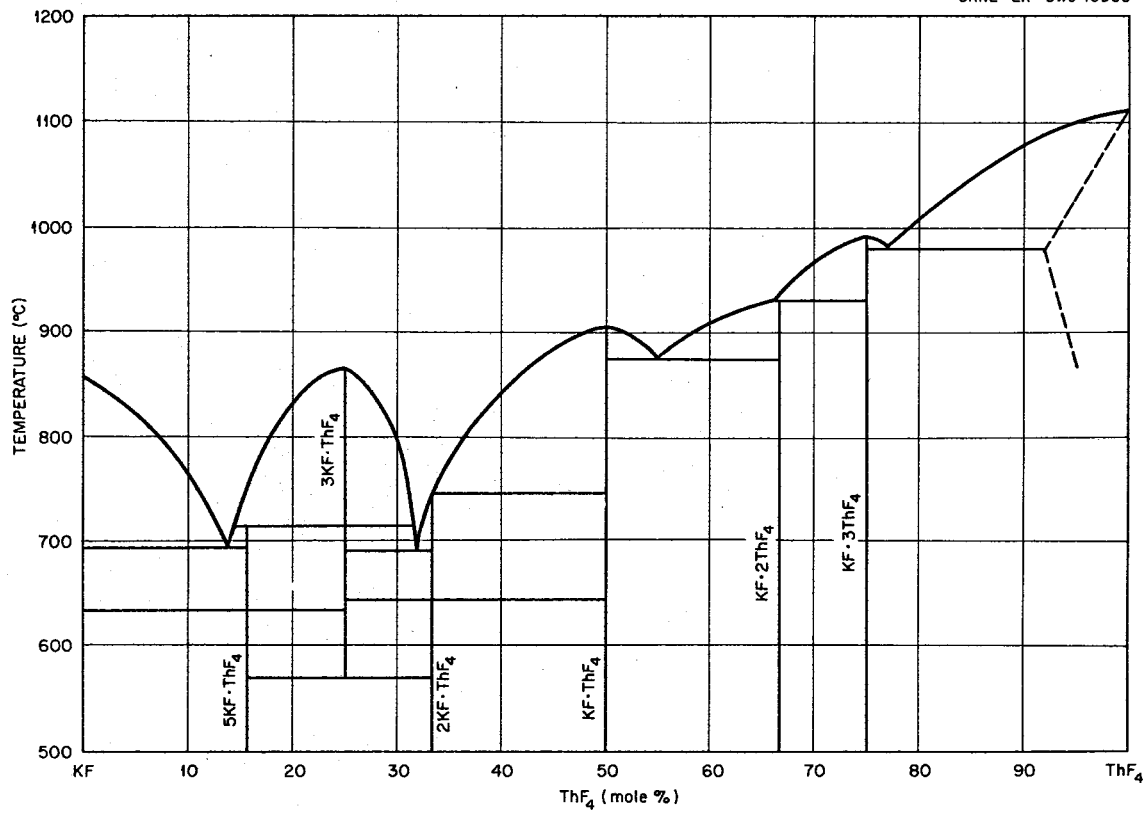
Fig. 3.46. The System KF—ThF₄.

3.47. The System RbF–ThF$_4$

E. P. Dergunov and A. G. Bergman, "Complex Formation Between Alkali Metal Fluorides and Fluorides of Metals of the Fourth Group," *Doklady Akad. Nauk S.S.S.R.* **60**, 391–94 (1948).

Invariant Equilibria

Mole % ThF$_4$ in Liquid	Invariant Temperature (°C)	Type of Equilibrium	Phase Reaction at Invariant Temperature
15	664	Eutectic	$L \rightleftharpoons RbF + 3RbF \cdot ThF_4$
25	974	Congruent melting point	$L \rightleftharpoons 3RbF \cdot ThF_4$
37	762	Eutectic	$L \rightleftharpoons 3RbF \cdot ThF_4 + RbF \cdot ThF_4$
50	852	Congruent melting point	$L \rightleftharpoons RbF \cdot ThF_4$
54	848	Eutectic	$L \rightleftharpoons RbF \cdot ThF_4 + RbF \cdot 3ThF_4$
75	1004	Congruent melting point	$L \rightleftharpoons RbF \cdot 3ThF_4$
80	1000	Eutectic	$L \rightleftharpoons RbF \cdot 3ThF_4 + ThF_4$
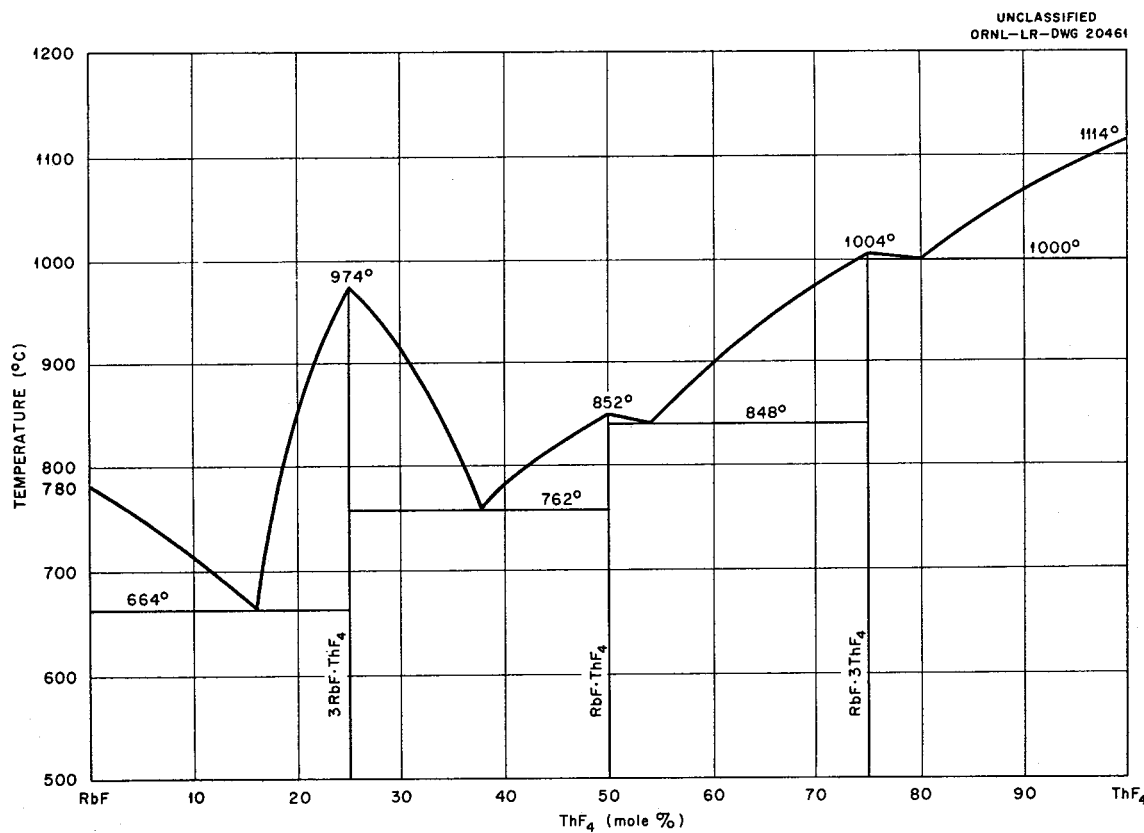
Fig. 3.47. The System RbF–ThF$_4$.

3.48. The System BeF$_2$–ThF$_4$

R. E. Thoma, H. Insley, H. A. Friedman, and C. F. Weaver, "Phase Equilibria in the Systems BeF$_2$–ThF$_4$ and LiF–BeF$_2$–ThF$_4$," paper to be presented at the 136th National Meeting of the American Chemical Society, Atlantic City, N. J., Sept. 13–18, 1959.

The system BeF$_2$–ThF$_4$ contains a single eutectic at 98.5 BeF$_2$–1.5 ThF$_4$ (mole %), m.p. 526 ± 3°C.
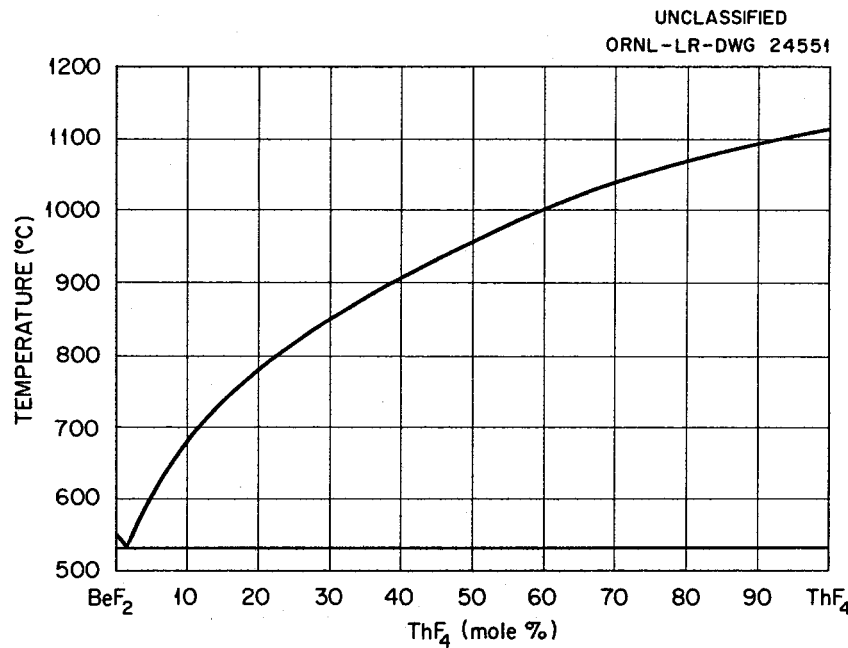
Fig. 3.48. The System BeF$_2$–ThF$_4$.

3.49. The System BeF$_2$-UF$_4$

T. B. Rhinehammer, P. A. Tucker, and E. F. Joy, *Phase Equilibria in the System BeF$_2$-UF$_4$*, MLM-1082 (to be published).

Preliminary diagram. The system BeF$_2$-UF$_4$ contains a single eutectic at 99.5 BeF$_2$-0.5 UF$_4$ (mole %), m.p. 535 ±2°C.
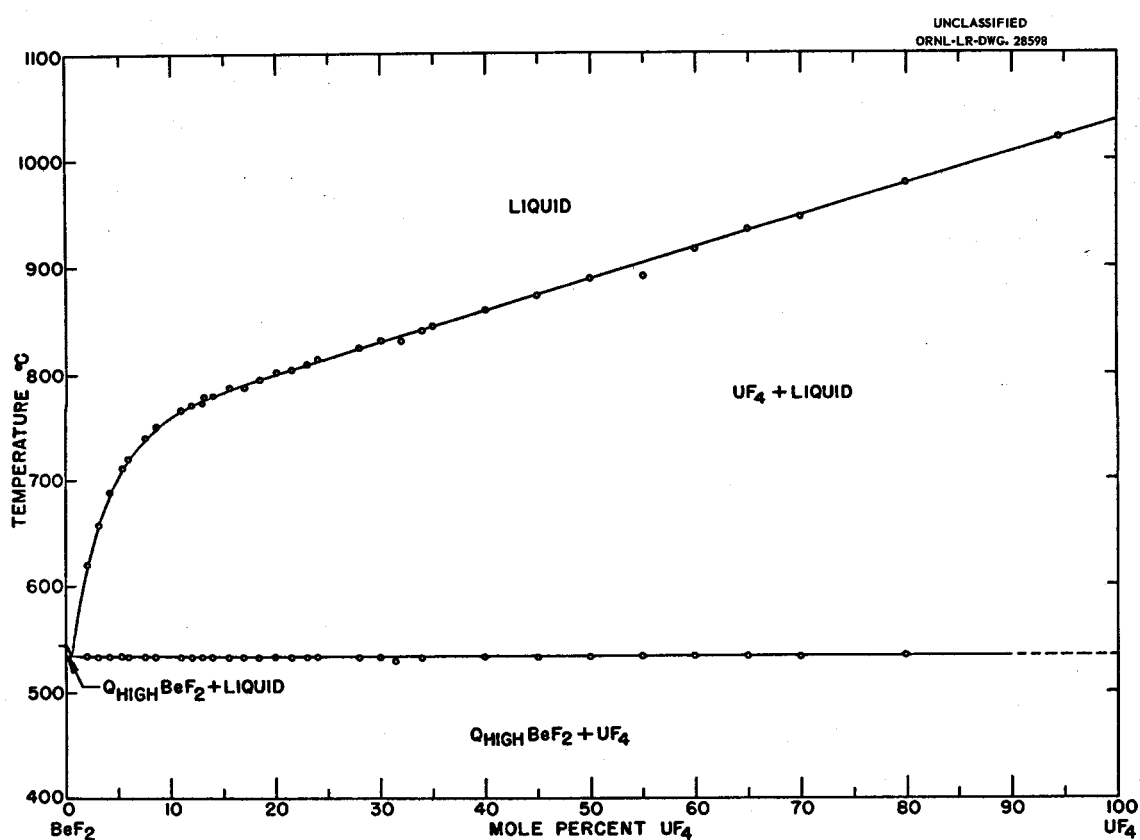
Fig. 3.49. The System BeF$_2$-UF$_4$.

3.50. The System MgF$_2$-ThF$_4$

J. O. Blomeke, *An Investigation of the ThF$_4$-Fused Salt Solutions for Homogeneous Reactors*, ORNL-1030 (June 19, 1951) (declassified with deletions).

Invariant Equilibria

Mole % ThF$_4$ in Liquid	Invariant Temperature (°C)	Type of Equilibrium	Phase Reaction at Invariant Temperature
25	915	Eutectic	$L \rightleftharpoons ThF_4 + MgF_2 \cdot 2ThF_4$
33.3	937	Congruent melting point	$L \rightleftharpoons MgF_2 \cdot 2ThF_4$
40	925	Eutectic	$L \rightleftharpoons MgF_2 \cdot 2ThF_4 + MgF_2$
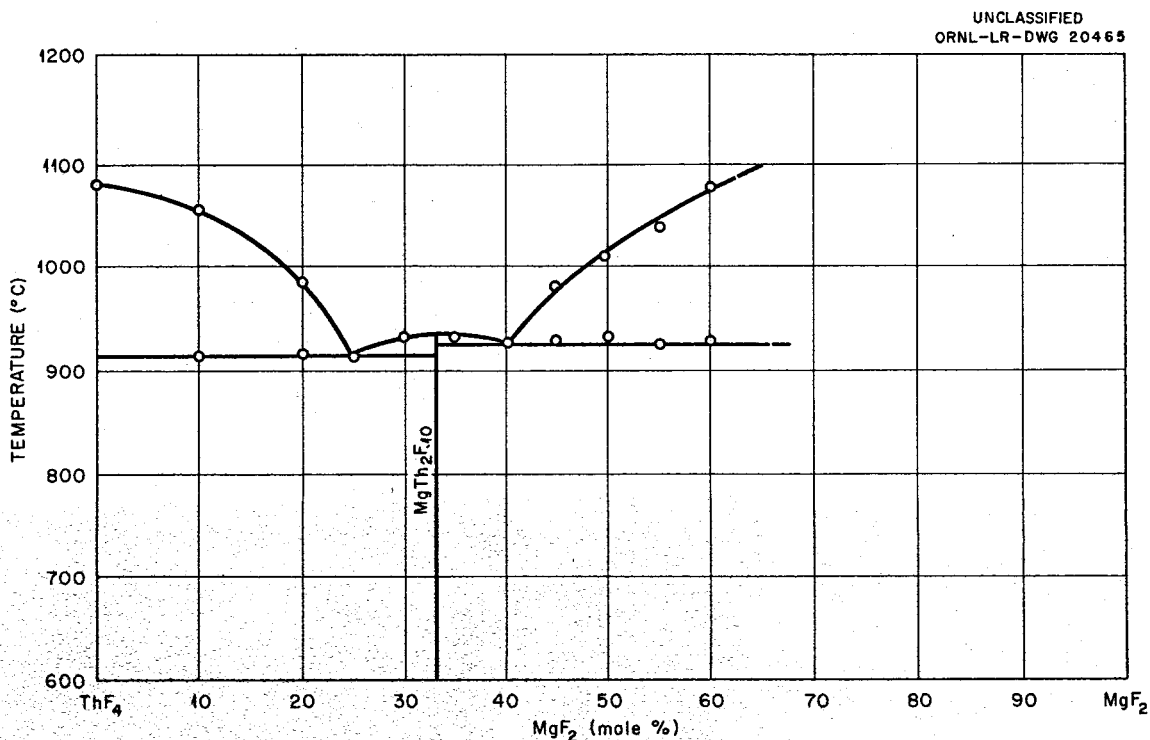
Fig. 3.50. The System MgF$_2$-ThF$_4$

3.51. The System LiF–BeF$_2$–ThF$_4$

R. E. Thoma, H. Insley, H. A. Friedman, and C. F. Weaver, "Phase Equilibria in the Systems BeF$_2$–ThF$_4$ and LiF–BeF$_2$–ThF$_4$," paper to be presented at the 136th National Meeting of the American Chemical Society, Atlantic City, N. J., Sept. 13–18, 1959.

Invariant Equilibria

Composition of Liquid (mole %)			Invariant Temperature (°C)	Type of Invariant	Solids Present at Invariant Point
LiF	BeF$_2$	ThF$_4$			
15	83	2	497 ± 4	Peritectic	ThF$_4$, LiF·4ThF$_4$, and BeF$_2$
33.5	64	2.5	455 ± 4	Peritectic	LiF·4ThF$_4$, LiF·2ThF$_4$, and BeF$_2$
47	51.5	1.5	356 ± 6	Eutectic	2LiF·BeF$_2$, LiF·2ThF$_4$, and BeF$_2$
60.5	36.5	3	433 ± 5	Peritectic	LiF·2ThF$_4$, 3LiF·ThF$_4$ss, and 2LiF·BeF$_2$
65.5	30.5	4	444 ± 4	Peritectic	LiF, 2LiF·BeF$_2$, and 3LiF·ThF$_4$ss
63	30.5	6.5	448 ± 5	Peritectic	3LiF·ThF$_4$ss, 7LiF·6ThF$_4$, and LiF·2ThF$_4$
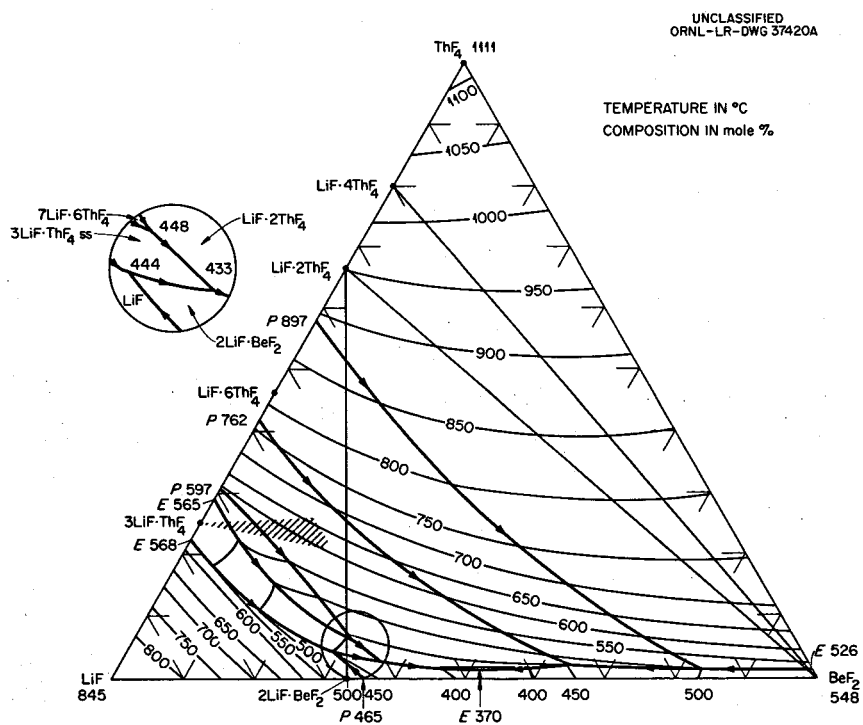
Fig. 3.51a. The System LiF–BeF$_2$–ThF$_4$.

Limits of Single-Phase 3LiF·ThF₄ Solid Solution

Composition (mole %)		
LiF	BeF₂	ThF₄
75	0	25
58	16	26
59	20	21

A three-dimensional model of the system $LiF-BeF_2-ThF_4$ is shown in Fig. 3.51b.
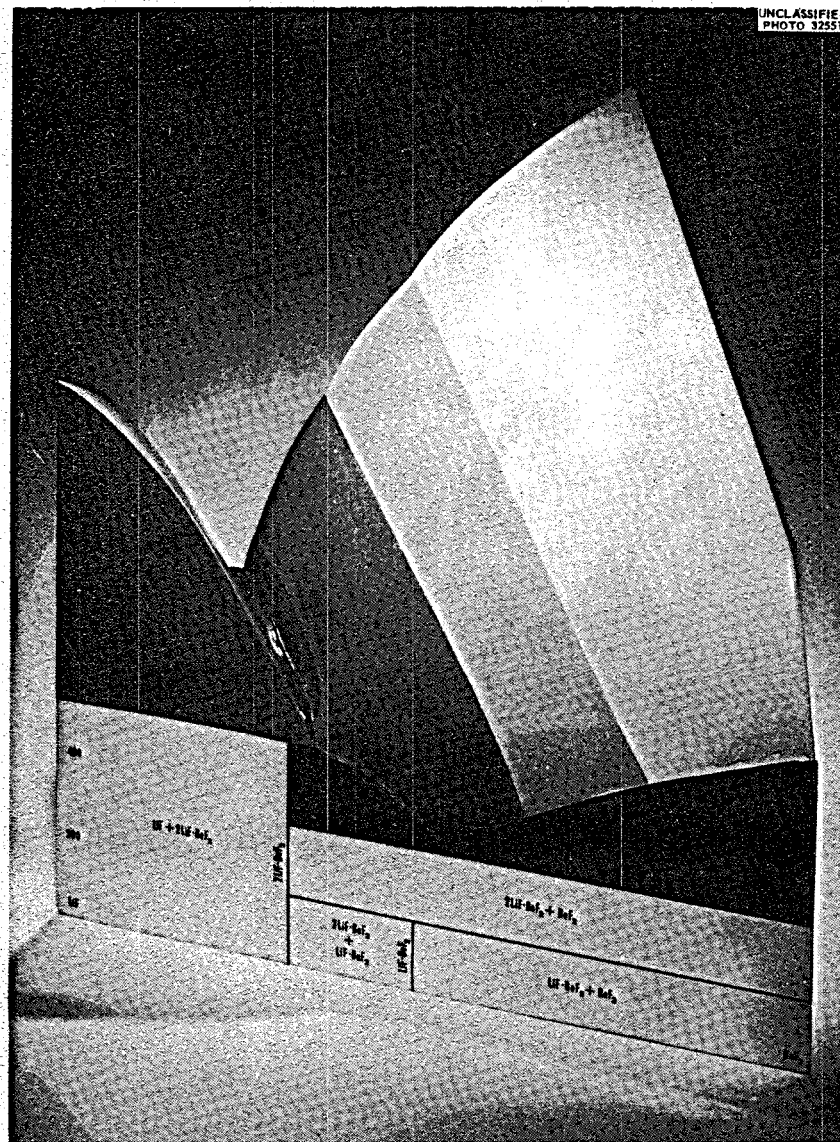
Fig. 3.51b. Model of the System $LiF-BeF_2-ThF_4$.

3.52. The System $NaF-ZrF_4-ThF_4$

R. E. Thoma, H. Insley, B. S. Landau, H. A. Friedman, and W. R. Grimes, unpublished work performed at the Oak Ridge National Laboratory, 1956–57.

Preliminary diagram.

Invariant Equilibria

Composition of Liquid (mole %)			Invariant Temperature ($^\circ$C)	Type of Equilibrium	Solids Present at Invariant Point
NaF	ZrF_4	ThF_4			
77	3	20	645	Peritectic	NaF, α-$4NaF \cdot ThF_4$, and $3NaF \cdot ZrF_4$
75.5	2.5	22	618	Eutectic	α-$4NaF \cdot ThF_4$, $2NaF \cdot ThF_4$, and $3NaF \cdot ZrF_4$
63	6	31*	683	Decomposition point of $3NaF \cdot 2ThF_4$ in ternary system	$3NaF \cdot 2ThF_4$, $2NaF \cdot ThF_4$, and $NaF \cdot ThF_4$
65.5	21.5	13	622	Peritectic	$2NaF \cdot ThF_4$, $3NaF \cdot ZrF_4$, and $NaF \cdot ThF_4$
65.5	24.5	10	615	Peritectic	$3NaF \cdot ZrF_4$, $NaF \cdot ThF_4$, and α-$5NaF \cdot 2ZrF_4$
64.5	25.5	10	593	Peritectic	α-$5NaF \cdot 2ZrF_4$, $NaF \cdot ThF_4$, and $NaF \cdot 2ThF_4$
58	38	4	538	Peritectic	α-$5NaF \cdot 2ZrF_4$, α-$2NaF \cdot ZrF_4$, and $NaF \cdot 2ThF_4$
58	40	2	495	Eutectic	β-$2NaF \cdot ZrF_4$, $NaF \cdot 2ThF_4$, and $7NaF \cdot 6ZrF_4$–$3NaF \cdot 2ZrF_4$ ss
53	42	4	510	Peritectic	$NaF \cdot 2ThF_4$, $Th(Zr)F_4$ ss, and $7NaF \cdot 6ZrF_4$–$3NaF \cdot 2ThF_4$ ss
49.5	48	2.5	505	Eutectic	$7NaF \cdot 6ZrF_4$, $3NaF \cdot 4ZrF_4$, and $Zr(Th)F_4$ ss

*Approximate composition.

Note: The boundary curve maximum on the Alkemade line $7NaF \cdot 6ZrF_4$–ThF_4 is unlikely to fall exactly on this line, because pure ThF_4 does not occur along this line. Since ThF_4 forms solid solutions with both ZrF_4 and $NaF \cdot 2ThF_4$, it is not readily determined on which side of the Alkemade line this maximum occurs.
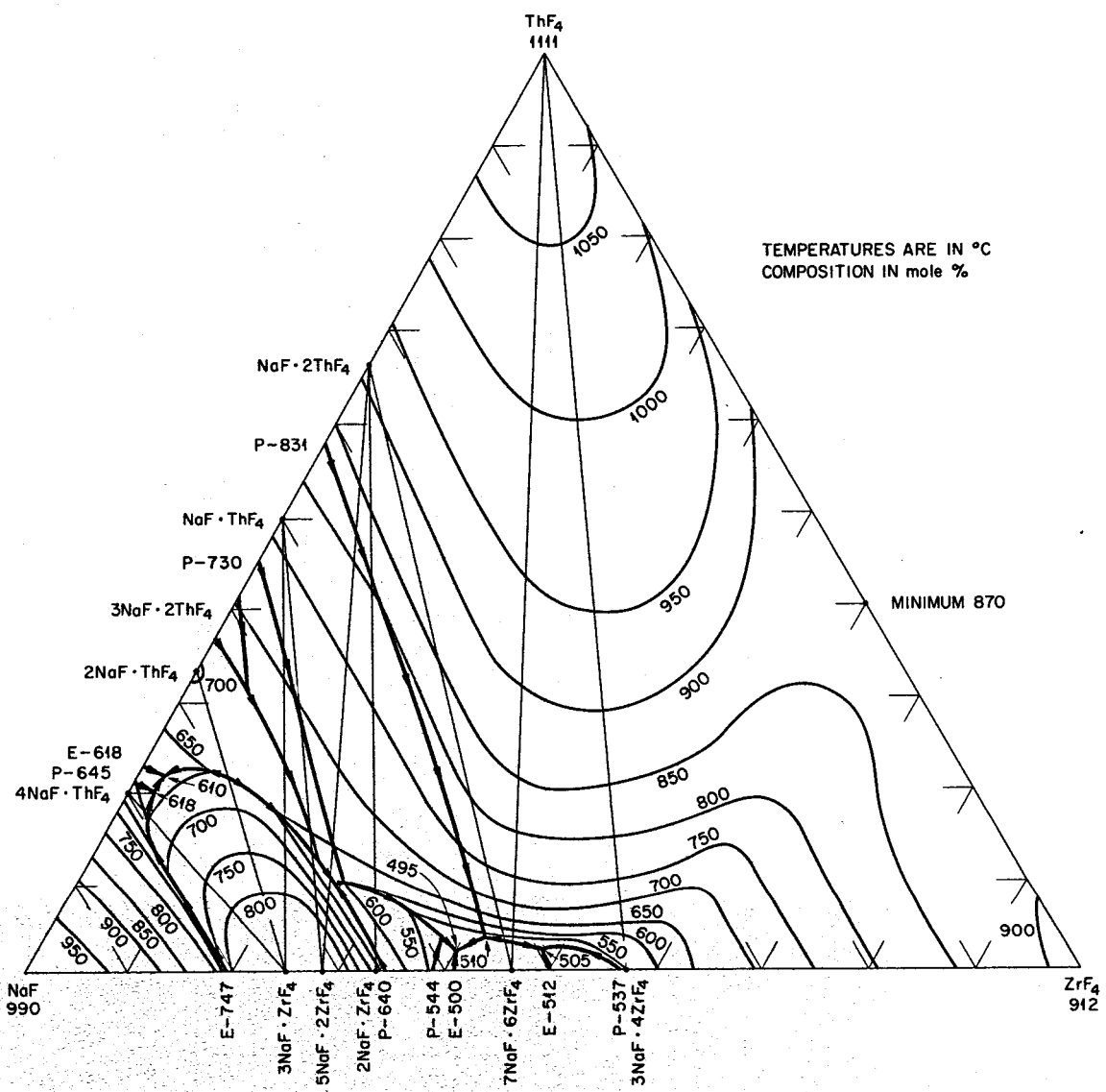
Fig. 3.52. The System NaF–ZrF$_4$–ThF$_4$.

3.53. The System LiF–UF₃

C. J. Barton, V. S. Coleman, L. M. Bratcher, and W. R. Grimes, unpublished work performed at the Oak Ridge National Laboratory, 1953–54.

Preliminary diagram. The system LiF–UF₃ contains a single eutectic at 73 LiF–27 UF₃ (mole %), m.p. 770°C.
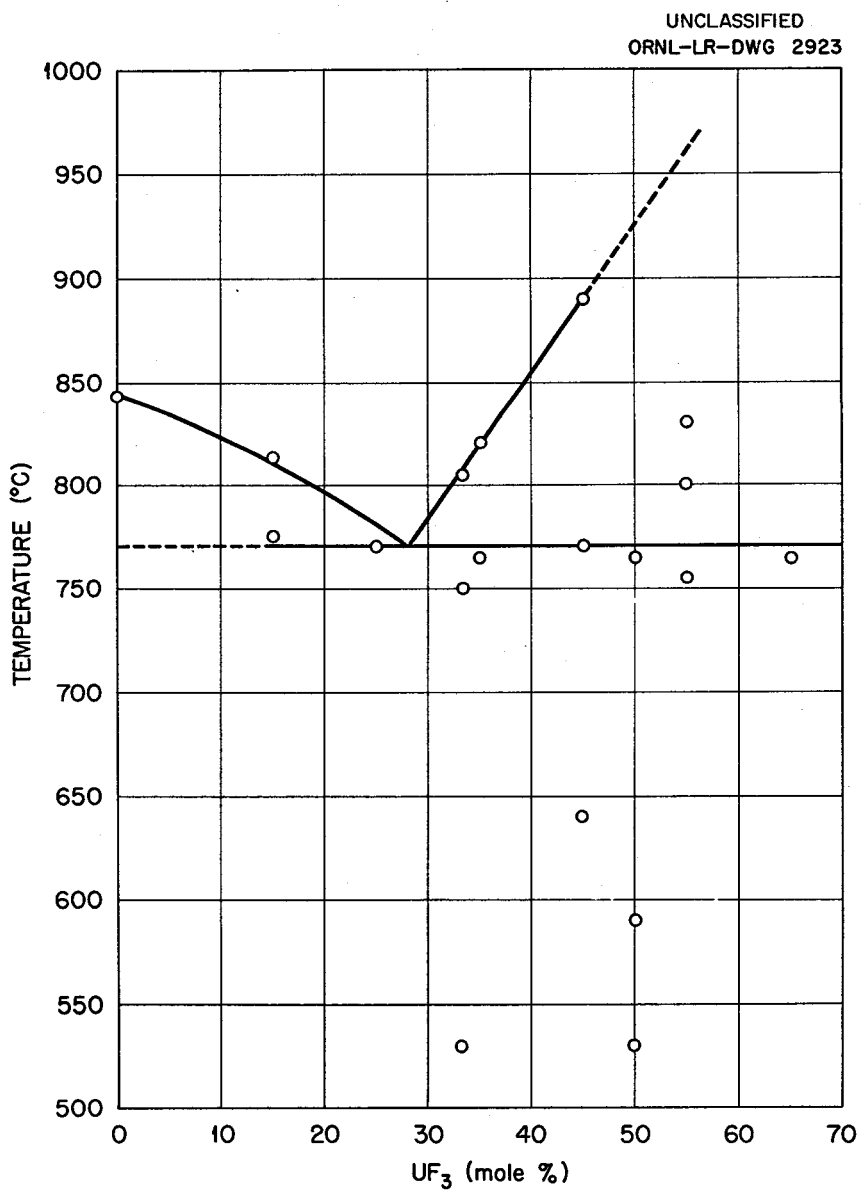
Fig. 3.53. The System LiF–UF₃.

3.54. The System LiF–UF$_4$

C. J. Barton, H. A. Friedman, W. R. Grimes, H. Insley, R. E. Moore, and R. E. Thoma, "Phase Equilibria in the Alkali Fluoride–Uranium Tetrafluoride Fused Salt Systems: I. The Systems LiF–UF$_4$ and NaF–UF$_4$," *J. Am. Ceram. Soc.* **41**, 63–69 (1958).

Invariant Equilibria

Mole % UF$_4$ in Liquid	Invariant Temperature (°C)	Type of Equilibrium	Phase Reaction at Invariant Temperature
–	470	Decomposition	$4LiF \cdot UF_4 \rightleftharpoons LiF + 7LiF \cdot 6UF_4$
26	500	Peritectic	$LiF + L \rightleftharpoons 4LiF \cdot UF_4$
27	490	Eutectic	$L \rightleftharpoons 4LiF \cdot UF_4 + 7LiF \cdot 6UF_4$
40	610	Peritectic	$L + LiF \cdot 4UF_4 \rightleftharpoons 7LiF \cdot 6UF_4$
57	775	Peritectic	$L + UF_4 \rightleftharpoons LiF \cdot 4UF_4$
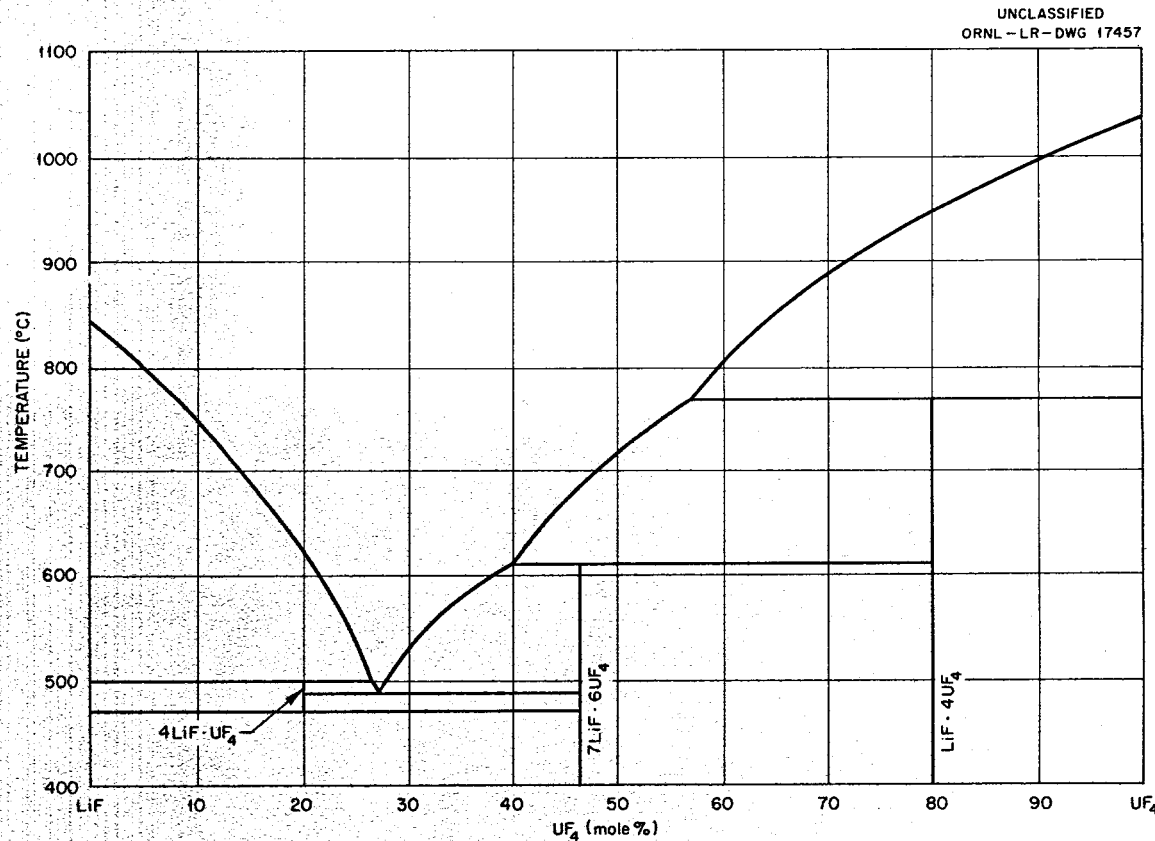
Fig. 3.54. The System LiF–UF$_4$.

3.55. The System NaF–UF$_3$

C. J. Barton, V. S. Coleman, T. N. McVay, and W. R. Grimes, unpublished work performed at the Oak Ridge National Laboratory, 1953–54.

Preliminary diagram.

Invariant Equilibria

| Mole % UF$_3$ in Liquid	Invariant Temperature (°C)	Type of Equilibrium	Phase Reaction at Invariant Temperature
27	715	Eutectic	$L \rightleftharpoons NaF + \alpha\text{-}NaF\cdot UF_3$
35	775	Peritectic	$L + UF_3 \rightleftharpoons \alpha\text{-}NaF\cdot UF_3$
–	595	Inversion	$\alpha\text{-}NaF\cdot UF_3 \rightleftharpoons \beta\text{-}NaF\cdot UF_3$
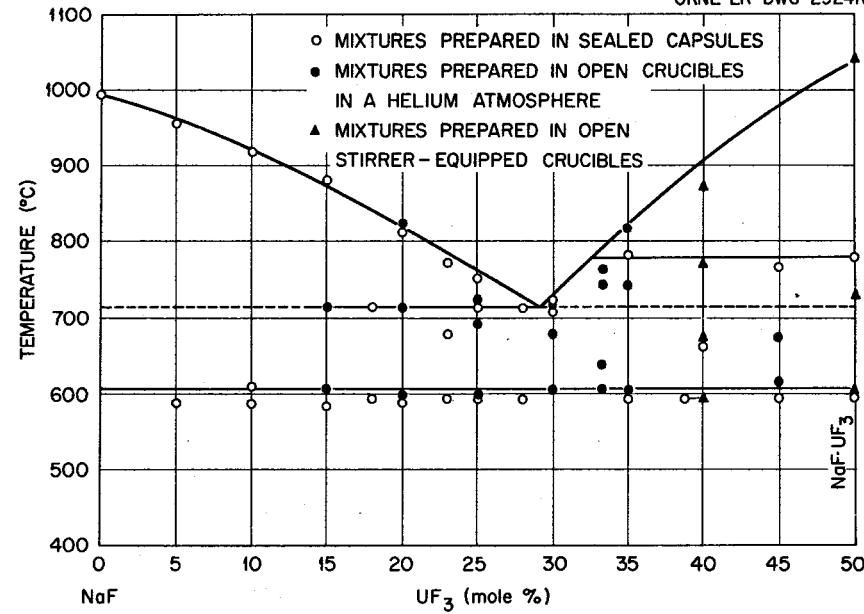
Fig. 3.55. The System NaF-UF$_3$.

3.56. The System NaF–UF$_4$

C. J. Barton, H. A. Friedman, W. R. Grimes, H. Insley, R. E. Moore, and R. E. Thoma, "Phase Equilibria in the Alkali Fluoride–Uranium Tetrafluoride Fused Salt Systems: I. The Systems LiF–UF$_4$ and NaF–UF$_4$," *J. Am. Ceram. Soc.* **41**, 63–69 (1958).

Invariant Equilibria

Mole % UF$_4$ in Liquid	Invariant Temperature (°C)	Type of Equilibrium	Phase Reaction at Invariant Temperature
21.5	618	Eutectic	$L \rightleftharpoons \alpha\text{-}3NaF\cdot UF_4 + NaF$
25	629	Congruent melting point	$L \rightleftharpoons \alpha\text{-}3NaF\cdot UF_4$
–	528	Inversion	$\alpha\text{-}3NaF\cdot UF_4 \rightleftharpoons \beta\text{-}3NaF\cdot UF_4$
–	497	Decomposition	$\beta\text{-}3NaF\cdot UF_4 \rightleftharpoons NaF + 2NaF\cdot UF_4$
28	623	Eutectic	$L \rightleftharpoons \alpha\text{-}3NaF\cdot UF_4 + 2NaF\cdot UF_4$
32.5	648	Peritectic	$L + 5NaF\cdot 3UF_4 \rightleftharpoons 2NaF\cdot UF_4$
37	673	Peritectic	$L + 7NaF\cdot 6UF_4 \rightleftharpoons 5NaF\cdot 3UF_4$
–	630	Decomposition	$5NaF\cdot 3UF_4 \rightleftharpoons 2NaF\cdot UF_4 + 7NaF\cdot 6UF_4$
46.2	718	Congruent melting point	$L \rightleftharpoons 7NaF\cdot 6UF_4$
56	680	Eutectic	$L \rightleftharpoons 7NaF\cdot 6UF_4 + UF_4$
–	660	Upper stability limit of NaF·2UF$_4$	$7NaF\cdot 6UF_4 + UF_4 \rightleftharpoons NaF\cdot 2UF_4$
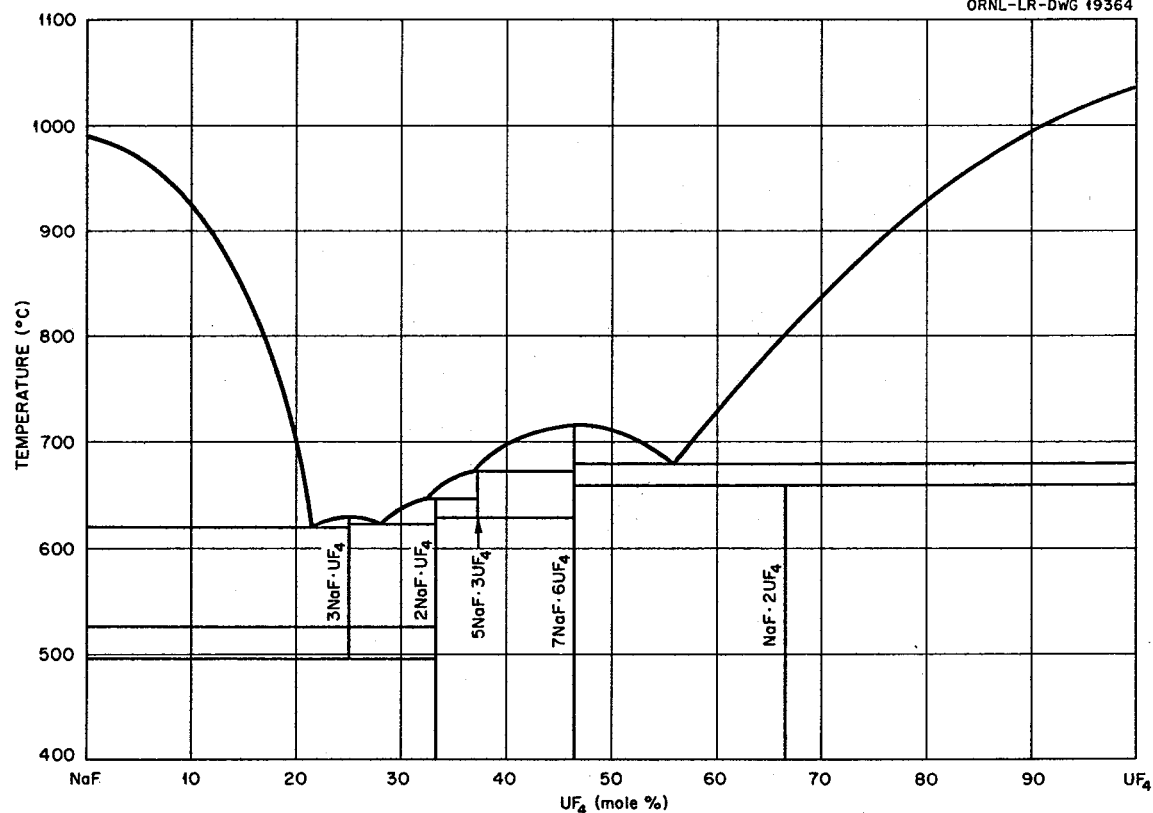
Fig. 3.56. The System NaF–UF$_4$.

3.57. The System KF–UF$_4$

R. E. Thoma, H. Insley, B. S. Landau, H. A. Friedman, and W. R. Grimes, "Phase Equilibria in the Alkali Fluoride–Uranium Tetrafluoride Fused Salt Systems: II. The Systems KF–UF$_4$ and RbF–UF$_4$," *J. Am. Ceram. Soc.* **41,** 538–44 (1958).

Invariant Equilibria

| Mole % UF$_4$ in Liquid	Invariant Temperature (°C)	Type of Equilibrium	Phase Reaction at Invariant Temperature
15	735	Eutectic	$L \rightleftharpoons KF + 3KF \cdot UF_4$
25	957	Congruent melting point	$L \rightleftharpoons 3KF \cdot UF_4$
–	608	Decomposition	$2KF \cdot UF_4 \rightleftharpoons 3KF \cdot UF_4 + 7KF \cdot 6UF_4$
35	755	Peritectic	$3KF \cdot UF_4 + L \rightleftharpoons 2KF \cdot UF_4$
38.5	740	Eutectic	$L \rightleftharpoons 2KF \cdot UF_4 + 7KF \cdot 6UF_4$
46.2	789	Congruent melting point	$L \rightleftharpoons 7KF \cdot 6UF_4$
54.5	735	Eutectic	$L \rightleftharpoons 7KF \cdot 6UF_4 + KF \cdot 2UF_4$
65	765	Peritectic	$UF_4 + L \rightleftharpoons KF \cdot 2UF_4$
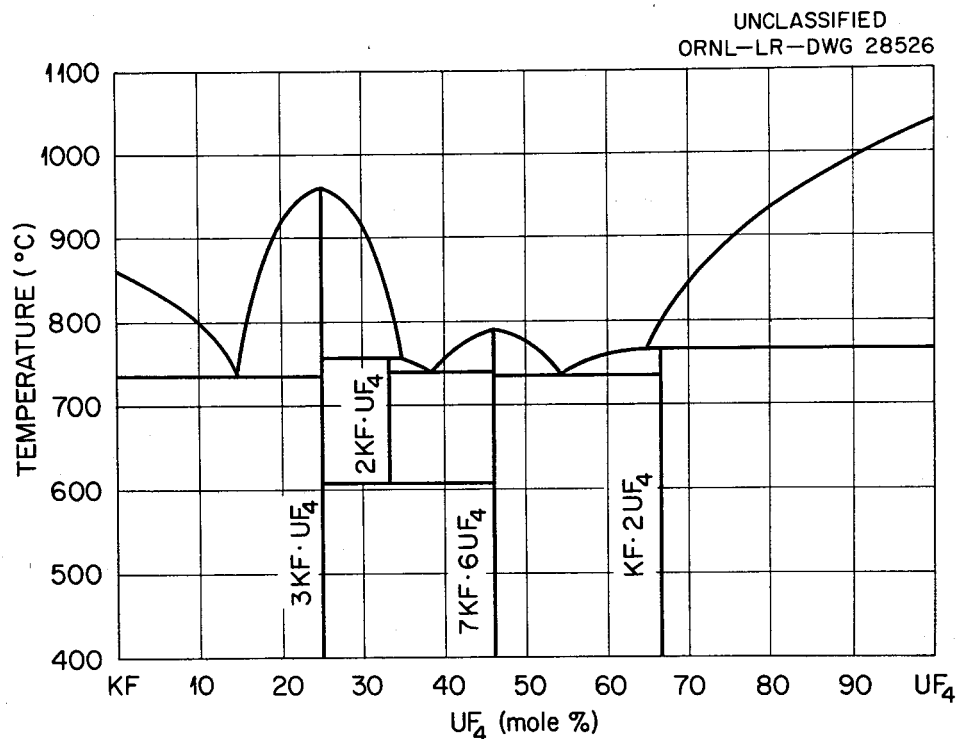
Fig. 3.57. The System KF–UF$_4$.

3.58. The System RbF–UF$_4$

R. E. Thoma, H. Insley, B. S. Landau, H. A. Friedman, and W. R. Grimes, "Phase Equilibria in the Alkali Fluoride–Uranium Tetrafluoride Fused Salt Systems: II. The Systems KF–UF$_4$ and RbF–UF$_4$," *J. Am. Ceram. Soc.* 41, 538–44 (1958).

Invariant Equilibria

Mole % UF$_4$ in Liquid	Invariant Temperature (°C)	Type of Equilibrium	Phase Reaction at Invariant Temperature
10	710	Eutectic	$L \rightleftharpoons RbF + 3RbF \cdot UF_4$
25	995	Congruent melting point	$L \rightleftharpoons 3RbF \cdot UF_4$
38	818	Peritectic	$L + 3RbF \cdot UF_4 \rightleftharpoons 2RbF \cdot UF_4$
43.5	675	Eutectic	$L \rightleftharpoons 2RbF \cdot UF_4 + 7RbF \cdot 6UF_4$
44	693	Peritectic	$RbF \cdot UF_4 + L \rightleftharpoons 7RbF \cdot 6UF_4$
50	735	Congruent melting point	$L \rightleftharpoons RbF \cdot UF_4$
55	714	Eutectic	$L \rightleftharpoons RbF \cdot UF_4 + 2RbF \cdot 3UF_4$
56.5	722	Peritectic	$RbF \cdot 3UF_4 + L \rightleftharpoons 2RbF \cdot 3UF_4$
57	730	Peritectic	$RbF \cdot 6UF_4 + L \rightleftharpoons RbF \cdot 3UF_4$
70.5	832	Peritectic	$UF_4 + L \rightleftharpoons RbF \cdot 6UF_4$
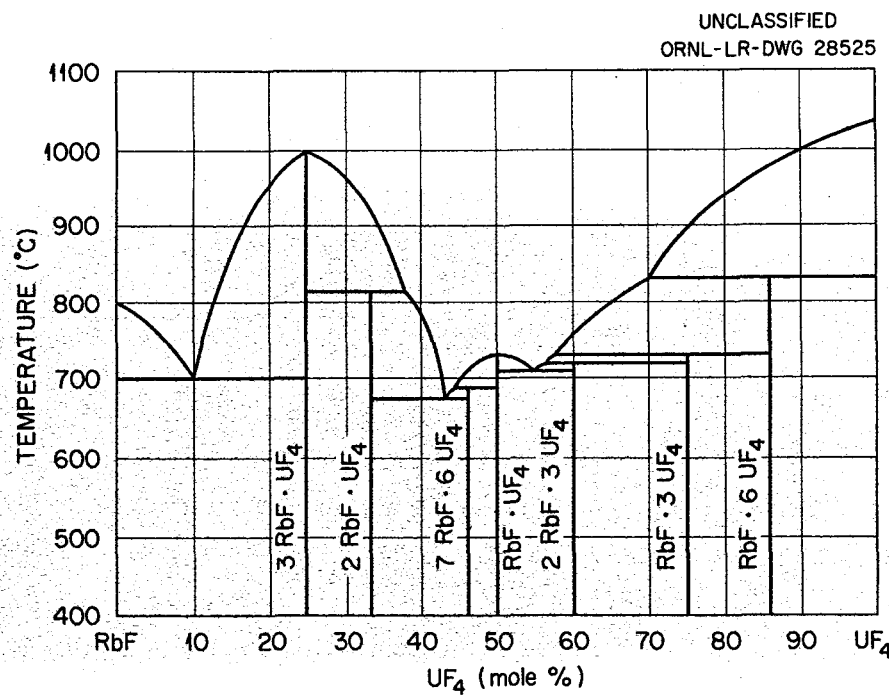
Fig. 3.58. The System RbF–UF$_4$

3.59. The System CsF–UF$_4$

C. J. Barton, L. M. Bratcher, J. P. Blakely, G. J. Nessle, and W. R. Grimes, unpublished work performed at the Oak Ridge National Laboratory, 1951–53.

Preliminary diagram.

Invariant Equilibria

Mole % UF$_4$ in Liquid	Invariant Temperature (°C)	Type of Equilibrium	Phase Reaction at Invariant Temperature
7.5	650	Eutectic	$L \rightleftharpoons CsF + 3CsF \cdot UF_4$
25	970	Congruent melting point	$L \rightleftharpoons 3CsF \cdot UF_4$
34	800	Peritectic	$L + 3CsF \cdot UF_4 \rightleftharpoons 2CsF \cdot UF_4$
41	695	Eutectic	$L \rightleftharpoons 2CsF \cdot UF_4 + \alpha\text{-}CsF \cdot UF_4$
50	735	Congruent melting point	$L \rightleftharpoons \alpha\text{-}CsF \cdot UF_4$
–	550	Inversion	$\alpha\text{-}CsF \cdot UF_4 \rightleftharpoons \beta\text{-}CsF \cdot UF_4$
53	725	Eutectic	$L \rightleftharpoons \alpha\text{-}CsF \cdot UF_4 + UF_4$
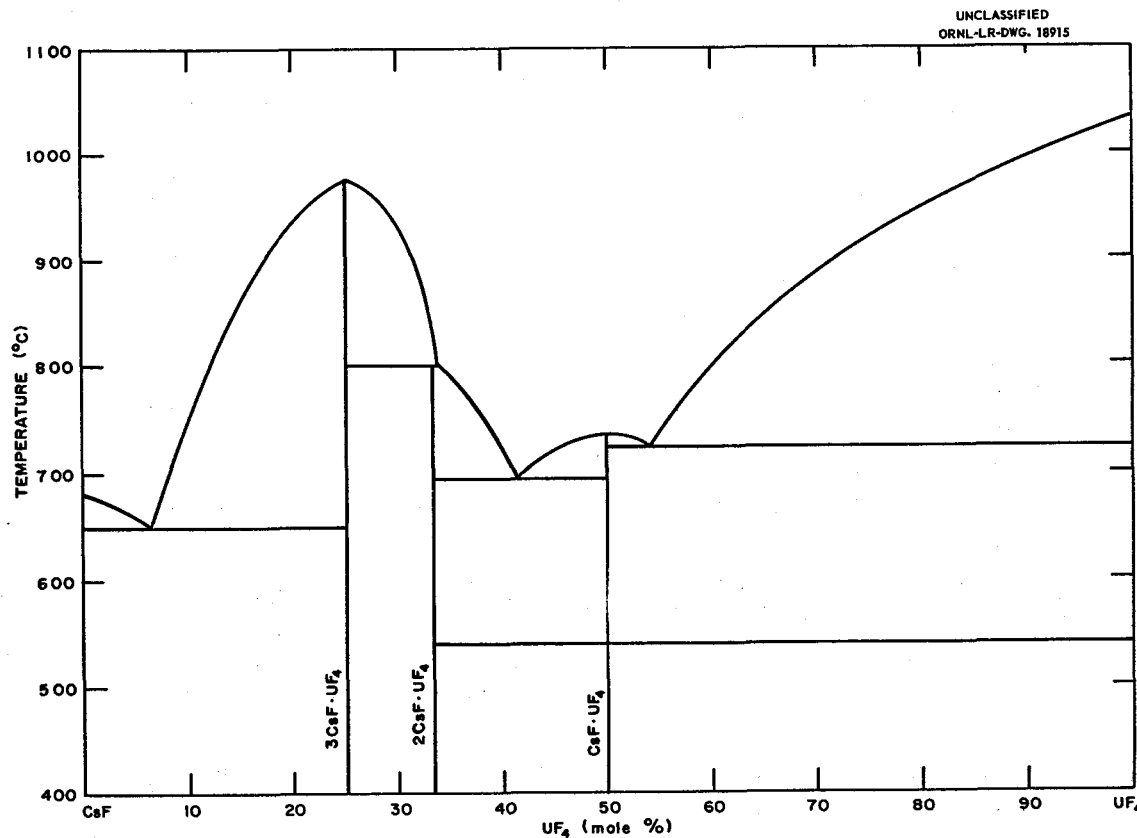
Fig. 3.59. The System CsF–UF$_4$.

3.60. The System ZrF$_4$–UF$_4$

C. J. Barton, W. R. Grimes, H. Insley, R. E. Moore, and R. E. Thoma, "Phase Equilibria in the Systems NaF–ZrF$_4$, UF$_4$–ZrF$_4$, and NaF–ZrF$_4$–UF$_4$," *J. Phys. Chem.* **62**, 665–76 (1958).

The system ZrF$_4$–UF$_4$ forms a continuous series of solid solutions having a minimum melting temperature of 765°C at 77 ZrF$_4$–23 UF$_4$ (mole %).
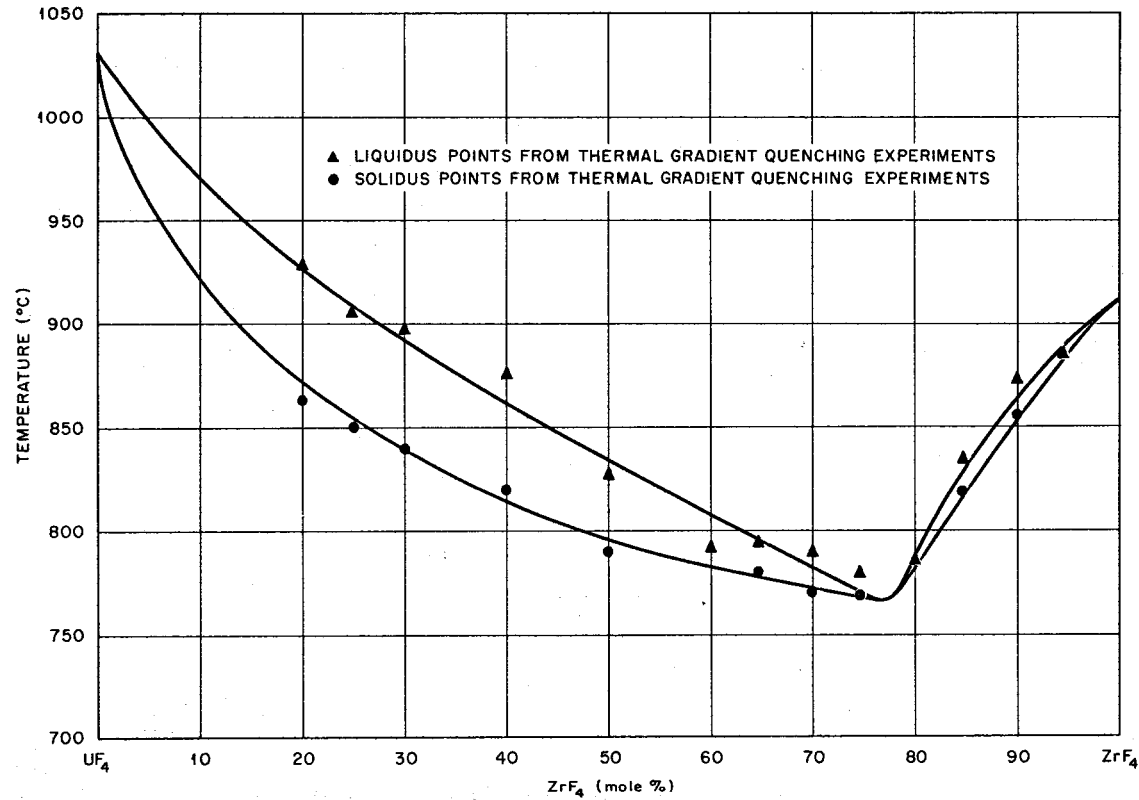
Fig. 3.60. The System ZrF$_4$–UF$_4$.

3.61. The System SnF$_2$–UF$_4$

B. J. Thamer and G. E. Meadows, *The Systems UF$_4$–SnF$_2$ and PuF$_3$–SnF$_2$,* LA-2286 (July 1959).

Invariant Equilibria

Mole % UF$_4$ in Liquid	Invariant Temperature (°C)	Type of Equilibrium	Phase Reaction at Invariant Temperature
0.5	212	Eutectic	$L \rightleftharpoons SnF_2 + 2SnF_2 \cdot UF_4$
4.5	340	Peritectic	$L + SnF_2 \cdot UF_4 \rightleftharpoons 2SnF_2 \cdot UF_4$
7.8	371	Peritectic	$L + UF_4 \rightleftharpoons SnF_2 \cdot UF_4$

UNCLASSIFIED
ORNL–LR–DWG 36864

Inset legend:
▲ SOLUBILITIES BY FILTRATION
△ LIQUIDUS POINTS FROM DTA HEATING CURVES
▼ LIQUIDUS POINTS FROM DTA COOLING CURVES
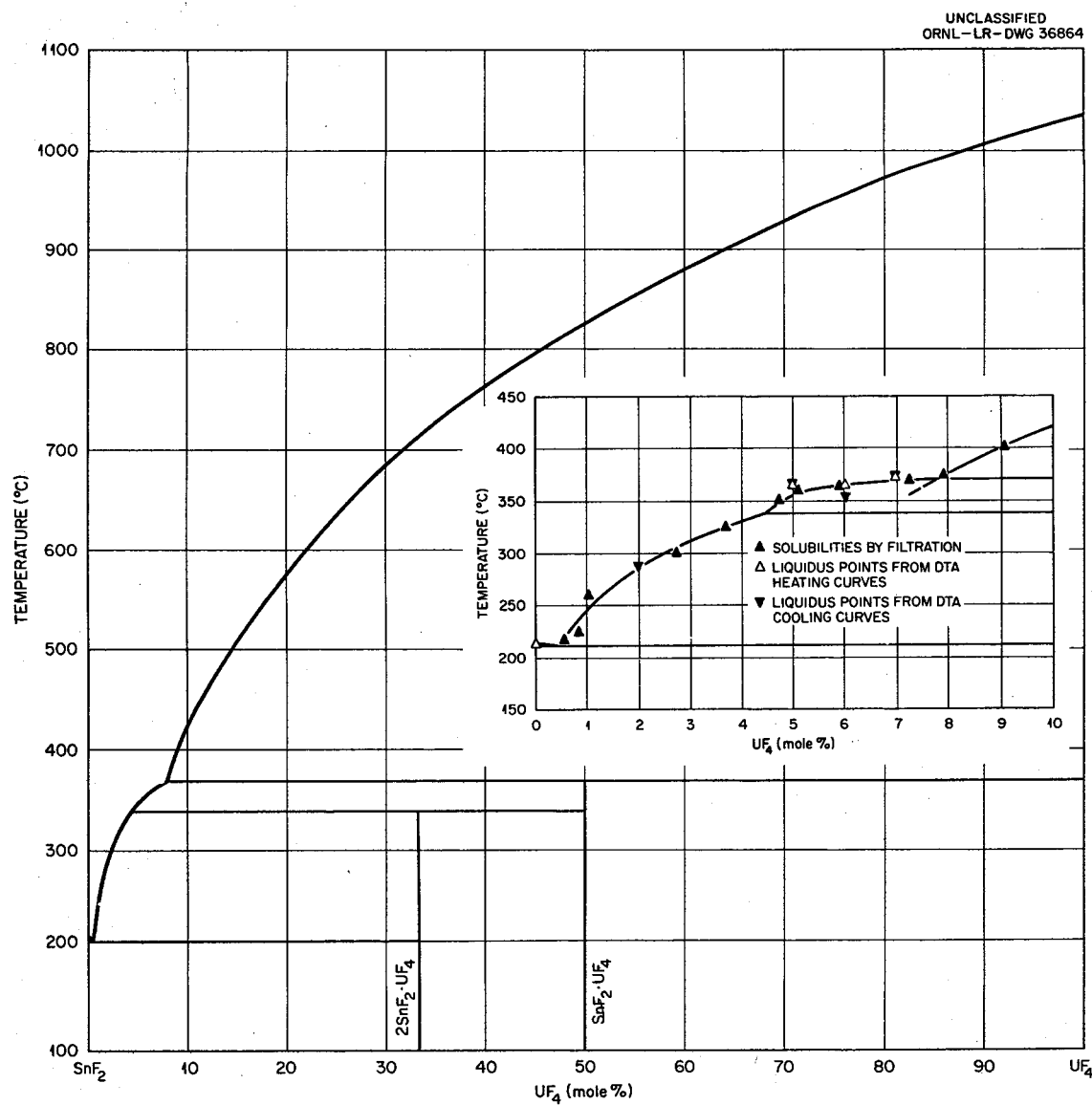
Fig. 3.61. The System SnF$_2$–UF$_4$.

3.62. The System PbF_2-UF_4

C. J. Barton, L. M. Bratcher, J. P. Blakely, G. J. Nessle, and W. R. Grimes, unpublished work performed at the Oak Ridge National Laboratory, 1950–51.

Preliminary diagram.

Invariant Equilibria

Mole % UF_4 in Liquid	Invariant Temperature (°C)	Type of Equilibrium	Phase Reaction at Invariant Temperature
14.3	920	Congruent melting point	$L \rightleftharpoons 6PbF_2 \cdot UF_4$
35	835	Eutectic	$L \rightleftharpoons 6PbF_2 \cdot UF_4 + 3PbF_2 \cdot 2UF_4$
40	840	Congruent melting point	$L \rightleftharpoons 3PbF_2 \cdot 2UF_4$
62	762 ± 10	Eutectic	$L \rightleftharpoons 3PbF_2 \cdot 2UF_4 + UF_4$

The eutectic at quite high PbF_2 concentrations is not shown on this diagram. The authors examined thermal data but found no evidence of a eutectic thermal effect.
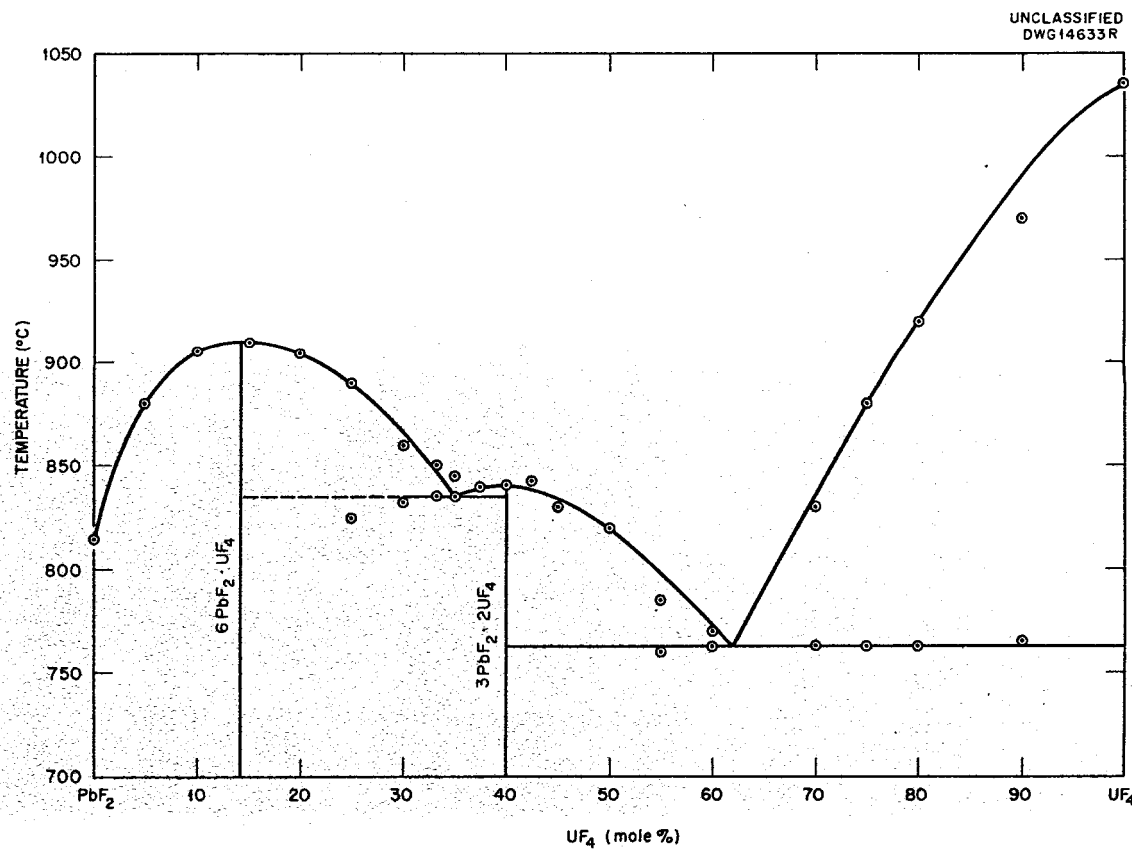
Fig. 3.62. The System PbF_2-UF_4.

3.63. The System ThF_4-UF_4

C. F. Weaver, R. E. Thoma, H. A. Friedman, and H. Insley, "Phase Equilibria in the Systems UF_4-ThF_4 and LiF-ThF_4-UF_4," paper presented at the 61st National Meeting of the American Ceramic Society, Chicago, Ill., May 17–21, 1959.

The system ThF_4-UF_4 forms a continuous series of solid solutions without a minimum.
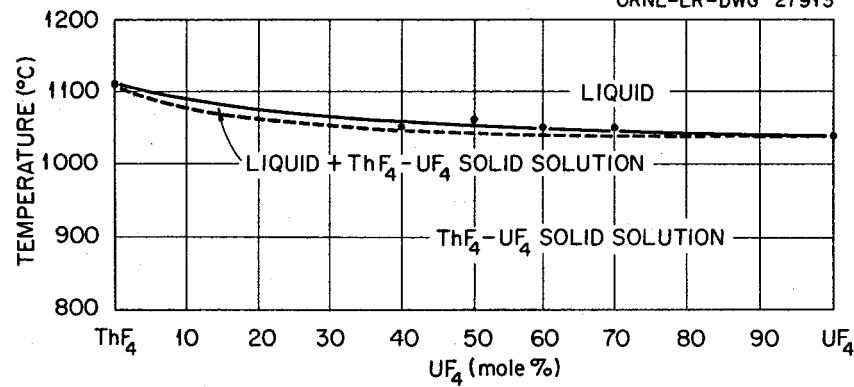
Fig. 3.63. The System ThF_4–UF_4.

3.64. The System LiF–NaF–UF$_4$

R. E. Thoma, H. Insley, B. S. Landau, H. A. Friedman, and W. R. Grimes, "Phase Equilibria in the Alkali Fluoride–Uranium Tetrafluoride Fused Salt Systems: III. The System NaF–LiF–UF$_4$," *J. Am. Ceram. Soc.* **42**, 21–26 (1959).

Invariant Equilibria

| Composition of Liquid (mole %)			Invariant Temperature (°C)	Type of Equilibrium	Solid Phases Present at Invariant Point
NaF	LiF	UF$_4$			
60	21	19	480	Eutectic	2NaF·UF$_4$, NaF, and LiF
65	13	22	497	Peritectic	β-3NaF·UF$_4$, 2NaF·UF$_4$, and NaF
7	65.5	27.5	470	Peritectic	7LiF·6UF$_4$ss,* 4LiF·UF$_4$, and LiF
35	37	28	480	Eutectic	2NaF·UF$_4$, 7NaF·6UF$_4$ss, and LiF
57	13	30	630	Peritectic	2NaF·UF$_4$, 5NaF·3UF$_4$, and 7NaF·6UF$_4$ss
24.3	43.5	32.2	445	Eutectic	7NaF·6UF$_4$ss, LiF, and 7LiF·6UF$_4$ss
24.5	29	46.5	602	Eutectic	NaF·2UF$_4$, 7LiF·6UF$_4$ss, and 7NaF·6UF$_4$ss
24.3	28.7	47	605	Peritectic	NaF·2UF$_4$, LiF·4UF$_4$, and 7LiF·6UF$_4$ss
23.5	28	48.5	640	Peritectic	UF$_4$, NaF·2UF$_4$, and LiF·4UF$_4$
37.5	10.5	52	660	Peritectic	UF$_4$, NaF·2UF$_4$, and 7NaF·6UF$_4$ss

*The compounds 7LiF·6UF$_4$ and 7NaF·6UF$_4$ as they occur in the ternary system are members of the solid solution 7LiF·6UF$_4$–7NaF·6UF$_4$.
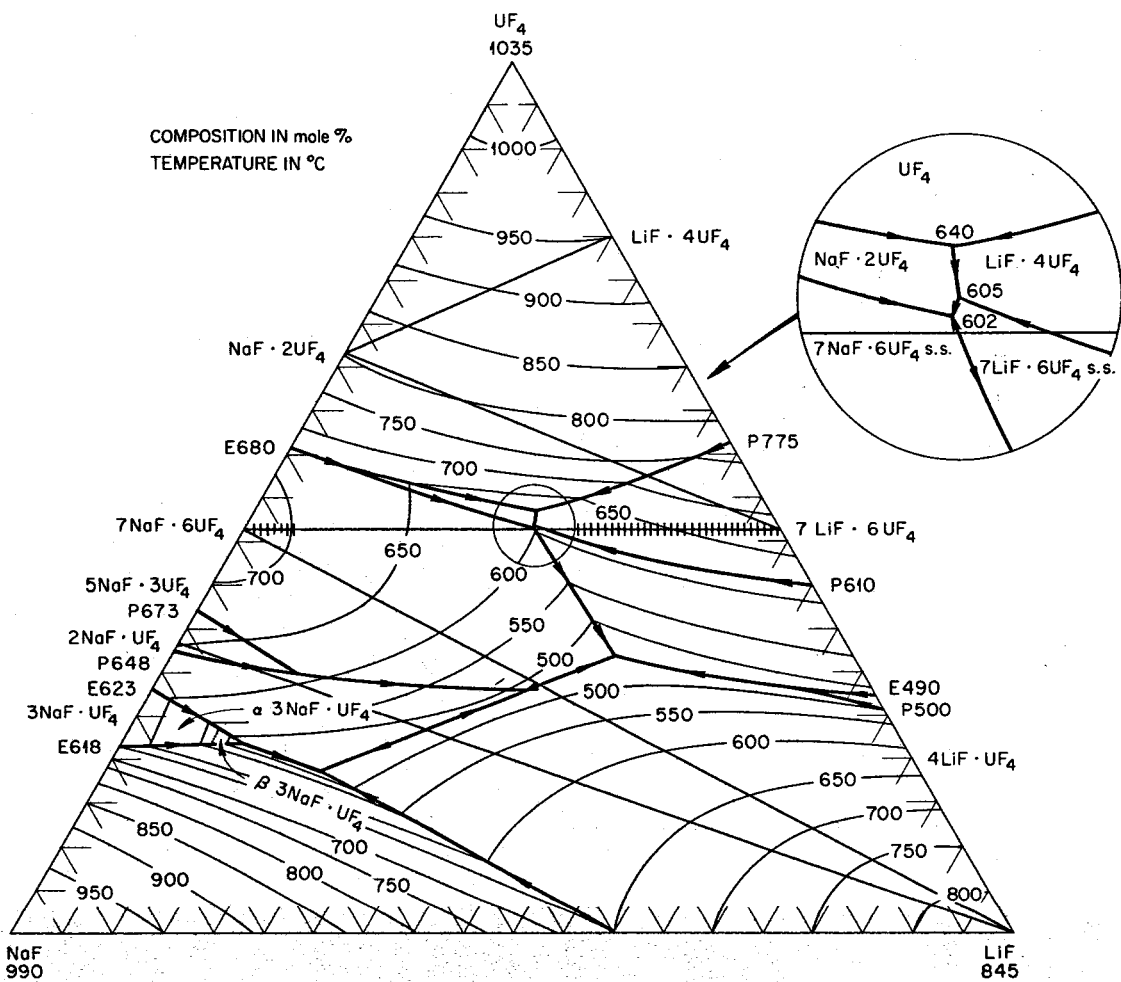
Fig. 3.64a. The System LiF–NaF–UF₄.
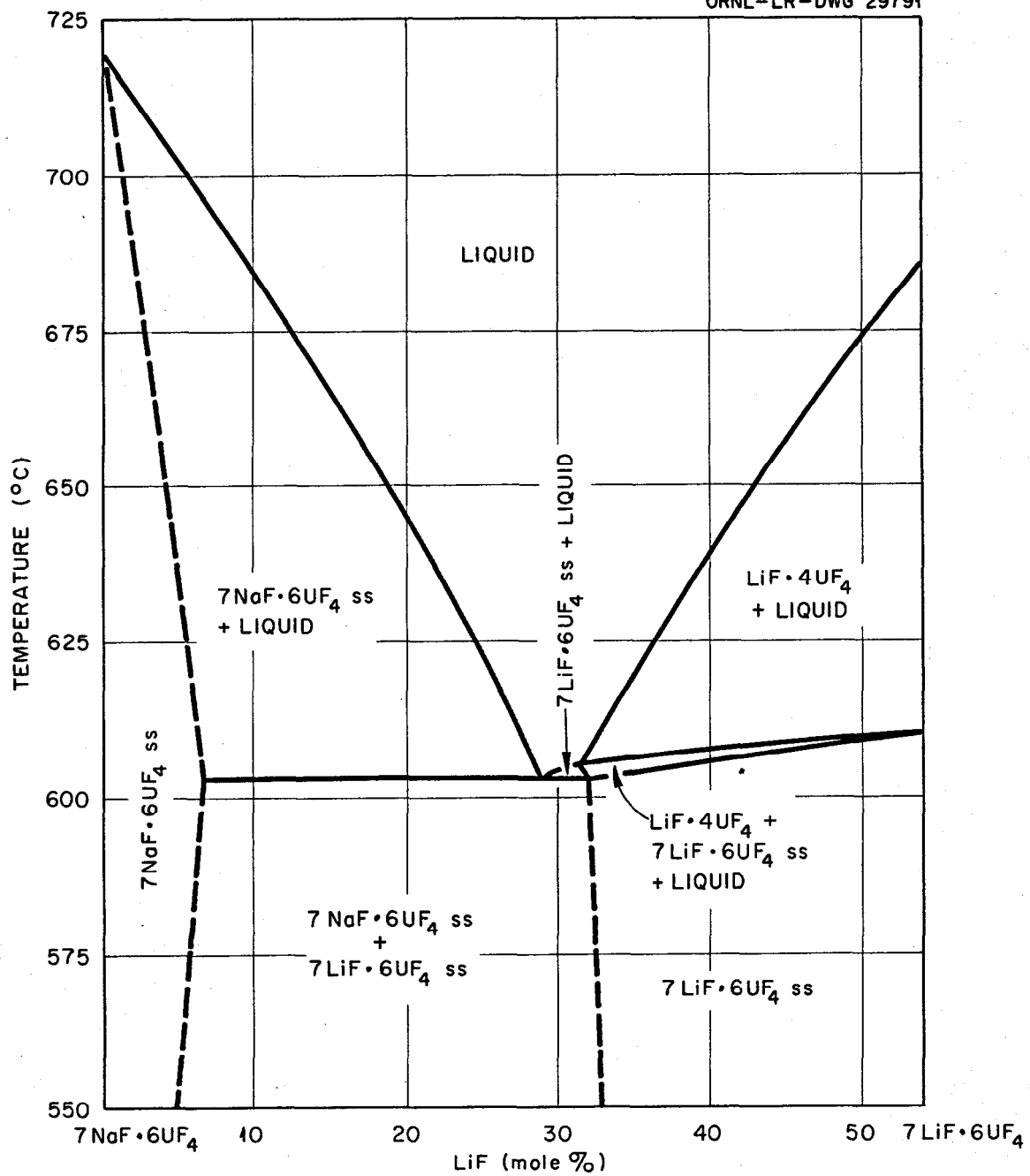
Fig. 3.64b. The Join $7NaF \cdot 6UF_4 - 7LiF \cdot 6UF_4$.

3.65. The System LiF–KF–UF$_4$

C. J. Barton, J. P. Blakely, L. M. Bratcher, and W. R. Grimes, unpublished work performed at the Oak Ridge National Laboratory, 1950–51.

Preliminary diagram. The system LiF–KF–UF$_4$ has not yet been defined at the Oak Ridge National Laboratory with sufficient precision to permit the temperatures and compositions of the invariant equilibria to be listed.
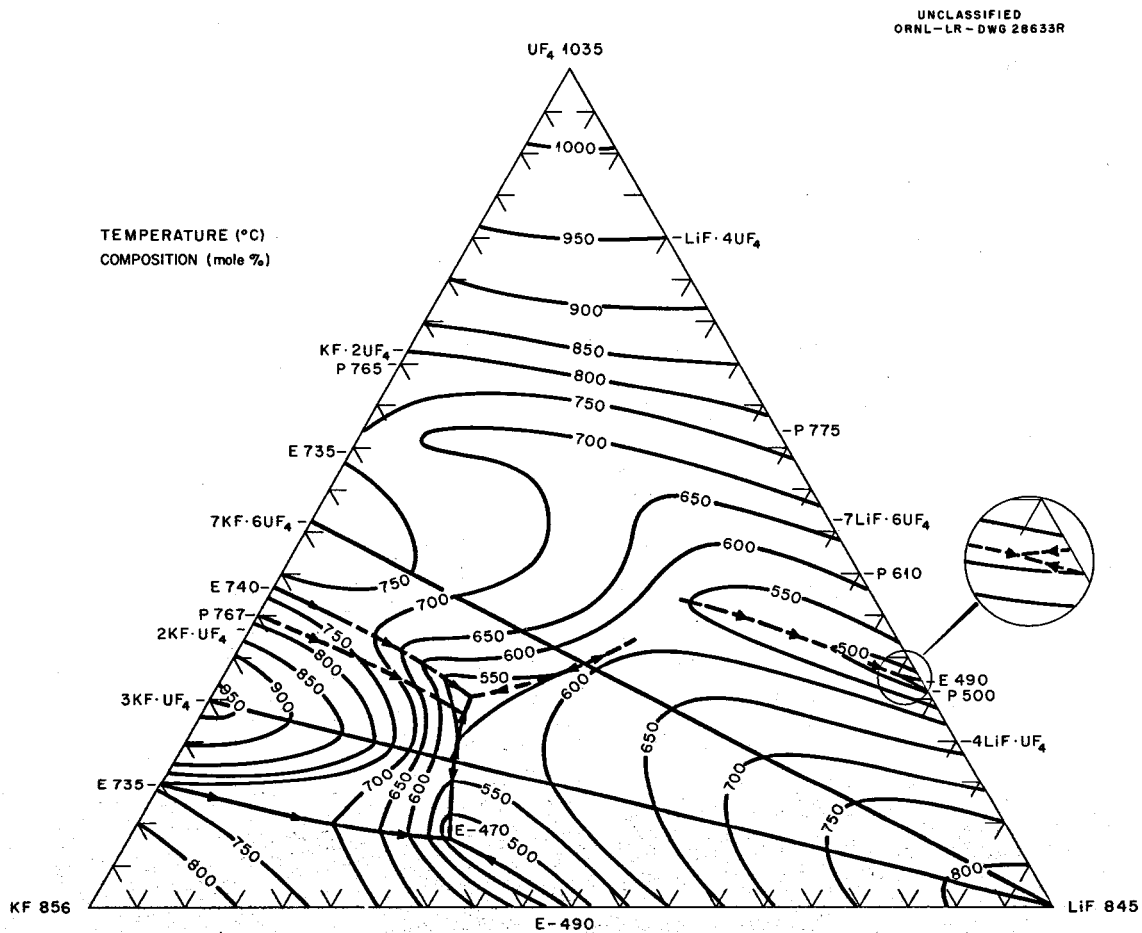
Fig. 3.65. The System LiF–KF–UF$_4$.

3.66. The System LiF–RbF–UF$_4$

C. J. Barton, J. P. Blakely, L. M. Bratcher, and W. R. Grimes, unpublished work performed at the Oak Ridge National Laboratory, 1950–51.

Preliminary diagram. Phase relationships within the system LiF–RbF–UF$_4$ have not yet become so well defined at the Oak Ridge National Laboratory that the compositions and temperatures of the invariant points may be listed.

UF$_4$ 1035

TEMPERATURE IN °C
COMPOSITION IN mole %

RbF·6UF$_4$

LiF·4UF$_4$

P–832

2RbF·3UF$_4$
P–730
P–722
E–714

P 775

RbF·UF$_4$

7RbF·6UF$_4$
P–693
E–675

7LiF·6UF$_4$

P–818

P 610

2RbF·UF$_4$

3RbF·UF$_4$

E 490
P 500

4LiF·UF$_4$

E–710

E–450

E–470

RbF
790

LiF
845

1000, 950, 900, 850, 800, 750, 700, 650, 600, 550, 550, 600, 650, 700, 750, 800, 850, 900, 950, 500, 750, 800
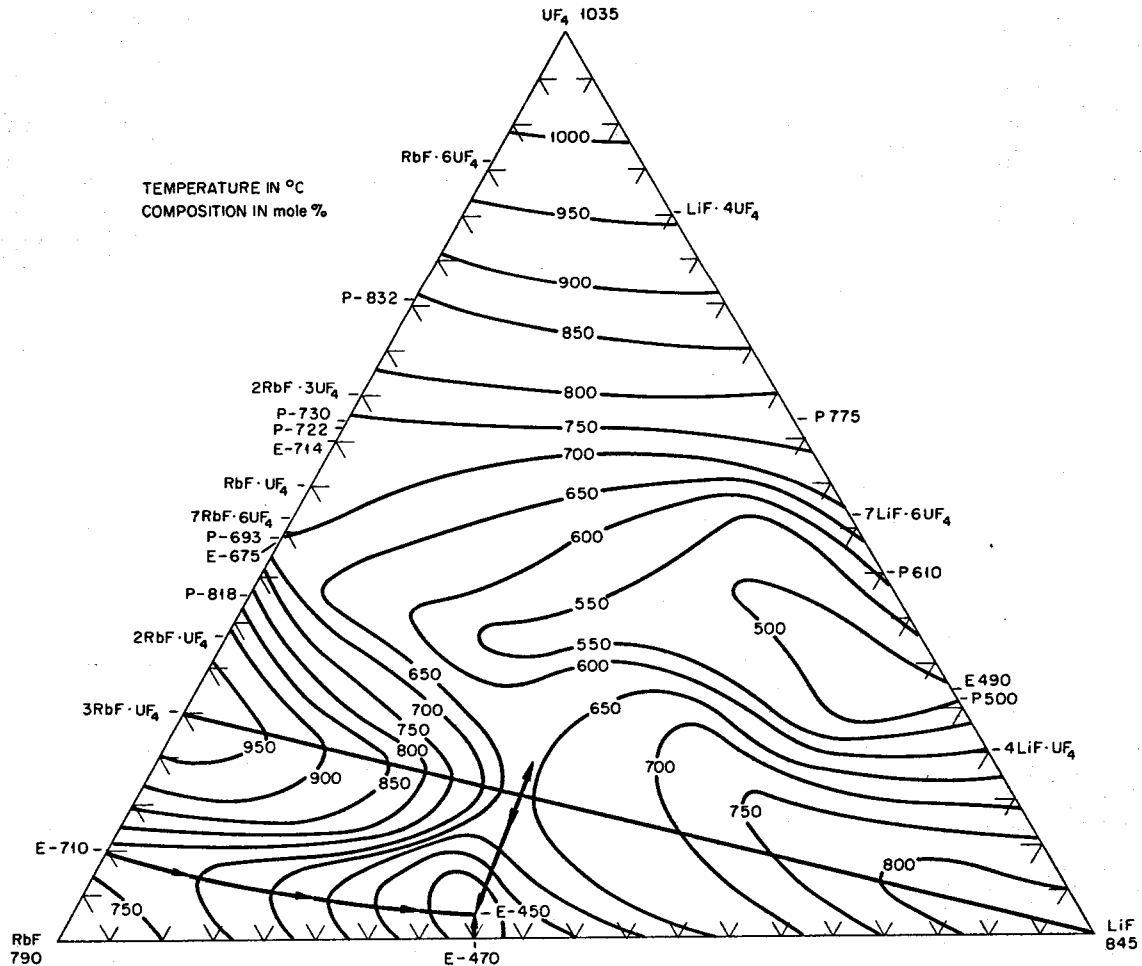
Fig. 3.66. The System LiF–RbF–UF$_4$.

102

3.67. The System NaF–KF–UF$_4$

R. E. Thoma, C. J. Barton, J. P. Blakely, R. E. Moore, G. J. Nessle, H. Insley, and H. A. Friedman, unpublished work performed at the Oak Ridge National Laboratory, 1950–58.

Preliminary diagram. Phase relationships within the system NaF–KF–UF$_4$ have not yet become so well defined at the Oak Ridge National Laboratory that the compositions and temperatures of the invariant points may be listed.
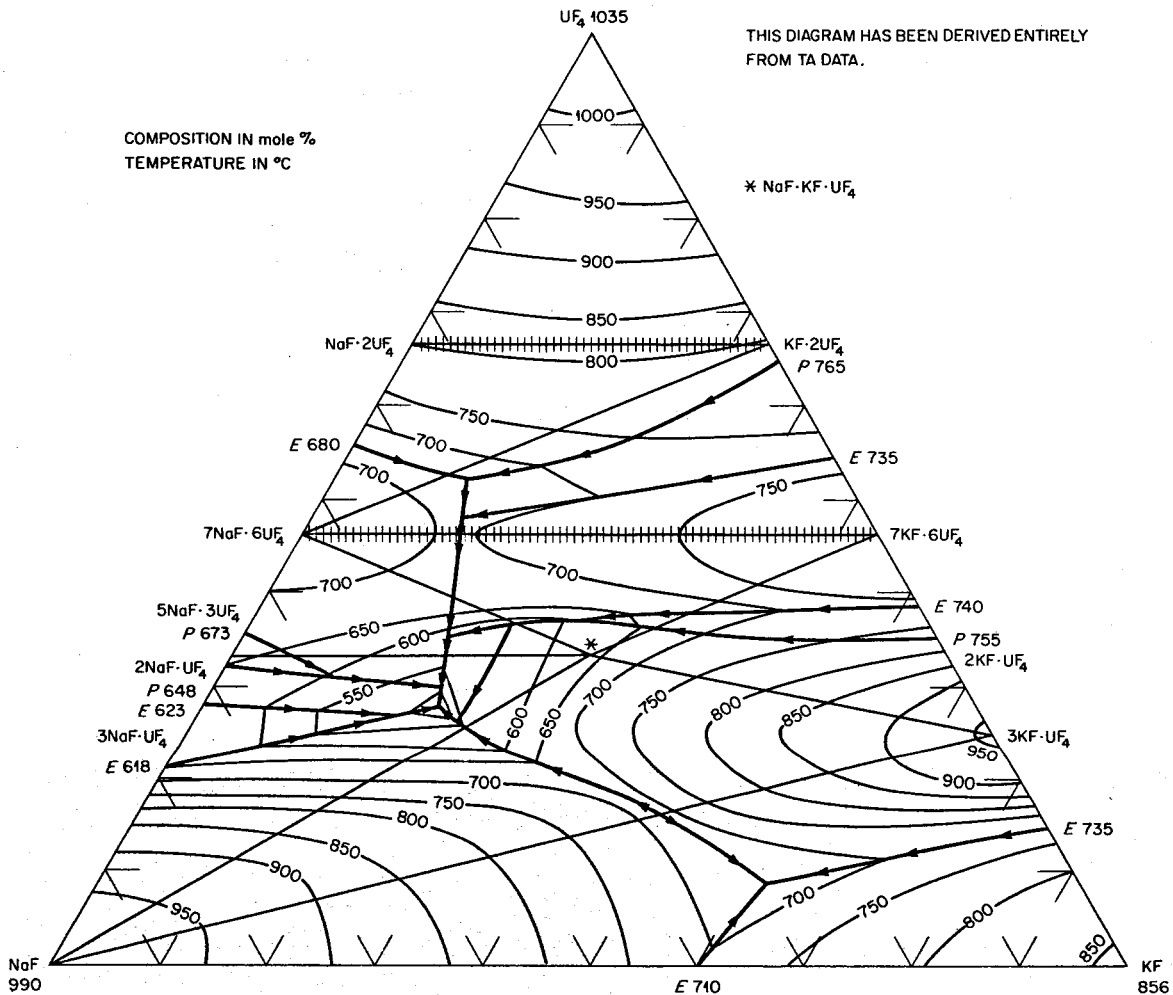
Fig. 3.67. The System NaF–KF–UF$_4$.
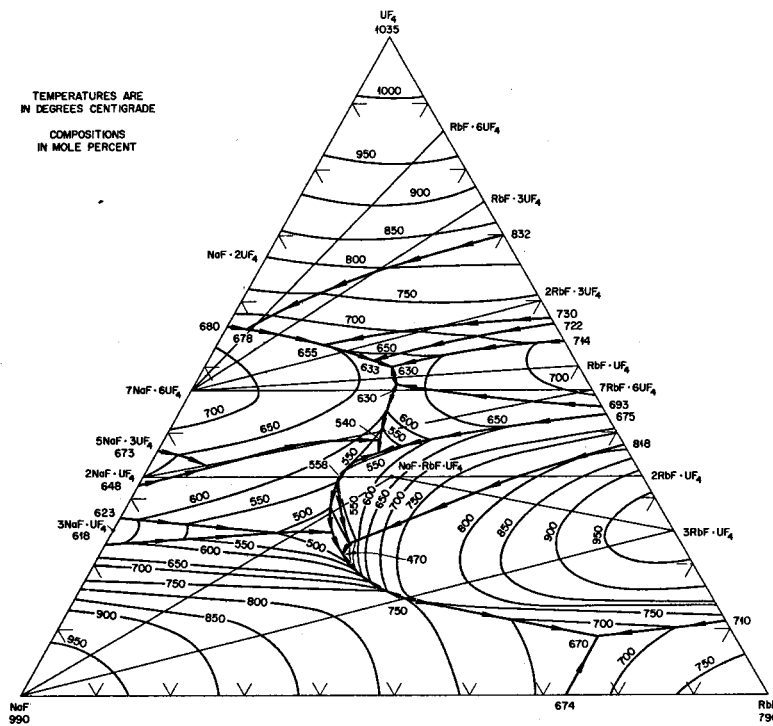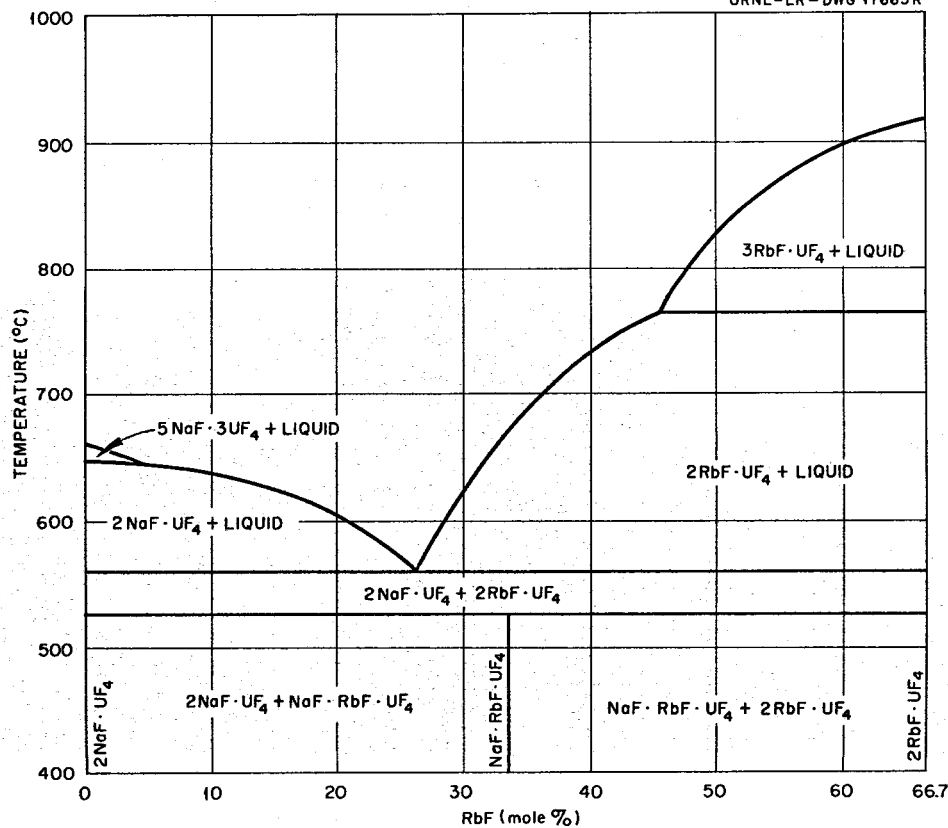
3.68. The System NaF–RbF–UF$_4$

R. E. Thoma, H. Insley, H. A. Friedman, and W. R. Grimes, unpublished work performed at the Oak Ridge National Laboratory, 1955–56.

Preliminary diagram.

Invariant Equilibria

| Composition of Liquid (mole %)			Invariant Temperature (°C)	Type of Equilibrium	Solid Phases Present at Invariant Point
NaF	RbF	UF$_4$			
18	73	9	670	Eutectic	RbF, NaF, and 3RbF·UF$_4$
46	33	21	470	Eutectic	NaF, NaF·RbF·UF$_4$, and 3RbF·UF$_4$
44	33	23	500	Peritectic	NaF·RbF·UF$_4$, 2RbF·UF$_4$, and 3RbF·UF$_4$
45	30	25	485	Peritectic	NaF, 2NaF·UF$_4$, and NaF·RbF·UF$_4$
52	23	25	500	Decomposition	3NaF·UF$_4$, NaF, and 2NaF·UF$_4$
41	26	33	555	Peritectic	2RbF·UF$_4$, 2NaF·UF$_4$, and NaF·RbF·UF$_4$
57	8	35	630	Decomposition	2NaF·UF$_4$, 5NaF·3UF$_4$, and 7NaF·6UF$_4$
33	30	37	535	Eutectic	2RbF·UF$_4$, 2NaF·UF$_4$, and 7RbF·6UF$_4$
32	29	39	540	Peritectic	7RbF·6UF$_4$, 2NaF·UF$_4$, and 7NaF·6UF$_4$
26	27	47	620	Eutectic	7RbF·6UF$_4$, 7NaF·6UF$_4$, and RbF·UF$_4$
25	25	50	630	Eutectic	7NaF·6UF$_4$, RbF·UF$_4$, and 2RbF·3UF$_4$
27	22	51	633	Peritectic	7NaF·6UF$_4$, 2RbF·3UF$_4$, and RbF·3UF$_4$
33	14	53	655	Peritectic	7NaF·6UF$_4$, RbF·3UF$_4$, and RbF·6UF$_4$
42	3	55	678	Peritectic	7NaF·6UF$_4$, RbF·6UF$_4$, and UF$_4$

Fig. 3.68a. The System NaF-RbF-UF$_4$.

Fig. 3.68b. The Section 2NaF·UF$_4$-2RbF·UF$_4$.
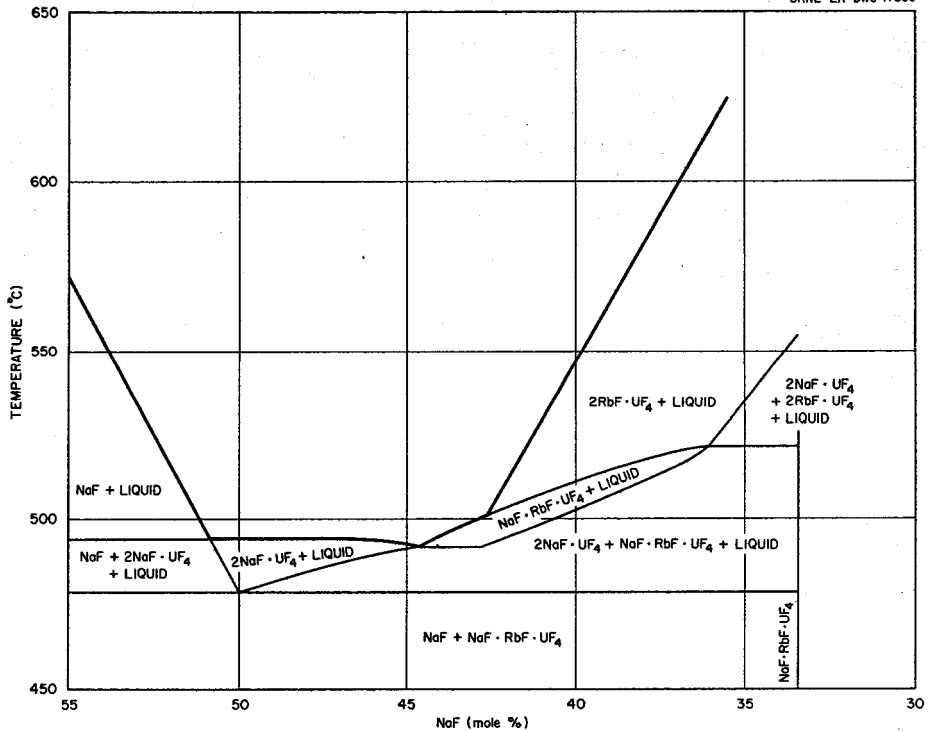
Fig. 3.68c. The Section NaF–NaF·RbF·UF$_4$.
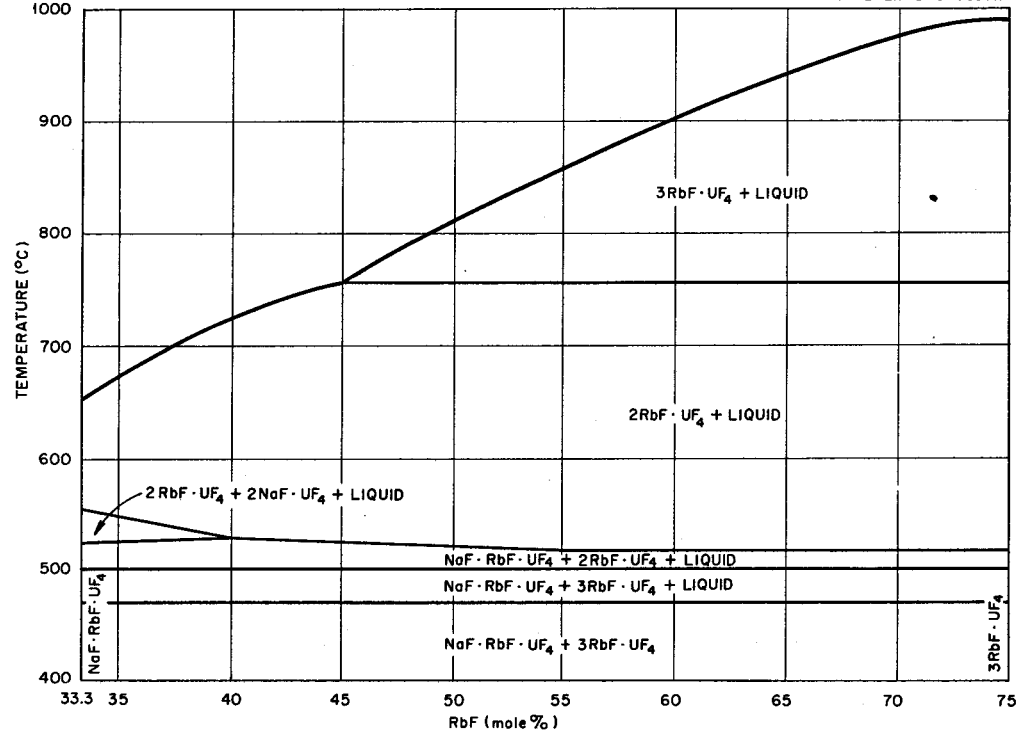
Fig. 3.68d. The Section 3RbF·UF₄-NaF·RbF·UF₄.

3.69. The System LiF–BeF$_2$–UF$_4$

L. V. Jones, D. E. Etter, C. R. Hudgens, A. A. Huffman, T. B. Rhinehammer, N. E. Rogers, P. A. Tucker, and L. J. Wittenberg, *Phase Equilibria in the LiF–BeF$_2$–UF$_4$ Ternary Fused Salt System*, MLM-1080 (Aug. 24, 1959).
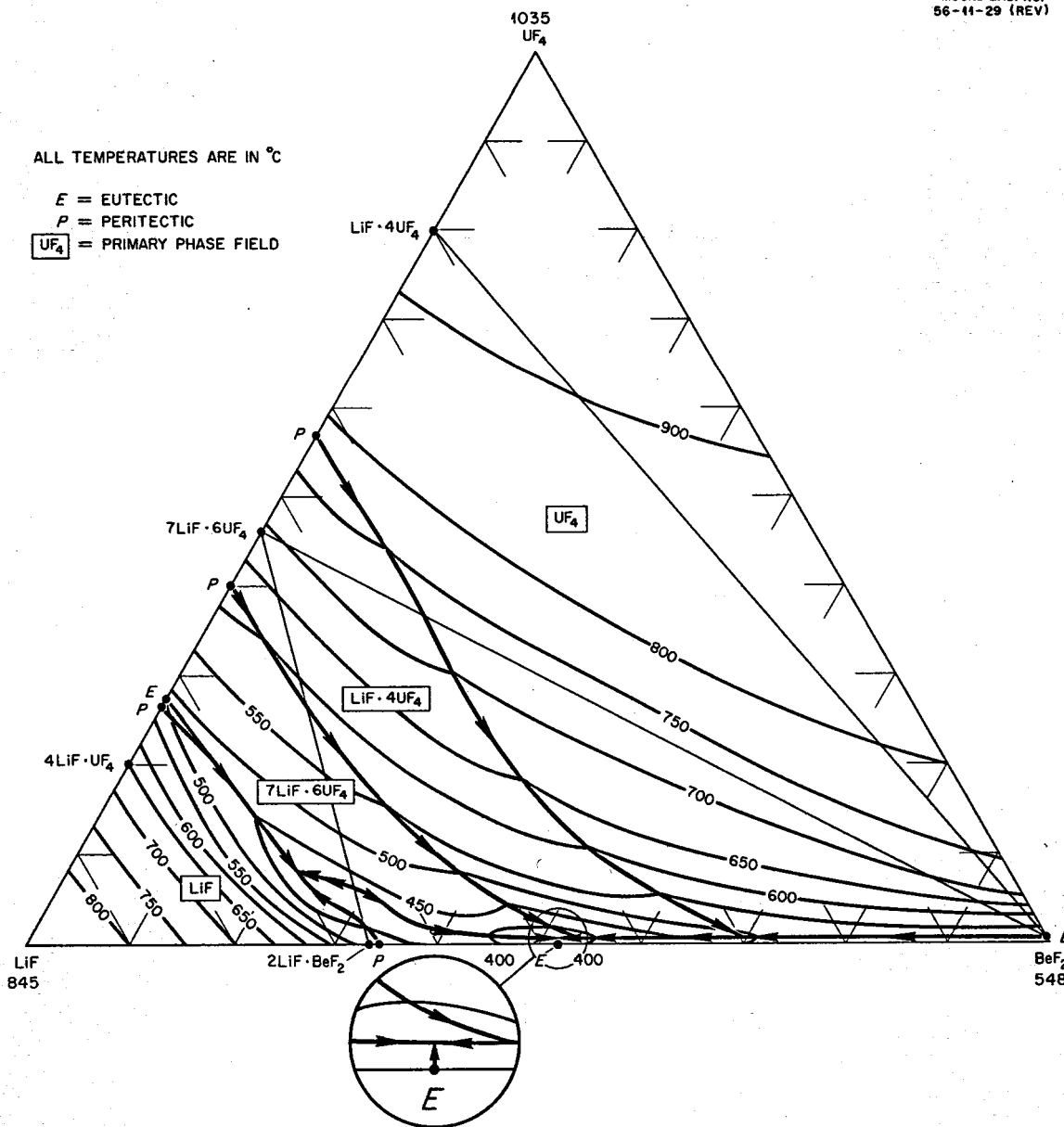
Fig. 3.69a. The System LiF–BeF$_2$–UF$_4$.

Preliminary diagram.

Composition of Liquid (mole %)			Temperature (°C)	Type of Equilibrium	Solid Phases Present at Invariant Temperature
LiF	BeF$_2$	UF$_4$			
72	6	22	480	Peritectic (decomposition of 4LiF·UF$_4$ in the ternary system)	4LiF·UF$_4$, LiF, and 7LiF·6UF$_4$
69	23	8	426	Eutectic	LiF, 2LiF·BeF$_2$, and 7LiF·6UF$_4$
48	51.5	0.5	350	Eutectic	7LiF·6UF$_4$, 2LiF·BeF$_2$, and BeF$_2$
45.5	54	0.5	381	Peritectic	LiF·4UF$_4$, 7LiF·6UF$_4$, and BeF$_2$
29.5	70	0.5	483	Peritectic	UF$_4$, LiF·4UF$_4$, and BeF$_2$

The minimum temperature in the quasi-binary system 2LiF·BeF$_2$–7LiF·6UF$_4$ occurs at 65 LiF–29 BeF$_2$–6 UF$_4$ (mole %) at 438°C.

A three-dimensional model of the system LiF–BeF$_2$-UF$_4$ is shown in Fig. 3.69b.
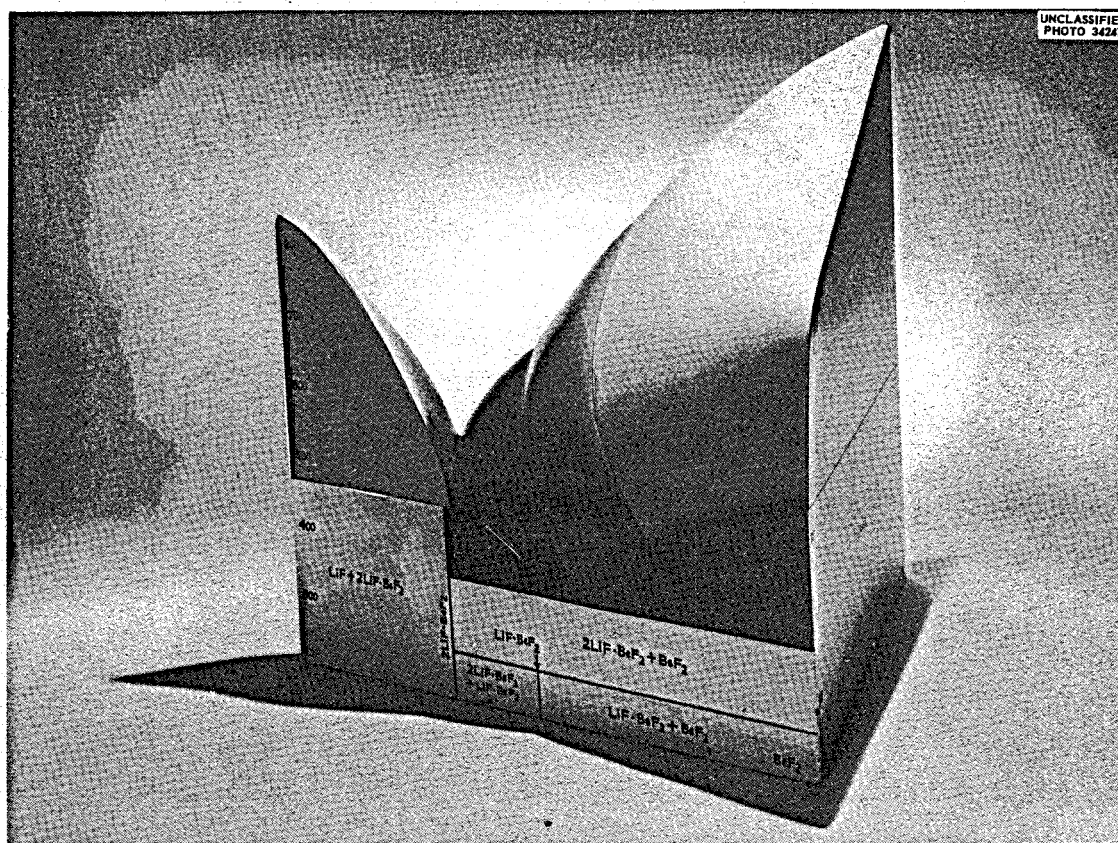
Fig. 3.69b. Model of the System LiF–BeF$_2$–UF$_4$.

3.70. The System $NaF-BeF_2-UF_4$

J. F. Eichelberger, C. R. Hudgens, L. V. Jones, G. Pish, T. B. Rhinehammer, P. A. Tucker, and L. J. Wittenberg, unpublished work performed at the Mound Laboratory, 1956–57.

Preliminary diagram.

Invariant Equilibria

Composition of Liquid (mole %)			Temperature (°C)	Type of Equilibrium	Solid Phases Present at Invariant Temperature
NaF	BeF$_2$	UF$_4$			
74	12	14	500	Peritectic (decomposition of 3NaF·UF$_4$ in ternary system)	3NaF·UF$_4$, NaF, and 2NaF·UF$_4$
72.5	17	19.5	486	Eutectic	NaF, 2NaF·UF$_4$, and 2NaF·BeF$_2$
64.5	9	26.5	630	Peritectic (decomposition of 5NaF·3UF$_4$ in the ternary system)	5NaF·3UF$_4$, 2NaF·UF$_4$, and 7NaF·6UF$_4$
57	42	1	378	Peritectic	2NaF·BeF$_2$, 2NaF·UF$_4$, and 7NaF·6UF$_4$
56	43.5	0.5	339	Eutectic	2NaF·BeF$_2$, NaF·BeF$_2$, and 7NaF·6UF$_4$
43.5	55.5	1	357	Eutectic	7NaF·6UF$_4$, BeF$_2$, and NaF·BeF$_2$
41	58	1	375	Peritectic	7NaF·6UF$_4$, NaF·2UF$_4$, and BeF$_2$
26	63	1	409	Peritectic	NaF·2UF$_4$, NaF·4UF$_4$, and BeF$_2$
44	18	38	665	Peritectic	7NaF·6UF$_4$, UF$_4$, and NaF·2UF$_4$
40	47	13	548	Peritectic	UF$_4$, NaF·2UF$_4$, and NaF·4UF$_4$
27	72	1	498	Peritectic	UF$_4$, BeF$_2$, and NaF·4UF$_4$

The minimum temperature in the quasi-binary system 2NaF·BeF$_2$–2NaF·UF$_4$ occurs at 66.7 LiF–25 BeF$_2$–8.3 UF$_4$ (mole %) at 528°C. The minimum temperature in the quasi-binary system NaF·BeF$_2$–7NaF·6UF$_4$ occurs at 50.5 NaF–48.5 BeF$_2$–1.0 UF$_4$ (mole %) at 367°C.

A three-dimensional model of the system $NaF-BeF_2-UF_4$ has been constructed by the authors and is shown in Fig. 3.70b.

ALL TEMPERATURES ARE IN °C

E = EUTECTIC
P = PERITECTIC
$\boxed{UF_4}$ = PRIMARY PHASE FIELD
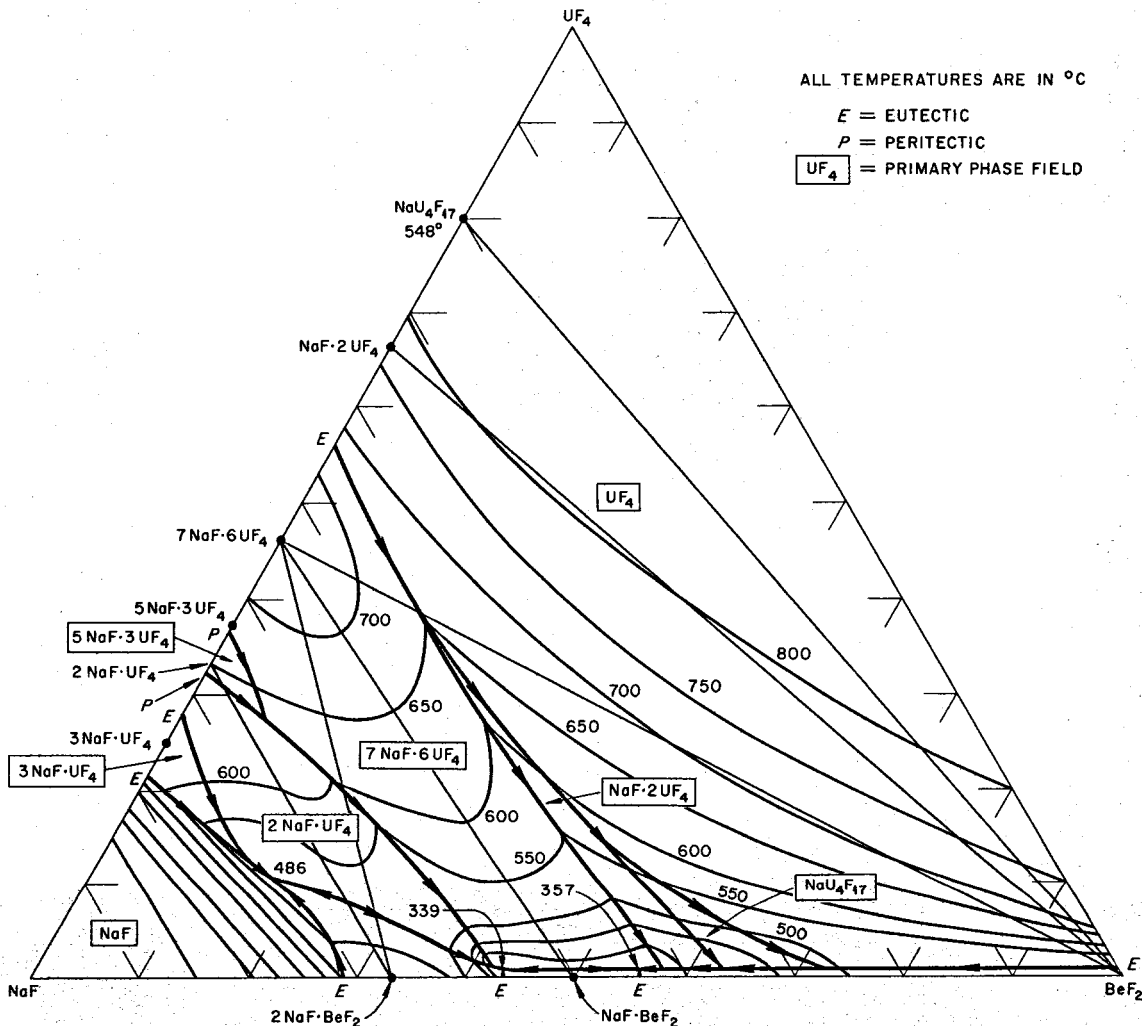
Fig. 3.70a. The System NaF–BeF$_2$–UF$_4$.
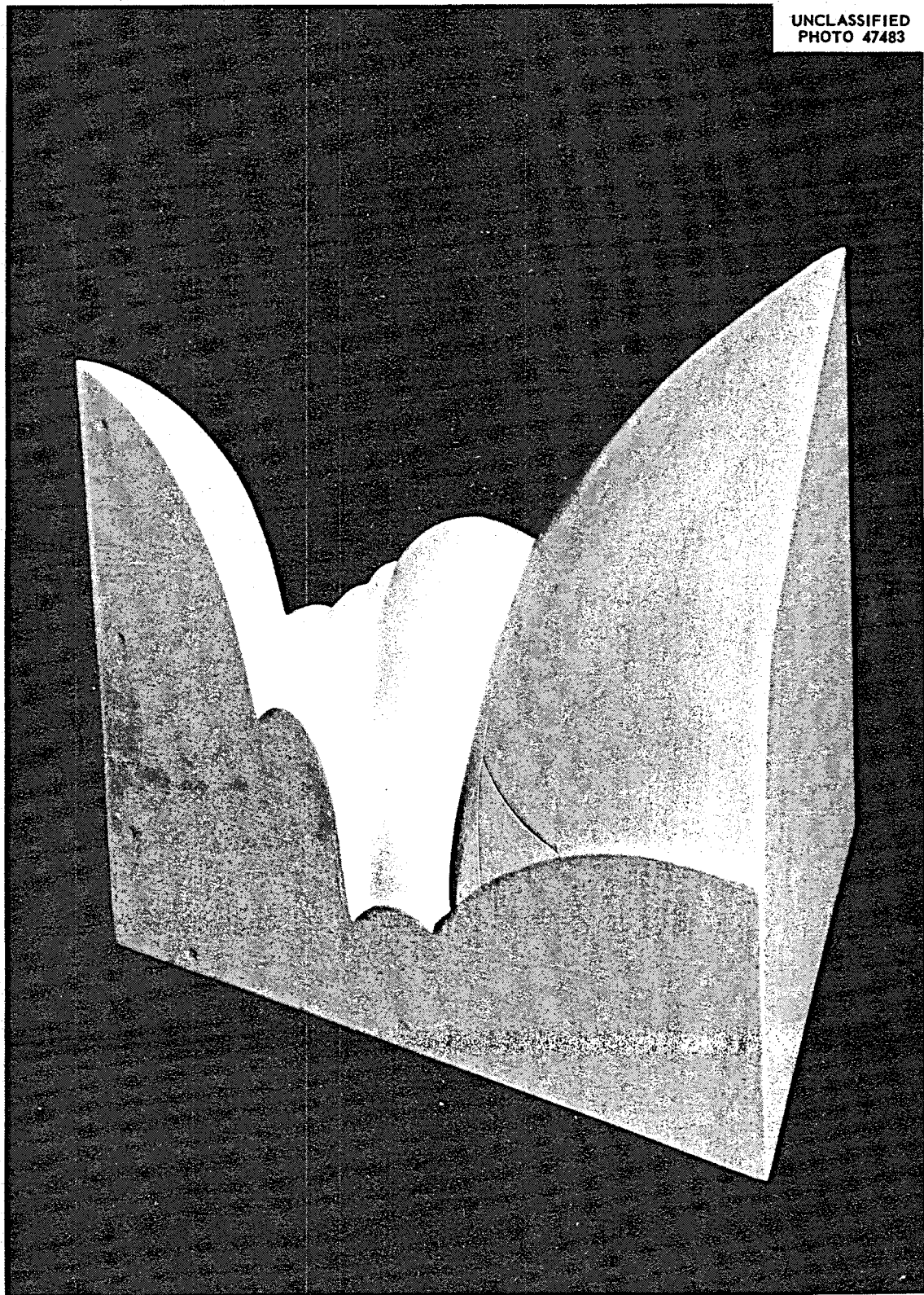
Fig. 3.70*b*. Model of the System NaF–BeF$_2$–UF$_4$.

3.71. The System $NaF-PbF_2-UF_4$

C. J. Barton, J. P. Blakely, G. J. Nessle, L. M. Bratcher, and W. R. Grimes, unpublished work performed at the Oak Ridge National Laboratory, 1950–51.

Preliminary diagram. No study has been made at the Oak Ridge National Laboratory of the phase relationships within the system $NaF-PbF_2-UF_4$.
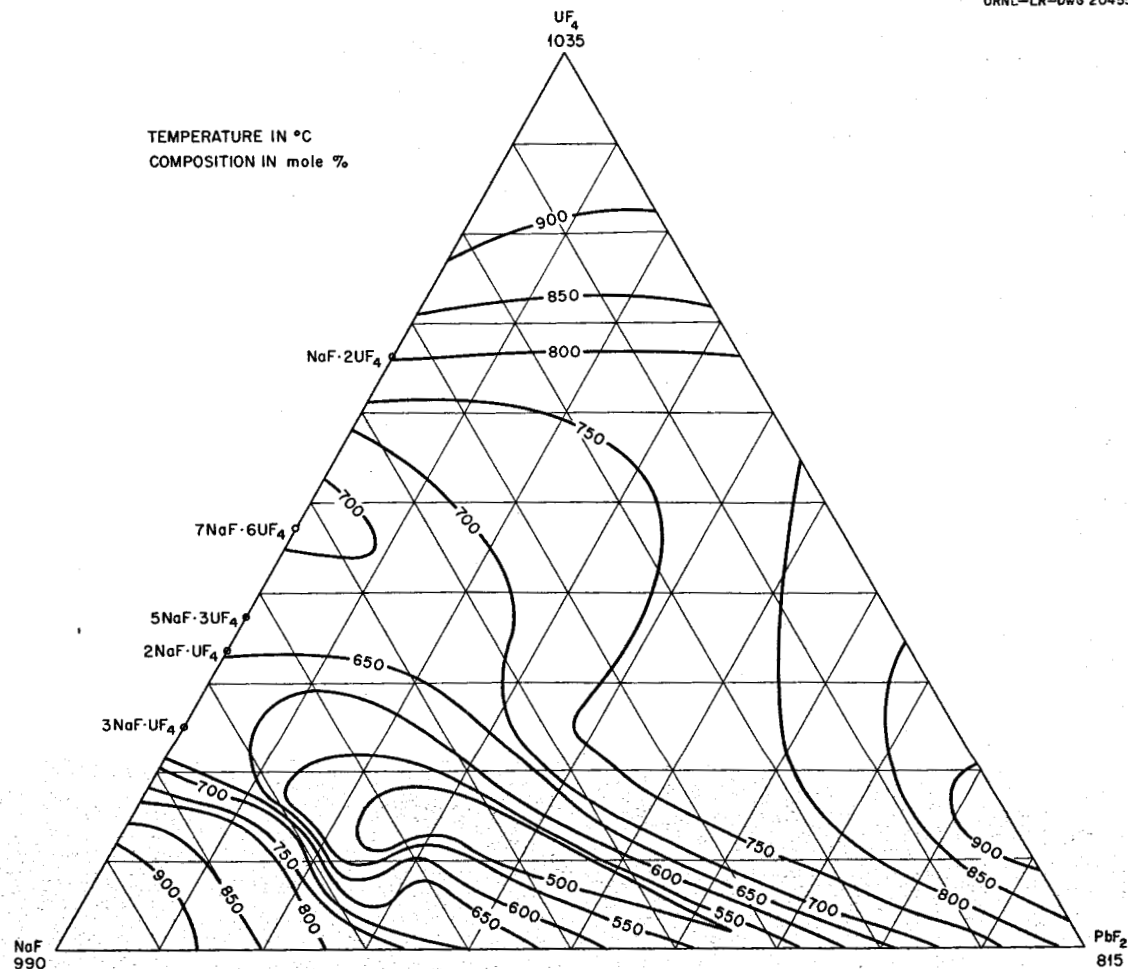
Fig. 3.71. The System $NaF-PbF_2-UF_4$.

3.72. The system $KF-PbF_2-UF_4$

C. J. Barton, J. P. Blakely, G. J. Nessle, L. M. Bratcher, and W. R. Grimes, unpublished work performed at the Oak Ridge National Laboratory, 1950–51.

Preliminary diagram. No study has been made at the Oak Ridge National Laboratory of the phase relationships within the system $KF-PbF_2-UF_4$.
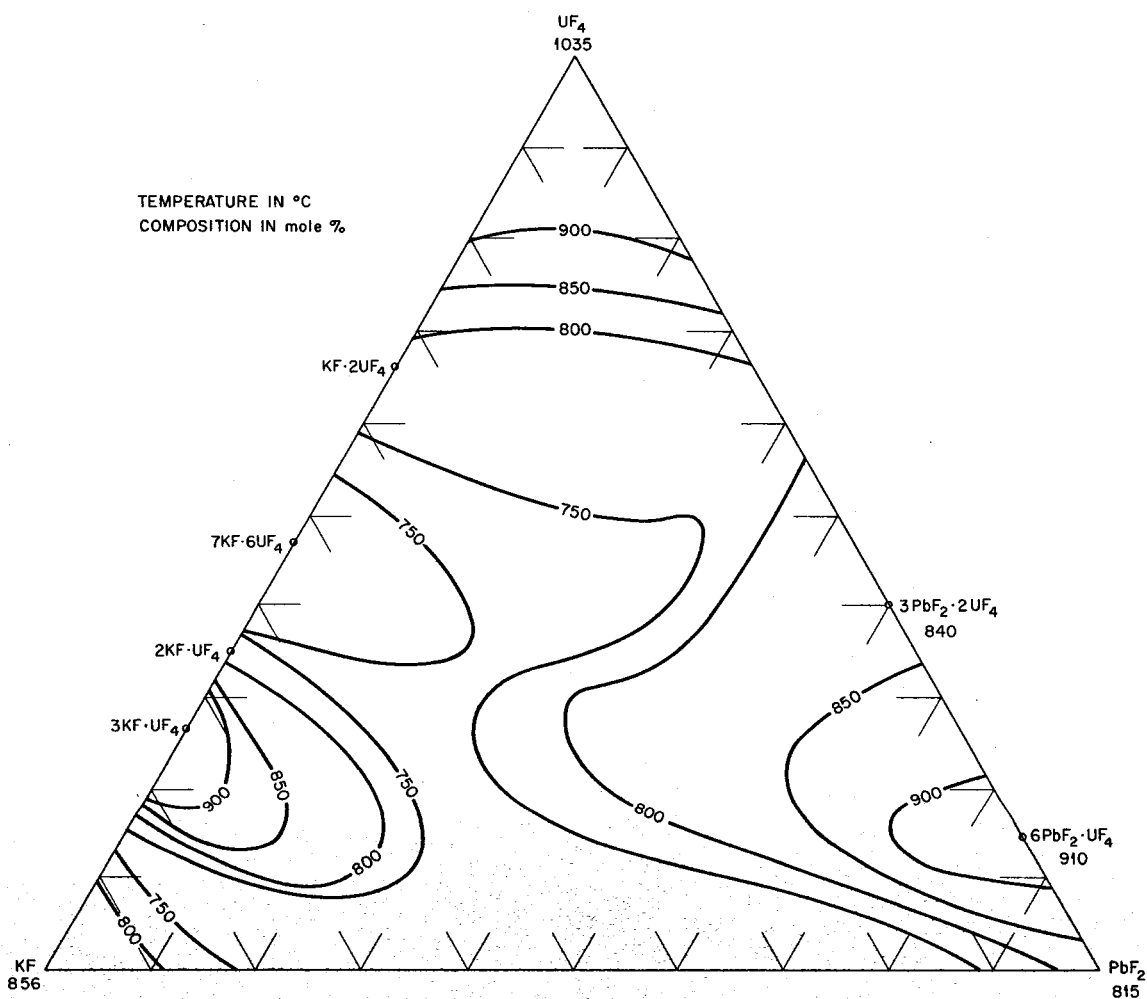
Fig. 3.72. The System KF–PbF$_2$–UF$_4$.

3.73. The System NaF-ZrF$_4$-UF$_4$

C. J. Barton, W. R. Grimes, H. Insley, R. E. Moore, and R. E. Thoma, "Phase Equilibria in the Systems NaF-ZrF$_4$, UF$_4$-ZrF$_4$, and NaF-ZrF$_4$-UF$_4$," *J. Phys. Chem.* **62**, 665–76 (1958).
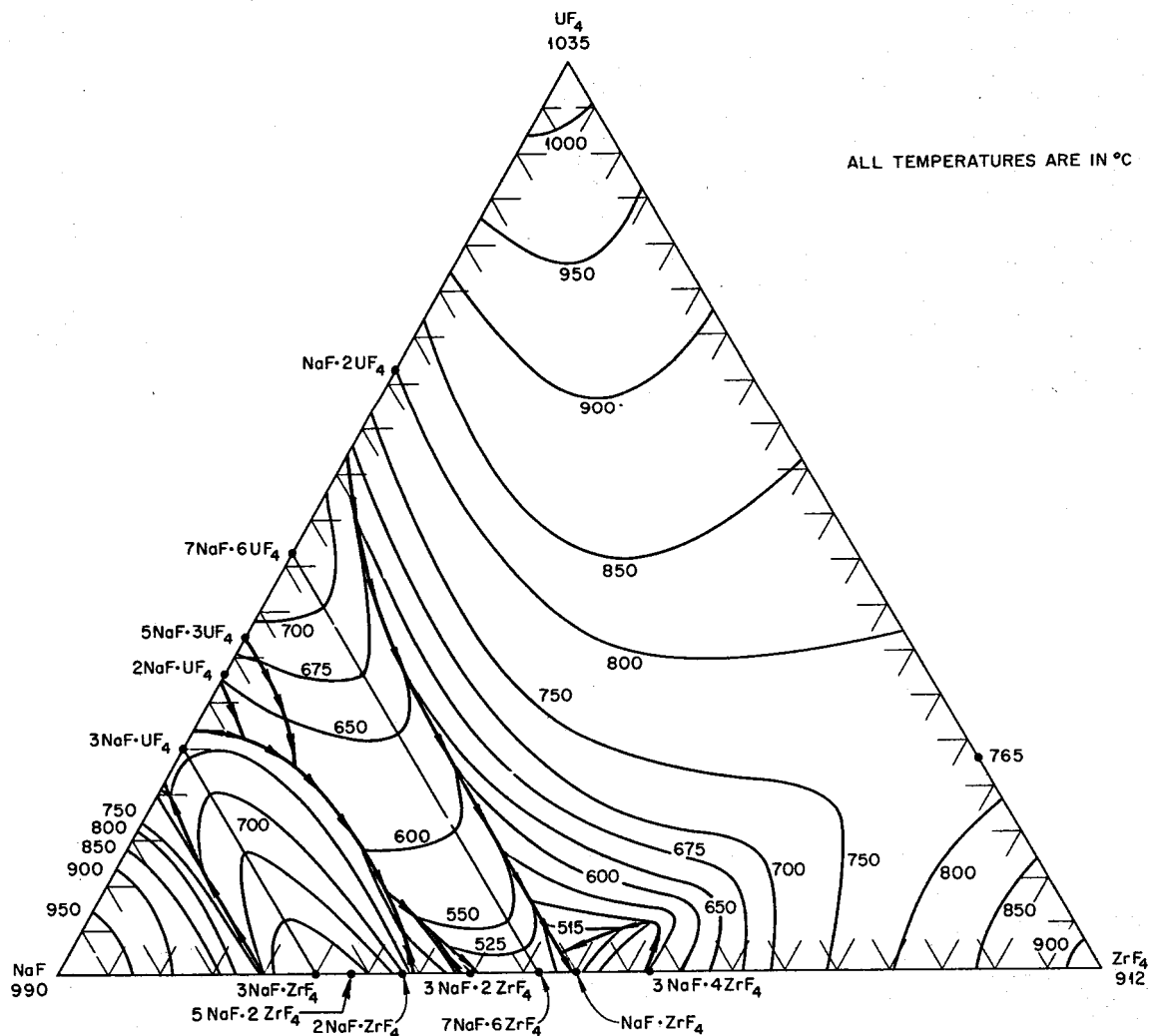
Fig. 3.73a. The System NaF-ZrF$_4$-UF$_4$.

Composition of Liquid (mole %)			Temperature (°C)	Type of Equilibrium	Solids Present at Invariant Point
NaF	ZrF$_4$	UF$_4$			
69.5	4.0	26.5	646	Maximum temperature of boundary curve	3NaF·(U,Zr)F$_4$ and 2NaF·UF$_4$
68.5	5.5	26.0	640	Peritectic	3NaF·(U,Zr)F$_4$, 2NaF·UF$_4$, and 5NaF·3UF$_4$ss
65.5	12.0	22.5	613	Peritectic or decomposition	3NaF·(U,Zr)F$_4$, 5NaF·3UF$_4$ss, and 7NaF·6(U,Zr)F$_4$
64.0	27.0	9.0	592	Peritectic	3NaF·(U,Zr)F$_4$, 5NaF·2ZrF$_4$ss, and 7NaF·6(U,Zr)F$_4$
61.5	34.5	4.0	540	Peritectic	5NaF·2ZrF$_4$ss, 2NaF·ZrF$_4$, and 7NaF·6(U,Zr)F$_4$
50.5	47	2.5	513	Peritectic	7NaF·6(U,Zr)F$_4$, (U,Zr)F$_4$, and 3NaF·4ZrF$_4$

UNCLASSIFIED
ORNL–LR–DWG 19888

▲ LIQUIDUS POINTS FROM THERMAL GRADIENT QUENCHING EXPERIMENTS
● SOLIDUS POINTS FROM THERMAL GRADIENT QUENCHING EXPERIMENTS
■ LIQUIDUS POINTS FROM THERMAL ANALYSIS
△ INITIAL COMPOSITION OF FILTRATION MIXTURES
□ FILTRATION RESIDUE COMPOSITIONS
○ FILTRATE COMPOSITIONS
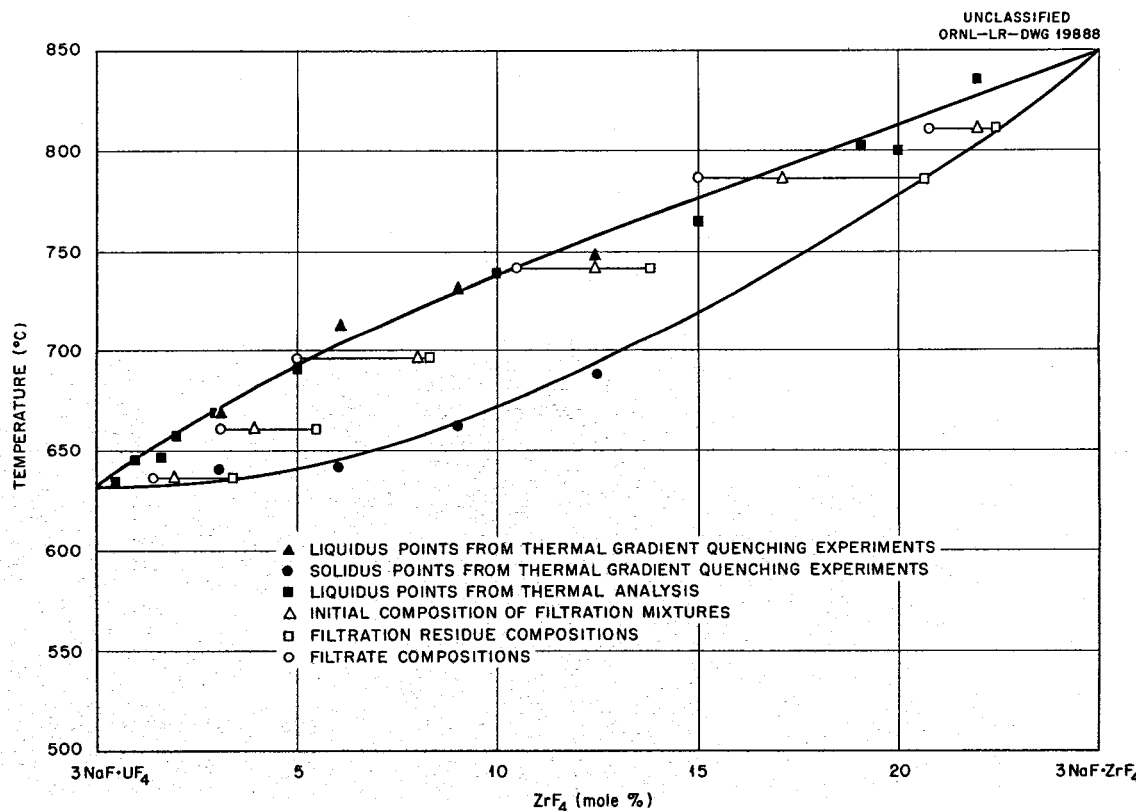
Fig. 3.73b. The Subsystem 3NaF·UF$_4$–3NaF·ZrF$_4$.
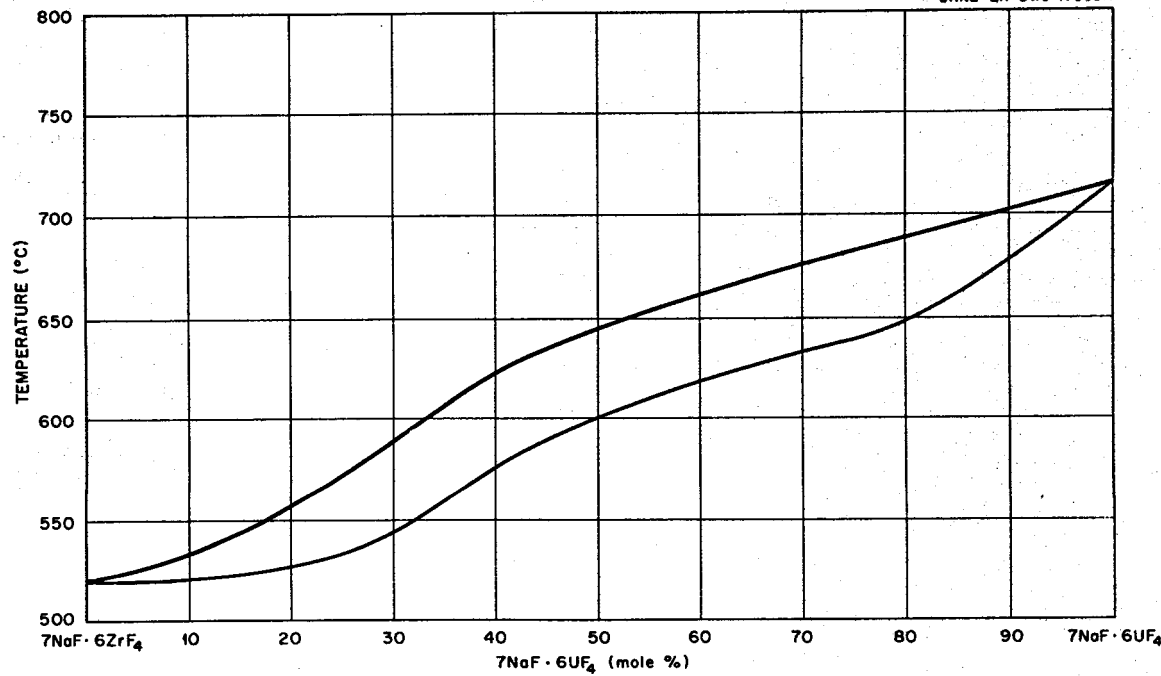
Fig. 3.73c. The Subsystem 7NaF·6ZrF$_4$–7NaF·6UF$_4$.

3.74. The System LiF–ThF$_4$–UF$_4$

C. F. Weaver, R. E. Thoma, H. Insley, and H. A. Friedman, "Phase Equilibria in the Systems UF$_4$–ThF$_4$ and LiF–ThF$_4$–UF$_4$," paper presented at the 61st National Meeting of the American Ceramic Society, Chicago, Ill., May 17–21, 1959.

<div align="center">Invariant Equilibria</div>

Composition of Liquid (mole %)			Invariant Temperature (°C)	Type of Equilibrium	Solids Present at Invariant Point
LiF	ThF$_4$	UF$_4$			
72.5	7.0	20.5	500	Peritectic	LiF, 3LiF·(Th,U)F$_4$, and 7LiF·6(U,Th)F$_4$
72.0	1.5	26.5	488	Eutectic	LiF, 4LiF·UF$_4$, and 7LiF·6(U,Th)F$_4$
53	18	19	609	Peritectic	7LiF·6(U,Th)F$_4$, LiF·2(Th,U)F$_4$, and LiF·4(U,Th)F$_4$

A three-dimensional model of the system LiF–ThF$_4$–UF$_4$ is shown in Fig. 3.74e.
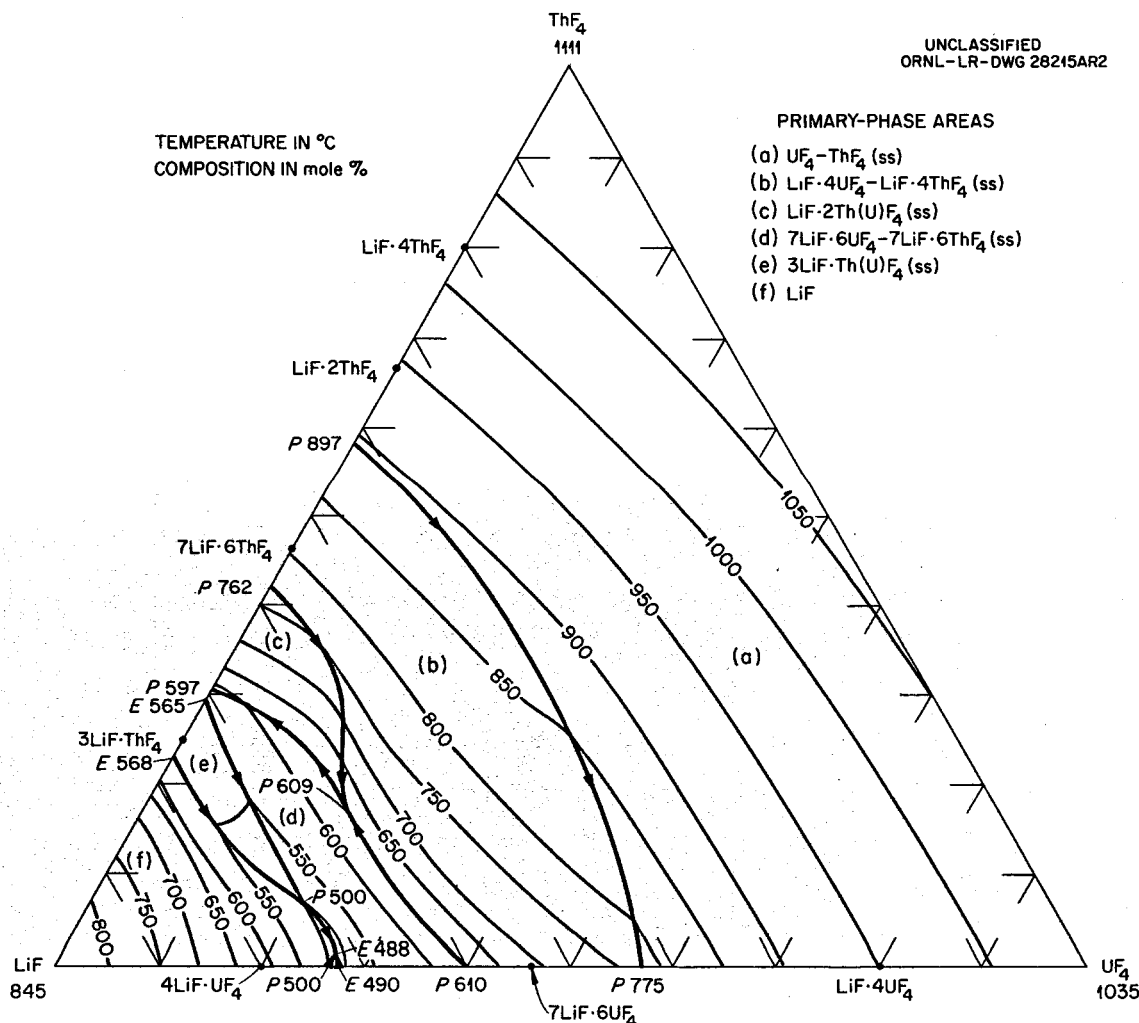
Fig. 3.74a. The System LiF–ThF$_4$–UF$_4$.

119

(a) LIQUID + 3 LiF · ThF$_4$ ss

(b) LiF + LIQUID

(c) LiF + 3 LiF · ThF$_4$ ss + LIQUID

(d) LiF + 7 LiF · 6 ThF$_4$ − 7 LiF · 6 UF$_4$ ss + LIQUID

(e) 4 LiF · UF$_4$ + LIQUID + LiF

(f) 4 LiF · UF$_4$ + LIQUID

(g) 4 LiF · UF$_4$ + 7 LiF · 6 ThF$_4$ − 7 LiF · 6 UF$_4$ ss + LIQUID

(h) 3 LiF · ThF$_4$ ss

(i) 3 LiF · ThF$_4$ ss + 7 LiF · 6 ThF$_4$ − 7 LiF · 6 UF$_4$ ss + LiF

(j) LiF + 7 LiF · 6 ThF$_4$ − 7 LiF · 6 UF$_4$ ss

(k) LiF + 4 LiF · UF$_4$ + 7 LiF · 6 ThF$_4$ − 7 LiF · 6 UF$_4$ ss

(l) 4 LiF · UF$_4$ + 7 LiF · 6 ThF$_4$ − 7 LiF · 6 UF$_4$ ss
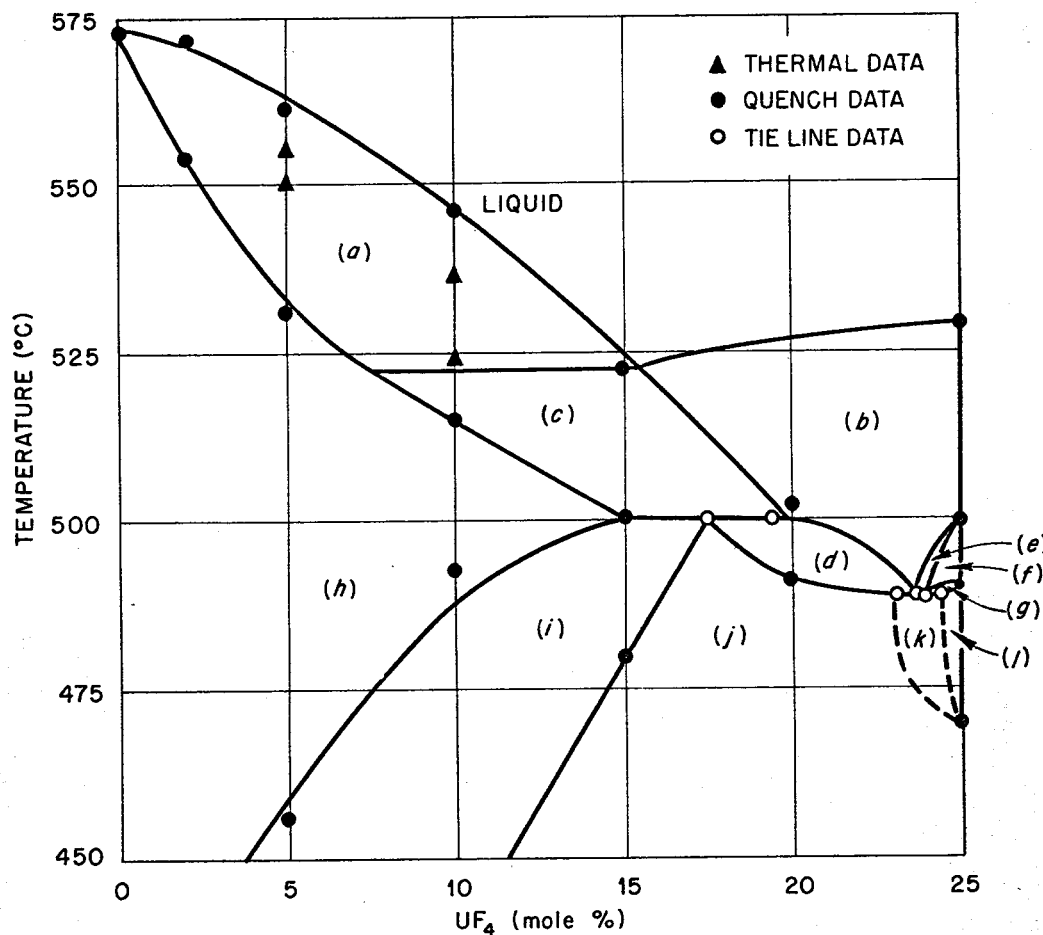
Fig. 3.74b. The System LiF–ThF$_4$–UF$_4$: The Section at 75 Mole % LiF.
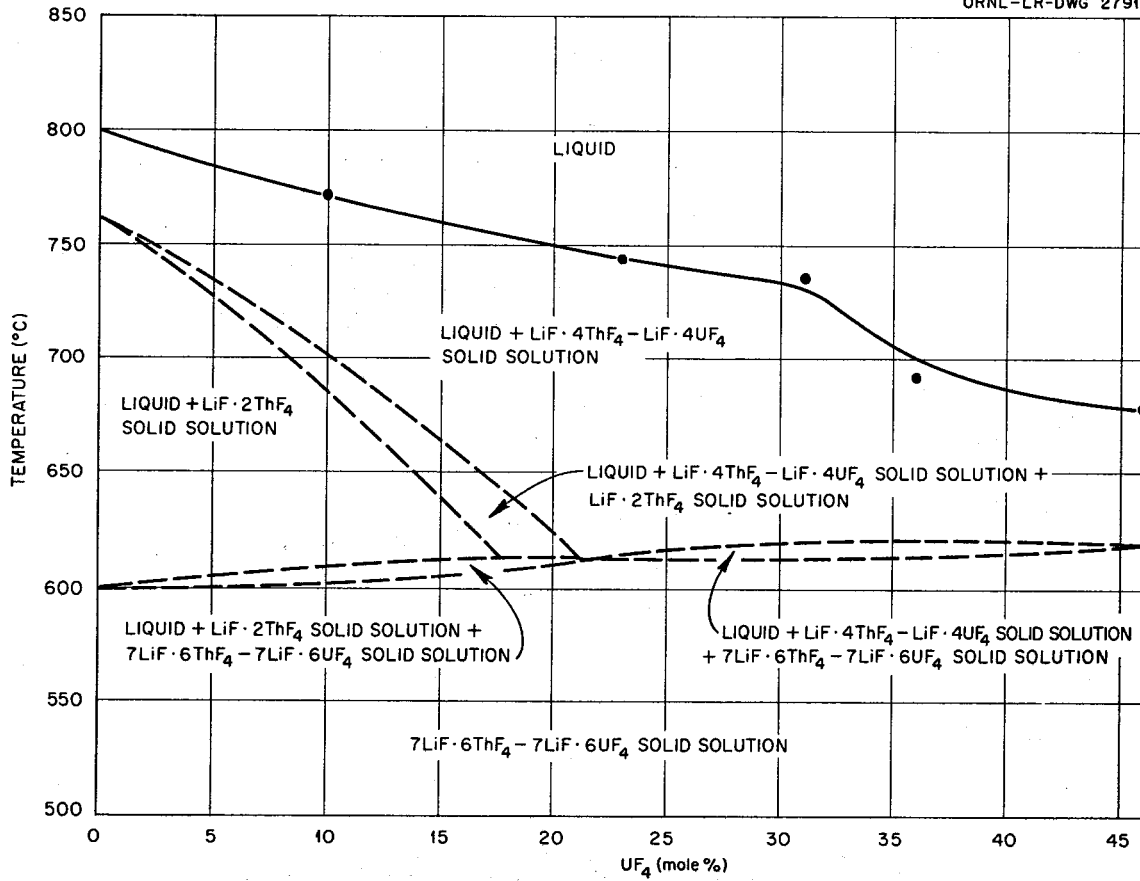
Fig. 3.74c. The System LiF–ThF$_4$–UF$_4$: The Section at 53.8 Mole % LiF.

(a) $UF_4 - ThF_4$ ss + LIQUID

(b) $LiF \cdot 4UF_4 - LiF \cdot 4ThF_4$ + LIQUID

(c) $UF_4 - ThF_4$ ss + LIQUID + $LiF \cdot 4UF_4 - LiF \cdot 4ThF_4$ ss

(d) $LiF \cdot 2ThF_4$ ss + LIQUID + $LiF \cdot 4UF_4 - LiF \cdot 4ThF_4$ ss

(e) $LiF \cdot 4UF_4 - LiF \cdot 4ThF_4$ ss + LIQUID + $7LiF \cdot 6UF_4 - 7LiF \cdot 6ThF_4$ ss

(f) $LiF \cdot 2ThF_4$ ss

(g) $LiF \cdot 4UF_4 - LiF \cdot 4ThF_4$ ss + $7LiF \cdot 6UF_4 - 7LiF \cdot 6ThF_4$ ss

(h) $LiF \cdot 4UF_4 - LiF \cdot 4ThF_4$ ss + $7LiF \cdot 6UF_4 - 7LiF \cdot 6ThF_4$ ss + $LiF \cdot 2ThF_4$ ss

▲ THERMAL BREAKS
● QUENCH RESULTS
○ TIE LINE INTERSECTION

LIQUID

TEMPERATURE (°C)

UF_4 (mole %)
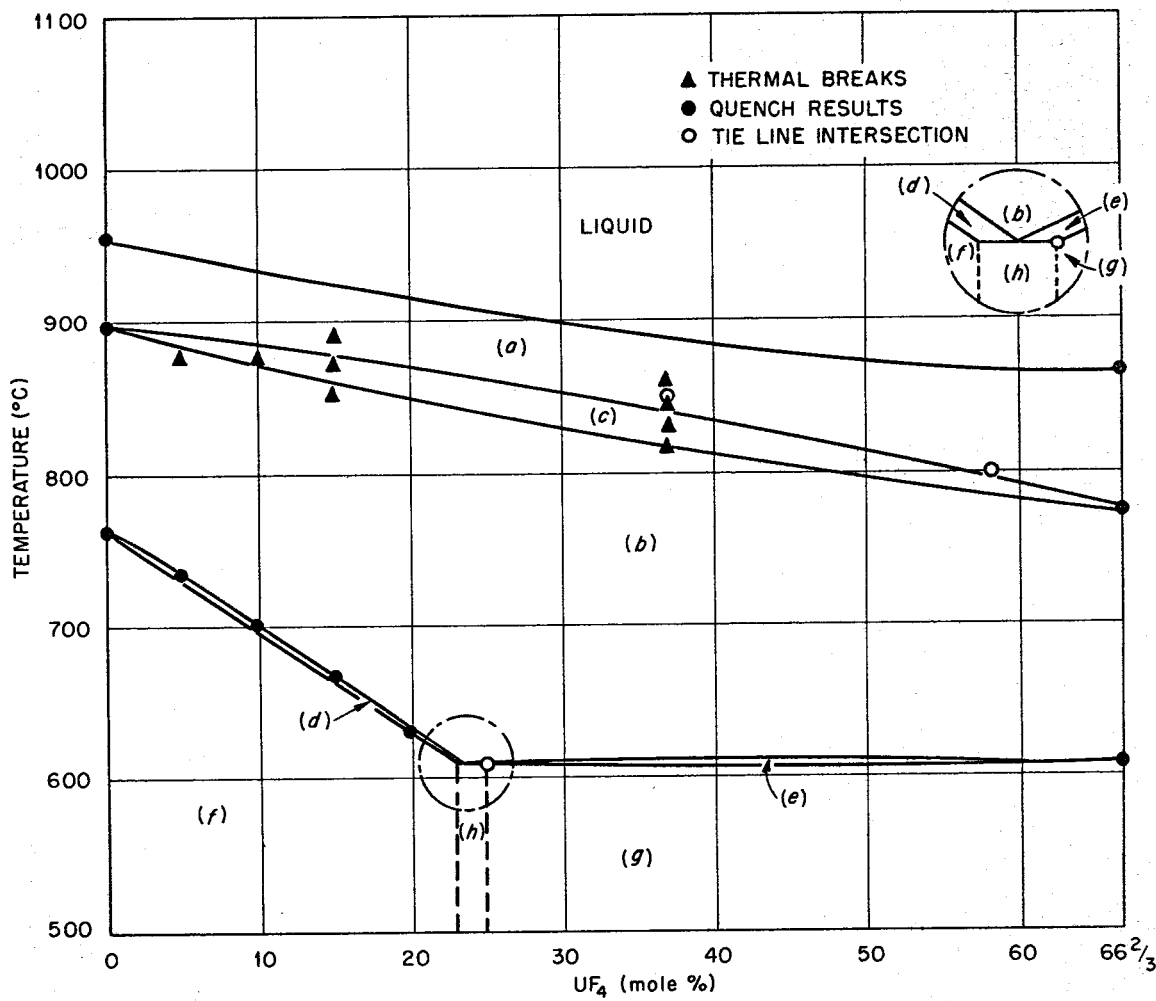
Fig. 3.74d. The System $LiF-ThF_4-UF_4$: The Section at 33.3 Mole % LiF.
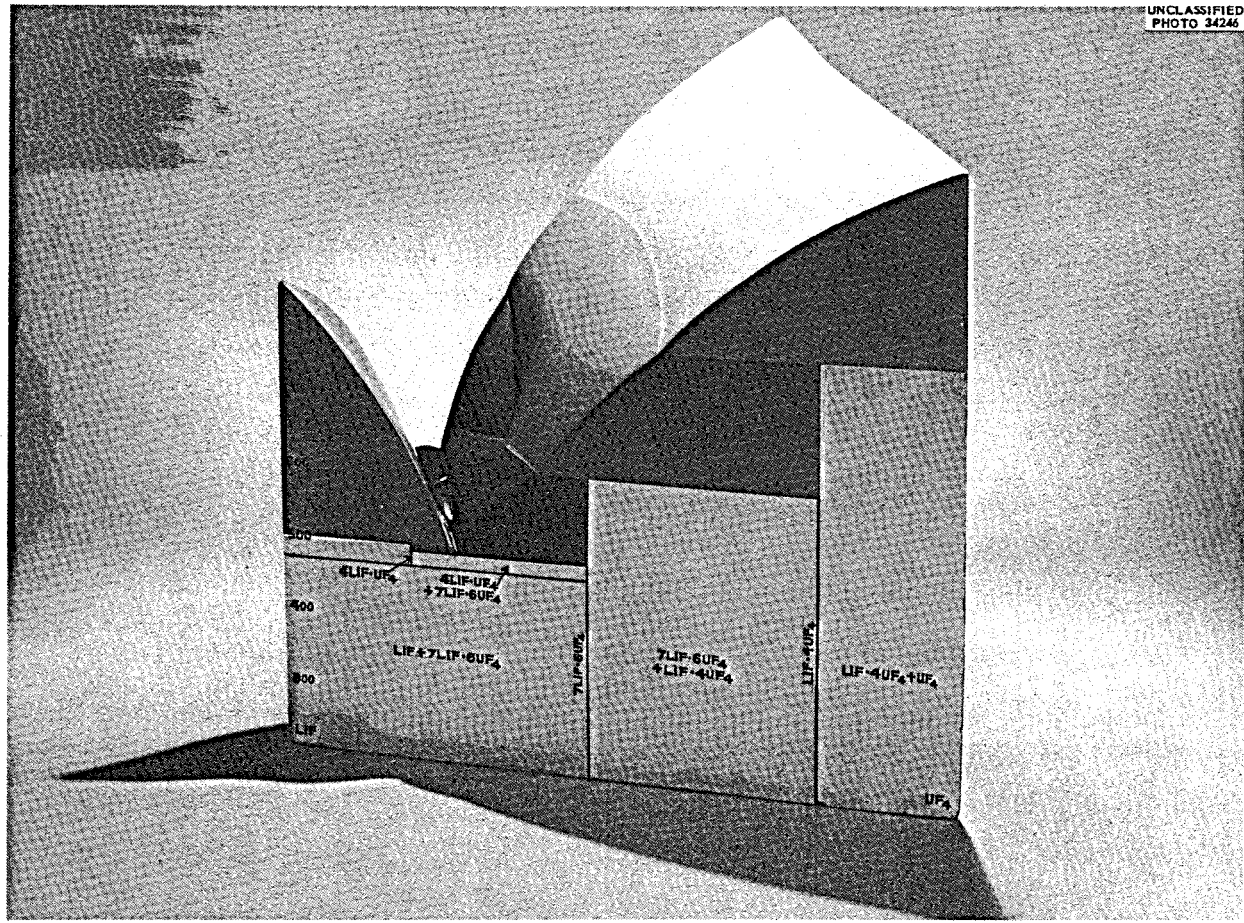
Fig. 3.74e. Model of the System LiF–ThF$_4$–UF$_4$.

3.75. The System NaF–ThF$_4$–UF$_4$: The Section 2NaF·ThF$_4$–2NaF·UF$_4$

R. E. Thoma, H. Insley, H. A. Friedman, and C. F. Weaver, unpublished work performed at the Oak Ridge National Laboratory, 1958–59.

Preliminary diagram.
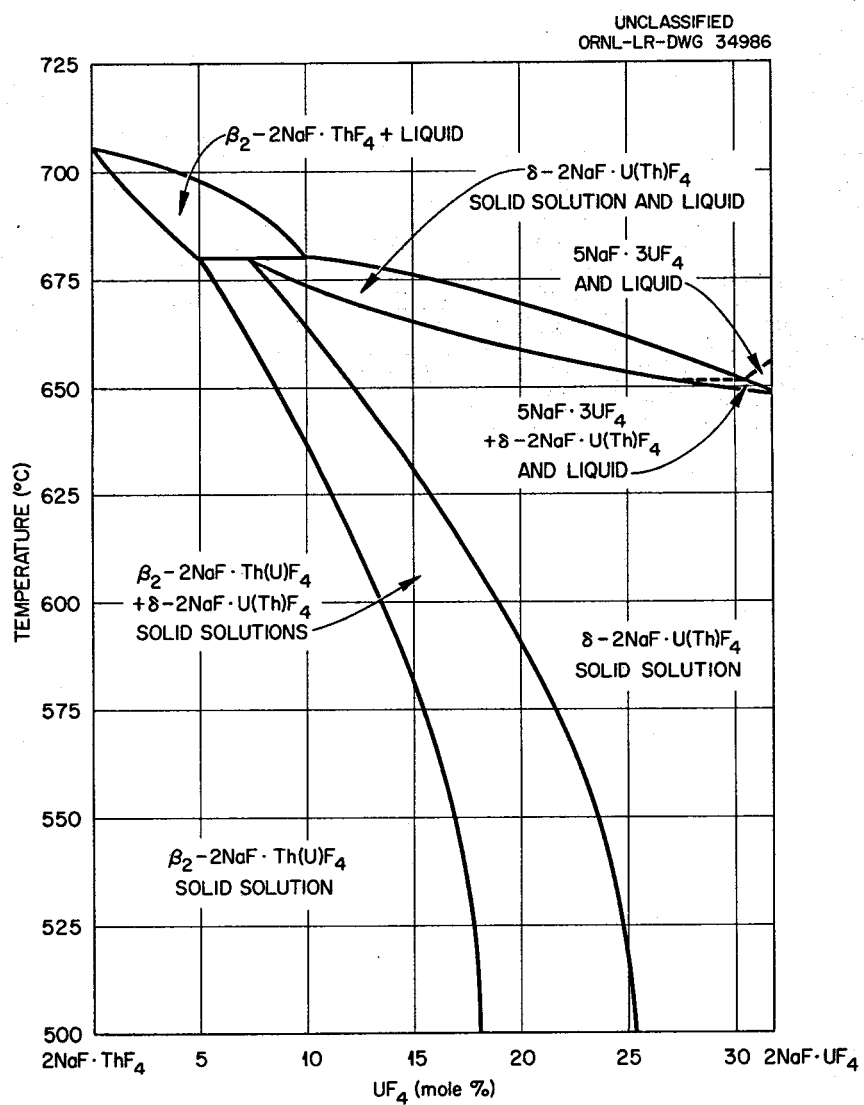
Fig. 3.75. The Section 2NaF·ThF$_4$–2NaF·UF$_4$.

3.76. The System LiF–PuF$_3$

C. J. Barton and R. A. Strehlow, "Phase Relationships in the System Lithium Fluoride–Plutonium Fluoride," paper presented at the 135th National Meeting of the American Chemical Society, Boston, Mass., Apr. 5–10, 1959.

The system LiF–PuF$_3$ contains a single eutectic at 80.5 LiF–19.5 PuF$_3$ (mole %), m.p. 743°C.
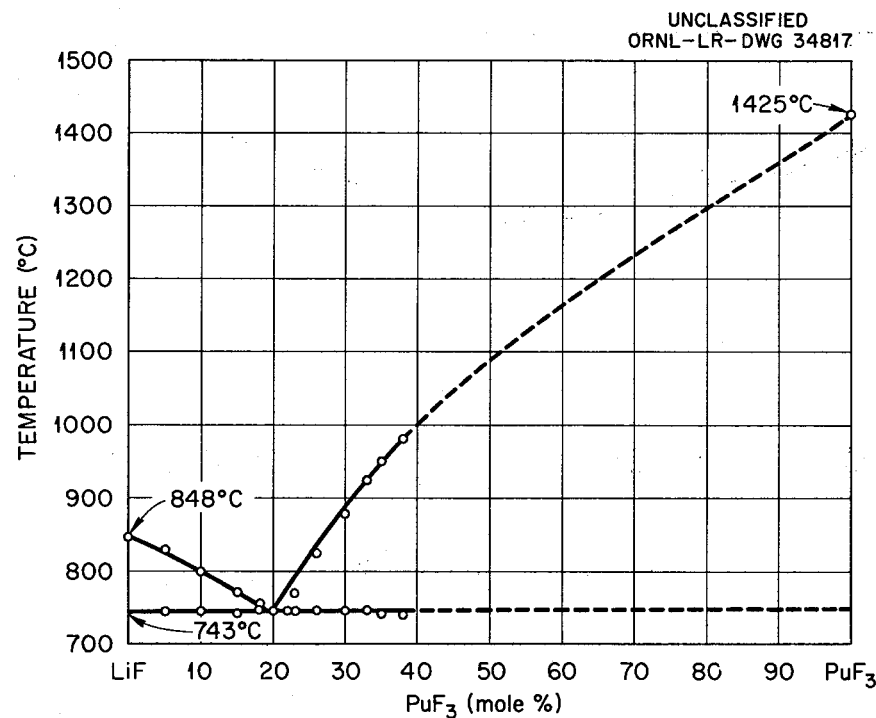
Fig. 3.76. The System LiF–PuF$_3$.

3.77. The System LiCl-FeCl$_2$

C. Beusman, *Activities in the KCl-FeCl$_2$ and LiCl-FeCl$_2$ Systems*, ORNL-2323 (May 15, 1957).

The system LiCl-FeCl$_2$ forms a continuous series of solid solutions with a minimum at 60 LiCl-40 FeCl$_2$ (mole %), m.p. 540°C.
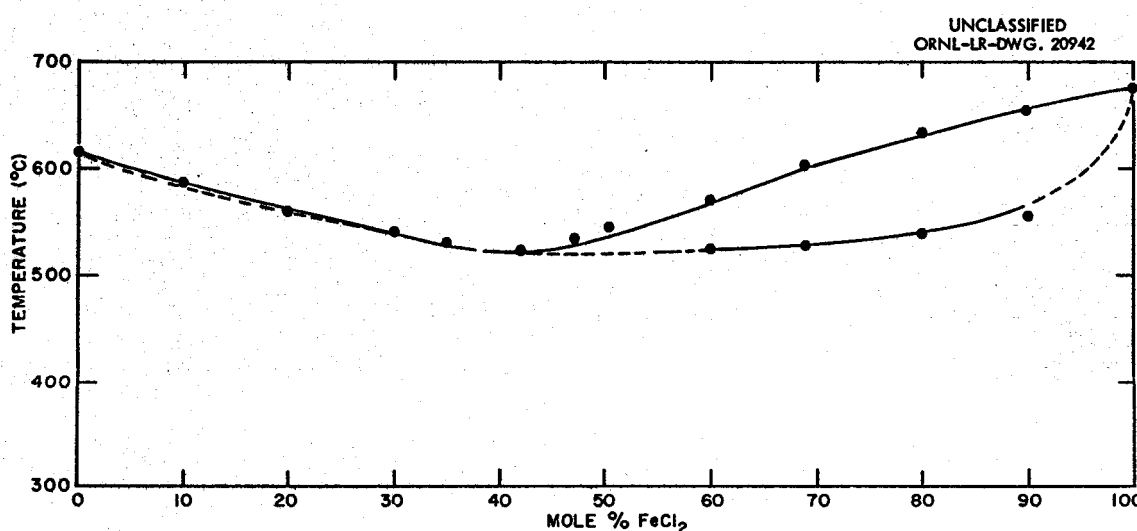
Fig. 3.77. The System LiCl-FeCl$_2$

3.78. The System KCl–FeCl$_2$

C. Beusman, *Activities in the KCl–FeCl$_2$ and LiCl–FeCl$_2$ Systems*, ORNL-2323 (May 15, 1957). A nearly identical diagram to this one has been reported by H. L. Pinch and J. M. Hirshon, "Thermal Analysis of the Ferrous Chloride–Potassium Chloride System," *J. Am. Chem. Soc.* **79**, 6149–50 (1957).

Invariant Equilibria

Mole % FeCl$_2$ in Liquid	Invariant Temperature (°C)	Type of Equilibrium	Phase Reaction at Invariant Temperature
35	385	Peritectic	$L + KCl \rightleftharpoons \alpha\text{-}2KCl\cdot FeCl_2$
–	255	Inversion	$\alpha\text{-}2KCl\cdot FeCl_2 \rightleftharpoons \beta\text{-}2KCl\cdot FeCl_2$
39	355	Eutectic	$L \rightleftharpoons \alpha\text{-}2KCl\cdot FeCl_2 + \alpha\text{-}KCl\cdot FeCl_2$
50	400	Congruent melting point	$L \rightleftharpoons \alpha\text{-}KCl\cdot FeCl_2$
–	300	Inversion	$\alpha\text{-}KCl\cdot FeCl_2 \rightleftharpoons \beta\text{-}KCl\cdot FeCl_2$
53	390	Eutectic	$L \rightleftharpoons \alpha\text{-}KCl\cdot FeCl_2 + FeCl_2$
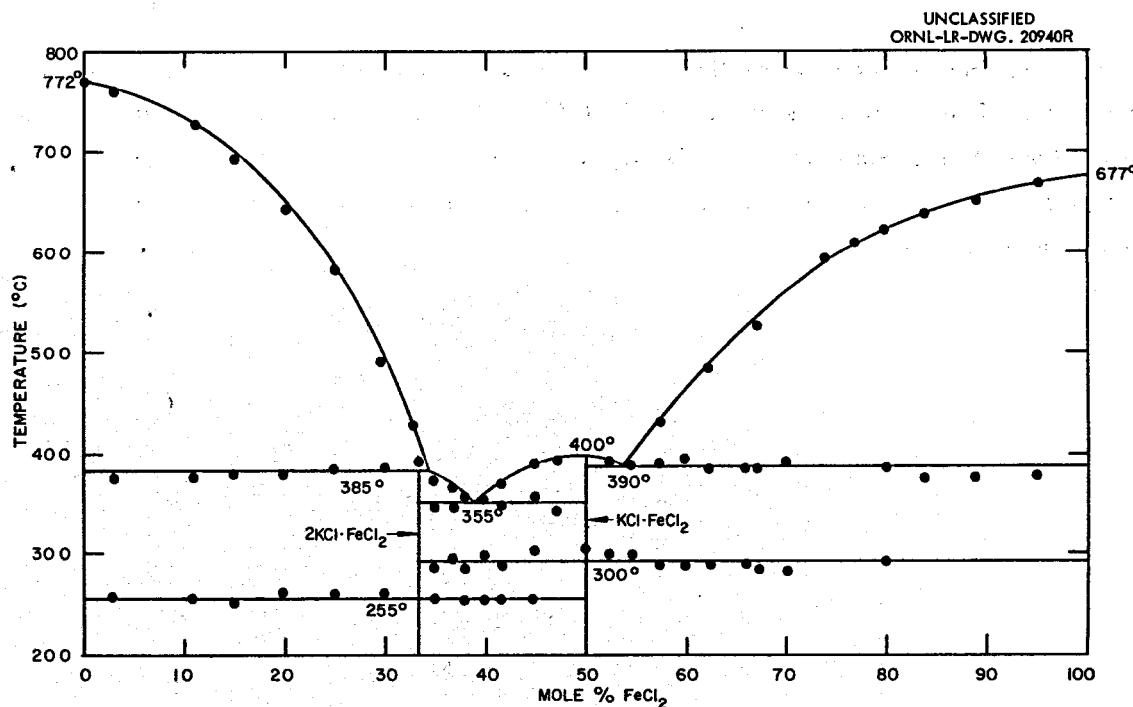
Fig. 3.78. The System KCl–FeCl$_2$

3.79. The System $NaCl-ZrCl_4$

C. J. Barton, R. J. Sheil, and W. R. Grimes, unpublished work performed at the Oak Ridge National Laboratory, 1956.

Preliminary diagram.

Invariant Equilibria

| Mole % $ZrCl_4$ in Liquid	Invariant Temperature (°C)	Type of Equilibrium	Phase Reaction at Invariant Temperature
28.0	535 ± 5	Peritectic	$L + NaCl \rightleftharpoons 3NaCl \cdot ZrCl_4$
–	445 ± 5	Decomposition	$3NaCl \cdot ZrCl_4 \rightleftharpoons NaCl + \alpha\text{-}2NaCl \cdot ZrCl_4$
28.5	525 ± 5	Eutectic	$L \rightleftharpoons 3NaCl \cdot ZrCl_4 + \alpha\text{-}2NaCl \cdot ZrCl_4$
33.3	626 + 5	Congruent melting point	$L \rightleftharpoons \alpha\text{-}2NaCl \cdot ZrCl_4$
–	370 ± 5	Inversion	$\alpha\text{-}2NaCl \cdot ZrCl_4 \rightleftharpoons \beta\text{-}2NaCl \cdot ZrCl_4$
58	352 ± 5	Peritectic	$L + \beta\text{-}2NaCl \cdot ZrCl_4 \rightleftharpoons \alpha\text{-}3NaCl \cdot 4ZrCl_4$
–	312 ± 5	Inversion	$\alpha\text{-}3NaCl \cdot 4ZrCl_4 \rightleftharpoons \beta\text{-}3NaCl \cdot 4ZrCl_4$
63	312 ± 5	Eutectic	$L \rightleftharpoons \beta\text{-}3NaCl \cdot 4ZrCl_4 + ZrCl_4$

Previous reports on the system $NaCl-ZrCl_4$ have been made by N. A. Berlozerskts and O. A. Kucherenko, *Zhur. Priklad. Khim.* 13, 1552 (1940), I. S. Morozov and B. G. Korshunov, *Zhur. Neorg. Khim.* 1, 145(1956), and H. H. Kellogg, L. J. Howell, and R. C. Sommer, *Physical Chemical Properties of the Systems $NaCl-ZrCl_4$, $KCl-ZrCl_4$, and $NaCl-KCl-ZrCl_4$, Summary Report*, NYO-3108 (April 7, 1955).
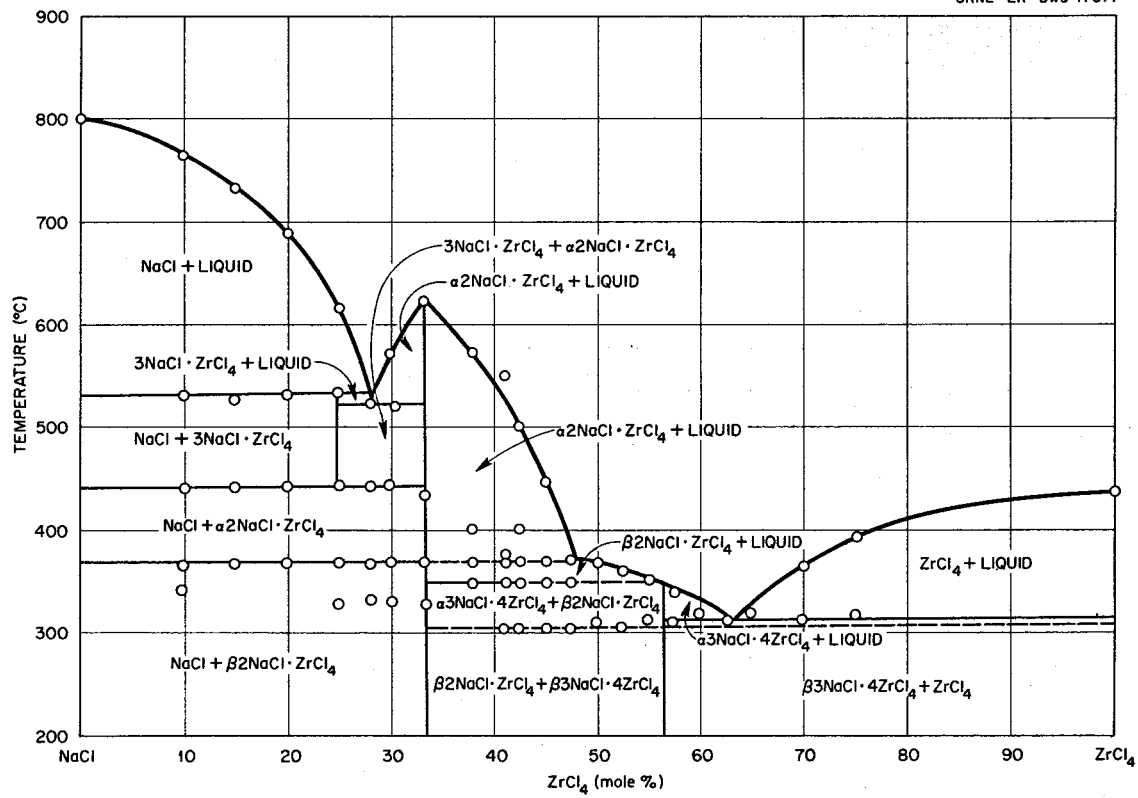
Fig. 3.79. The System NaCl—ZrCl$_4$.

3.80. The System KCl–ZrCl$_4$

C. J. Barton, R. J. Sheil, and W. R. Grimes, unpublished work performed at the Oak Ridge National Laboratory, 1955.

Preliminary diagram.

Invariant Equilibria

Mole % ZrCl$_4$ in Liquid	Invariant Temperature (°C)	Type of Equilibrium	Phase Reaction at Invariant Temperature
23	600 ± 5	Eutectic	$L \rightleftharpoons KCl + 2KCl \cdot ZrCl_4$
33.3	790 ± 5	Congruent melting point	$L \rightleftharpoons 2KCl \cdot ZrCl_4$
48	565 ± 5	Peritectic	$L + 2KCl \cdot ZrCl_4 \rightleftharpoons \alpha\text{-}7KCl \cdot 6ZrCl_4$
–	222 ± 4	Inversion	$\alpha\text{-}7KCl \cdot 6ZrCl_4 \rightleftharpoons \beta\text{-}7KCl \cdot 6ZrCl_4$
65	225 ± 4	Eutectic	$L \rightleftharpoons \alpha\text{-}7KCl \cdot 6ZrCl_4 + ZrCl_4$

Some phase work on this system has been reported by H. H. Kellogg, L. J. Howell, and R. C. Sommer, *Physical Chemical Properties of the Systems NaCl–ZrCl$_4$, KCl–ZrCl$_4$, and NaCl–KCl–ZrCl$_4$, Summary Report*, NYO-3108 (April 7, 1955).
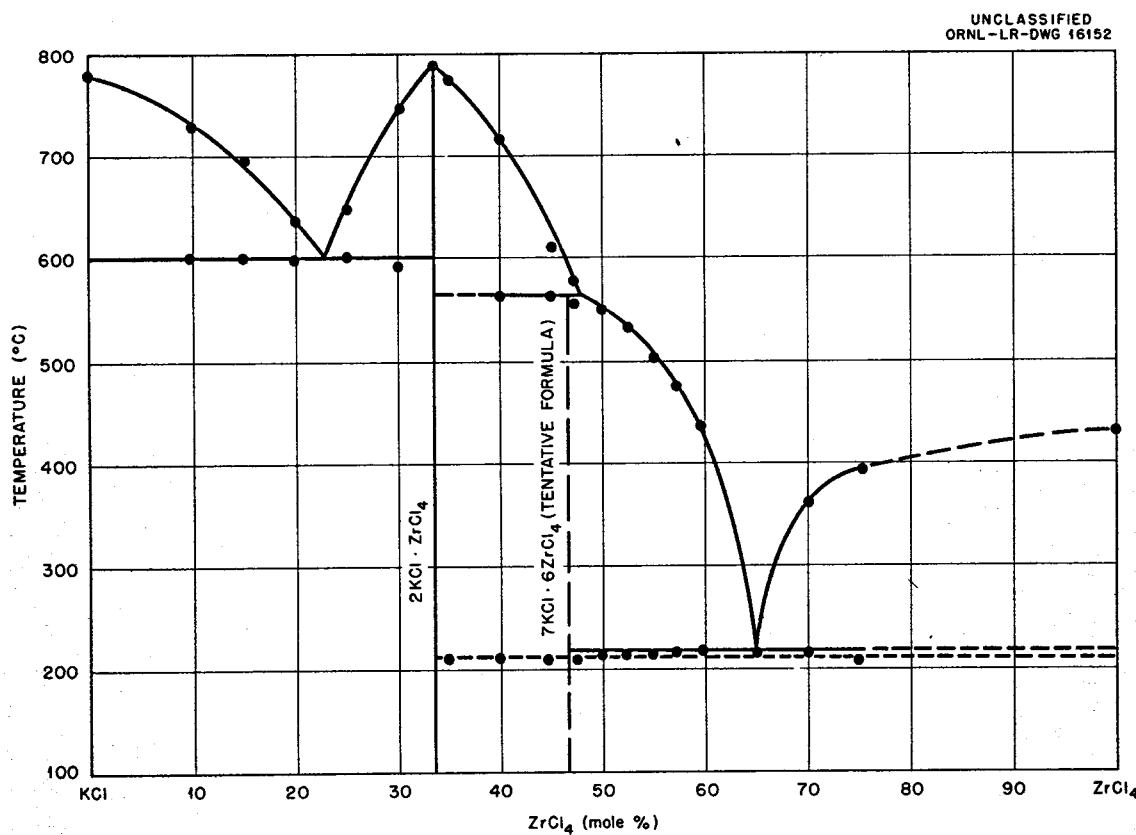
Fig. 3.80. The System KCl–ZrCl$_4$.

3.81. The System LiCl–UCl$_3$

C. J. Barton, A. B. Wilkerson, and W. R. Grimes, unpublished work performed at the Oak Ridge National Laboratory, 1953.

Preliminary diagram. The system LiCl–UCl$_3$ contains a single eutectic at 75 LiCl–25 UCl$_3$ (mole %), m.p. 495 ±5°C.
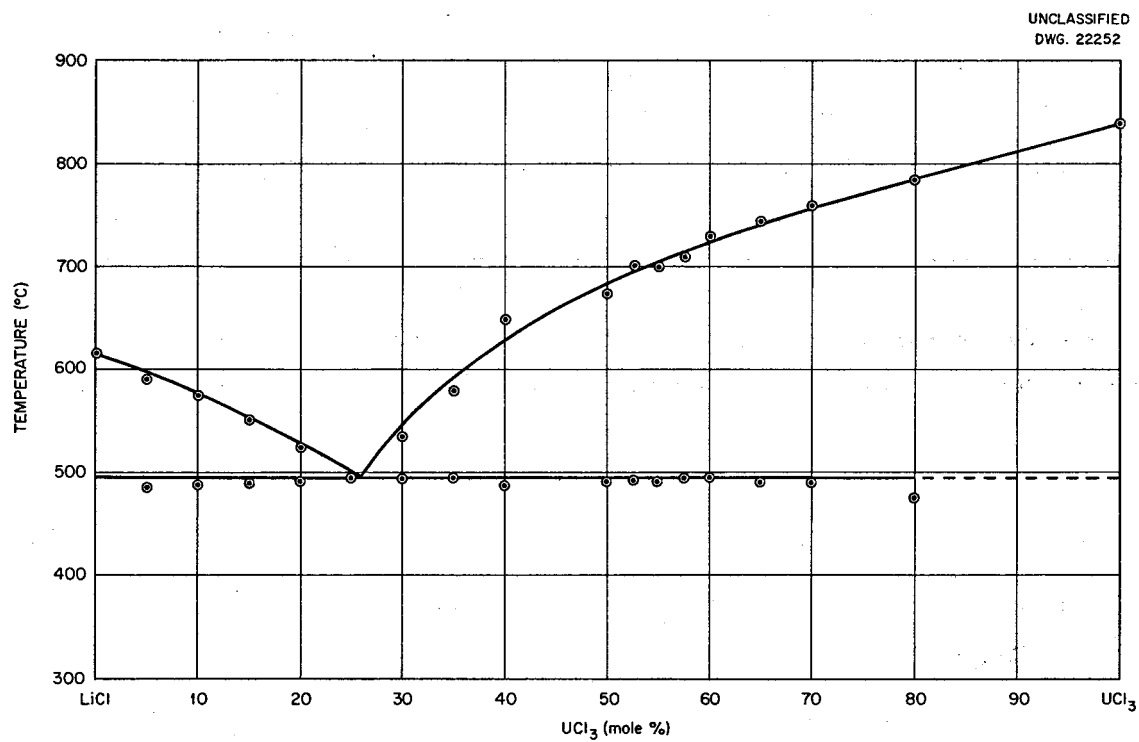
Fig. 3.81. The System LiCl–UCl$_3$

3.82. The System LiCl–UCl$_4$

C. J. Barton, R. J. Sheil, and W. R. Grimes, unpublished work performed at the Oak Ridge National Laboratory, 1953.

Preliminary diagram.

Invariant Equilibria

Mole % UCl$_4$ in Liquid	Invariant Temperature (°C)	Type of Equilibrium	Phase Reaction at Invariant Temperature
29	415	Eutectic	$L \rightleftharpoons 2LiCl{\cdot}UCl_4 + LiCl$
33.3	430 ± 10	Congruent melting point	$L \rightleftharpoons 2LiCl{\cdot}UCl_4$
48	405	Eutectic	$L \rightleftharpoons 2LiCl{\cdot}UCl_4 + UCl_4$

Some data on this system were reported by C. A. Kraus in *Phase Diagrams of Some Complex Salts of Uranium with Halides of the Alkali and Alkaline Earth Metals*, M-251 (July 1, 1943).
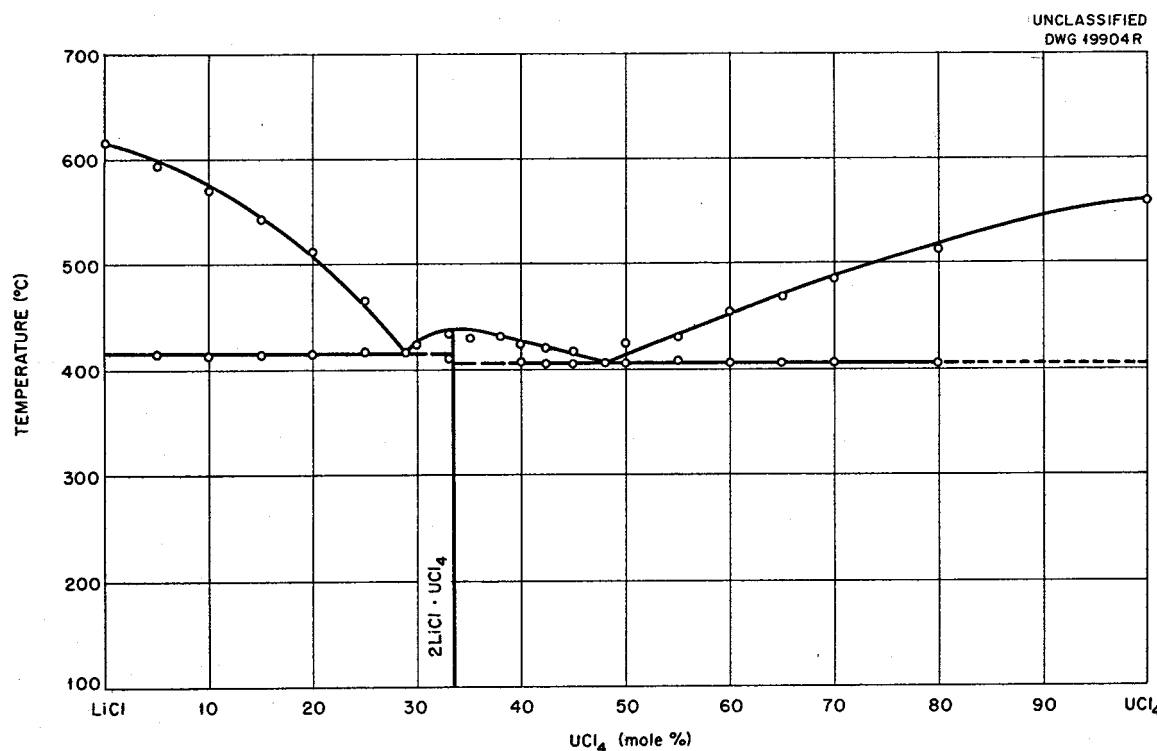
Fig. 3.82. The System LiCl–UCl$_4$

3.83. The System NaCl–UCl₃

C. A. Kraus, unpublished work.

Preliminary diagram constructed with the author's permission from data reported in *Phase Diagrams of Some Complex Salts of Uranium with Halides of the Alkali and Alkaline Earth Metals*, M-251 (July 1, 1943).

The system NaCl–UCl₃ contains a single eutectic at 67 NaCl–33 UCl₃ (mole %), m.p. 525°C.
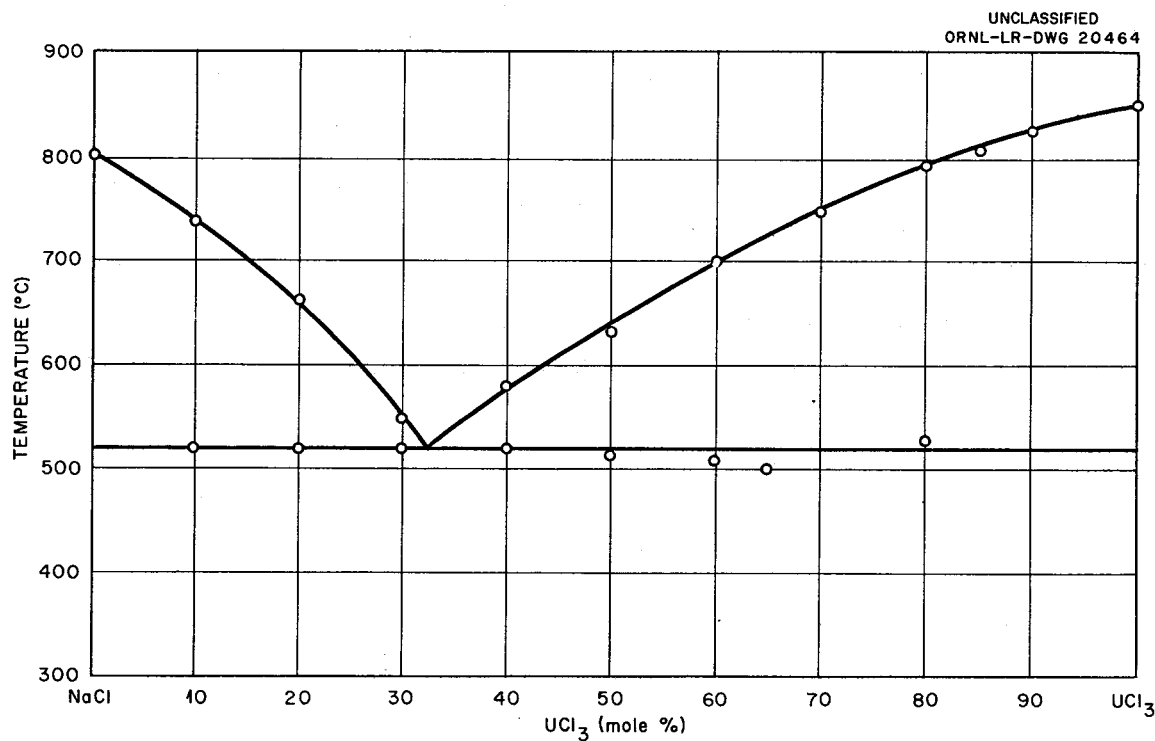
Fig. 3.83. The System NaCl–UCl₃.

3.84. The System NaCl–UCl$_4$

C. J. Barton, R. J. Sheil, A. B. Wilkerson, and W. R. Grimes, unpublished work performed at the Oak Ridge National Laboratory, 1953.

Preliminary diagram.

Invariant Equilibria

Mole % UCl$_4$ in Liquid	Invariant Temperature (°C)	Type of Equilibrium	Phase Reaction at Invariant Temperature
30	430 ± 5	Eutectic	$L \rightleftharpoons NaCl + 2NaCl \cdot UCl_4$
33.3	440 ± 5	Congruent melting point	$L \rightleftharpoons 2NaCl \cdot UCl_4$
47	370 ± 5	Eutectic	$L \rightleftharpoons 2NaCl \cdot UCl_4 +$ unidentified compound
57	415 ± 5	Peritectic	$L + UCl_4 \rightleftharpoons$ unidentified compound

A phase diagram of this system has been reported by C. A. Kraus in *Phase Diagrams of Some Complex Salts of Uranium with Halides of the Alkali and Alkaline Earth Metals*, M-251 (July 1, 1943).
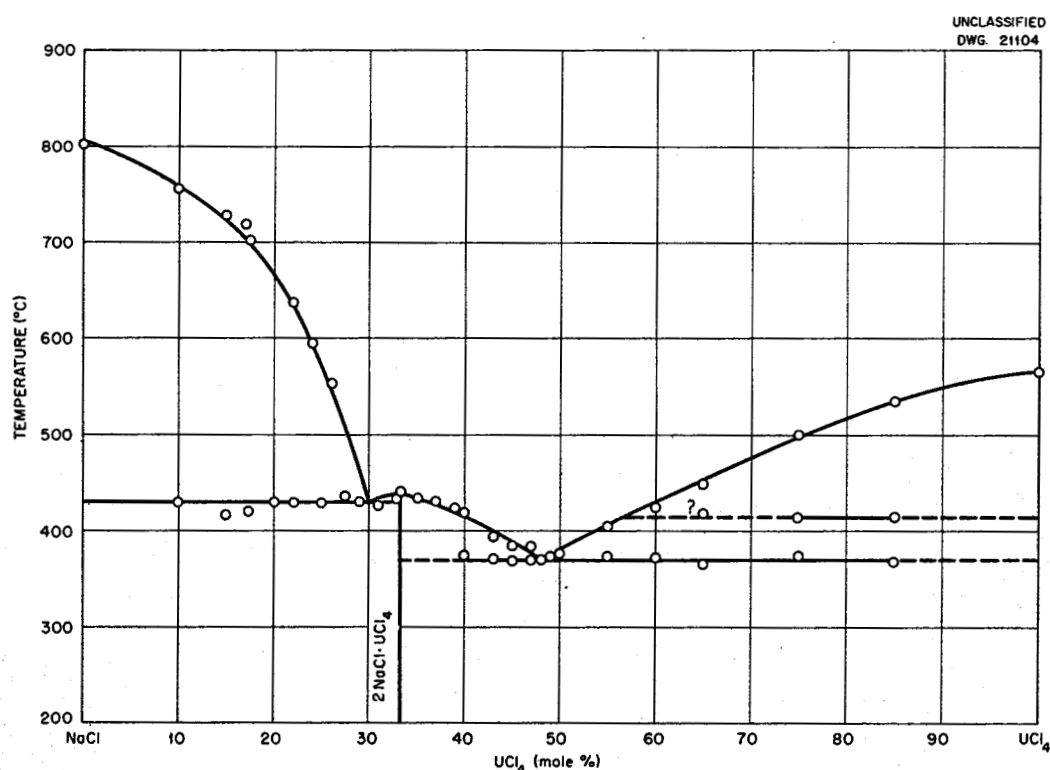
Fig. 3.84. The System NaCl–UCl$_4$.

3.85. The System KCl–UCl$_4$

C. J. Barton, A. B. Wilkerson, T. N. McVay, R. J. Sheil, and W. R. Grimes, unpublished work performed at the Oak Ridge National Laboratory, 1954.

Preliminary diagram.

Invariant Equilibria

Mole % UCl$_4$ in Liquid	Invariant Temperature (°C)	Type of Equilibrium	Phase Reaction at Invariant Temperature
25	550	Eutectic	$L \rightleftharpoons KCl + 2KCl \cdot UCl_4$
33.3	630	Congruent melting point	$L \rightleftharpoons 2KCl \cdot UCl_4$
44	330	Eutectic	$L \rightleftharpoons 2KCl \cdot UCl_4 + KCl \cdot UCl_4$
49	345	Peritectic	$L + KCl \cdot 3UCl_4 \rightleftharpoons KCl \cdot UCl_4$
61	395	Peritectic	$L + UCl_4 \rightleftharpoons KCl \cdot 3UCl_4$

A phase diagram of this system has been reported by C. A. Kraus in *Phase Diagrams of Some Complex Salts of Uranium with Halides of the Alkali and Alkaline Earth Metals*, M-251 (July 1, 1943).
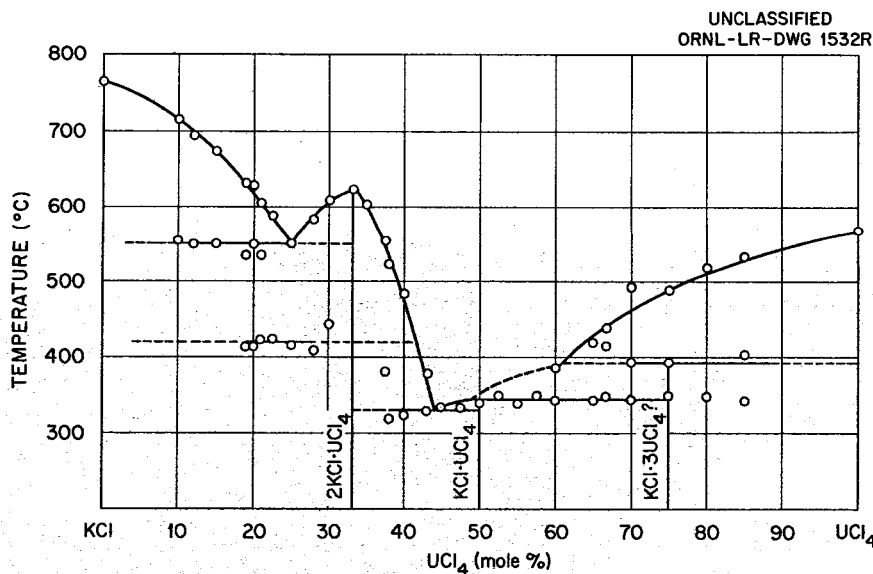

Fig. 3.85. The System KCl–UCl$_4$

3.86. The System $RbCl-UCl_3$

C. J. Barton, R. J. Sheil, A. B. Wilkerson, and W. R. Grimes, unpublished work performed at the Oak Ridge National Laboratory, 1954.

Preliminary diagram.

Invariant Equilibria

Mole % UCl_3 in Liquid	Invariant Temperature (°C)	Type of Equilibrium	Phase Reaction at Invariant Temperature
15	610	Eutectic	$L \rightleftharpoons RbCl + 3RbCl \cdot UCl_3$
25	745 ± 10	Congruent melting point	$L \rightleftharpoons 3RbCl \cdot UCl_3$
40	560 ± 10	Peritectic	$L + 3RbCl \cdot UCl_3 \rightleftharpoons 2RbCl \cdot UCl_3$
45.5	513 ± 5	Eutectic	$L \rightleftharpoons 2RbCl \cdot UCl_3 + RbCl \cdot UCl_3$
49	550 ± 10	Peritectic	$L + UCl_3 \rightleftharpoons RbCl \cdot UCl_3$
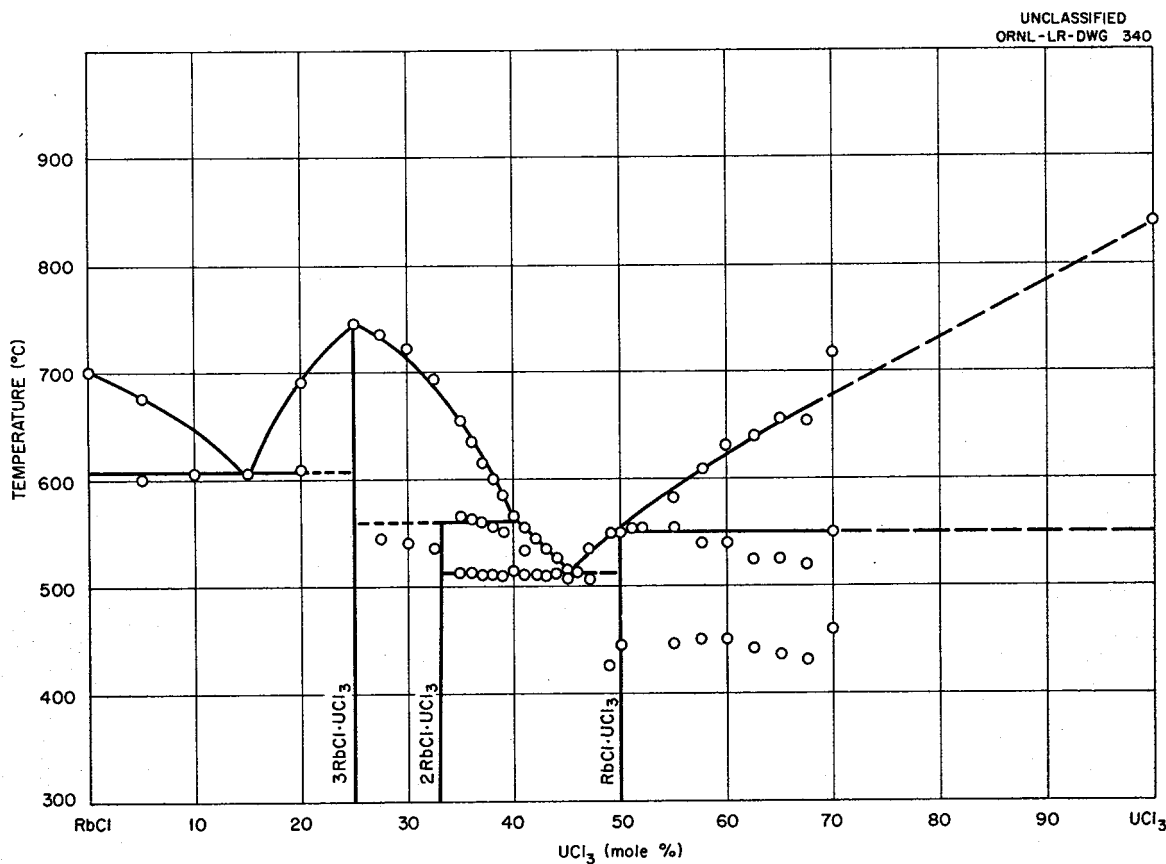
Fig. 3.86. The System $RbCl-UCl_3$.

3.87. The System CsCl-UCl$_4$

C. J. Barton, A. B. Wilkerson, and W. R. Grimes, unpublished work performed at the Oak Ridge National Laboratory, 1953.

Preliminary diagram.

Invariant Equilibria

Mole % UCl$_4$ in Liquid	Invariant Temperature (°C)	Type of Equilibrium	Phase Reaction at Invariant Temperature
20	505 ± 5	Eutectic	$L \rightleftarrows CsCl + 2CsCl \cdot UCl_4$
33.3	657 ± 5	Congruent melting point	$L \rightleftarrows 2CsCl \cdot UCl_4$
58	370 ± 5	Eutectic	$L \rightleftarrows 2CsCl \cdot UCl_4 + CsCl \cdot 2UCl_4$
63	382 ± 5	Peritectic	$L + UCl_4 \rightleftarrows CsCl \cdot 2UCl_4$
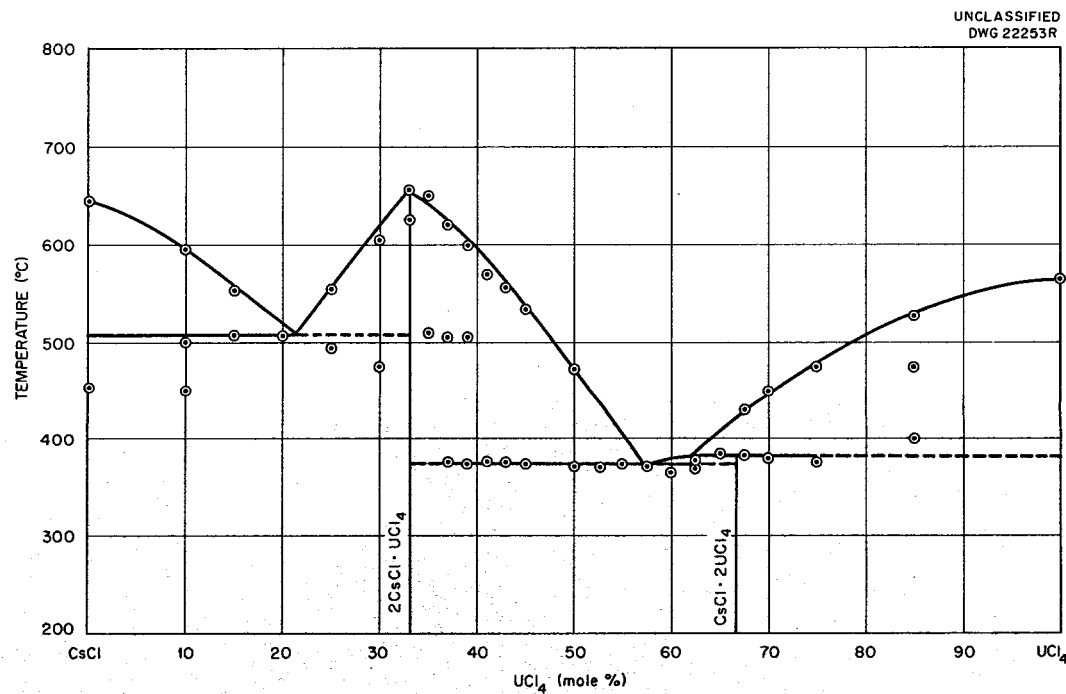
Fig. 3.87. The System CsCl-UCl$_4$

3.88. The System K_3CrF_6–Na_3CrF_6–Li_3CrF_6

B. J. Sturm, L. G. Overholser, and W. R. Grimes, unpublished work performed at the Oak Ridge National Laboratory, 1951–52.

Preliminary diagram.
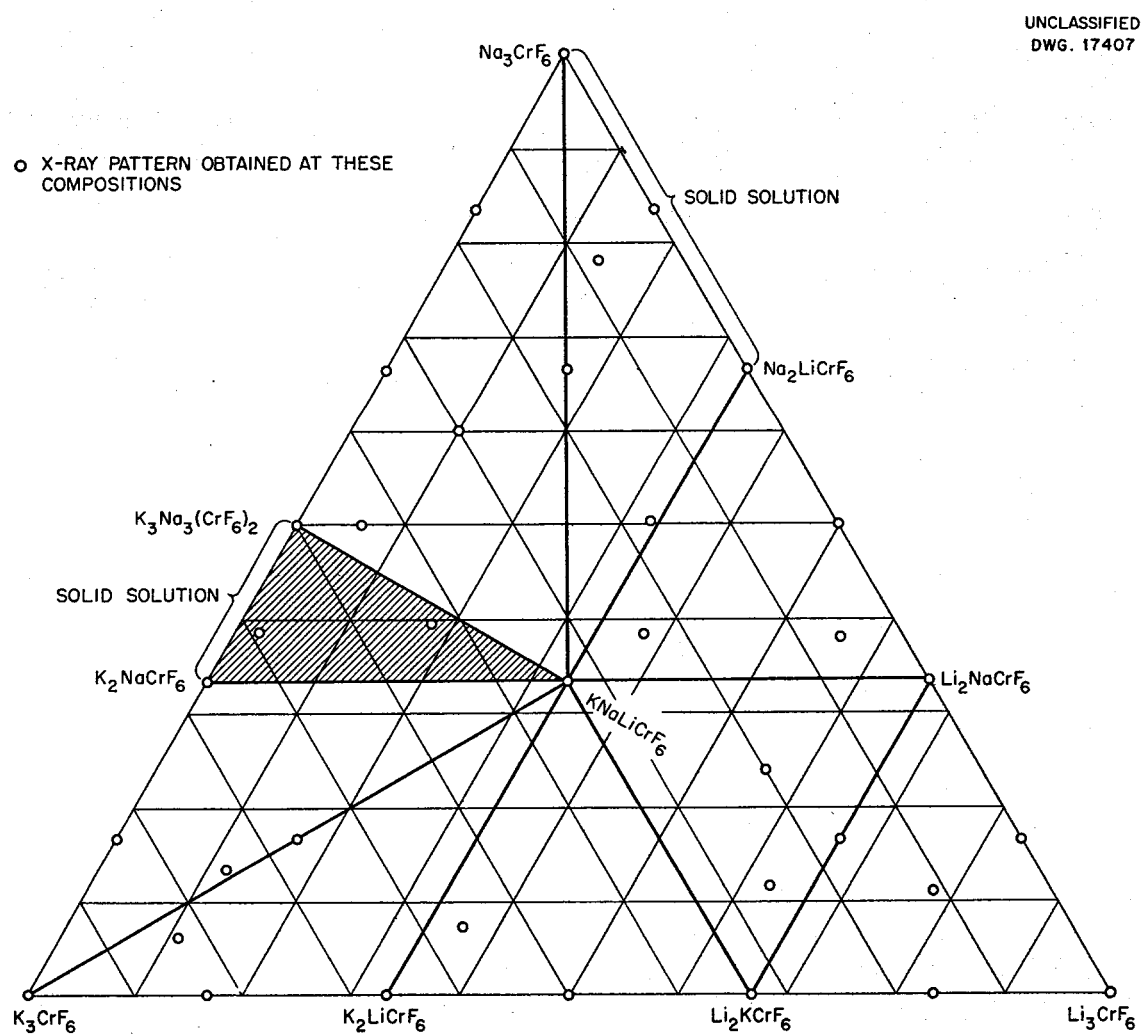
Fig. 3.88. The System K_3CrF_6–Na_3CrF_6–Li_3CrF_6.

4. OXIDE AND HYDROXIDE SYSTEMS

4.1. The System SiO_2-ThO_2

L. A. Harris, "A Preliminary Study of the Phase Equilibria Diagram of ThO_2-SiO_2," *J. Am. Ceram. Soc.* **42**, 74–77 (1959).
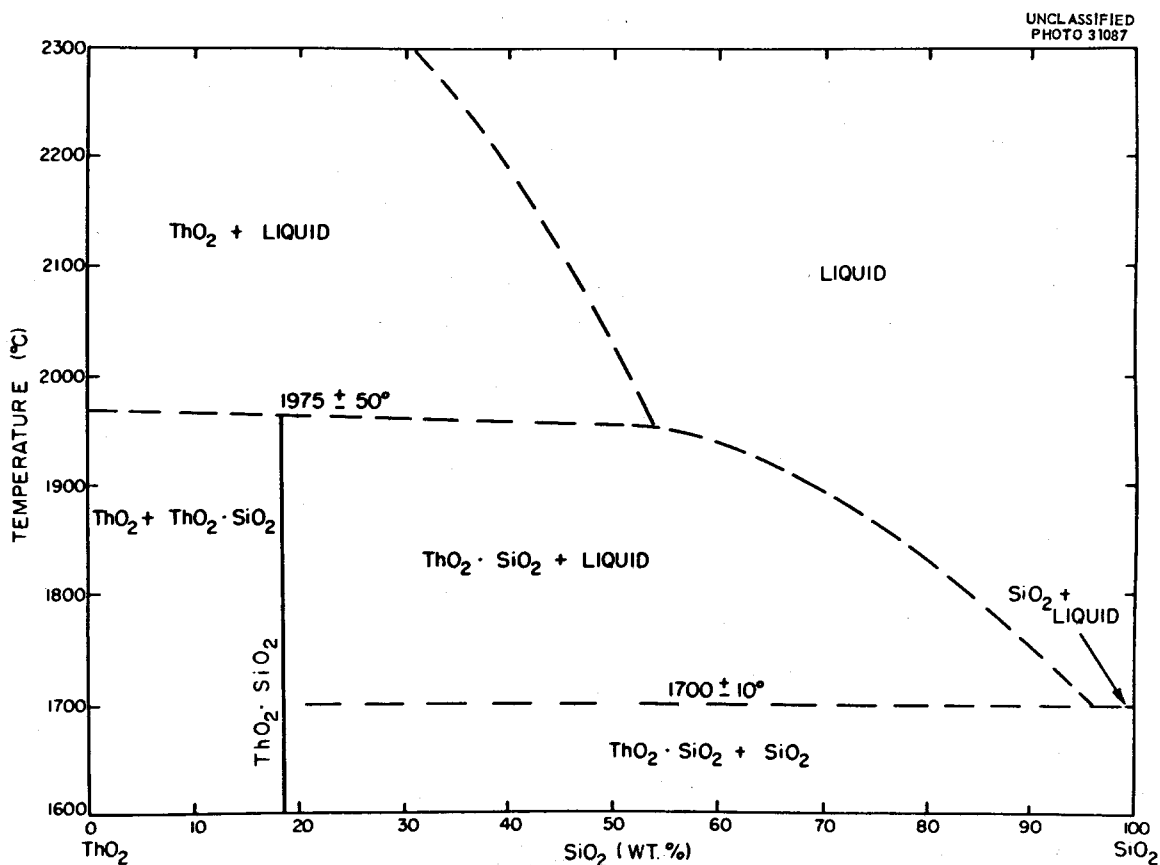
Fig. 4.1. The System SiO_2-ThO_2.

4.2. The System LiOH–NaOH

C. J. Barton, J. P. Blakely, K. A. Allen, W. C. Davis, and B. S. Weaver, unpublished work performed at the Oak Ridge National Laboratory, 1951.

Preliminary diagram. A phase diagram of the system LiOH–NaOH has been reported more recently by N. A. Reshetnikov and G. M. Oonzhakov, *Zhur. Neorg. Khim.* 3, 1433 (1958).

Invariant Equilibria

Mole % LiOH in Liquid	Invariant Temperature (°C)	Type of Equilibrium	Phase Reaction at Invariant Temperature
27	219	Eutectic	$L \rightleftharpoons NaOH + \alpha\text{-}NaOH\cdot LiOH$
40	250	Peritectic	$L + LiOH \rightleftharpoons \alpha\text{-}LiOH\cdot NaOH$
–	180	Inversion	$\alpha\text{-}LiOH\cdot NaOH \rightleftharpoons \beta\text{-}LiOH\cdot NaOH$

UNCLASSIFIED
ORNL-LR-DWG 20463R
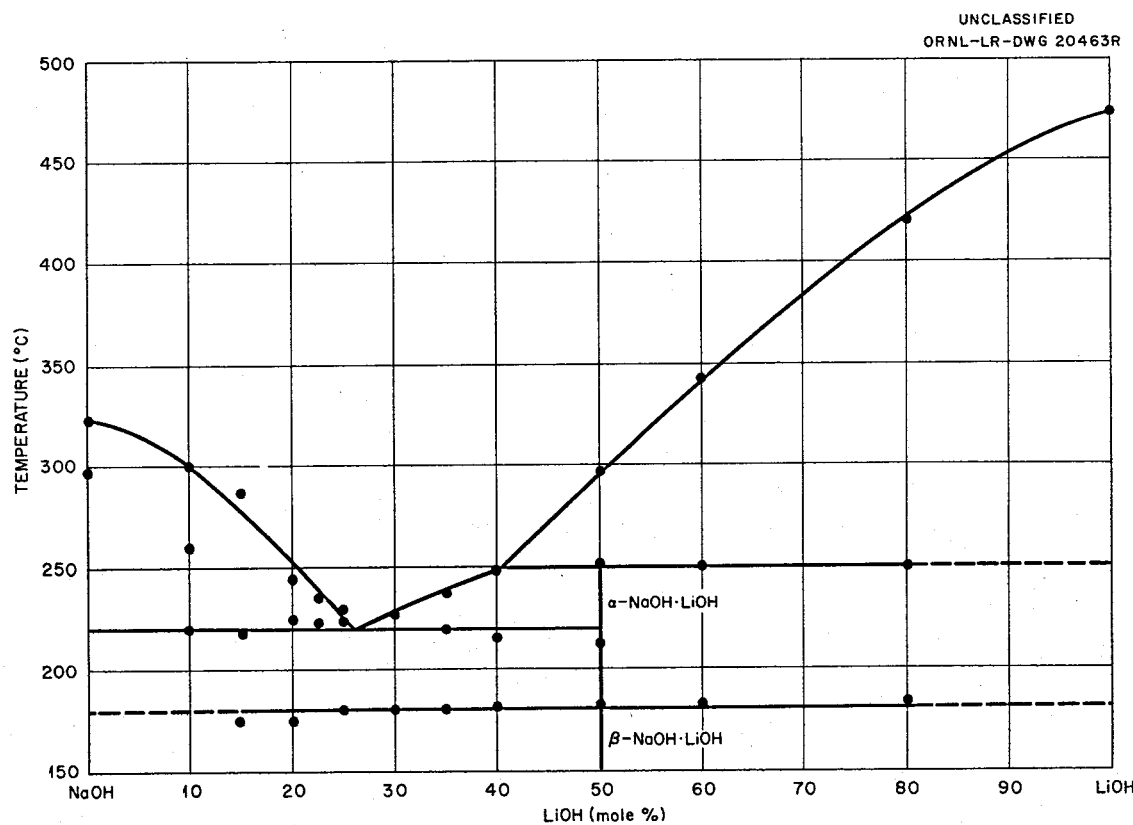
Fig. 4.2. The System LiOH–NaOH.

4.3. The System LiOH–KOH

C. J. Barton, J. P. Blakely, L. M. Bratcher, and W. R. Grimes, unpublished work performed at the Oak Ridge National Laboratory, 1951.

Preliminary diagram.

Invariant Equilibria

Mole % KOH in Liquid	Invariant Temperature (°C)	Type of Equilibrium	Phase Reaction at Invariant Temperature
40	315	Incongruent melting point of 3LiOH·2KOH	$L + LiOH \rightleftharpoons 3LiOH \cdot 2KOH$
70	245	Eutectic	$L \rightleftharpoons 3LiOH \cdot 2KOH + \beta\text{-}KOH$
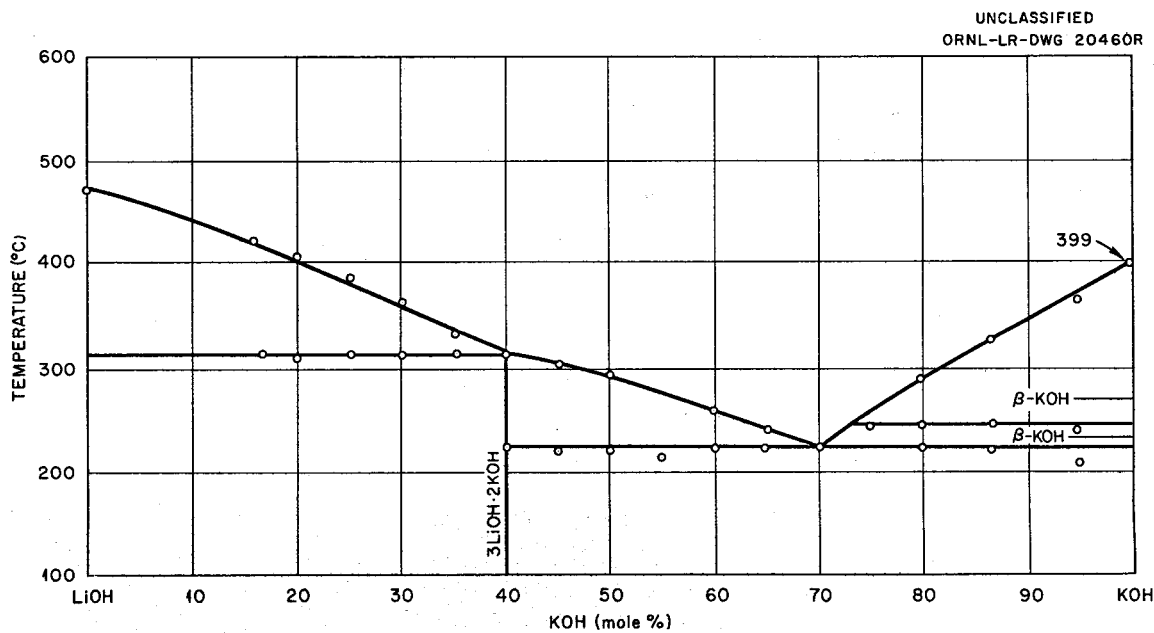
Fig. 4.3. The System LiOH–KOH.

4.4. The System NaOH–KOH

G. von Hevesy, "The Binary Systems NaOH–KOH, KOH–RbOH, and RbOH–NaOH," *Z. physik. Chem.* **73**, 667–84 (1910).
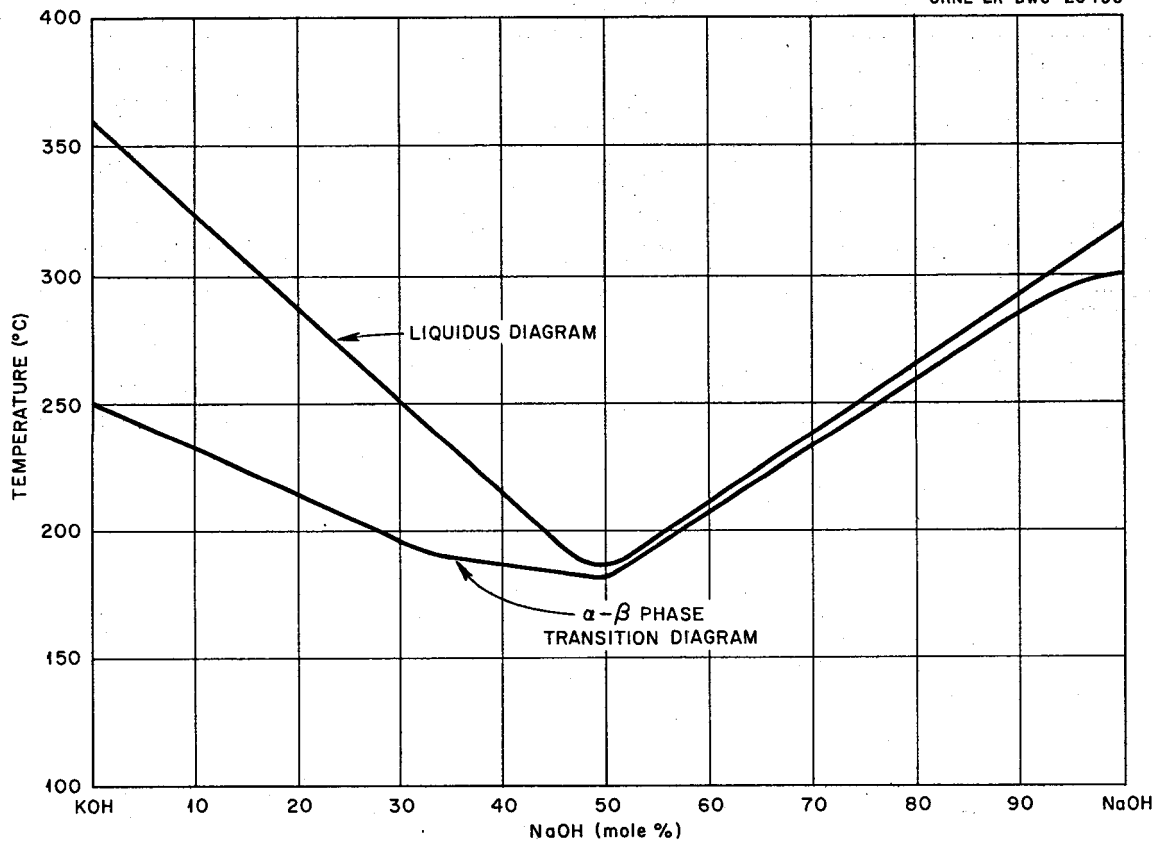
Fig. 4.4 The System NaOH–KOH.

4.5. The System NaOH–RbOH

G. von Hevesy, "The Binary Systems NaOH–KOH, KOH–RbOH, and RbOH–NaOH," Z. *physik. Chem.* **73,** 667–84 (1910).
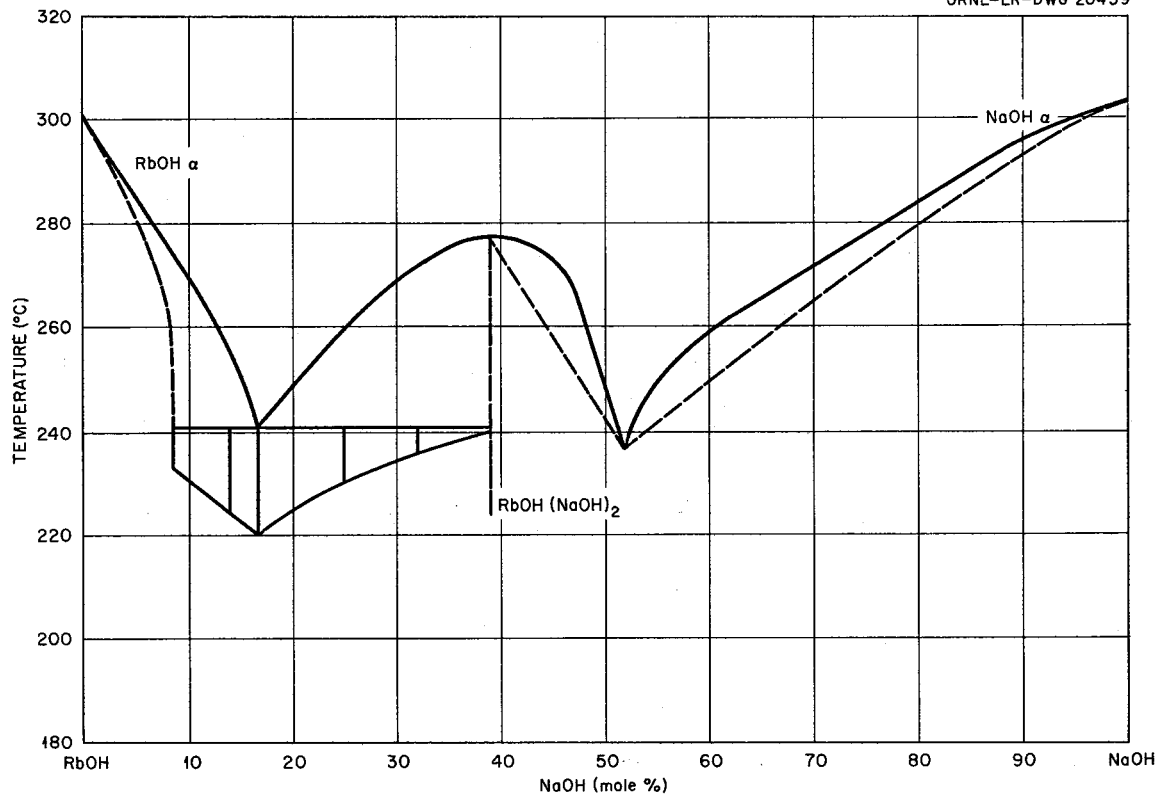
Fig. 4.5. The System NaOH–RbOH.

4.6. The System Ba(OH)$_2$–Sr(OH)$_2$

K. A. Allen, W. C. Davis, and B. S. Weaver, unpublished work performed at the Oak Ridge National Laboratory, 1951.

Preliminary diagram. The system Ba(OH)$_2$–Sr(OH)$_2$ contains a single eutectic at 37 Sr(OH)$_2$–63 Ba(OH)$_2$ (mole %), m.p. 360°C.
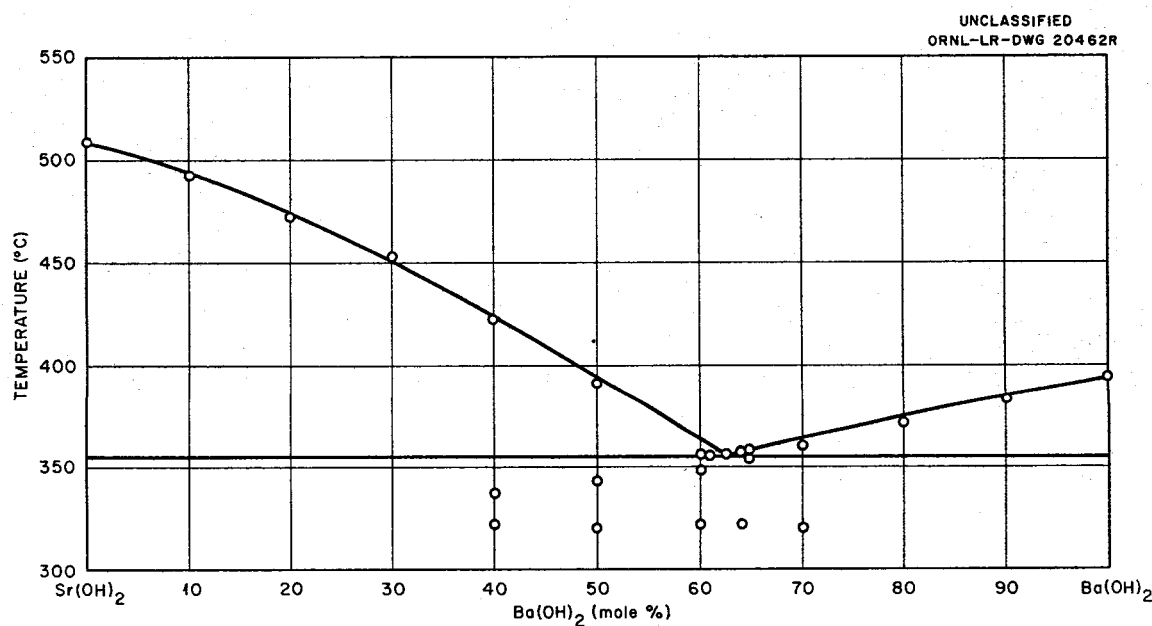
Fig. 4.6. The System Ba(OH)$_2$–Sr(OH)$_2$.

5. AQUEOUS SYSTEMS

5.1. The System UO_2–P_2O_5–H_2O, 25°C Isotherm

J. M. Schreyer, "The Solubility of Uranium(IV) Orthophosphates in Phosphoric Acid Solutions," *J. Am. Chem. Soc.* **77**, 2972 (1955).

The transition point between $U(HPO_4)_2 \cdot 6H_2O$ and $U(HPO_4)_2 \cdot H_3PO_4 \cdot H_2O$ as stable solids was at 0.62 ± 0.02 M U (10.3 wt % UO_2) and 9.8 ± 0.1 M PO_4 (42.6 wt % P_2O_5), density 1.63 ± 0.03 g/ml. The compound $U(HPO_4)_2 \cdot H_3PO_4 \cdot H_2O$ is incongruently soluble in water.
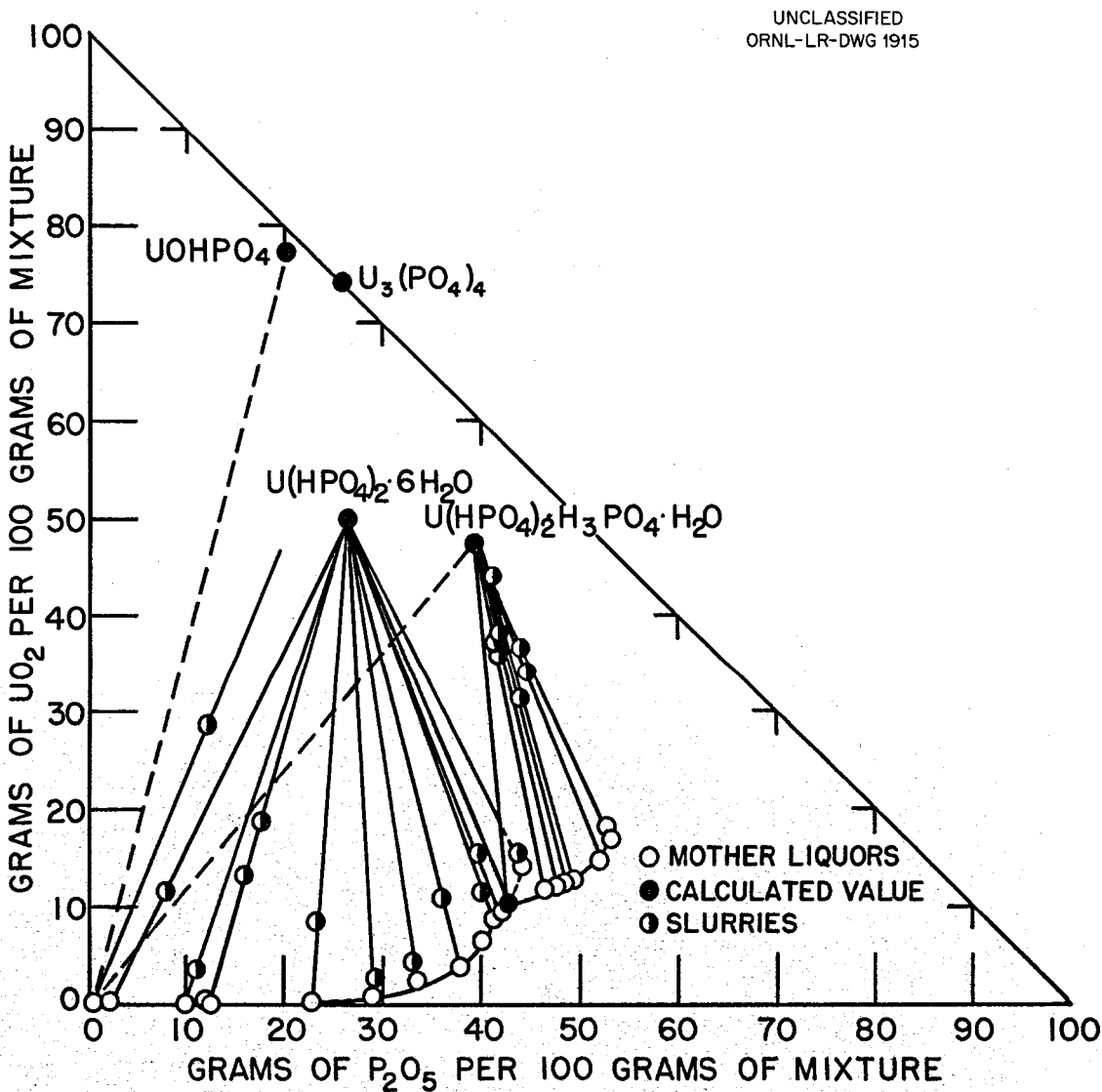
Fig. 5.1. The System UO_2–P_2O_5–H_2O, 25°C Isotherm.

5.2. The System UO_3–H_3PO_4–H_2O, 25°C Isotherm

J. M. Schreyer and C. F. Baes, Jr., "The Solubility of Uranium(VI) Orthophosphates in Phosphoric Acid Solution," *J. Am. Chem. Soc.* **76**, 354 (1954).

The normal phosphate $(UO_2)_3(PO_4)_2 \cdot 6H_2O$ is stable below 0.025 mole % H_3PO_4. The stability ranges are as follows:

Compound	Total Phosphate Molarity
$(UO_2)_3(PO_4)_2 \cdot 6H_2O$	<0.014
$UO_2HPO_4 \cdot 4H_2O$	0.014–6.1
$UO_2(H_2PO_4)_2 \cdot 3H_2O$	>6.1
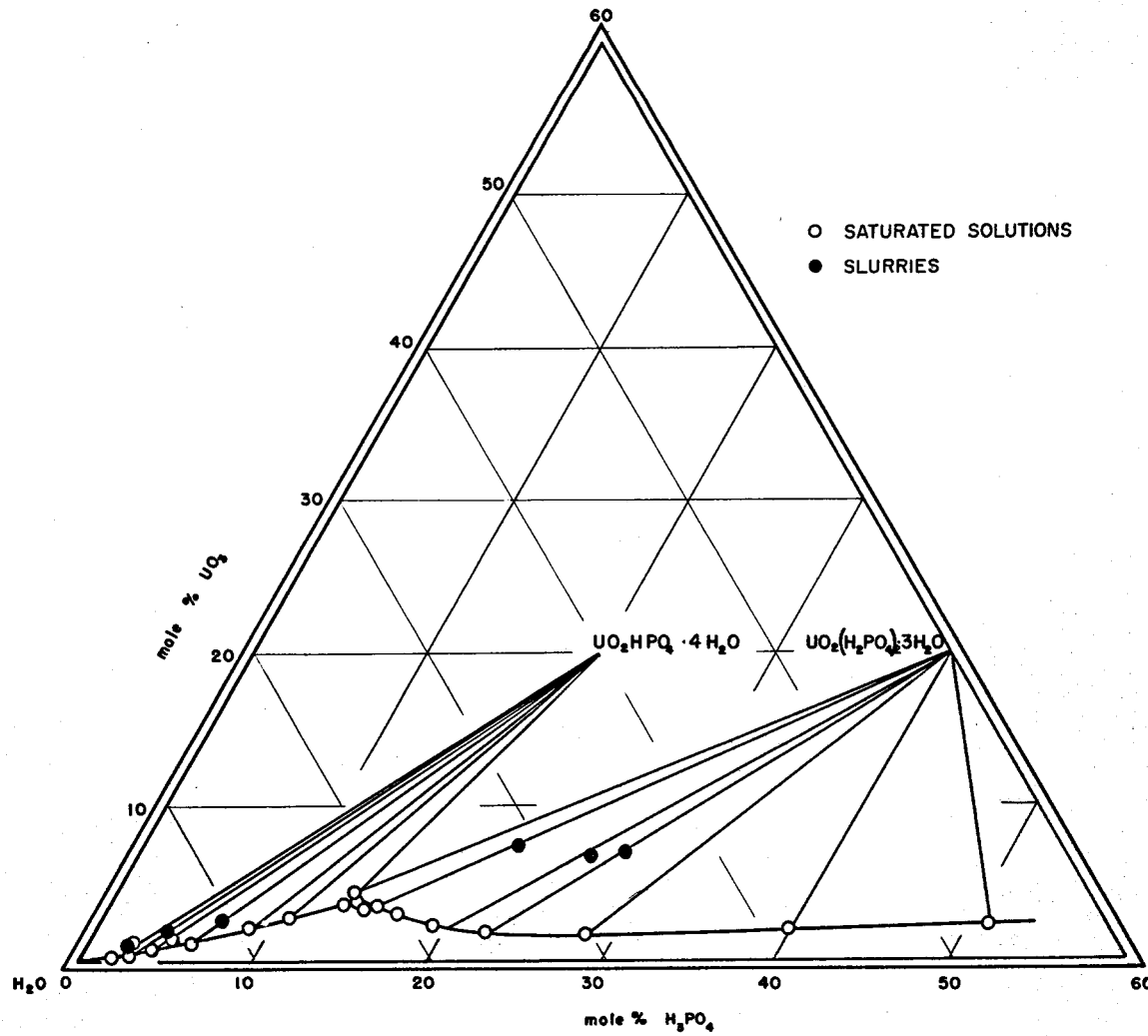
Fig. 5.2 The System UO_3–H_3PO_4–H_2O, 25°C Isotherm. 0–60 mole % UO_3, 0–60 mole % H_3PO_4.

5.3. The System $U(HPO_4)_2-Cl_2O_7-H_2O$, 25°C Isotherm

J. M. Schreyer and L. R. Phillips, "The Solubility of Uranium(VI) Orthophosphates in Perchloric Acid Solutions," *J. Phys. Chem.* **60**, 588 (1956).

The stable solids in this system are $U(HPO_4)_2\cdot 2H_2O$, $U(H_2PO_4)_2(ClO_4)_2\cdot 4H_2O$, and $U(H_2PO_4)_2(ClO_4)_2\cdot 6H_2O$. Metastable anhydrous $U(HPO_4)_2$ formed readily in all solution compositions tested. X-ray diffraction patterns indicated the existence of three polymorphic forms of $U(H_2PO_4)_2(ClO_4)_2\cdot 6H_2O$.
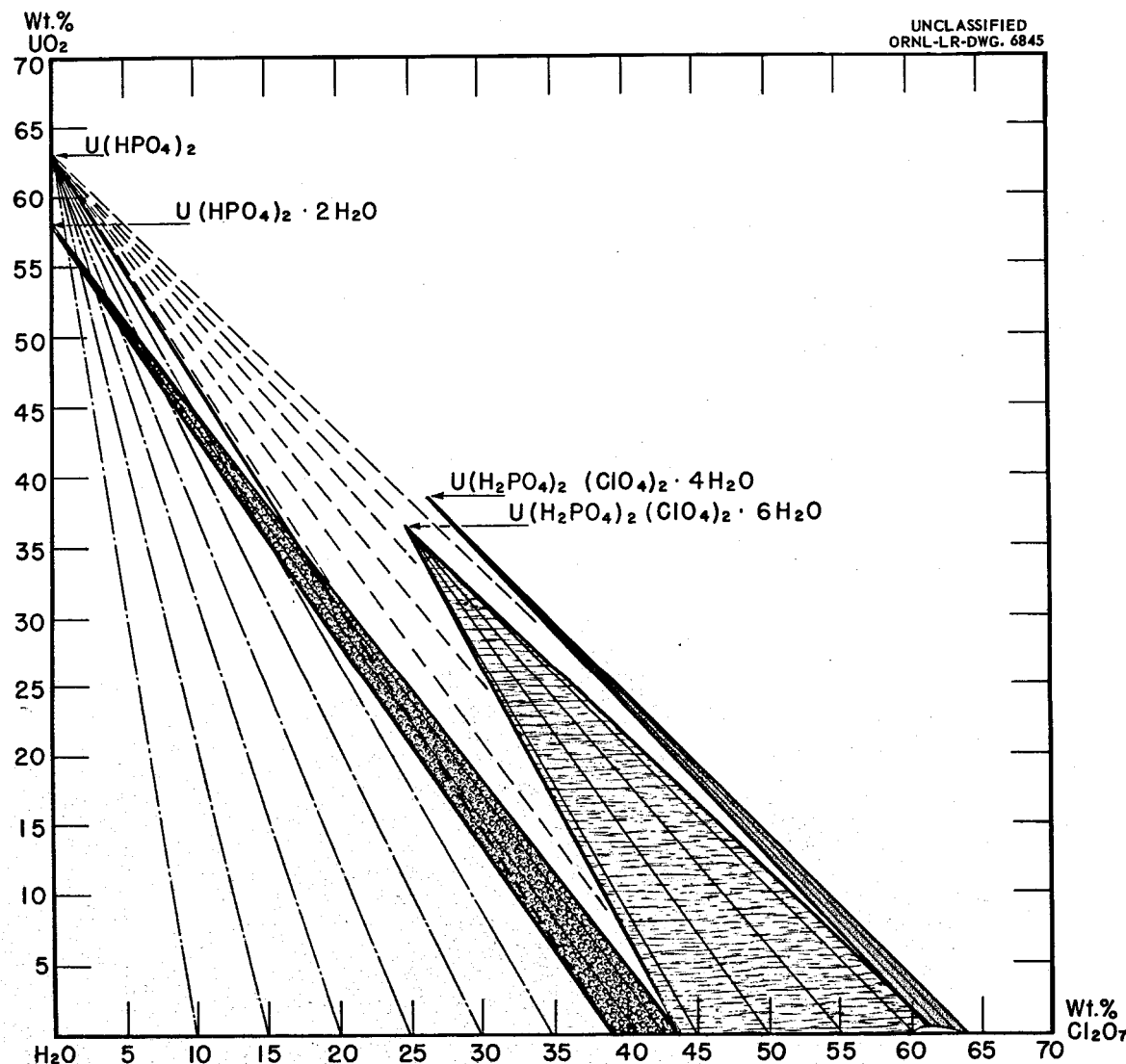
Fig. 5.3. Schreinemakers' Projection of the System $UO_2-P_2O_5-Cl_2O_7-H_2O$ at 25°C. A projection on the $UO_2-Cl_2O_7-H_2O$ face, plotted in rectangular coordinates.

147

5.4. The System $UO_3-Na_2O-CO_2-H_2O$, 26°C Isotherm

C. A. Blake, C. F. Coleman, K. B. Brown, D. G. Hill, R. S. Lowrie, and J. M. Schmitt, "Studies in the Carbonate–Uranium System," *J. Am. Chem. Soc.* **78**, 5978 (1956).
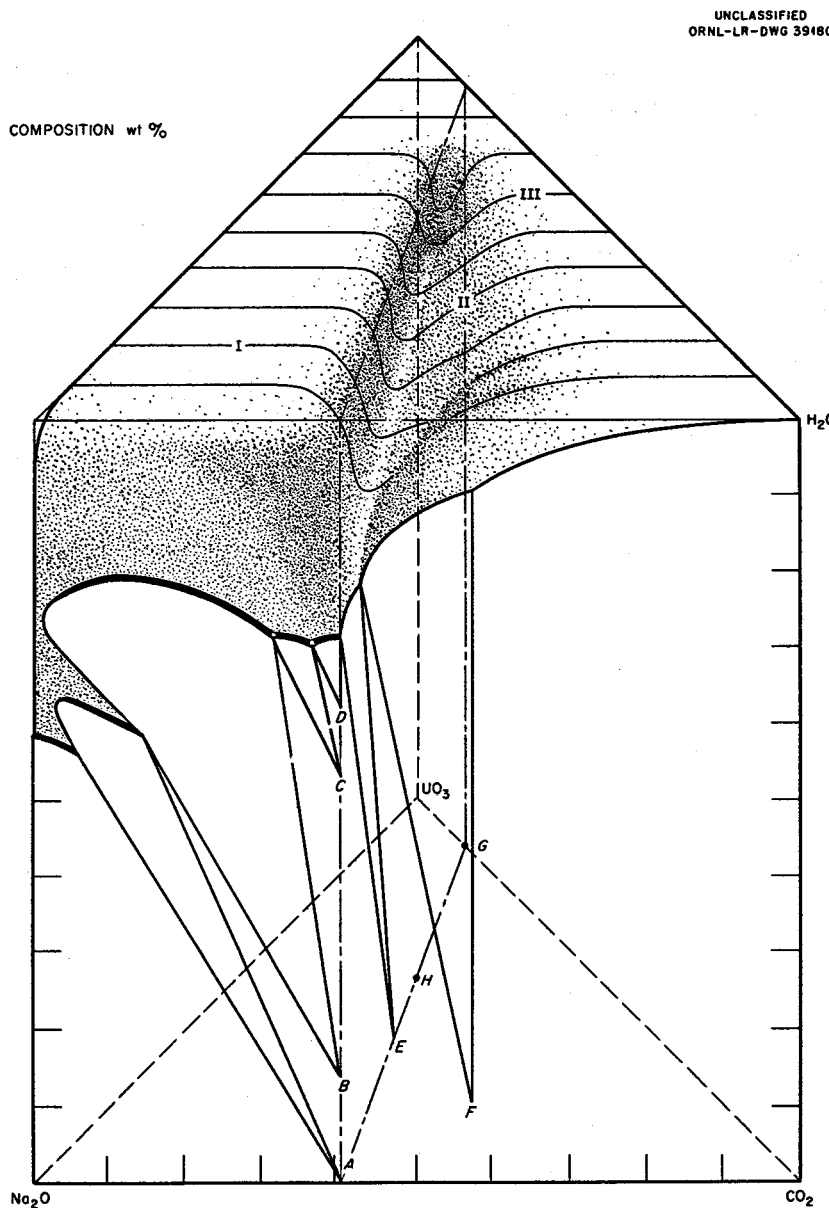
COMPOSITION wt %

Fig. 5.4a. The System $UO_3-Na_2O-CO_2-H_2O$ at 26°C. Compositions are plotted in weight per cent. I, solutions in equilibrium with sodium uranates; II, solutions in equilibrium with sodium uranyl tricarbonate; III, solutions in equilibrium with uranyl carbonate. A, Na_2CO_3; B, $Na_2CO_3 \cdot H_2O$; C, $Na_2CO_3 \cdot 7H_2O$; D, $Na_2CO_3 \cdot 10H_2O$; E, $Na_2CO_3 \cdot NaHCO_3 \cdot 2H_2O$ (trona); F, $NaHCO_3$; G, UO_2CO_3; H, $Na_4UO_2(CO_3)_3$. The entire upper face of the triangular prism represents pure water.

The stable uranium–carbonate solids found were UO_2CO_3 and $Na_4UO_2(CO_3)_3$. The solution composition at the transition point (not determined exactly) was at least 26 wt % UO_3, 5.6 wt % Na_2O, and 7.2 wt % CO_2 (mole ratio $UO_3:Na_2O:CO_2 = 1:1.0:1.8$).

Further data on this system are available from the American Documentation Institute (document No. 5079). These include compositions, pH's, and densities at points in and near the planes $Na_2O–CO_2–H_2O$, $UO_3–Na_2O–H_2O$, $UO_2CO_3–Na_2CO_3–H_2O$, $Na_4UO_2(CO_3)_3–NaHCO_3–H_2O$, $UO_3–Na_2CO_3–H_2O$, $UO_3–NaHCO_3–H_2O$, and $UO_2CO_3–Na_2O–H_2O$.

Related phase equilibria in the system $Na_2O–UO_3–H_2O$ at 50 and 75°C are reported by J. E. Ricci and F. J. Loprest, *J. Am. Chem. Soc.* **77**, 2119 (1955).
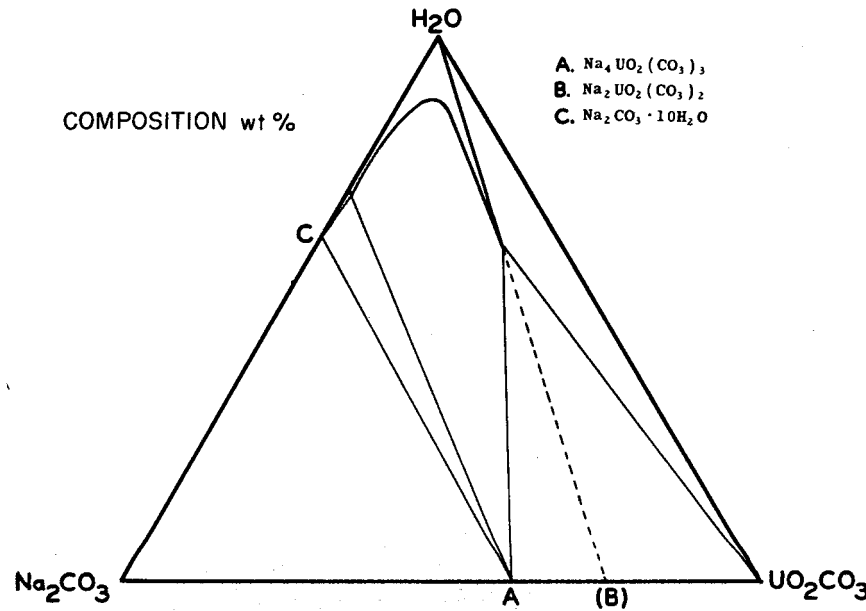
Fig. 5.4b. The Section $UO_2CO_3–Na_2CO_3–H_2O$ at 26°C.

5.5. Portions of the System $ThO_2-Na_2O-CO_2-H_2O$, 25°C Isotherm

F. A. Schimmel, unpublished work performed at the Oak Ridge National Laboratory, 1955.
The stable thorium–carbonate solids found were $ThOCO_3 \cdot 8H_2O$ and $Na_6Th(CO_3)_5 \cdot 12H_2O$.

Ternary Points

Solid Phases Present	Composition of Solution (wt %)		
	ThO_2	Na_2O	CO_2
$Na_6Th(CO_3)_5 \cdot 12H_2O$, $NaHCO_3$, and $Na_2CO_3 \cdot NaHCO_3 \cdot 2H_2O$ (trona)	0.62	12.0	9.96
$Na_6Th(CO_3)_5 \cdot 12H_2O$, $Na_2CO_3 \cdot 10H_2O$, and trona	0.48	14.1	10.86

EQUILIBRIUM SOLID PHASES

a-b z + NaHCO₃
b   z + NaHCO₃ + TRONA
b-c NaHCO₃ + TRONA
b-d z + TRONA
d   z + TRONA + Na₂CO₃·10H₂O
d-e TRONA + Na₂CO₃·10H₂O
d-f z + Na₂CO₃·10H₂O
g-h z + ThOCO₃·8H₂O

(z = 3Na₂O · ThO₂ · 5CO₂ · 12H₂O)
(TRONA = Na₂CO₃ · NaHCO₃ · 2H₂O)
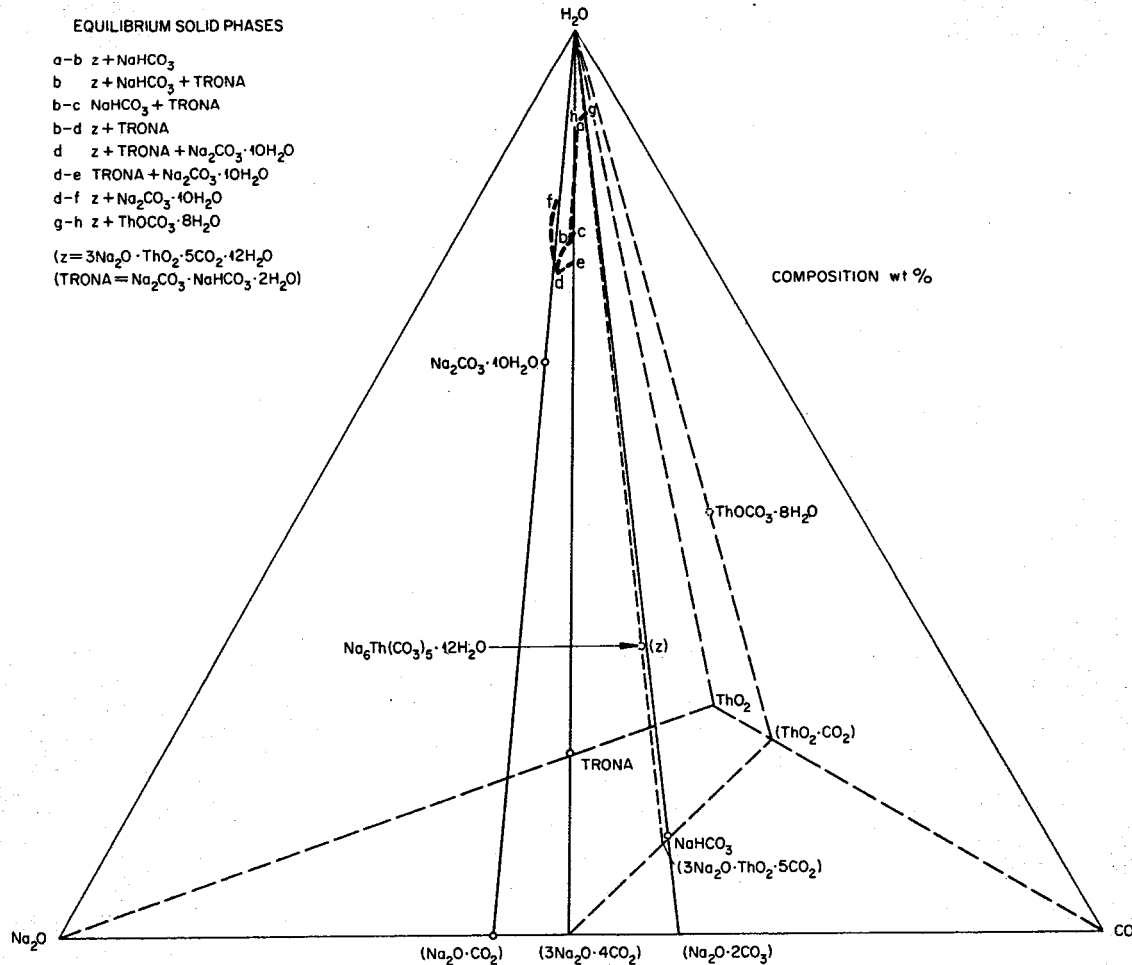
Fig. 5.5a. Perspective Representation of the System $ThO_2-Na_2O-CO_2-H_2O$ as a Tetrahedron.

The highest thorium solubility found was 3.35 wt % ThO_2 (3.06 wt % Na_2O, 3.60 wt % CO_2) in equilibrium with solid $Na_6Th(CO_3)_5 \cdot 12H_2O$ and $ThOCO_3 \cdot 8H_2O$. (The terminal points of this binary line were not established.) The maximum thorium solubility in equilibrium with $Na_6Th(CO_3)_5 \cdot 12H_2O$ and $Na_2CO_3 \cdot 10H_2O$ was 1.25 wt % ThO_2 (12.5 wt % Na_2O, 9.4 wt % CO_2); with $Na_6Th(CO_3)_5 \cdot 12H_2O$ and trona, the highest solubility was 0.7 wt % ThO_2 (12.6 wt % Na_2O, 10.4 wt % CO_2). The highest found with $Na_6Th(CO_3)_5 \cdot 12H_2O$ and $NaHCO_3$ was 1.2 wt % ThO_2 (5.0 wt % Na_2O, 6.0 wt % CO_2), which was the most dilute $NaHCO_3$ solution tested.

EQUILIBRIUM SOLID PHASES

a-b	$z + NaHCO_3$
b	$z + NaHCO_3 + TRONA$
b-c	$NaHCO_3 + TRONA$
b-d	$z + TRONA$
d	$z + TRONA + Na_2CO_3 \cdot 10H_2O$
d-e	$TRONA + Na_2CO_3 \cdot 10H_2O$
d-f	$z + Na_2CO_3 \cdot 10H_2O$
g-h	$z + ThOCO_3 \cdot 8H_2O$

$(z = Na_6Th(CO_3)_5 \cdot 12H_2O)$
$(TRONA = Na_2CO_3 \cdot NaHCO_3 \cdot 2H_2O)$
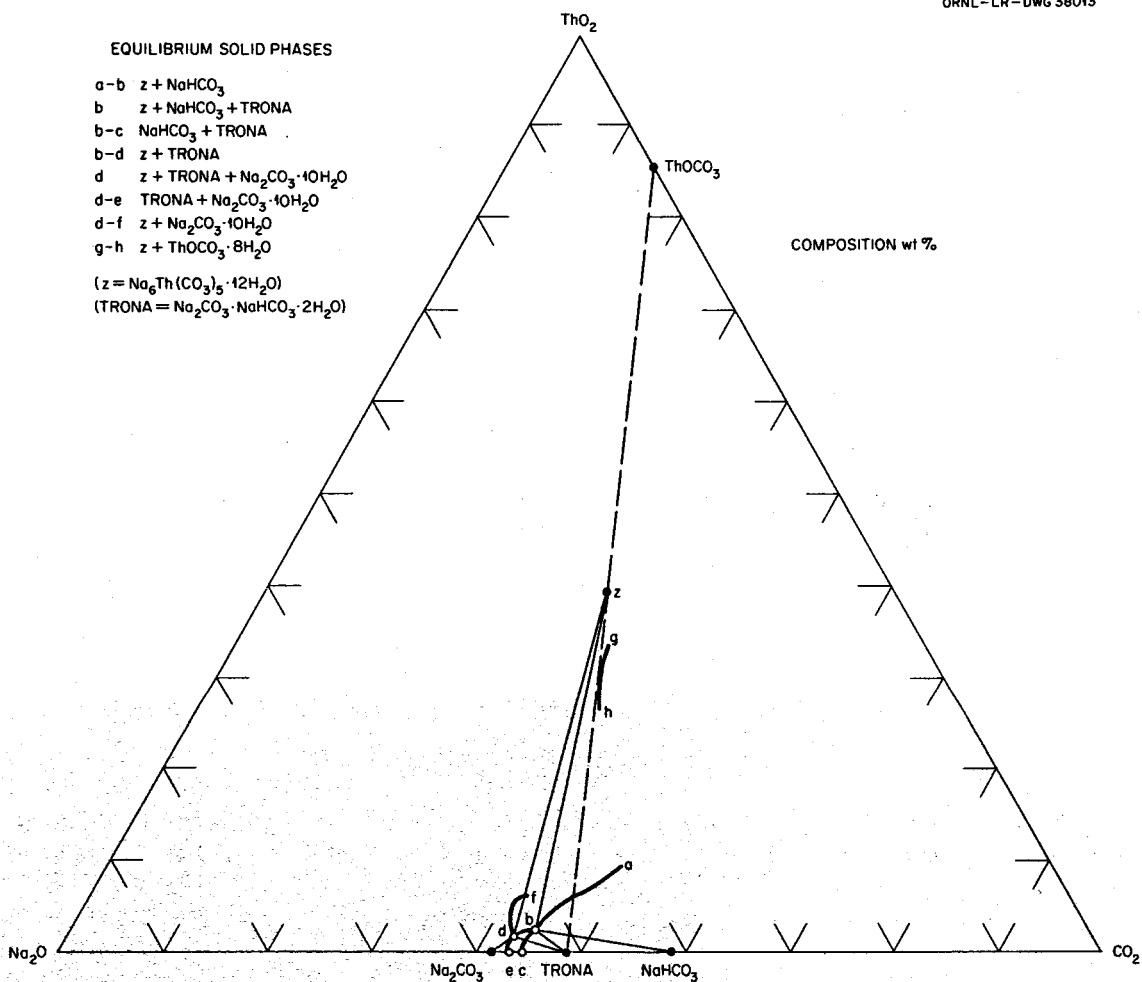
Fig. 5.5b. The System $ThO_2-Na_2O-CO_2-H_2O$ at 25°C. Projection to the $ThO_2-Na_2O-CO_2$ face along radii from the H_2O vertex.

151

EQUILIBRIUM SOLID PHASES

a–b   z + NaHCO₃
b   z + NaHCO₃ + TRONA
b–c   NaHCO₃ + TRONA
b–d   z + TRONA
d   z + TRONA + Na₂CO₃·10H₂O
d–e   TRONA + Na₂CO₃·10H₂O
d–f   z + Na₂CO₃·10H₂O
g–h   z + ThOCO₃·8H₂O

(z = 3Na₂O–ThO₂·5CO₂·12H₂O)
(TRONA = Na₂CO₃·NaHCO₃·2H₂O)

COMPOSITION wt %
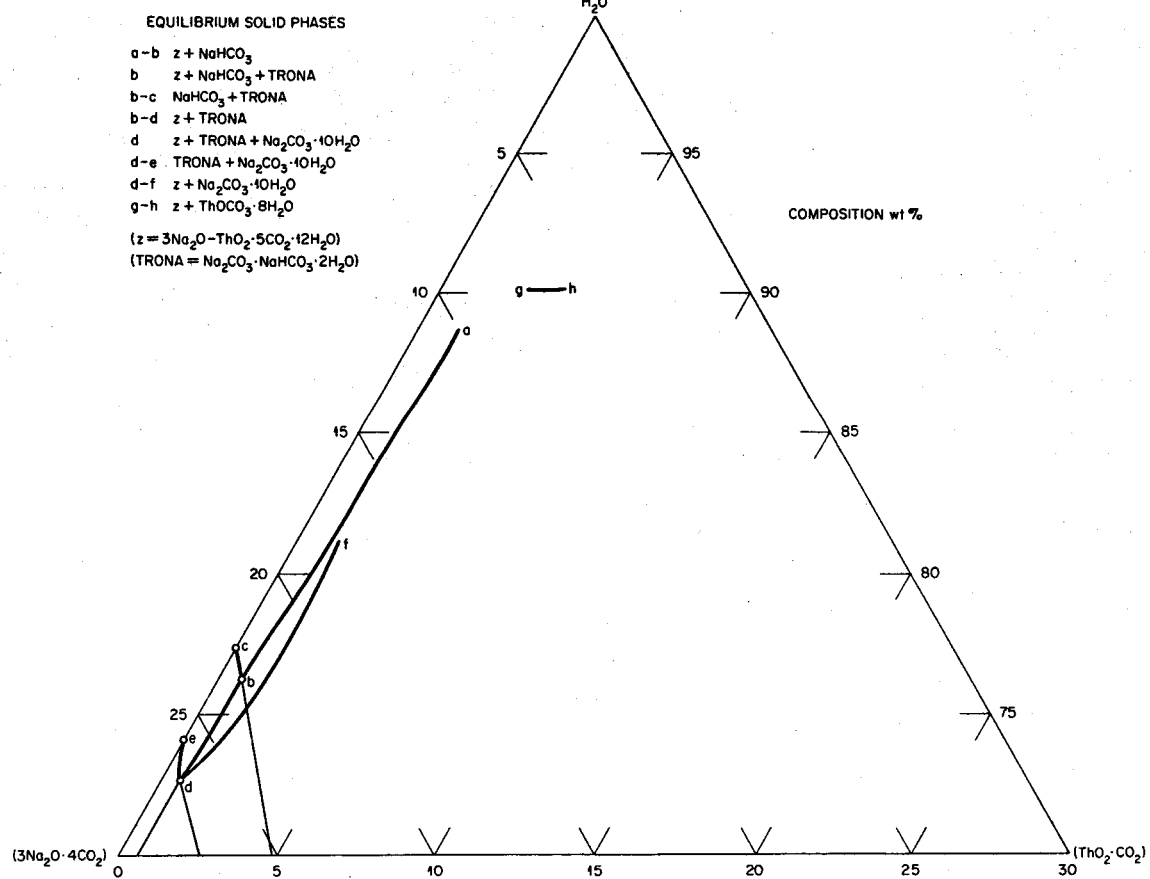
Fig. 5.5c. The System ThO_2–Na_2O–CO_2–H_2O at 25°C. Projection to the $ThO_2 \cdot CO_2$–$3Na_2O \cdot 4CO_2$–H_2O internal plane, represented as an equivalent triangle, along radii from the CO_2 vertex. Portion from 70 to 100 wt % H_2O.

5.6. The System $Na_2O-CO_2-H_2O$, 25°C Isotherm

F. A. Schimmel, unpublished work performed at the Oak Ridge National Laboratory, 1955.

Significant changes from the data of Freeth [*Phil. Trans. Roy. Soc. London* **233**, 35 (1922)] were found throughout the range; there was closer agreement in the bicarbonate range with the data of Hill and Bacon [*J. Am. Chem. Soc.* **49**, 2487 (1927)].

Transition Points

Solid Phases Present	Composition of Solution (wt %)	
	Na_2O	CO_2
$NaOH \cdot H_2O$ and Na_2CO_3	40.5	0.85
Na_2CO_3 and $Na_2CO_3 \cdot H_2O$	31.4	0.72
$Na_2CO_3 \cdot H_2O$ and $Na_2CO_3 \cdot 7H_2O$	18.7	6.9
$Na_2CO_3 \cdot 7H_2O$ and $Na_2CO_3 \cdot 10H_2O$	17.85	7.8
$Na_2CO_3 \cdot 10H_2O$ and $Na_2CO_3 \cdot NaHCO_3 \cdot 2H_2O$ (trona)	13.7	10.35
Trona and $NaHCO_3$	11.9	9.5

The System Na$_2$O–CO$_2$–H$_2$O, 25°C Isotherm

Composition of Saturated Solution (wt %)		Equilibrium Solid Phase
Na$_2$O	CO$_2$	
41.3	0	NaOH·H$_2$O
40.5	0.85	Na$_2$CO$_3$
40.45	0.8	Na$_2$CO$_3$
31.6	0.67	Na$_2$CO$_3$
31.4	0.72	Na$_2$CO$_3$ and Na$_2$CO$_3$·H$_2$O
31.1	0.78	Na$_2$CO$_3$·H$_2$O
29.9	0.5	Na$_2$CO$_3$·H$_2$O
26.6	0.4	Na$_2$CO$_3$·H$_2$O
25.2	0.55	Na$_2$CO$_3$·H$_2$O
23.2	0.9	Na$_2$CO$_3$·H$_2$O
23.15	1.0	Na$_2$CO$_3$·H$_2$O
21.15	2.3	Na$_2$CO$_3$·H$_2$O
19.3	4.3	Na$_2$CO$_3$·H$_2$O
18.95	6.0	Na$_2$CO$_3$·H$_2$O
18.57	7.5	Na$_2$CO$_3$·H$_2$O (metastable)
18.6	7.8	Na$_2$CO$_3$·H$_2$O (metastable)
18.7	6.9	Na$_2$CO$_3$·H$_2$O and Na$_2$CO$_3$·7H$_2$O
18.5	6.75	Na$_2$CO$_3$·7H$_2$O (metastable)
17.7	7.95	Na$_2$CO$_3$·7H$_2$O (metastable)
18.3	7.3	Na$_2$CO$_3$·7H$_2$O
17.85	7.8	Na$_2$CO$_3$·7H$_2$O and Na$_2$CO$_3$·10H$_2$O
17.3	7.88	Na$_2$CO$_3$·10H$_2$O
16.1	7.9	Na$_2$CO$_3$·10H$_2$O
15.6	7.92	Na$_2$CO$_3$·10H$_2$O
15.1	8.1	Na$_2$CO$_3$·10H$_2$O
13.7	8.85	Na$_2$CO$_3$·10H$_2$O
13.28	9.4	Na$_2$CO$_3$·10H$_2$O
13.55	10.15	Na$_2$CO$_3$·10H$_2$O
14.1	11.0	Na$_2$CO$_3$·10H$_2$O (metastable)
13.7	10.35	Na$_2$CO$_3$·10H$_2$O and trona*
17.0	13.0	Trona (metastable)
16.7	12.7	Trona (metastable)
13.8	10.35	Trona
11.9	9.5	Trona and NaHCO$_3$
11.55	9.3	NaHCO$_3$
10.5	8.8	NaHCO$_3$
9.4	.8.0	NaHCO$_3$
8.1	7.5	NaHCO$_3$
6.4	6.5	NaHCO$_3$
5.4	5.75	NaHCO$_3$
3.9	5.0	NaHCO$_3$
3.56	4.95	NaHCO$_3$
3.47	4.93	NaHCO$_3$

*The formula of trona is Na$_2$CO$_3$·NaHCO$_3$·2H$_2$O.
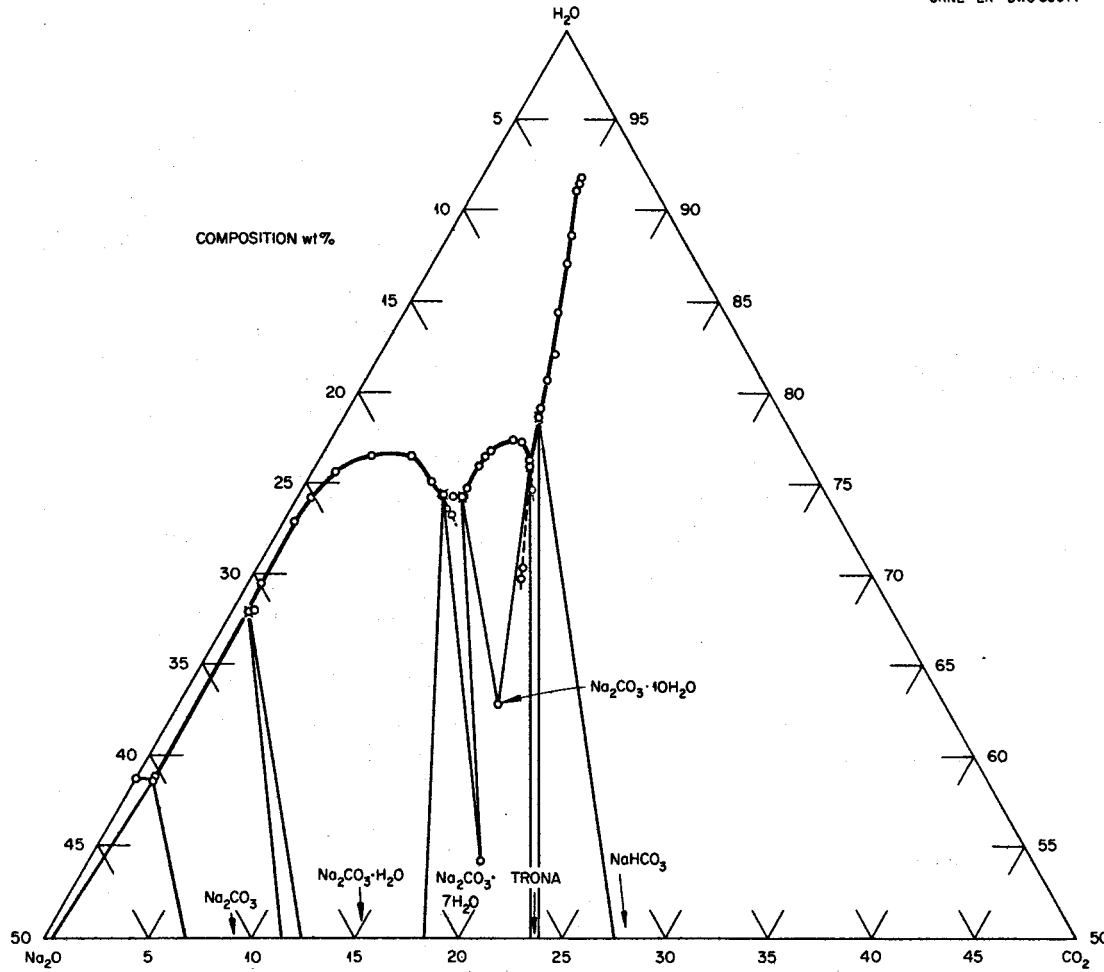
Fig. 5.6. The System $Na_2O-CO_2-H_2O$, 25°C Isotherm. 0–50 wt % Na_2O, 0–50 wt % CO_2.

5.7. Solubility of Uranyl Sulfate in Water

1. C. H. Secoy, *J. Am. Chem. Soc.* **72**, 3343 (1950) (data above 300°C).

2. C. H. Secoy, *J. Am. Chem. Soc.* **70**, 3450 (1948) (data up to 300°C).

3. L. Helmholtz and G. Friedlander, *Physical Properties of Uranyl Sulfate Solutions,* MDDC-808 (1943) (room temperature data).

4. C. Dittrich, *Z. physik. Chem.* **29**, 449 (1899).

5. E. V. Jones and W. L. Marshall, *HRP Quar. Prog. Rep. March 15, 1952,* ORNL-1280, p 180–83.

6. E. V. Jones and W. L. Marshall, *HRP Quar. Prog. Rep. Jan. 31, 1959,* ORNL-2696, p 210–11.

The two-liquid-phase region of this system in actuality must be represented by the three components UO_3, SO_3, and H_2O. The curve representing the boundary of liquid-liquid immiscibility is correct for stoichiometric solutions. However, the tie lines within the region of immiscibility do not connect two solutions containing stoichiometric UO_2SO_4 but rather connect solutions containing varying concentrations and ratios of UO_3 and SO_3 (Fig. 5.10). At low concentrations and high temperatures, that is, below 0.02 m UO_2SO_4 and above 250°C, hydrolysis occurs to produce a nonstoichiometric solution phase. The point of hydrolysis is dependent on concentration and temperature (see Sec 5.13).

Note: Revised data (ref 5) are used to construct the immiscibility boundary in the figure. Earlier data (ref 1) showed higher temperatures in this region and a possible likelihood of acid impurity in the solutions.
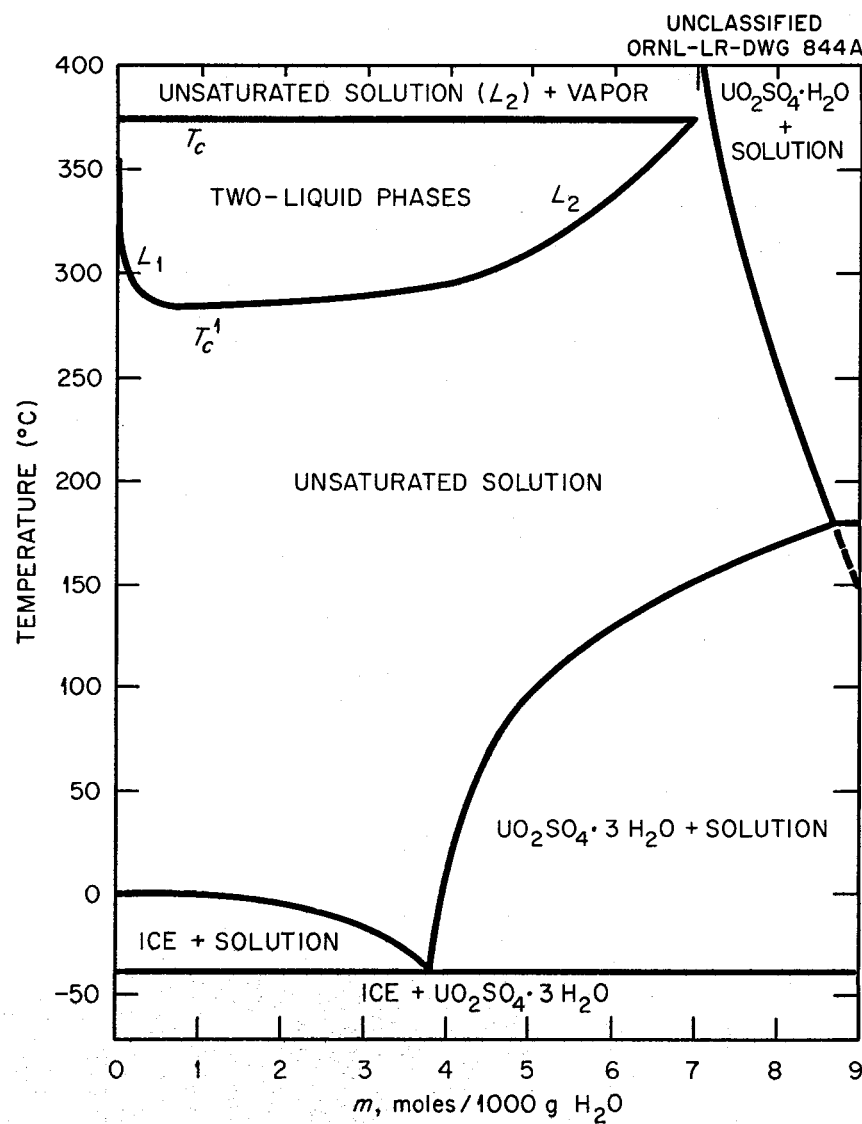
Fig. 5.7. The System UO_2SO_4–H_2O.

5.8. Two-Liquid-Phase Region of UO_2SO_4 in Ordinary and Heavy Water

E. V. Jones and W. L. Marshall, *HRP Quar. Prog. Rep. March 15, 1952,* ORNL-1280, p 180–83.

The two curves shown are boundary curves for liquid-liquid immiscibility obtained by observing the phase-transitional behavior of known UO_2SO_4–H_2O (D_2O) solutions in sealed tubes as a function of temperature. For later reference, this procedure is designated the visual-synthetic method. As was described in Sec 5.7, the concentrations and compositions of the two phases within the boundary region at equilibrium cannot be obtained from this figure. Mixtures which are solutions at lower temperatures separate into two liquid phases as the temperature is raised, according to the boundary curves.
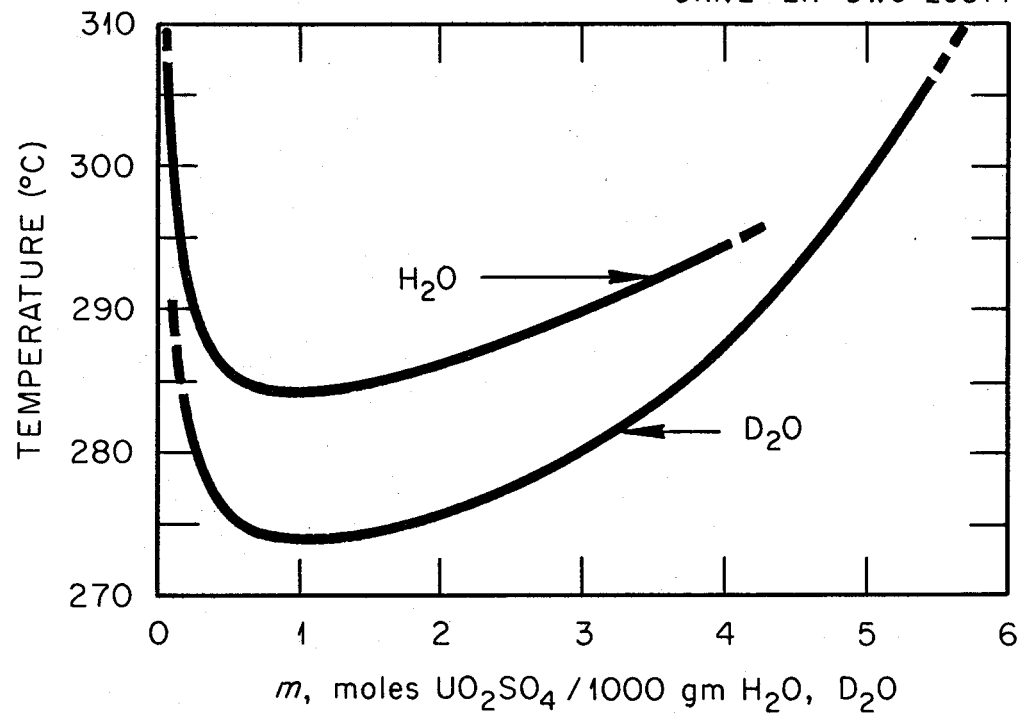
Fig. 5.8. Two-Liquid-Phase Region of UO_2SO_4 in Ordinary and Heavy Water.

5.9. The System $UO_3-SO_3-H_2O$

1. A. Colani, *Bull. soc. chim. France* [4] 43, 754–62 (1928).

2. J. S. Gill, E. V. Jones, and C. H. Secoy, *HRP Quar. Prog. Rep. Oct. 31, 1953,* ORNL-1658, p 87.

The 25° data on the SO_3–rich side are those of Colani. The higher temperature data are those of Gill, Jones, and Secoy, obtained by filtration techniques at temperature. The number and identity of the solid phases in the UO_3–rich regions at 25, 100, and 175°C are somewhat uncertain. Subsequent unpublished work of F. E. Clark and C. H. Secoy has disclosed that the K solid is identical (x-ray diffraction) with the mineral uranopilite, $6UO_3 \cdot SO_3 \cdot xH_2O$, that the G solid is not identifiable as any known mineral, and that at least one additional unidentified solid phase occurs at 25 and 100°. The liquidus curves for the 25 and 100° isotherms are essentially correct as shown except that the transition points (two solid phases) occur at somewhat lower concentrations than those indicated.

$F = UO_3 \cdot H_2O$

$K = $ URANOPILITE
$\qquad 6UO_3 \cdot SO_3 \cdot 18 \, (?) \, H_2O$

$G = G$ BASIC SALT
$\qquad (5UO_3 \cdot 2SO_3 \cdot yH_2O)?$

$E = UO_2SO_4 \cdot 3H_2O$

$D = UO_2SO_4 \cdot 2H_2O$

$C = UO_3 \cdot 2SO_3 \cdot 6H_2O$

$B = UO_3 \cdot 2SO_3 \cdot 3H_2O$

$A = UO_3 \cdot 2SO_3 \cdot 1.5H_2O$
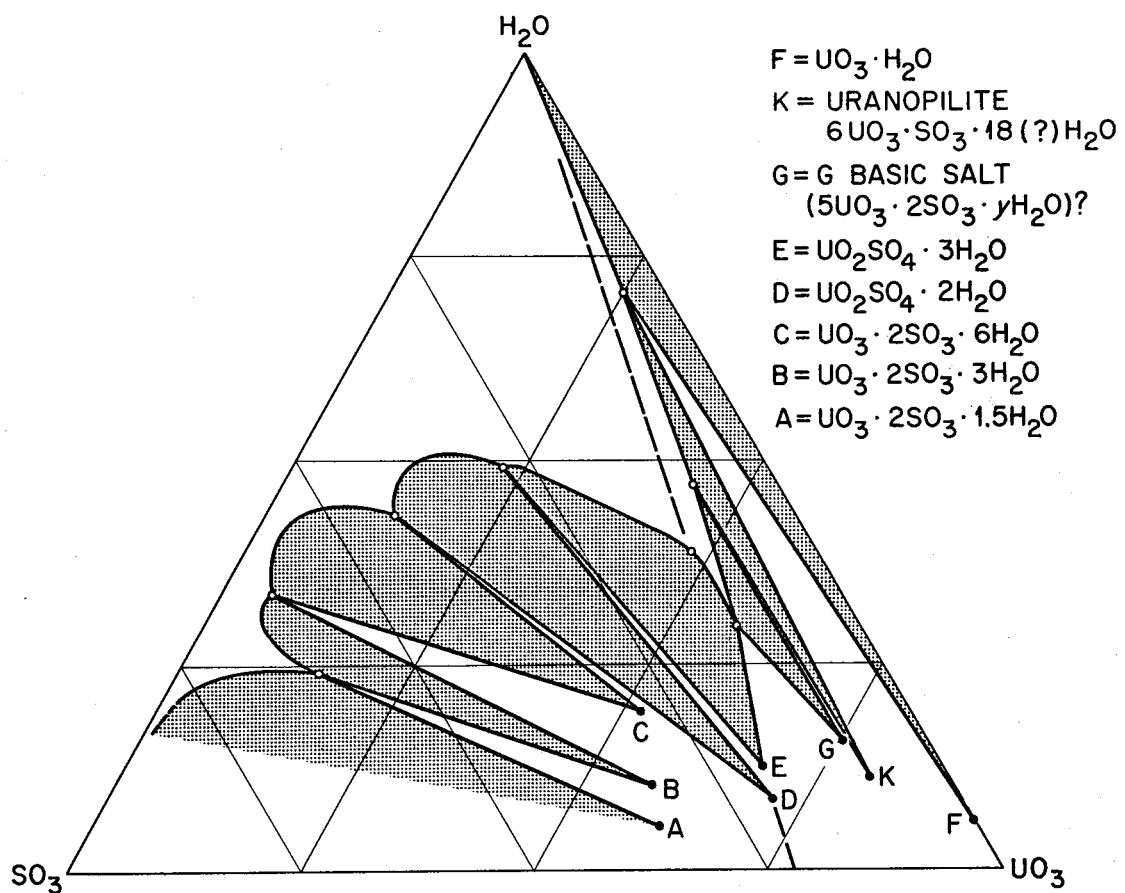
Fig. 5.9a. The System $UO_3-SO_3-H_2O$ at 25°C.

$F = UO_3 \cdot H_2O$
$G = G$ BASIC SALT
$E = UO_2SO_4 \cdot 3H_2O$
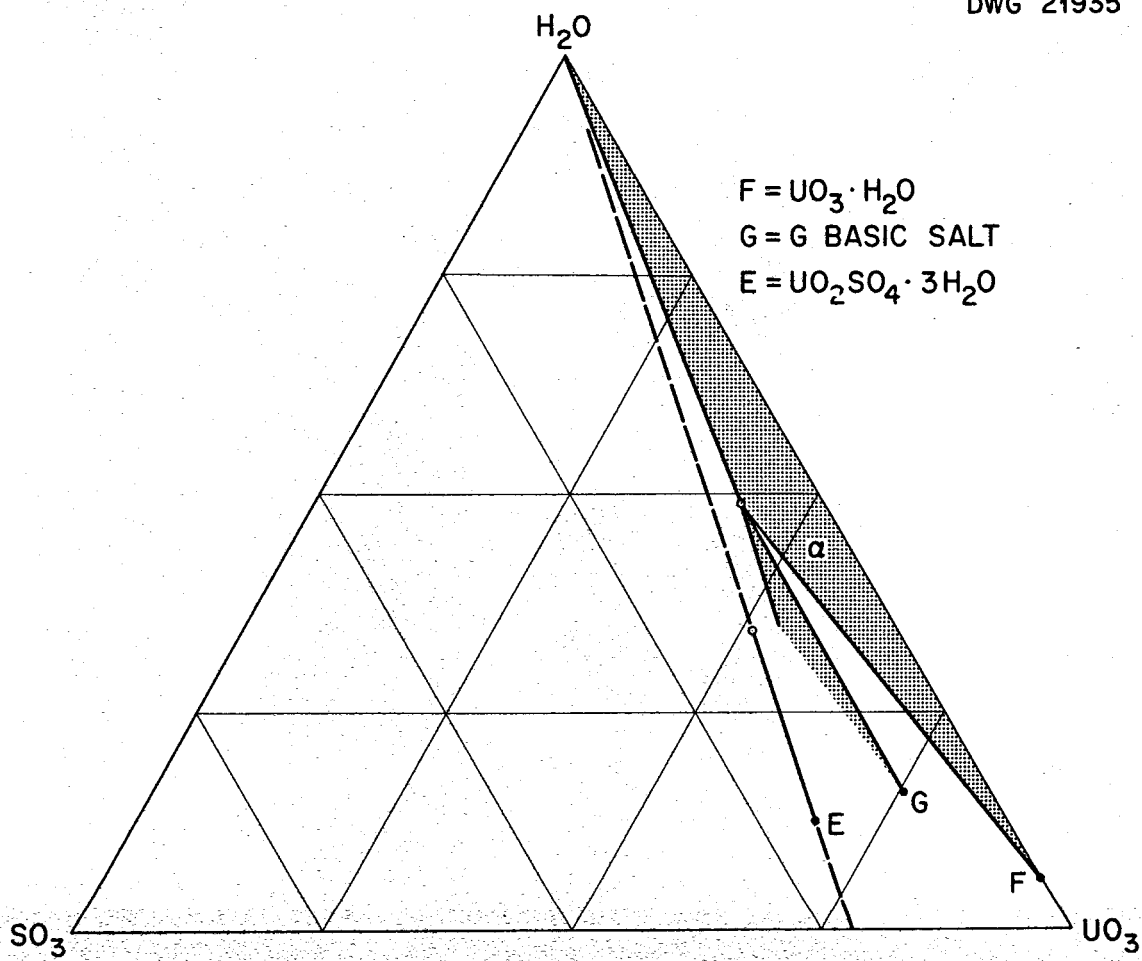
Fig. 5.9b. The System UO_3–SO_3–H_2O at 100°C.

$F = UO_3 \cdot H_2O$

$G = G$ BASIC SALT

$E = UO_2 \cdot SO_4 \cdot 3H_2O$
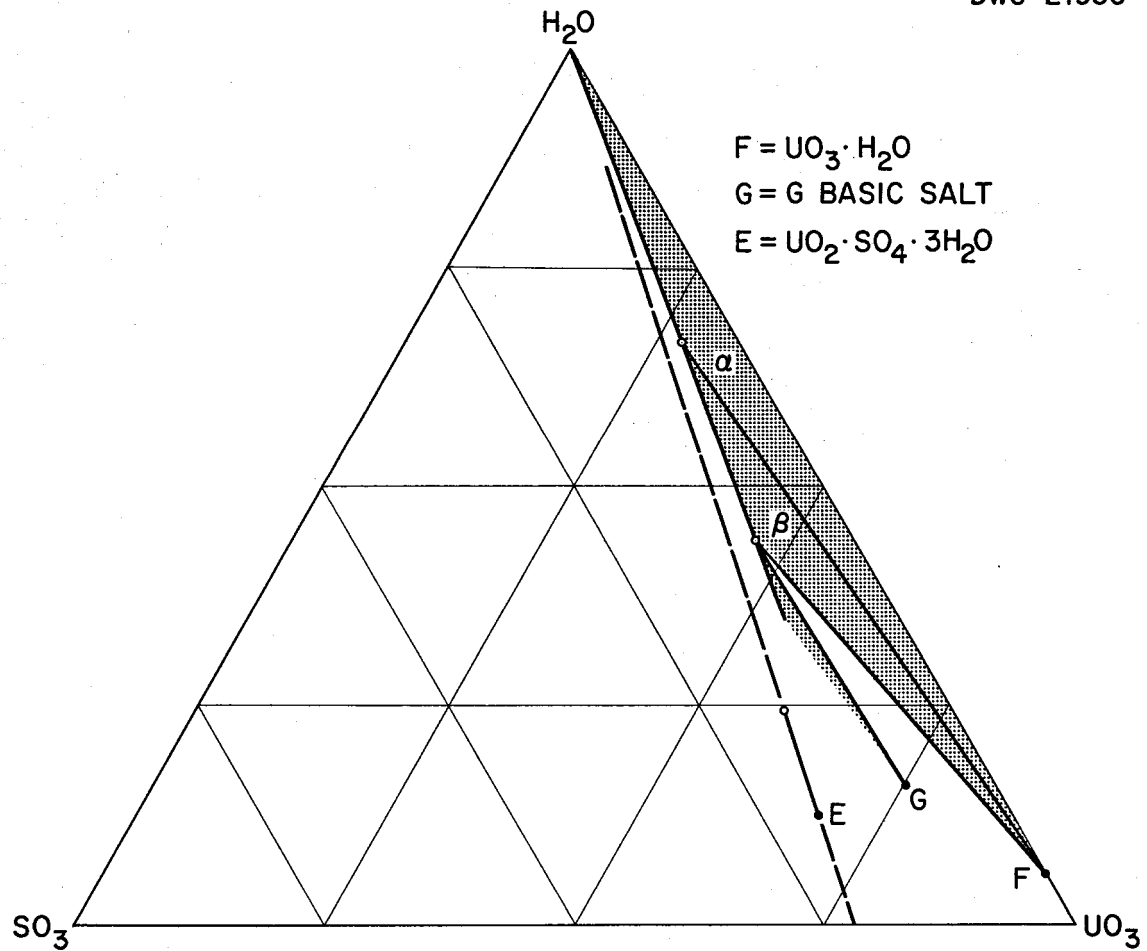
Fig. 5.9c. The System UO_3–SO_3–H_2O at 175°C.

SOLID PHASE : $\beta\ UO_3 \cdot H_2O$

H₂O

99.75

99.50

99.25

CROSS OVER

SO₃

UO₃

0.25

0.75

0.50

0.50

0.75

0.25
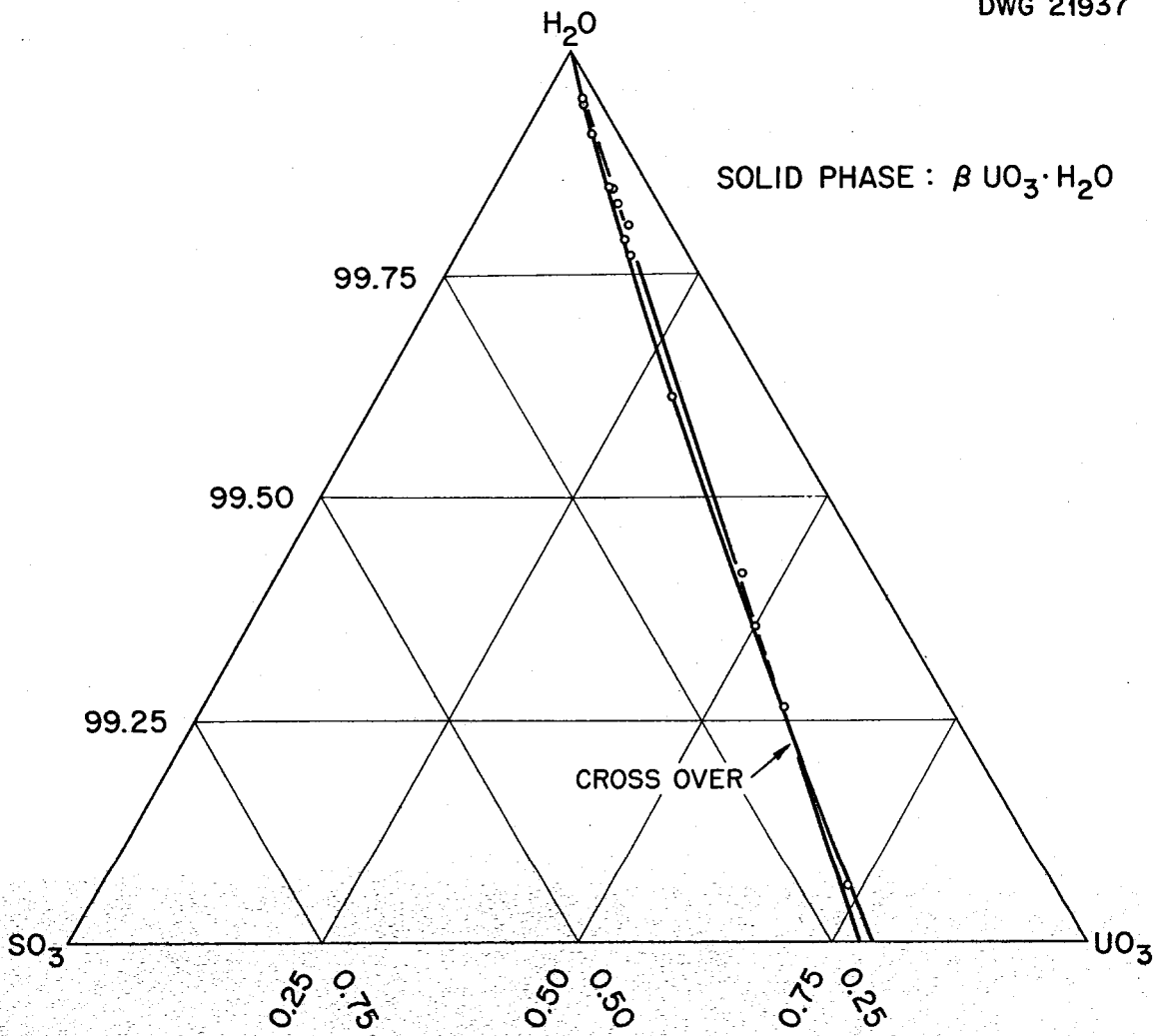
Fig. 5.9d. The System UO_3–SO_3–H_2O at 250°C.

163

5.10. Coexistence Curves for Two Liquid Phases in the System $UO_2SO_4-H_2SO_4-H_2O$

H. W. Wright, W. L. Marshall, and C. H. Secoy, *HRP Quar. Prog. Rep. Oct. 1, 1952,* ORNL-1424, p 108.

All curves in this figure must extrapolate to the critical temperature of water (374.2°C) at zero concentration of uranium. These are boundary curves which were determined by observing sealed tubes in which immiscibility occurred in $UO_3-SO_3-H_2O$ solutions upon varying the temperature. As was explained in Sec 5.7, they do not represent concentrations and compositions of the two liquid phases within the temperature-concentration region of immiscibility but are lower solution boundary curves.
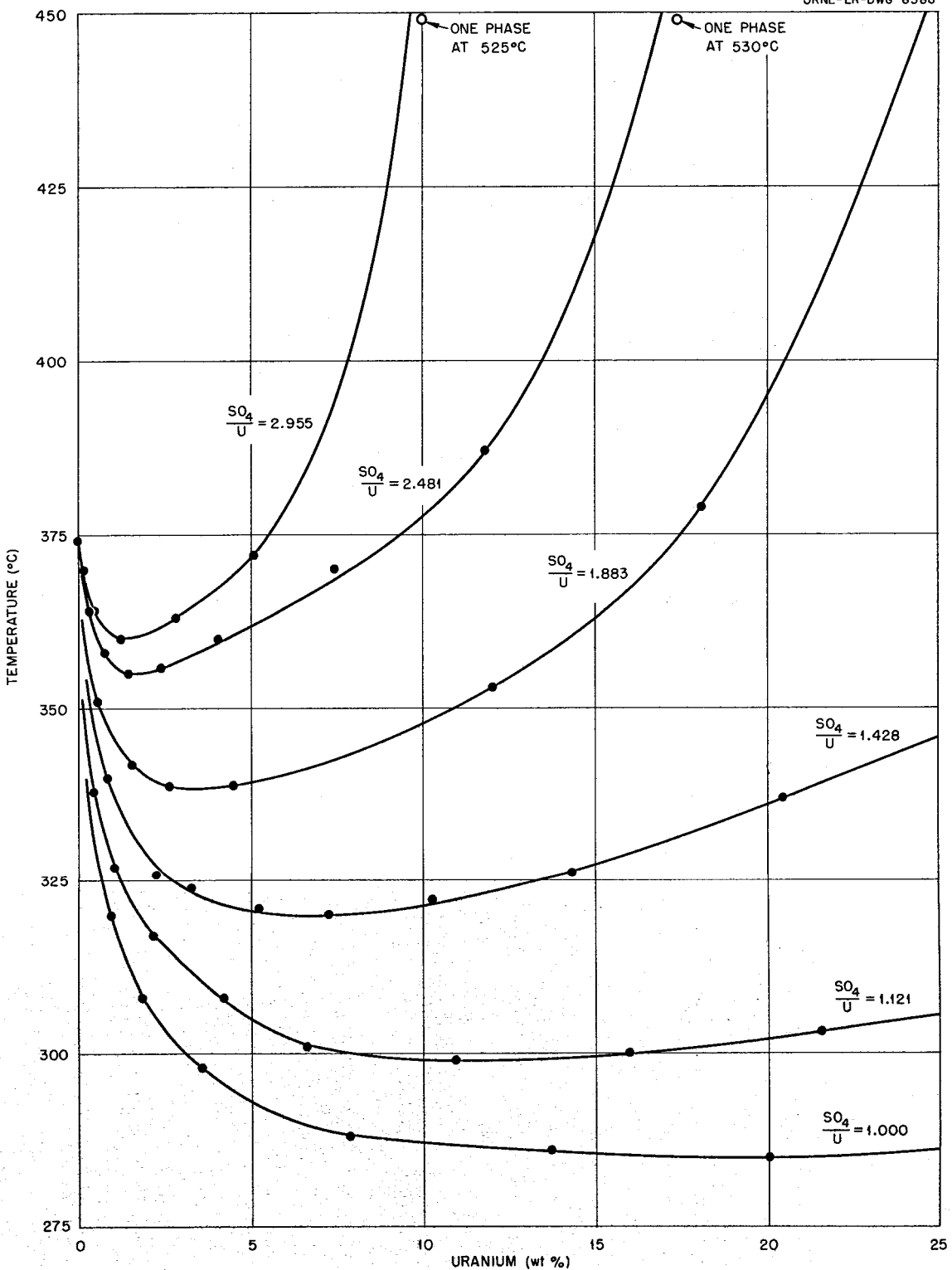
Fig. 5.10. Coexistence Curves for Two Liquid Phases in the System UO_2SO_4–H_2SO_4–H_2O.

5.11. Two-Liquid-Phase Region of the System $UO_2SO_4-H_2SO_4-H_2O$

R. E. Leed and C. H. Secoy, *Chem. Quar. Prog. Rep. Sept. 30, 1950*, ORNL-870, p 29–30; C. H. Secoy, *Chem. Quar. Prog. Rep. Dec. 31, 1949*, ORNL-607, p 33–38.

In contrast with the immiscibility curves shown in Fig. 5.10, each of these curves must extrapolate to a critical temperature curve for SO_3-H_2O in which a small or negligible amount of UO_3 is dissolved. Since SO_3 dissolved in H_2O (neglecting any dissolved UO_3) will elevate the critical temperature, the curves obtained from solutions containing a constant amount of free H_2SO_4 will all extrapolate to critical temperatures higher than that (374.2°C) for H_2O alone.
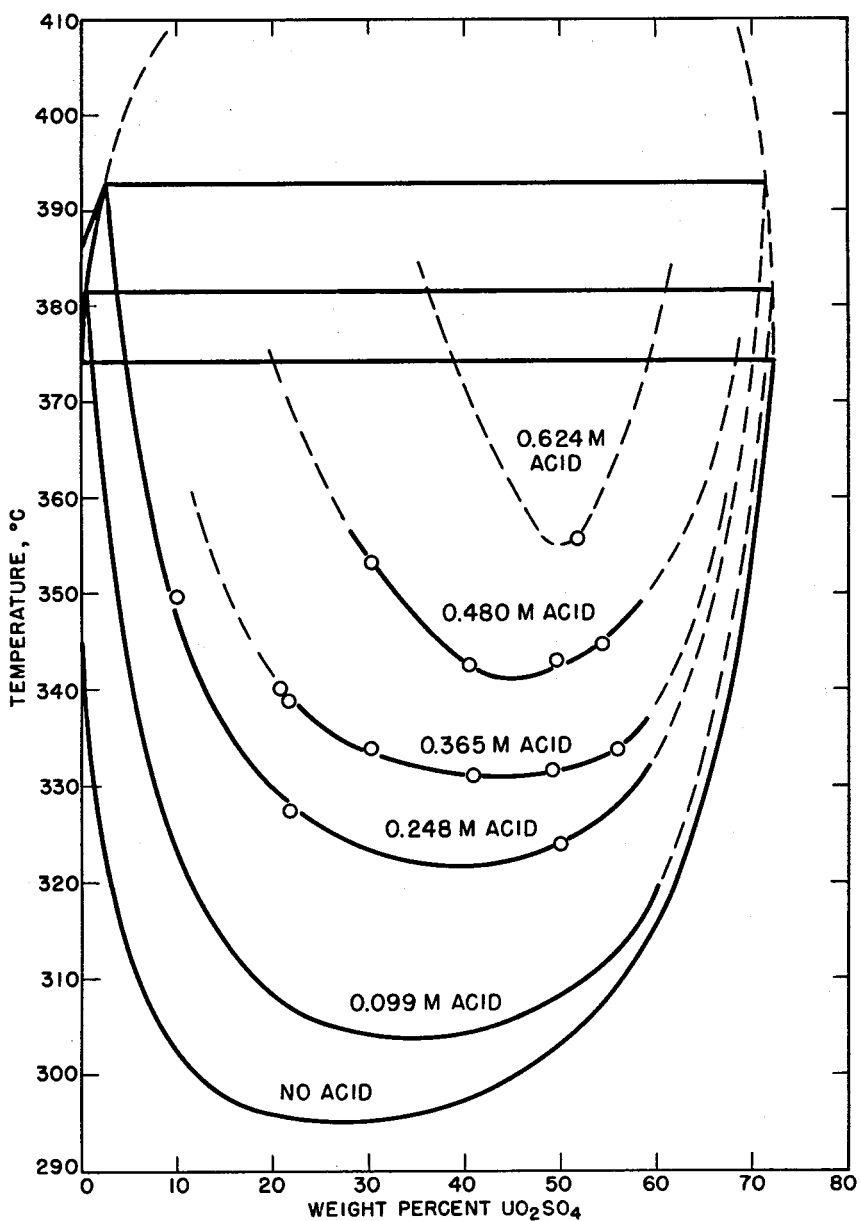
Fig. 5.11. Two-Liquid-Phase Region of the System $UO_2SO_4-H_2SO_4-H_2O$.

5.12. Two-Liquid-Phase Coexistence Curves for UO_3-Rich Solutions in the System UO_3-SO_3-H_2O With and Without HNO_3

E. V. Jones and W. L. Marshall, *HRP Quar. Prog. Rep. July 1, 1952*, ORNL-1318, p 147–48.

These curves have been obtained by the visual-synthetic method mentioned in Sec 5.8. They are therefore boundary curves and do not describe compositions and concentrations within the liquid-liquid immiscibility region.
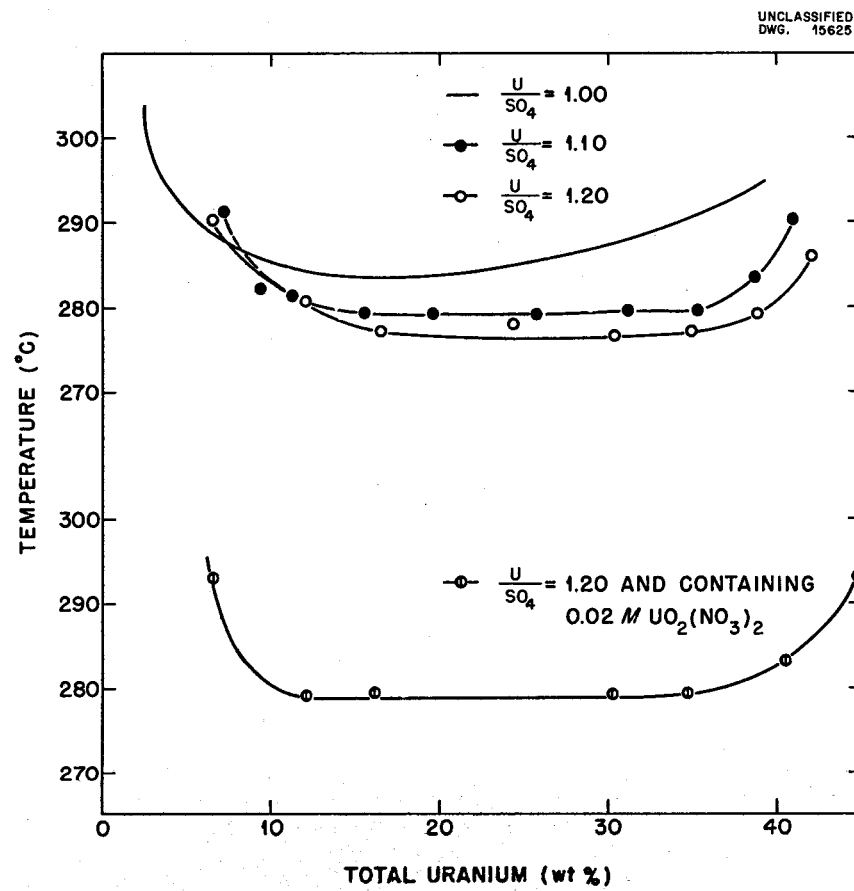
Fig. 5.12. Two-Liquid-Phase Coexistence Curves for UO_3-Rich Solutions in the System UO_3-SO_3-H_2O With and Without HNO_3.

5.13. Solubility of UO_3 in $H_2SO_4-H_2O$ Mixtures

W. L. Marshall, *Anal. Chem.* **27**, 1923 (1955).

The data are represented in this manner in order to show the full concentration range on one figure and to best indicate the degree of precision. The solid phase is α-$UO_3 \cdot H_2O$ below 205°C and β-$UO_3 \cdot H_2O$ above 205°C. These curves represent hydrolysis equilibria.
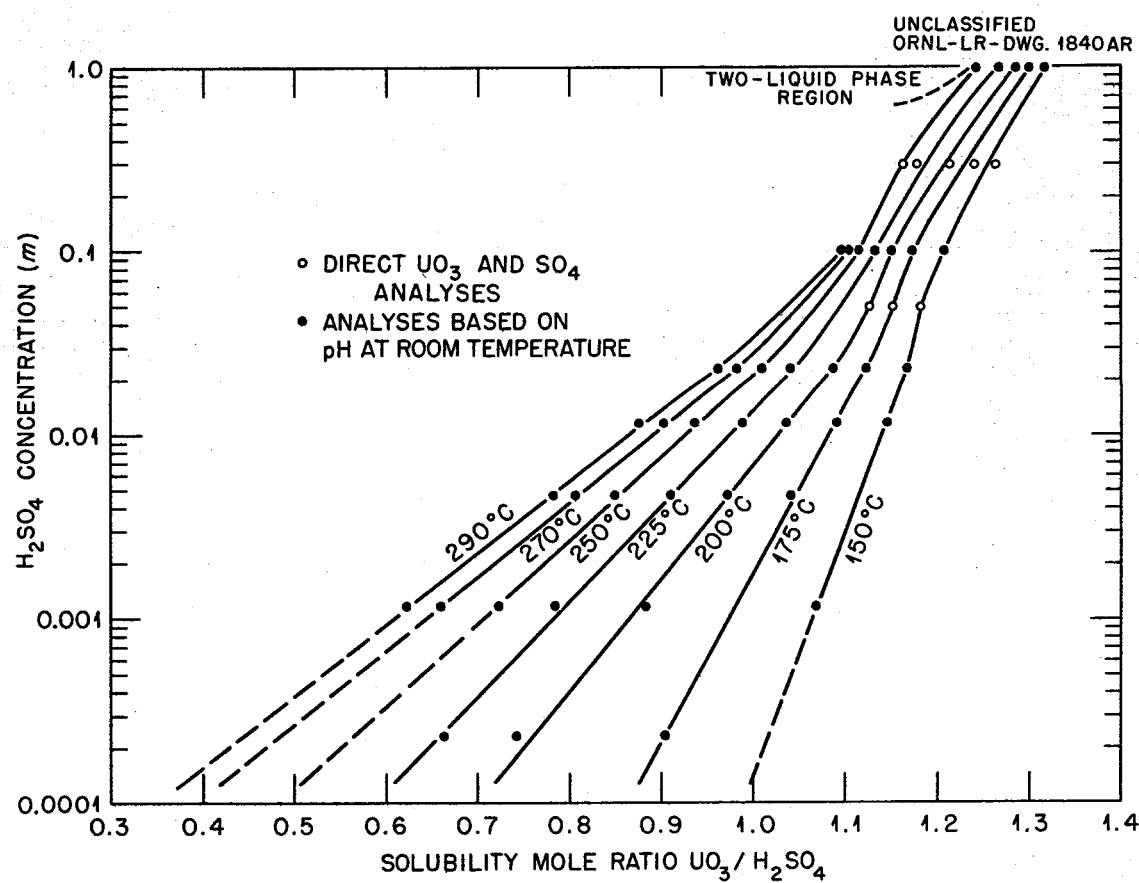
Fig. 5.13. Solubility of UO_3 in $H_2SO_4-H_2O$ Mixtures.

5.14. Effect of Excess H_2SO_4 on the Phase Equilibria in Very Dilute UO_2SO_4 Solutions

1. W. L. Marshall, *Anal. Chem.* **27**, 1923 (1955).

2. H. W. Wright, W. L. Marshall, and C. H. Secoy, *HRP Quar. Prog. Rep. Oct. 1, 1952,* ORNL-1424, p 108.

The curves were drawn by C. H. Secoy from data used for Figs. 5.10 and 5.13.
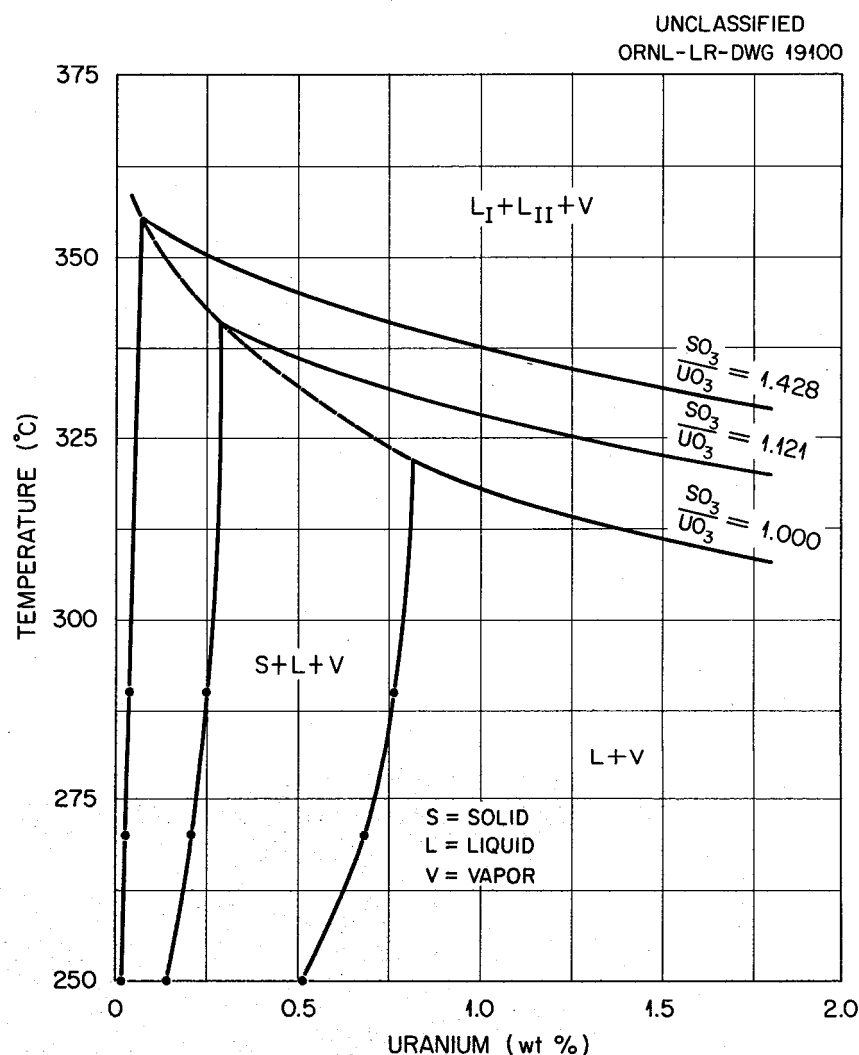
Fig. 5.14. Effect of Excess H_2SO_4 on the Phase Equilibria in Very Dilute UO_2SO_4 Solutions.

5.15. Second-Liquid-Phase Temperatures of UO_2SO_4–Li_2SO_4 Solutions

R. S. Greeley, S. R. Buxton, and J. C. Griess, "High Temperature Behavior of Aqueous UO_2SO_4–Li_2SO_4 and UO_2SO_4–$BeSO_4$," paper presented at American Nuclear Society 2nd Winter Meeting, New York City (Oct. 1957). Also R. S. Greeley and J. C. Griess, *HRP Dynamic Solution Corrosion Studies for Quarter Ending July 31, 1956*, ORNL CF-56-7-52, p 30–31.

These data were obtained by the visual-synthetic method mentioned in Sec 5.8.

UNCLASSIFIED
ORNL-LR-DWG 19101

▲ 0.42–0.45 *m* UO_2SO_4 PLUS Li_2SO_4
○ 1.3 *m* UO_2SO_4 PLUS Li_2SO_4
● 2.2 *m* UO_2SO_4 PLUS Li_2SO_4
CONCENTRATIONS ARE UNCORRECTED FOR LOSS OF WATER TO VAPOR PHASE AT ELEVATED TEMPERATURES
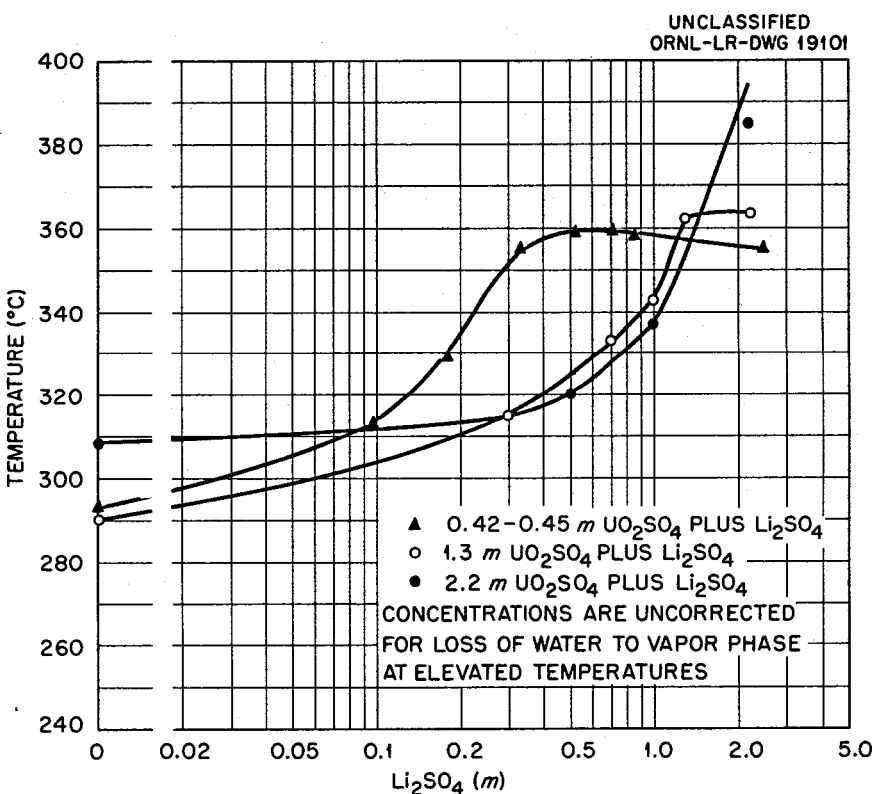
Fig. 5.15. Second-Liquid-Phase Temperatures of UO_2SO_4–Li_2SO_4 Solutions.

5.16. Second-Liquid-Phase Temperatures for UO_2SO_4 Solutions Containing Li_2SO_4 or $BeSO_4$

R. S. Greeley and J. C. Griess, *HRP Dynamic Solution Corrosion Studies for Quarter Ending July 31, 1956*, ORNL CF-56-7-52, p 30.

Liquid-liquid immiscibility occurs at the boundary curves as the temperature is raised.
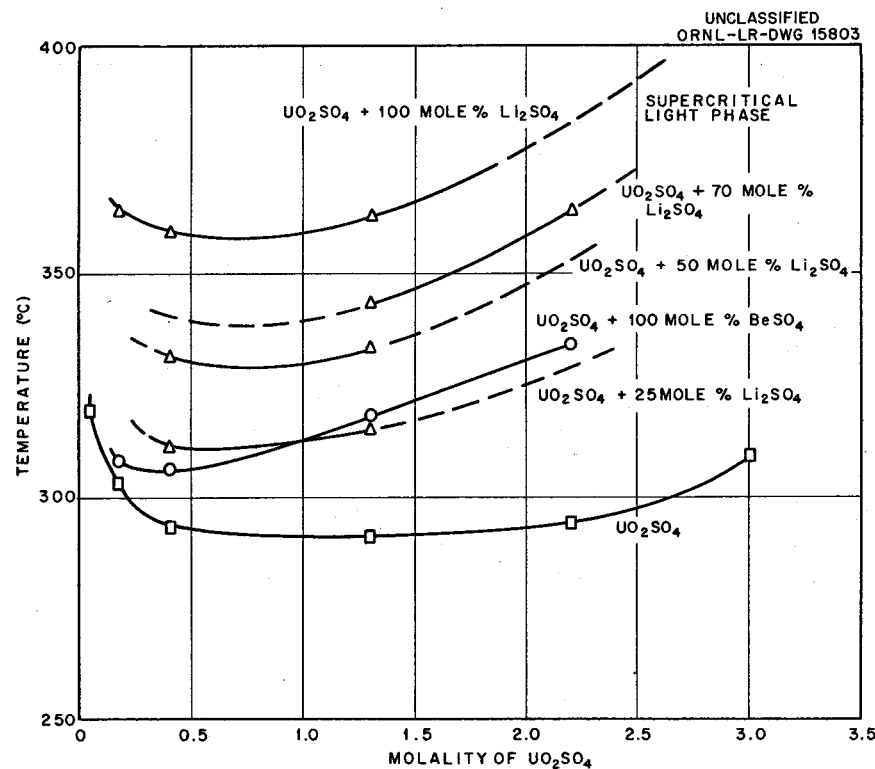
Fig. 5.16. Second-Liquid-Phase Temperatures for UO_2SO_4 Solutions Containing Li_2SO_4 or $BeSO_4$.

5.17. Second-Liquid-Phase Temperatures for BeSO$_4$ Solutions Containing UO$_3$

R. S. Greeley and J. C. Griess, *HRP Dynamic Solution Corrosion Studies for Quarter Ending July 31, 1956*, ORNL CF-56-7-52, p 31.

Liquid-liquid immiscibility occurs at the boundary curves as the temperature is raised.
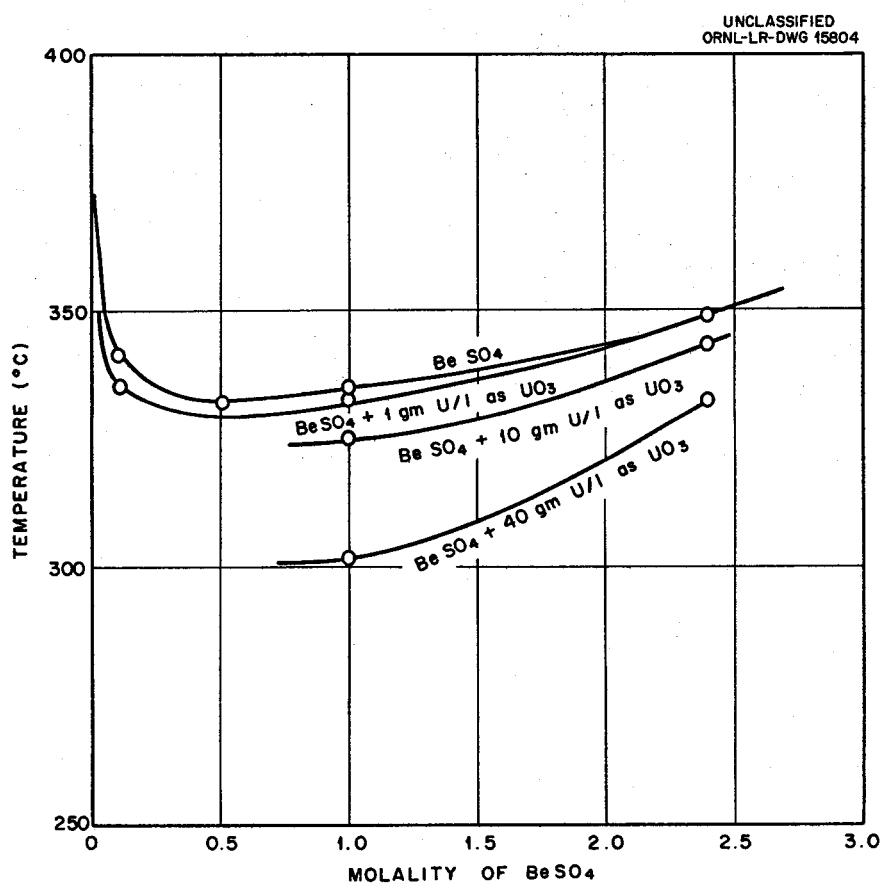
Fig. 5.17. Second-Liquid-Phase Temperatures for BeSO$_4$ Solutions Containing UO$_3$.

5.18. The System $NiSO_4-UO_2SO_4-H_2O$ at 25°C

E. V. Jones, J. S. Gill, and C. H. Secoy, *HRP Quar. Prog. Rep. Oct. 31, 1954*, ORNL-1813, p 166–67.

Also included in the reference are solubility data for this system at 175 and 250°C. The data at high temperature are not in sufficient quantity for a diagram to be presented.
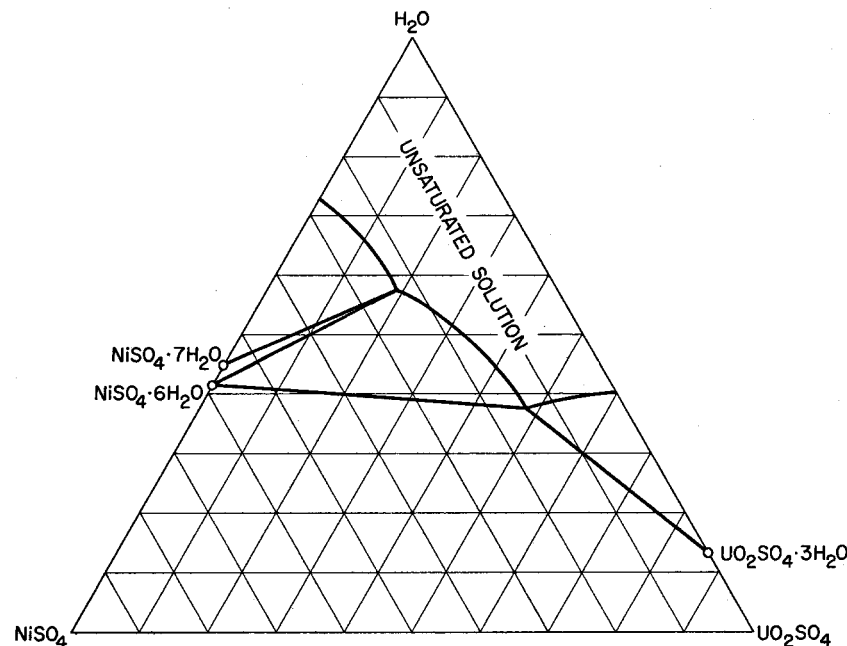
Fig. 5.18. The System $NiSO_4-UO_2SO_4-H_2O$ at 25°C. Compositions are plotted in weight per cent.

5.19. Phase-Transition Temperatures in Solutions Containing $CuSO_4$, UO_2SO_4, and H_2SO_4

F. E. Clark, J. S. Gill, R. Slusher, and C. H. Secoy, *J. Chem. Eng. Data* 4, 12 (1959).

All data were obtained by the visual-synthetic method mentioned in Sec 5.8 and represent temperatures at which immiscibility occurred upon raising the temperature. No deductions can be made regarding compositions within the two-liquid-phase region.
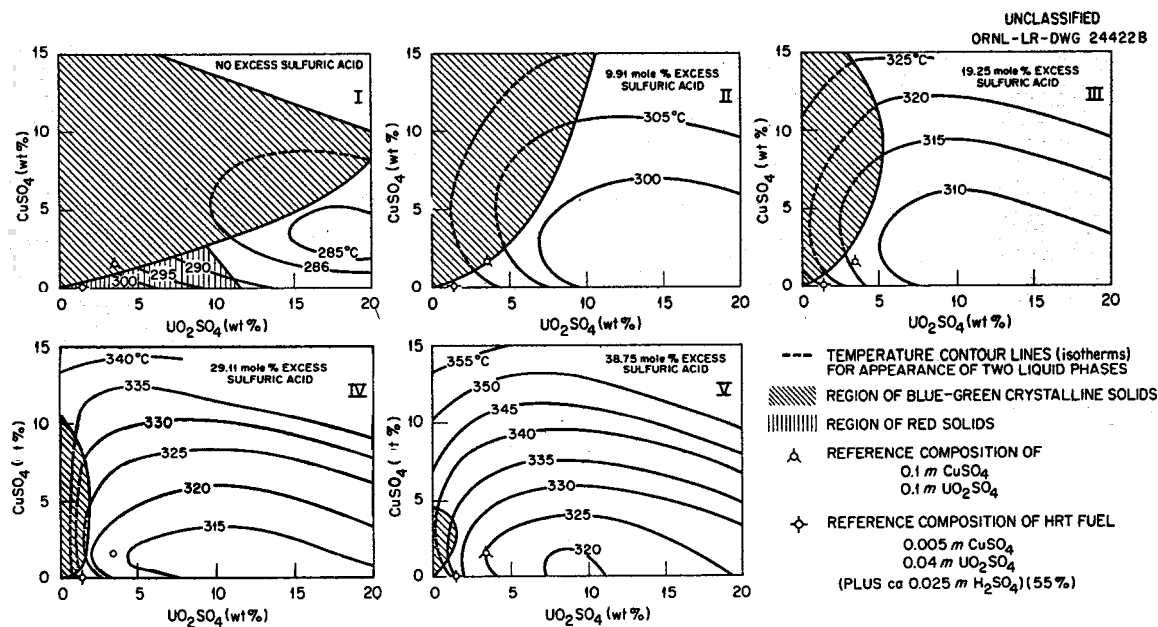
Fig. 5.19. Phase-Transition Temperatures in Solutions Containing $CuSO_4$, UO_2SO_4, and H_2SO_4.

5.20. The Effect of CuSO₄ and NiSO₄ on Phase-Transition Temperatures: 0.04 *m* UO₂SO₄; 0.01 *m* H₂SO₄

C. H. Secoy *et al.*, *HRP Quar. Prog. Rep. July 31, 1957*, ORNL-2379, p 163. Also additional data: F. Moseley, *Core Solution Stability in the Homogeneous Aqueous Reactor; the Effect of Corrosion Product and Copper Concentrations*, HARD(C)/P-41 (May 1957).

The curves for liquid-liquid immiscibility were drawn from data obtained by the visual-synthetic method mentioned in Sec 5.8. Saturation temperatures for solid-liquid equilibria were obtained by measuring solution concentrations as a function of temperature and determining a break in the curve. The numbers in parentheses are temperatures at which the indicated solid phase appeared upon raising the temperature. Solid phases indicated in parentheses were found in small quantity.
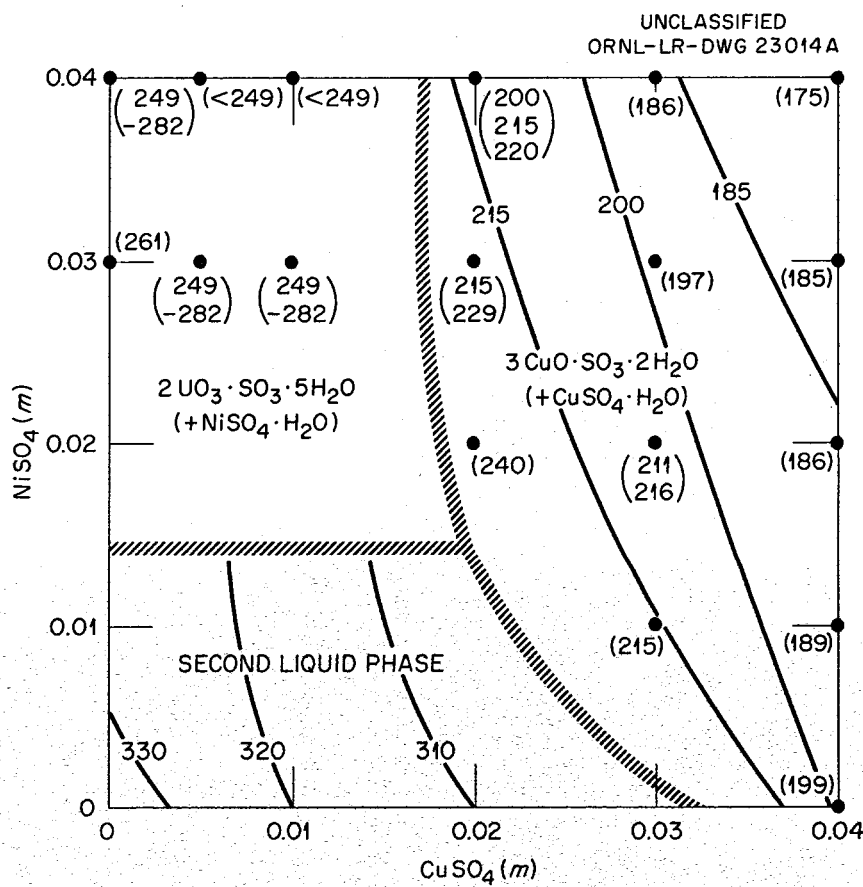
Fig. 5.20. The Effect of CuSO₄ and NiSO₄ on Phase-Transition Temperatures: 0.04 *m* UO₂SO₄; 0.01 *m* H₂SO₄.

5.21. The System UO_3-CuO-NiO-SO_3-D_2O at 300°C; 0.06 m SO_3

J. S. Gill, R. Slusher, and W. L. Marshall, *HRP Quar. Prog. Rep. Jan. 31, 1959*, ORNL-2696, p 205-13.

The variation in solution composition in the presence of one, two, and three solid phases was determined at 300°C from 0.04 to 0.2 m SO_3. Solubility relationships at 0.06 m SO_3 were obtained from these separate solubility curves, and the skeletal volume figure for the five-component system was drawn. Other skeletal figures can be drawn at various SO_3 concentrations. This investigation is still in progress, and the data are subject to revision.
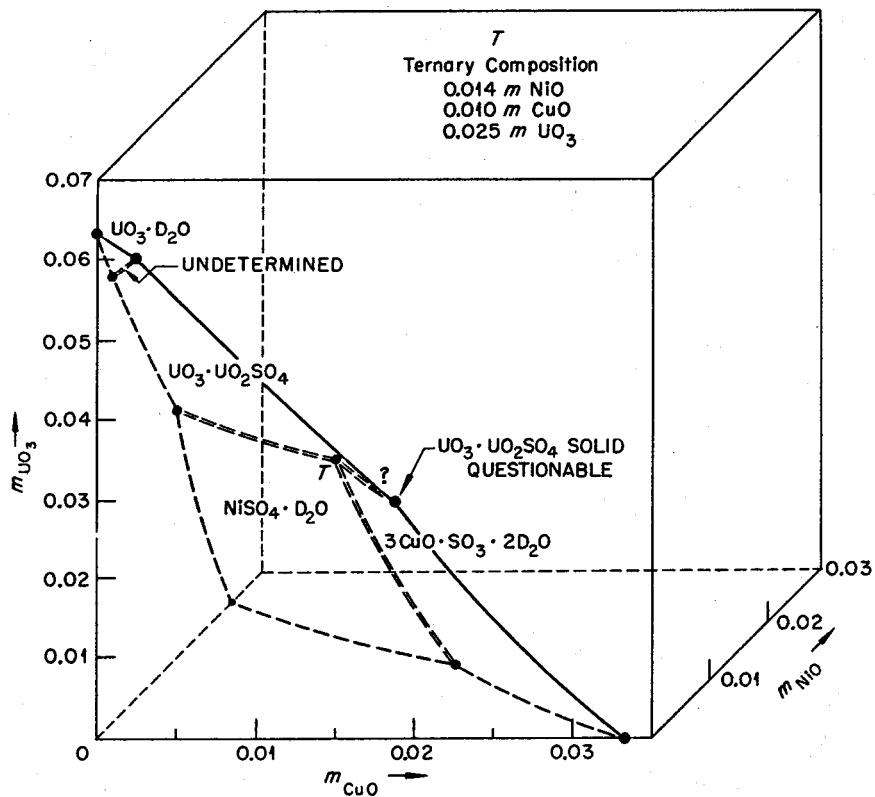
Fig. 5.21. The System UO_3-CuO-NiO-SO_3-D_2O at 300°C; 0.06 m SO_3.

5.22. Solubility of $Nd_2(SO_4)_3$ in 0.02 m UO_2SO_4 Solution Containing 0.005 m H_2SO_4 (180–300°C)

R. E. Leuze *et al.*, *HRP Quar. Prog. Rep. April 30, 1954*, ORNL-1753, p 176–79.

Also included in the reference are preliminary solubility data for rare earth sulfate mixtures as well as $Ce_2(SO_4)_3$ and $La_2(SO_4)_3$ in 0.02 m UO_2SO_4, 0.005 m H_2SO_4.
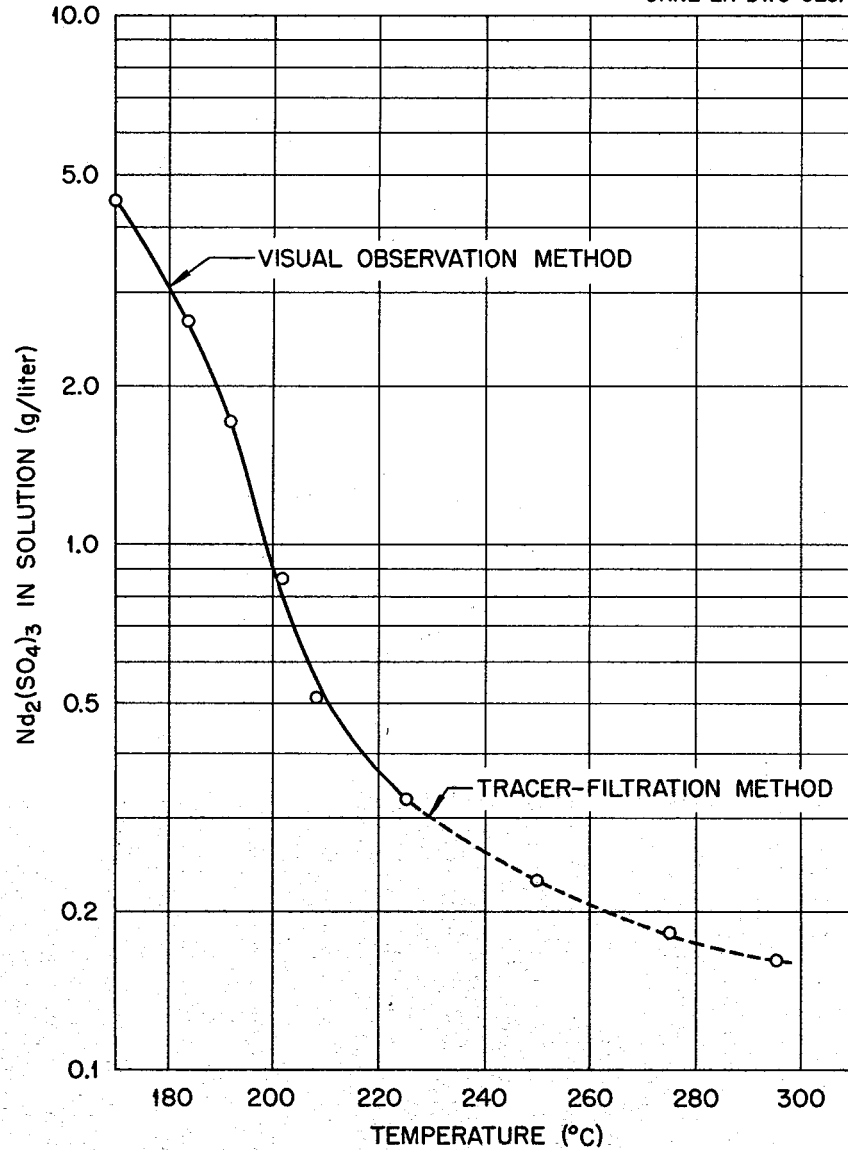
Fig. 5.22. Solubility of $Nd_2(SO_4)_3$ in 0.02 m UO_2SO_4 Solution Containing 0.005 m H_2SO_4 (180–300°C).

5.23. Solubility of $La_2(SO_4)_3$ in UO_2SO_4 Solutions

E. V. Jones, M. H. Lietzke, and W. L. Marshall, *J. Am. Chem. Soc.* **79**, 267 (1957); also *The Solubility of Several Metal Sulfates at High Temperatures and Pressures in Water and in Aqueous Uranyl Sulfate Solution*, ORNL CF-55-7-69 (declassified Aug. 23, 1955).

Experimental data for Figs. 5.23–5.27 were obtained by the visual-synthetic method described in Sec 5.8. The very large effect of UO_2SO_4 must be noted and indicates considerable solvation of other species by aqueous UO_2SO_4.
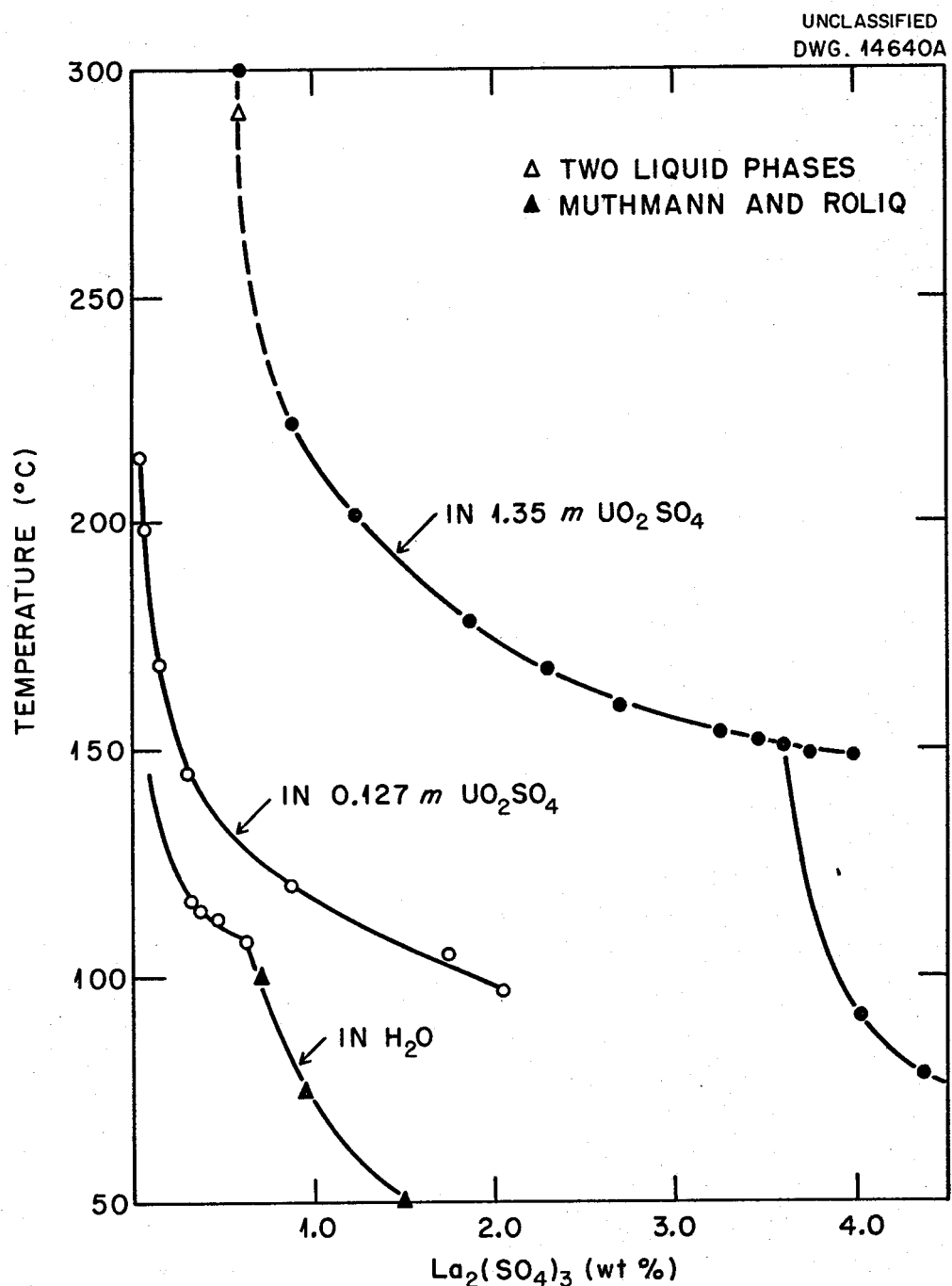
Fig. 5.23. Solubility of $La_2(SO_4)_3$ in UO_2SO_4 Solutions.

5.24. Solubility of CdSO$_4$ in UO$_2$SO$_4$ Solutions

E. V. Jones, M. H. Lietzke, and W. L. Marshall, *J. Am. Chem. Soc.* **79**, 267 (1957); also *The Solubility of Several Metal Sulfates at High Temperatures and Pressures in Water and in Aqueous Uranyl Sulfate Solution,* ORNL CF-55-7-69 (declassified Aug. 23, 1955).

See comments in Sec 5.23.
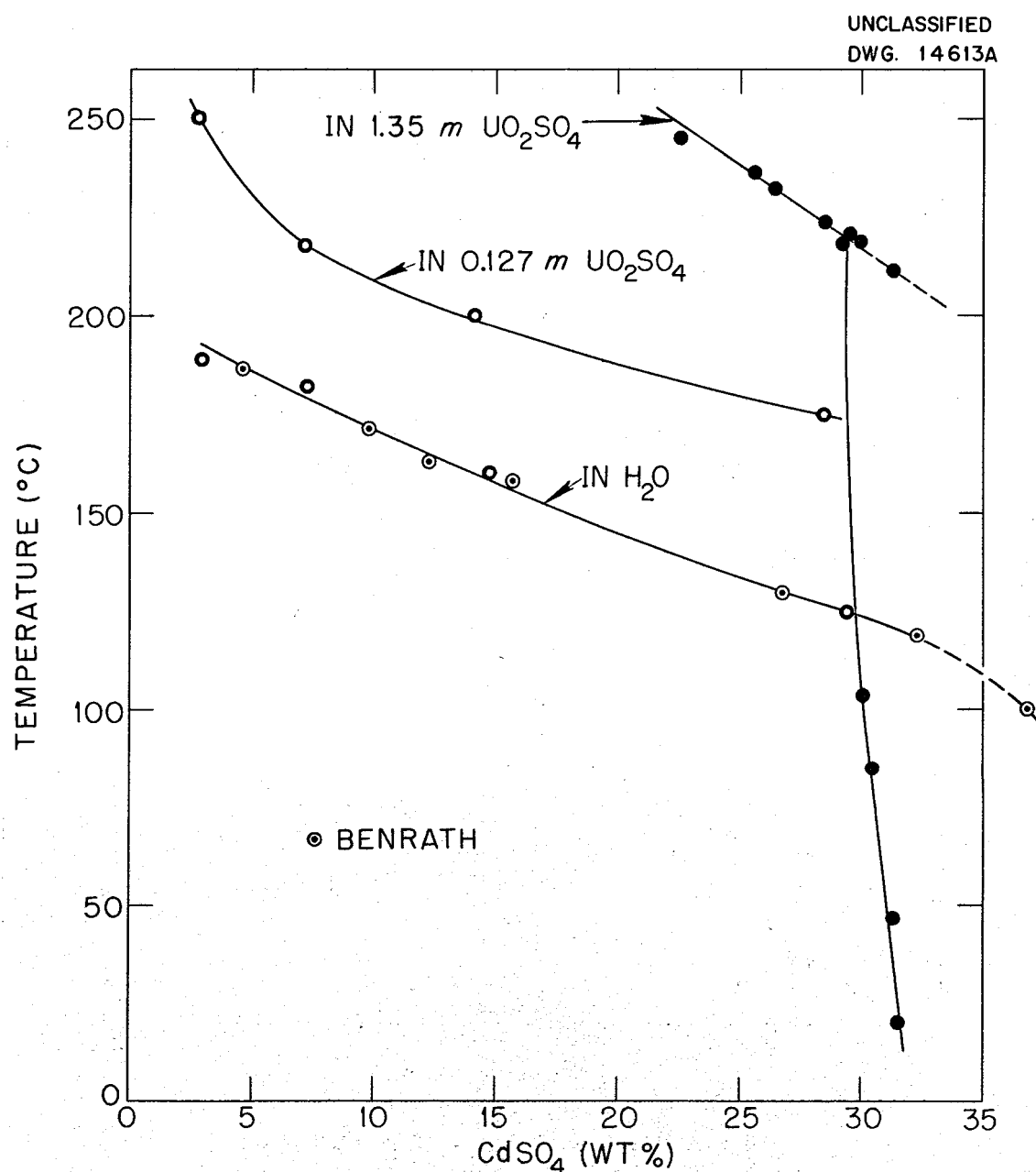
Fig. 5.24. Solubility of CdSO$_4$ in UO$_2$SO$_4$ Solutions.

5.25. Solubility of Cs_2SO_4 in UO_2SO_4 Solutions

E. V. Jones, M. H. Lietzke, and W. L. Marshall, *J. Am. Chem. Soc.* **79**, 267 (1957); also *The Solubility of Several Metal Sulfates at High Temperatures and Pressures in Water and in Aqueous Uranyl Sulfate Solution*, ORNL CF-55-7-69 (declassified Aug. 23, 1955).

See comments in Sec 5.23.
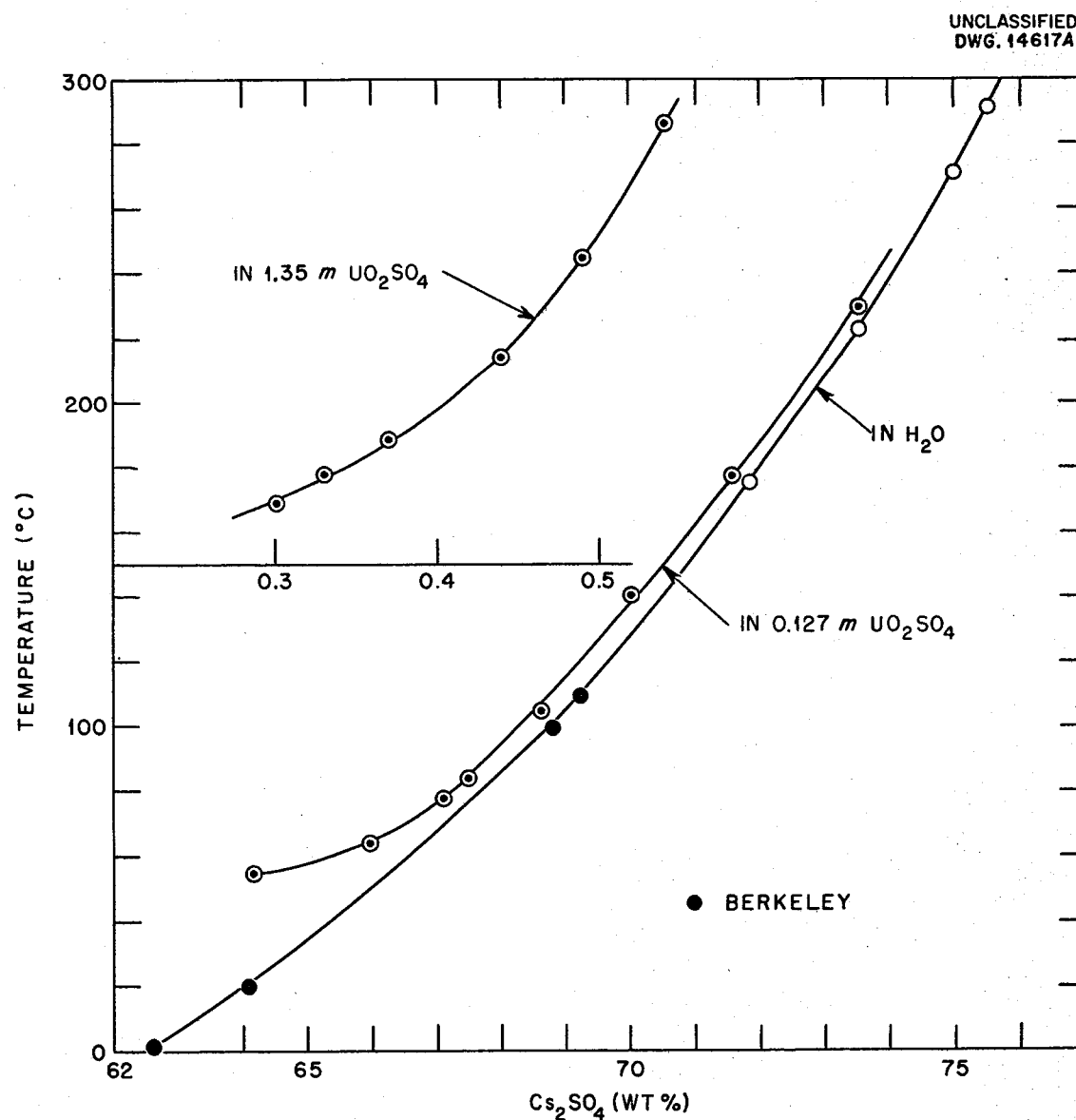
Fig. 5.25. Solubility of Cs_2SO_4 in UO_2SO_4 Solutions.

5.26. Solubility of Y$_2$(SO$_4$)$_3$ in UO$_2$SO$_4$ Solutions

E. V. Jones, M. H. Lietzke, and W. L. Marshall, *J. Am. Chem. Soc.* **79**, 267 (1957); also *The Solubility of Several Metal Sulfates at High Temperatures and Pressures in Water and in Aqueous Uranyl Sulfate Solution*, ORNL CF-55-7-69 (declassified Aug. 23, 1955).

See comments in Sec 5.23.
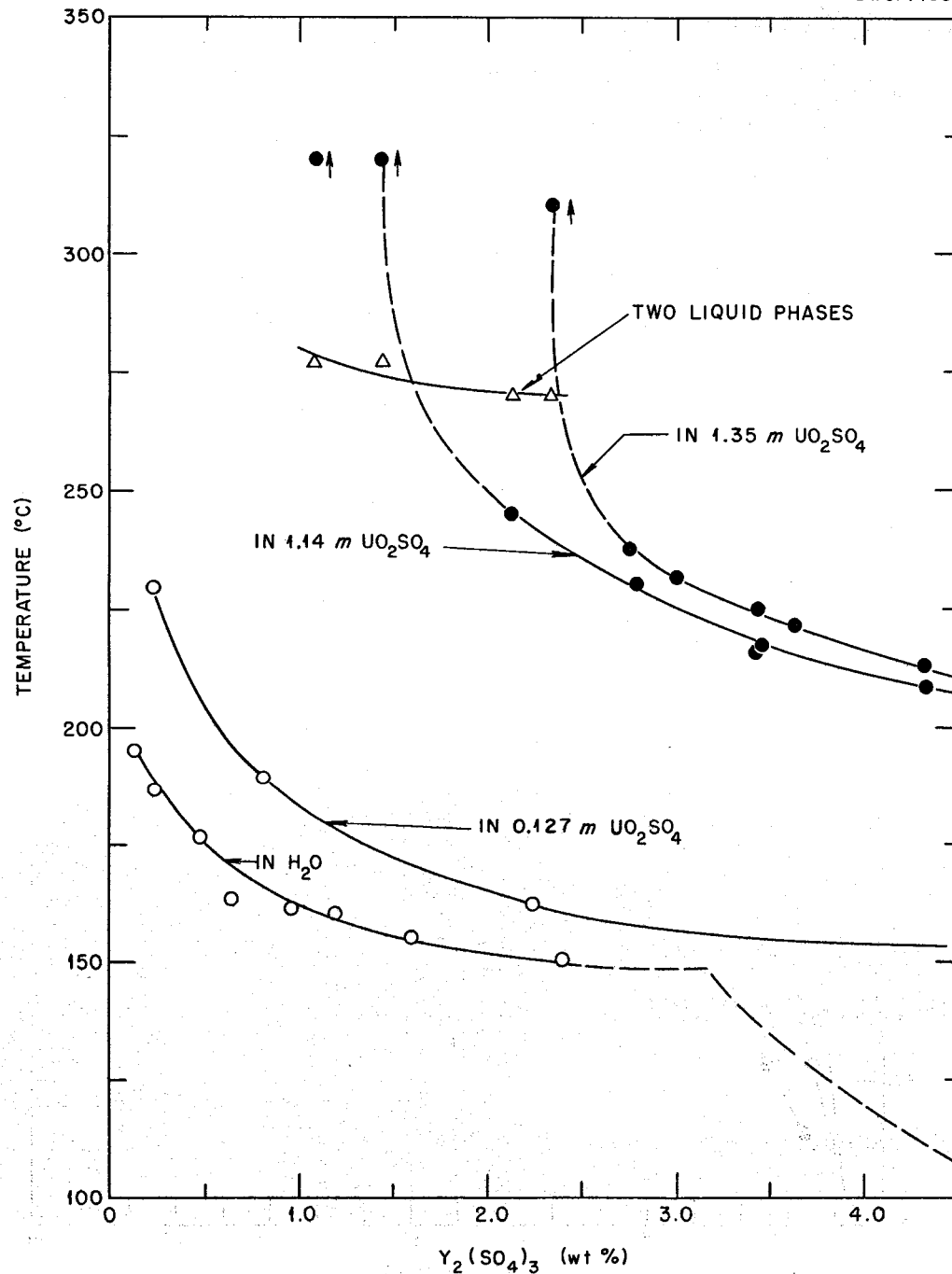
Fig. 5.26. Solubility of Y$_2$(SO$_4$)$_3$ in UO$_2$SO$_4$ Solutions.

5.27. Solubility of Ag₂SO₄ in UO₂SO₄ Solutions

E. V. Jones, M. H. Lietzke, and W. L. Marshall, *J. Am. Chem. Soc.* **79**, 267 (1957); also *The Solubility of Several Metal Sulfates at High Temperatures and Pressures in Water and in Aqueous Uranyl Sulfate Solution*, ORNL CF-55-7-69 (declassified Aug. 23, 1955).

See comments in Sec 5.23.
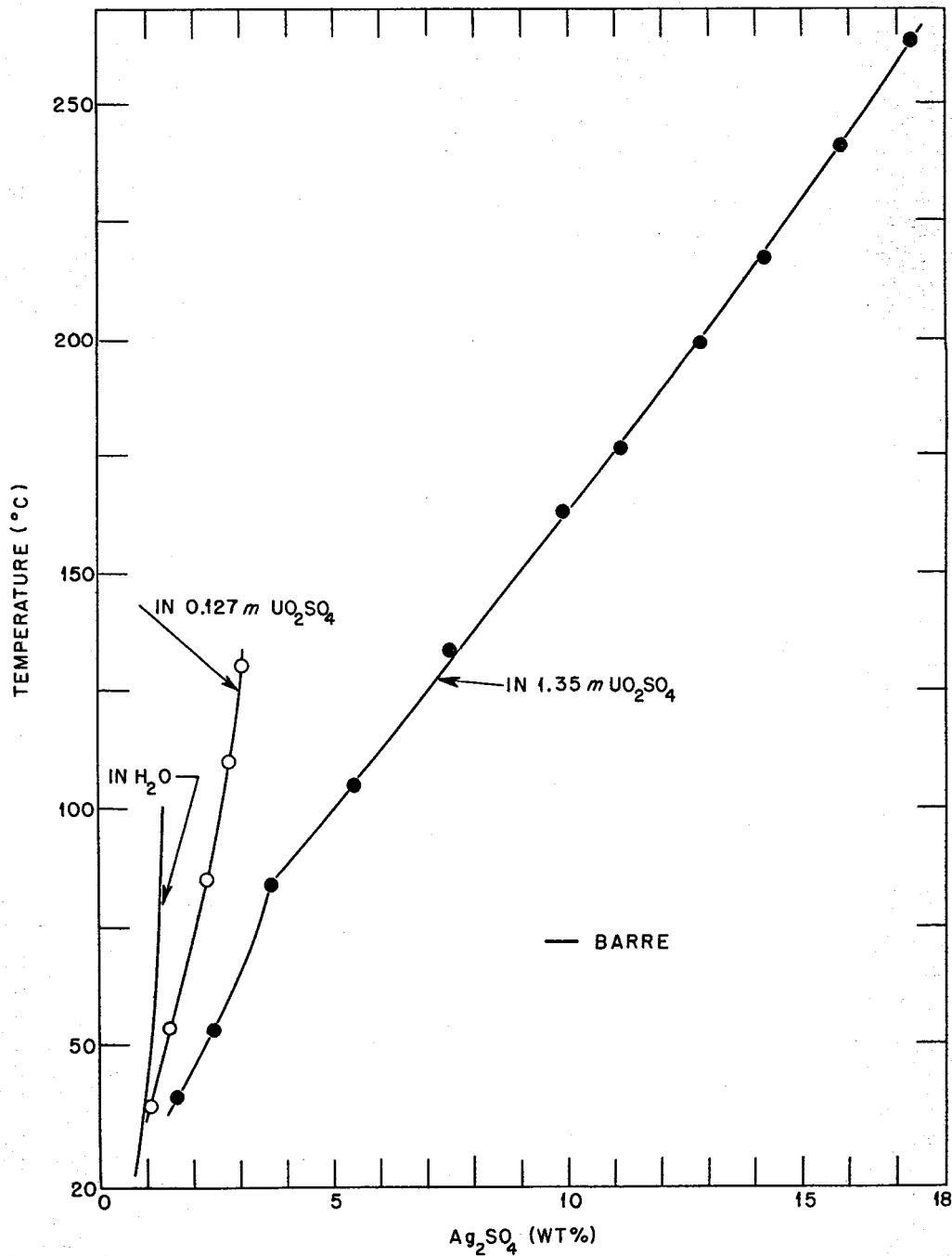
Fig. 5.27. Solubility of Ag₂SO₄ in UO₂SO₄ Solutions.

5.28. Solubility at 250°C of BaSO₄ in UO₂SO₄–H₂O Solutions

E. V. Jones, M. H. Lietzke, and W. L. Marshall, *J. Am. Chem. Soc.* **79**, 267 (1957); also *The Solubility of Several Metal Sulfàtes at High Temperatures and Pressures in Water and in Aqueous Uranyl Sulfate Solutions*, ORNL CF-55-7-69 (declassified Aug. 23, 1955).

Solutions were filtered from solids at 250°C to obtain the solubility of BaSO₄ in H₂O. Counting of radioactive barium was used to determine the solubility concentration. The very large effect of UO₂SO₄ must be noted and indicates considerable solvation of other species by aqueous UO₂SO₄.
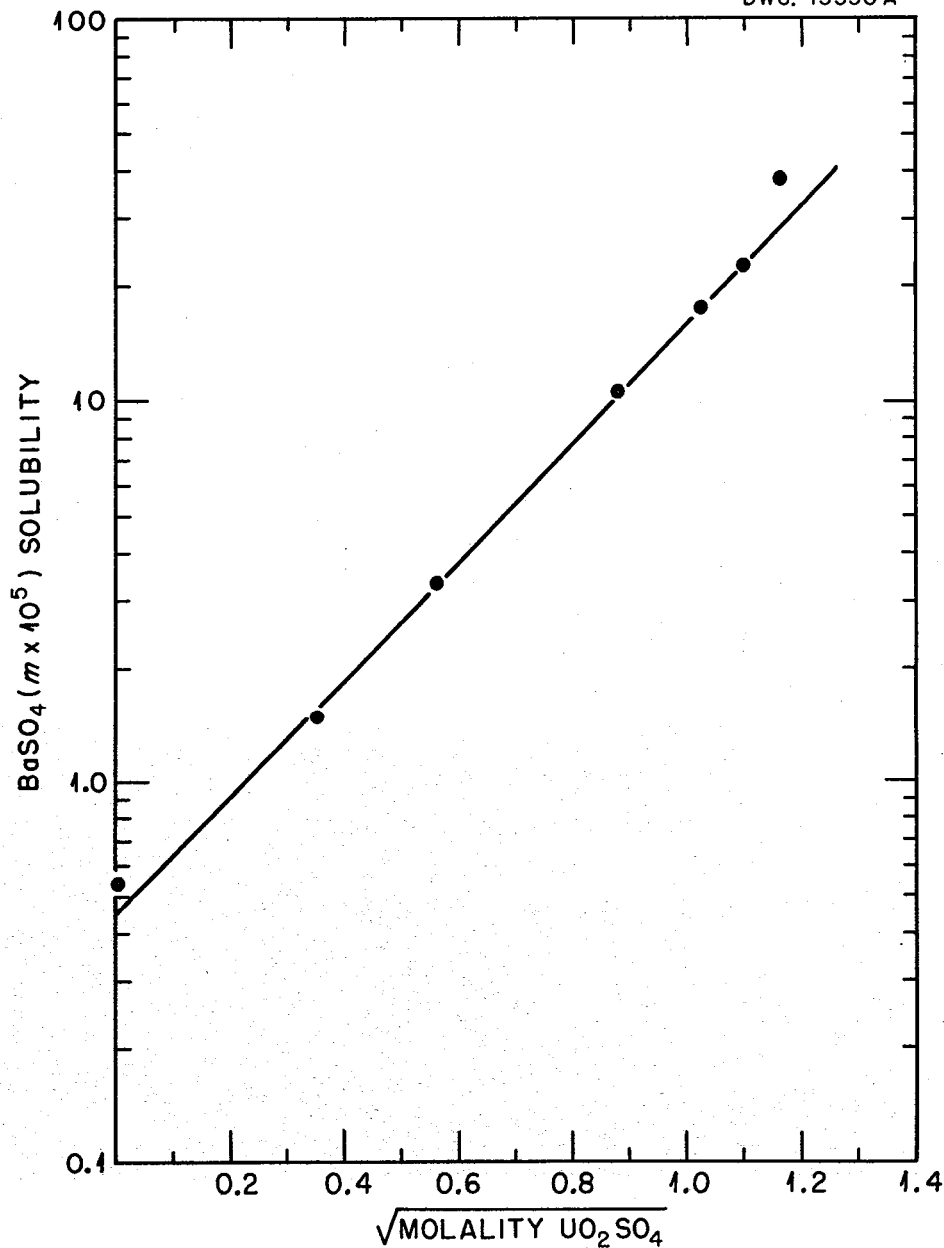
Fig. 5.28. Solubility at 250°C of BaSO₄ in UO₂SO₄–H₂O Solutions.

5.29. Solubility of H_2WO_4 in 0.126 and 1.26 M UO_2SO_4

C. E. Coffey, W. L. Marshall, and G. H. Cartledge, *HRP Quar. Prog. Rep. Oct. 31, 1953,* ORNL-1658, p 96-99.

The data shown in the figures were obtained by direct sampling of equilibrated solutions, by the filter bomb method, and by the synthetic method described previously in Sec 5.8. In 0.126 M UO_2SO_4 the solubility of H_2WO_4 first shows a positive temperature coefficient of solubility and then, above 100°C, a negative coefficient of solubility. In 1.26 M UO_2SO_4 the temperature coefficient of solubility is positive up to 285°, the temperature at which two liquid phases form — a characteristic of UO_2SO_4-H_2O solutions.
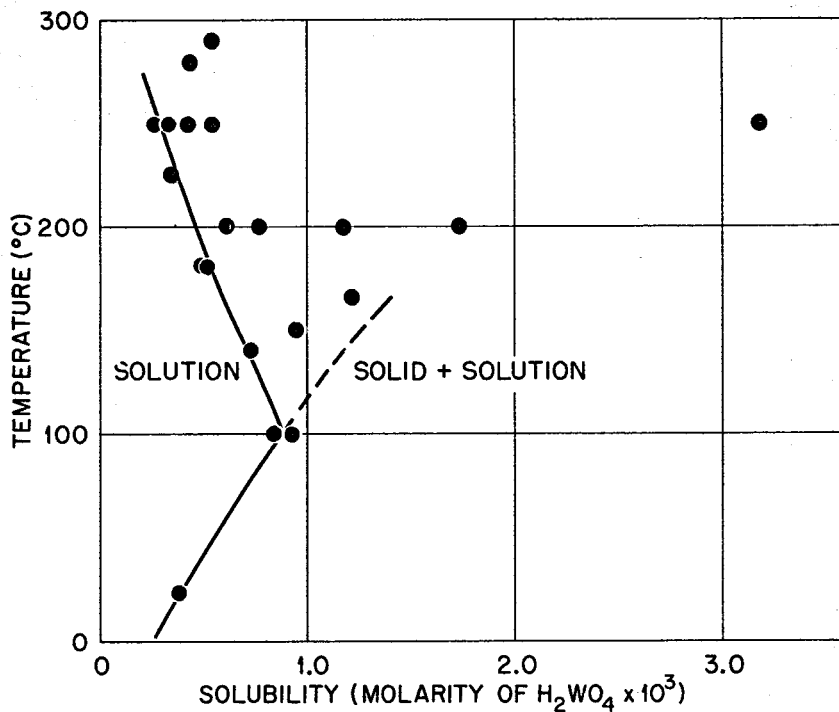
Fig. 5.29a. Solubility of H_2WO_4 in 0.126 M UO_2SO_4.
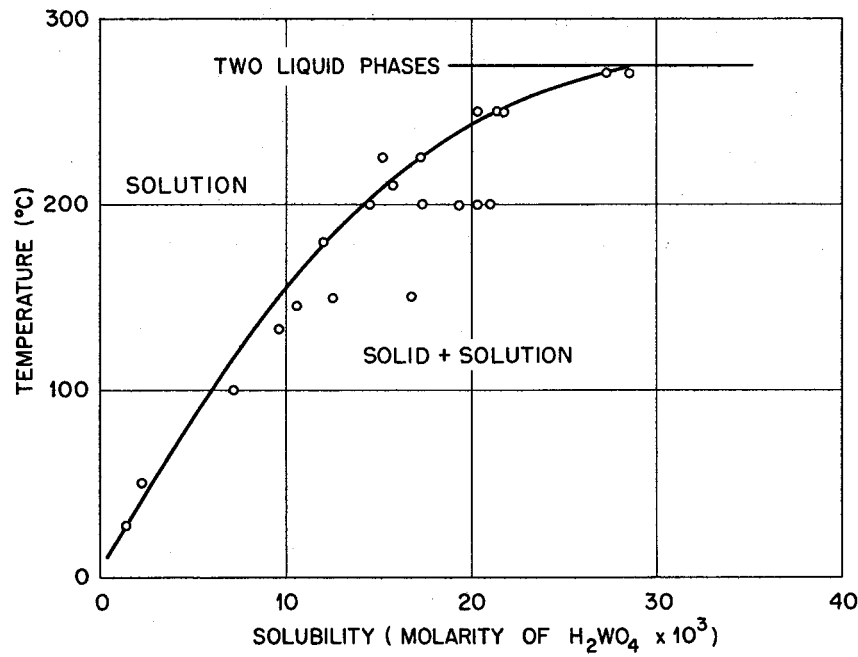
Fig. 5.29b. Solubility of H_2WO_4 in 1.26 M UO_2SO_4.

5.30. Phase Stability of H_2WO_4 in 1.26 M UO_2F_2

C. E. Coffey, W. L. Marshall, and G. H. Cartledge, *HRP Quar. Prog. Rep. Oct. 31, 1953,* ORNL-1658, p 96–99.

The methods of solubility and stability determination were the same as for analogous studies of H_2WO_4 in UO_2SO_4 (Sec 5.29). The data on the figure as drawn show temperatures at which hydrolytic precipitation of an unidentified solid phase occurs from solutions stable at lower temperatures.
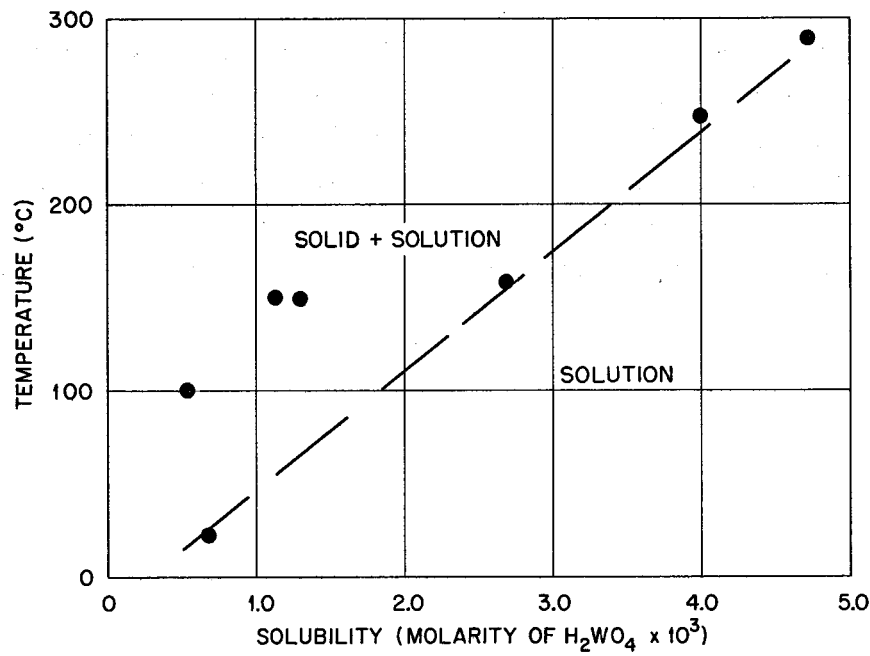
Fig. 5.30. Phase Stability of H_2WO_4 in 1.26 M UO_2F_2.

5.31. The System $UO_2(NO_3)_2$–H_2O

1. Reported in full by W. L. Marshall, J. S. Gill, and C. H. Secoy, *Chem. Quar. Prog. Rep. March 31, 1951*, ORNL-1053, p 22–25.

2. Reported in part by W. L. Marshall, J. S. Gill, and C. H. Secoy, *J. Am. Chem. Soc. 73,* 1867 (1951).

As in the case of the system UO_2SO_4–H_2O, hydrolysis occurs at high temperatures and low concentrations, resulting in precipitation of $UO_3 \cdot H_2O$ from stoichiometric $UO_2(NO_3)_2$ solutions. In addition, decomposition of NO_3^- occurs at elevated temperature to produce an equilibrium vapor phase of nitrogen oxides. Letter A represents a region of complete solution. Data at low temperature up to point F were obtained by direct analysis of equilibrated solutions, whereas the high-temperature data were obtained by the visual-synthetic method described in Sec 5.8.

Fig. 5.31. The System $UO_2(NO_3)_2-H_2O$.

○ = PRECIPITATION LIMITS
● = VAPOR PHASE COLORATION
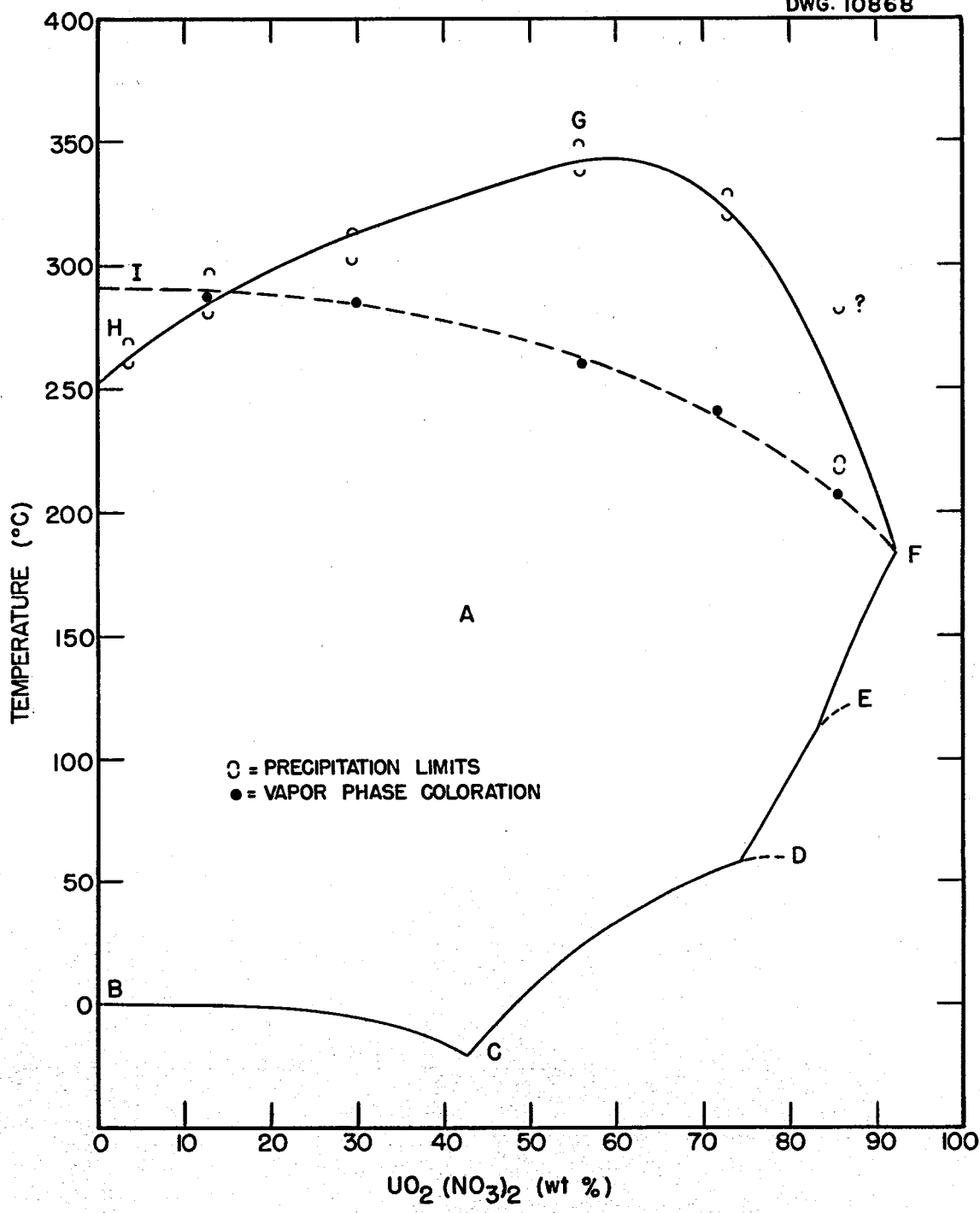
5.32. Phase Equilibria of UO₃ and HF in Stoichiometric Concentrations (Aqueous System)

W. L. Marshall, J. S. Gill, and C. H. Secoy, *J. Am. Chem. Soc.* **76**, 4279 (1954).

The two-liquid-phase region and the region of "basic" solid solution + saturated solution are in actuality segments of the three-component system UO_3–HF–H_2O, in which the equilibrium phases are nonstoichiometric with regard to UO_2F_2. This system is somewhat analogous to the system UO_3–H_2SO_4–H_2O (see Sec 5.7).
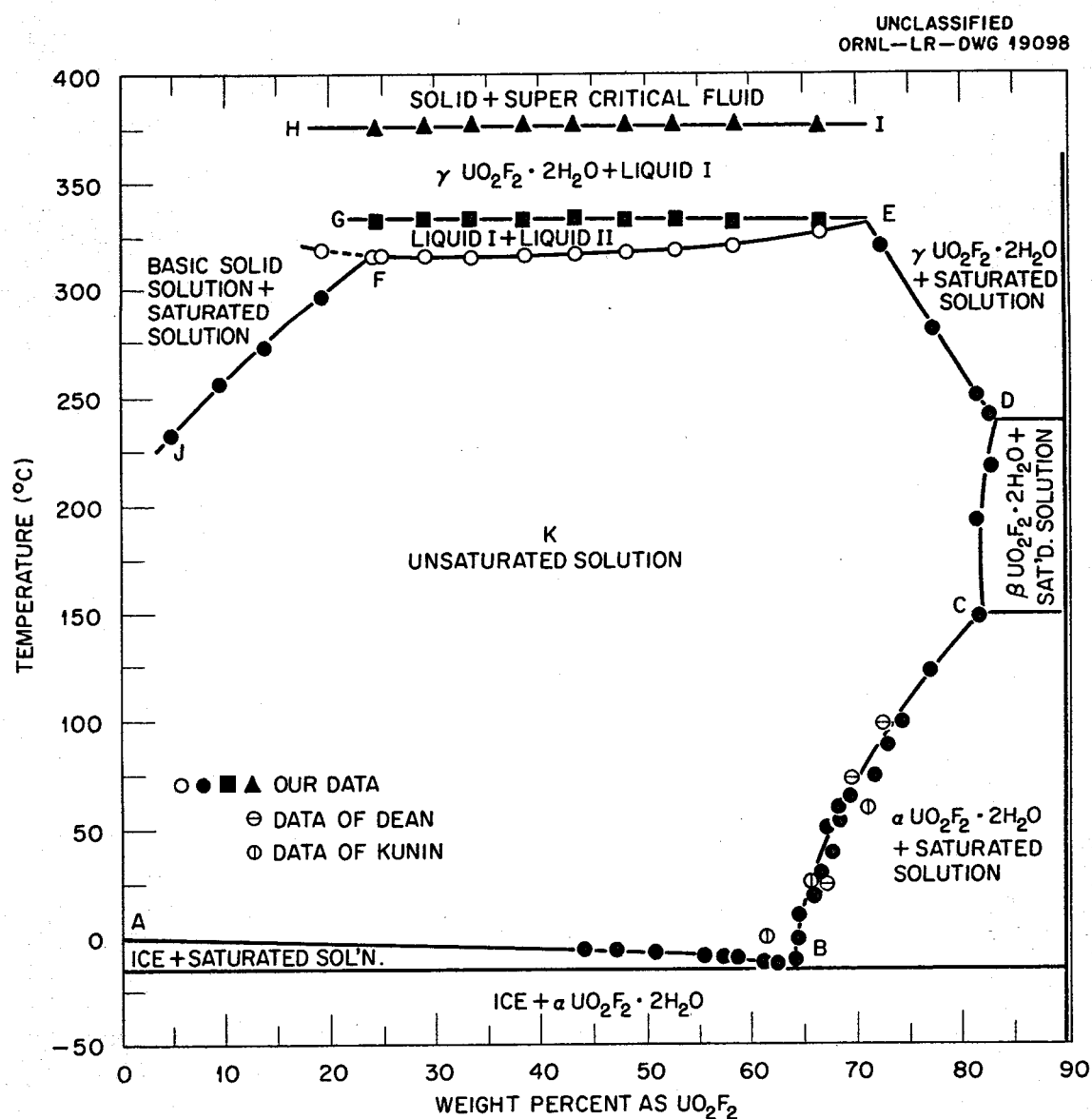
Fig. 5.32. Phase Equilibria of UO₃ and HF in Stoichiometric Concentrations (Aqueous System).

5.33. Solubility of Uranium Trioxide in Orthophosphoric Acid Solutions

W. L. Marshall, J. S. Gill, and H. W. Wright, *HRP Quar. Prog. Rep. May 15, 1951*, ORNL-1057, p 112–15.

The data were obtained for the most part by equilibrating solutions of known concentration in sealed tubes for various times at different temperatures. Phase changes were observed visually.

CURVE A 1 MOLAR H_3 PO_4
CURVE B 2 MOLAR H_3 PO_4
CURVE C 3 MOLAR H_3 PO_4

O ● ■ OUR DATA
△ ▲ KUHN AND RYON
▫ LOS ALAMOS
Ω MORSE
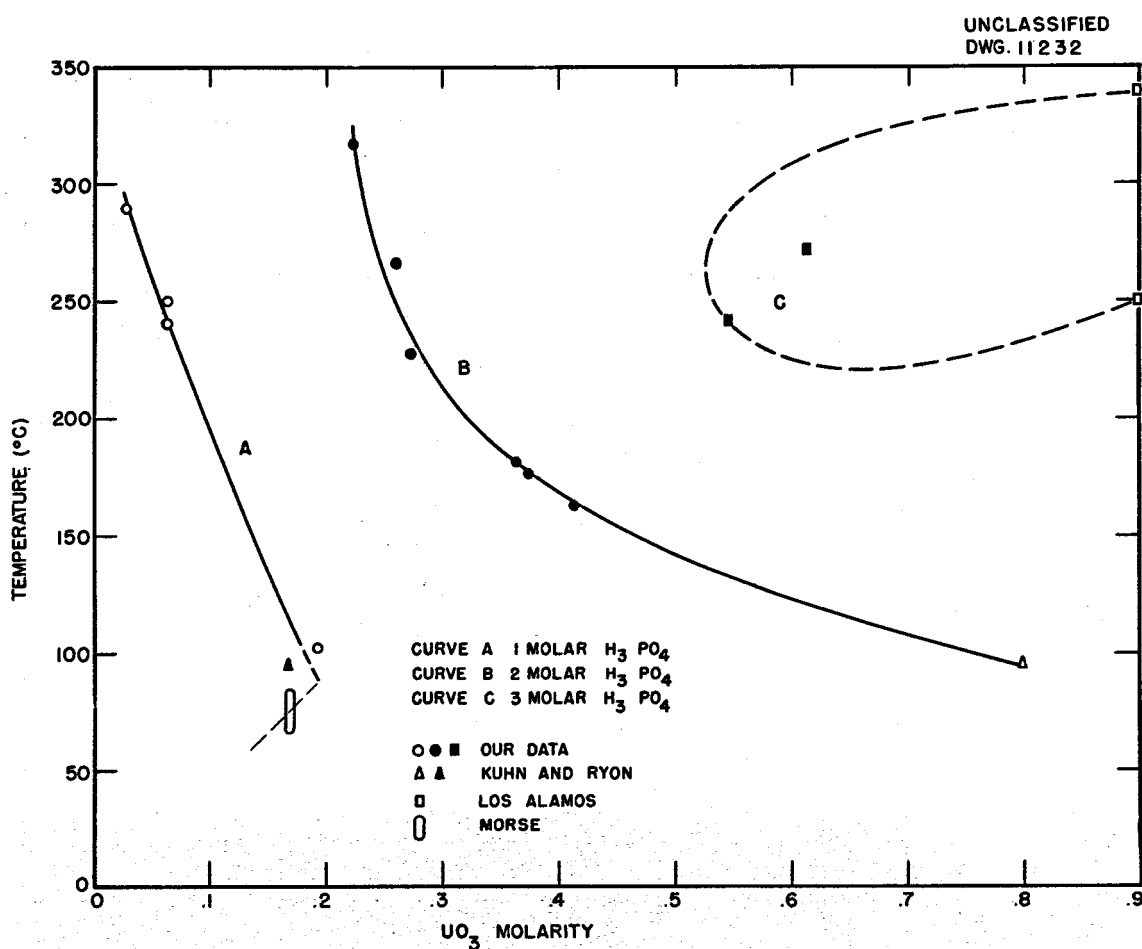
Fig. 5.33. Solubility of Uranium Trioxide in Orthophosphoric Acid Solutions.

5.34. Solubility of Uranium Trioxide in Phosphoric Acid at 250°C

J. S. Gill, W. L. Marshall, and H. W. Wright, *HRP Quar. Prog. Rep. Aug. 15, 1951*, ORNL-1121, p 119–21.

Solution and solid mixtures were equated at 250°C in sealed glass tubes. The tubes were cooled rapidly to room temperature, and the solution and solid phases were analyzed. The slow reversibility of equilibrium conditions made this procedure possible.
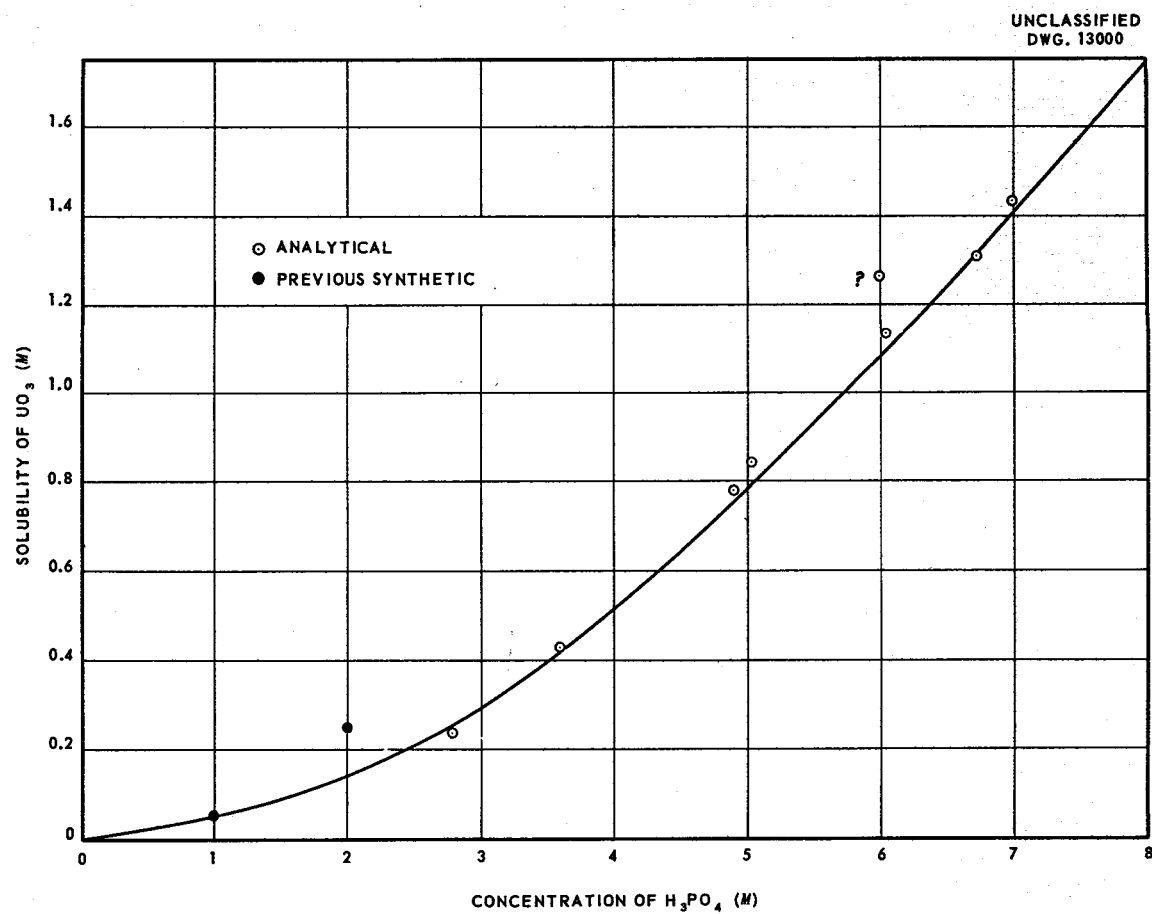
Fig. 5.34. Solubility of Uranium Trioxide in Phosphoric Acid at 250°C.

5.35. Solubility of UO₃ in H₃PO₄ Solution

B. J. Thamer *et al.*, *The Properties of Phosphoric Acid Solutions of Uranium as Fuels for Homogeneous Reactors*, LA-2043 (March 6, 1956); W. L. Marshall, J. S. Gill, and H. W. Wright, *HRP Quar. Prog. Rep. May 15, 1951*, ORNL-1057, p 112–15; and J. S. Gill, W. L. Marshall, and H. W. Wright, *HRP Quar. Prog. Rep. Aug. 15, 1951*, ORNL-1121, p 119–21.

This figure represents a compilation from the data of B. J. Thamer *et al.* of Los Alamos and W. L. Marshall *et al.* of Oak Ridge National Laboratory.
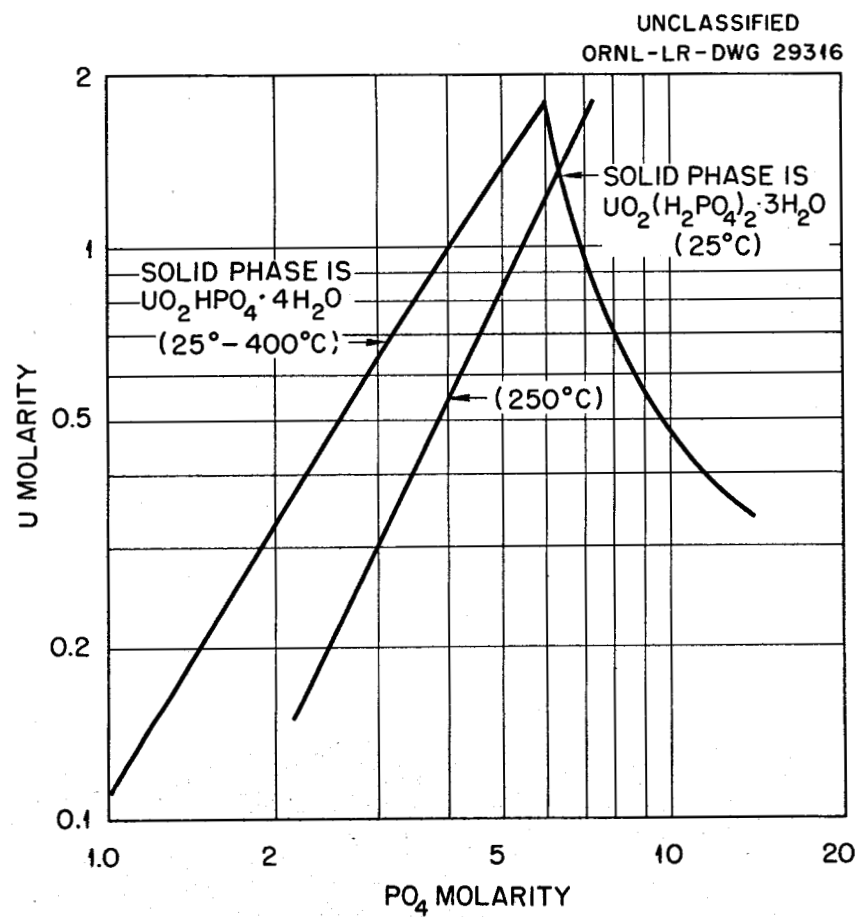
Fig. 5.35. Solubility of UO₃ in H₃PO₄ Solution.

5.36. The System $UO_2CrO_4-H_2O$

1. F. J. Loprest, W. L. Marshall, and C. H. Secoy, *J. Am. Chem. Soc.* **77**, 4705 (1955).

2. W. L. Marshall, *HRP Quar. Prog. Rep. March 31, 1953*, ORNL-1554, p 105-6.

The solid phases are $UO_2CrO_4 \cdot 5\frac{1}{2}H_2O$ (*A*) and $UO_2CrO_4 \cdot xH_2O$ (*B*). Curve *rs* represents the boundary of a region in which hydrolytic precipitation of a basic uranyl chromate occurs. In the same concentration range the dichromate, $UO_2Cr_2O_7$, is stable to the critical temperature and apparently dissolves in the supercritical fluid (ref 2).
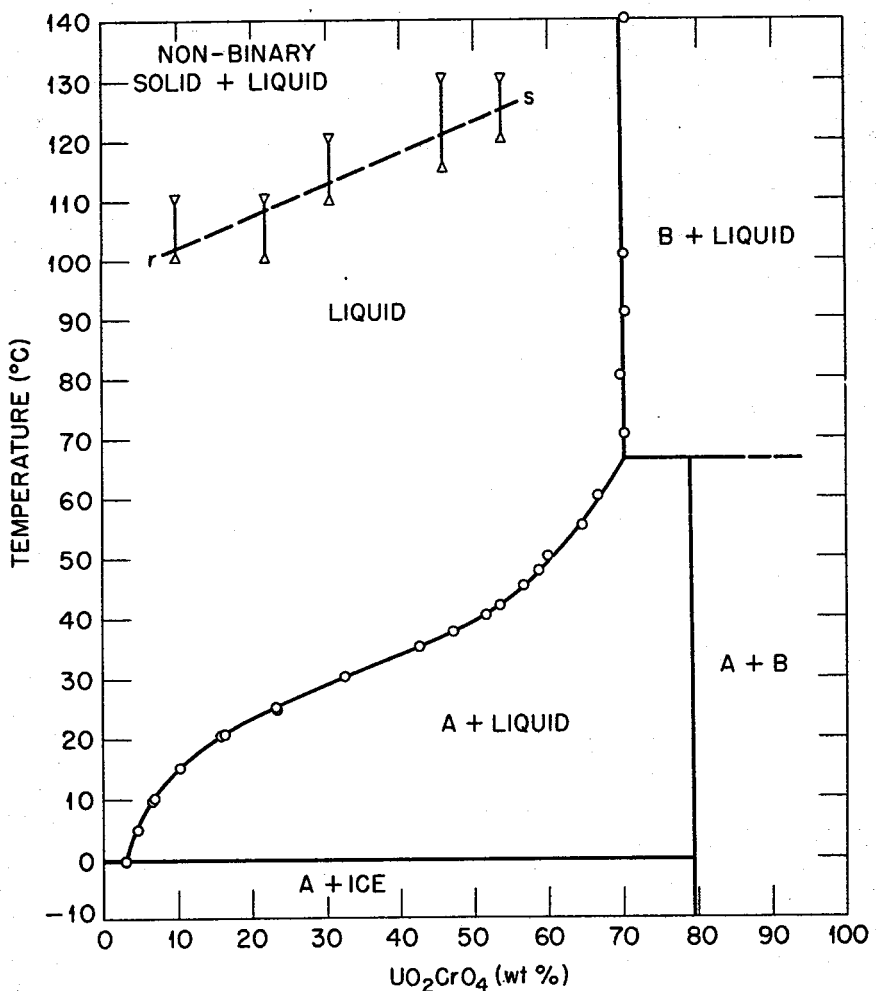
Fig. 5.36. The System $UO_2CrO_4-H_2O$.

5.37. Variation of Li_2CO_3 Solubility with UO_2CO_3 Concentration at Constant CO_2 Pressure (250°C)

1. F. J. Loprest, W. L. Marshall, and C. H. Secoy, *HRP Quar. Prog. Rep. July 31, 1955,* ORNL-1943, p 227–35.

2. W. L. Marshall, F. J. Loprest, and C. H. Secoy, *HRP Quar. Prog. Rep. Jan. 31, 1956,* ORNL-2057, p 131–32.

The solubility relationships in the figure indicate strong complexing of UO_2CO_3 with Li_2CO_3 under CO_2 pressure. The formation of HCO_3^- species in solution is indicated.
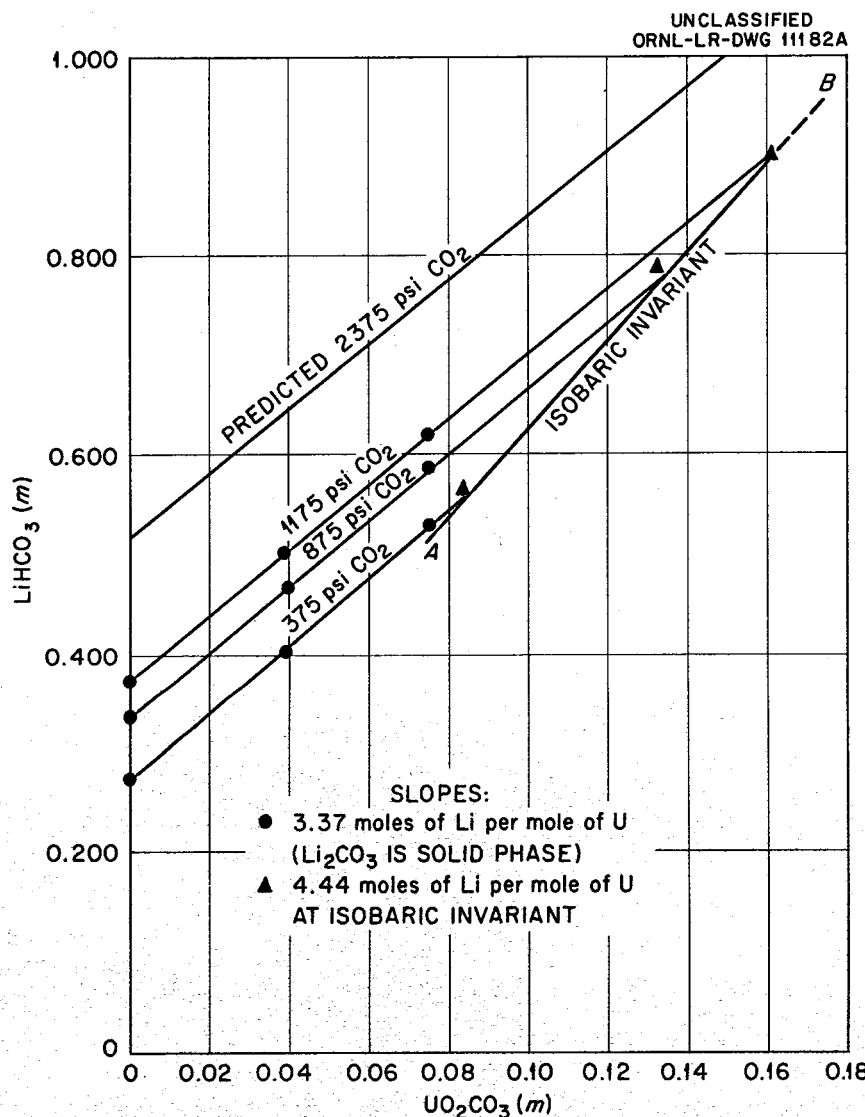
Fig. 5.37. Variation of Li_2CO_3 Solubility with UO_2CO_3 Concentration at Constant CO_2 Pressure (250°C).

5.38. The System $Li_2O–UO_3–CO_2–H_2O$ at 250°C and 1500 psi

1. F. J. Loprest, W. L. Marshall, and C. H. Secoy, *HRP Quar. Prog. Rep. July 31, 1955*, ORNL-1943, p 227–35.

2. W. L. Marshall, F. J. Loprest, and C. H. Secoy, *HRP Quar. Prog. Rep. Jan. 31, 1956*, ORNL-2057, p 131–32.

As CO_2 pressure is increased, the area of complete solution (indicated by the shading) increases. As temperature is increased, the solution area decreases.
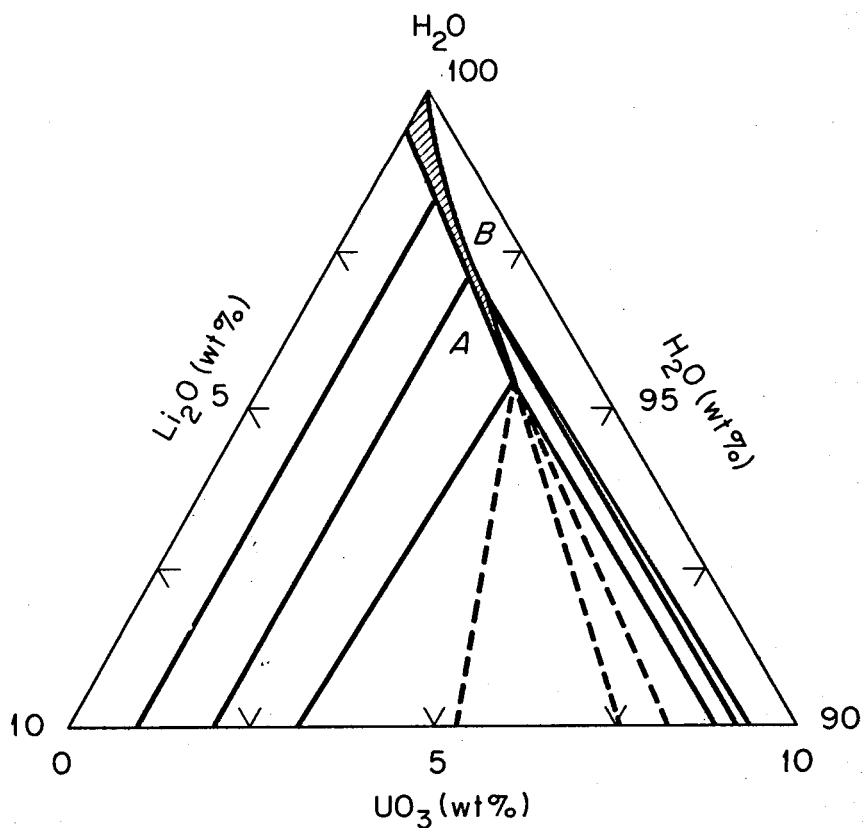
Fig. 5.38. The System $Li_2O–UO_3–CO_2–H_2O$ at 250°C and 1500 psi.

5.39. The System Th(NO$_3$)$_4$-H$_2$O

1. Reported in full by W. L. Marshall, J. S. Gill, and C. H. Secoy, *HRP Quar. Prog. Rep. Nov. 30, 1950*, ORNL-925, p 279–90.

2. W. L. Marshall, J. S. Gill, and C. H. Secoy, *J. Am. Chem. Soc.* **73**, 4991 (1951).

Hydrolytic precipitation of ThO$_2$ and thermal decomposition of NO$_3^-$ in this system occur in an analogous manner to the reactions occurring in the system UO$_2$(NO$_3$)$_2$-H$_2$O (see Sec 5.31). At higher temperatures the two-component system in actuality must be considered in terms of the three components ThO$_2$, HNO$_3$, and H$_2$O.
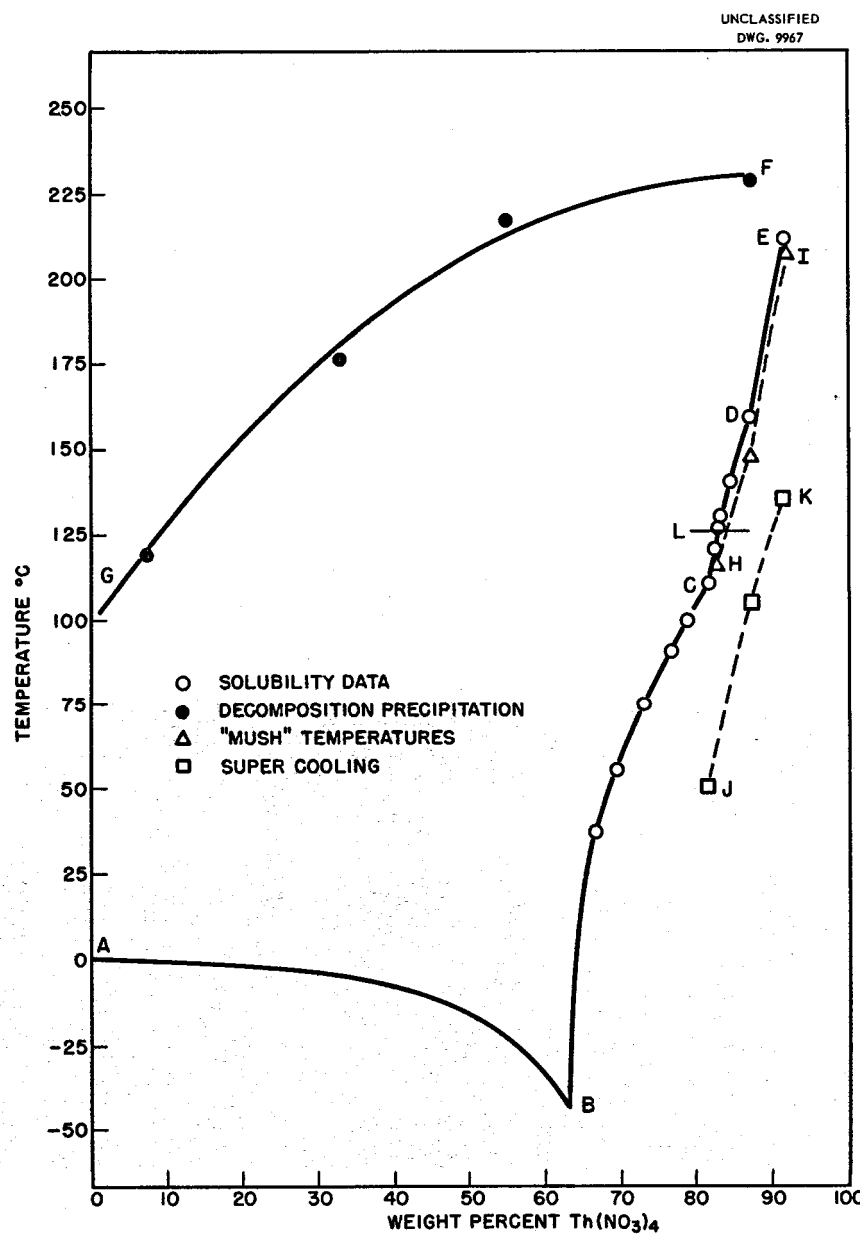
Fig. 5.39. The System Th(NO$_3$)$_4$-H$_2$O.

5.40. Hydrolytic Stability of Thorium Nitrate—Nitric Acid and Uranyl Nitrate Solutions

1. W. L. Marshall and C. H. Secoy, *HRP Quar. Prog. Rep. Oct. 31, 1953,* ORNL-1658, p 93–96.

2. W. L. Marshall, J. S. Gill, and C. H. Secoy, *Chem. Quar. Prog. Rep. March 31, 1951,* ORNL-1053, p 22–25.

The data used to draw the individual curves were obtained by observations at various temperatures of tubes that contained different solutions of known concentration. The procedure was analogous to that used for obtaining data for Fig. 5.33. The curve for hydrolytic precipitation of $UO_2(NO_3)_2$ is taken from ref 2.
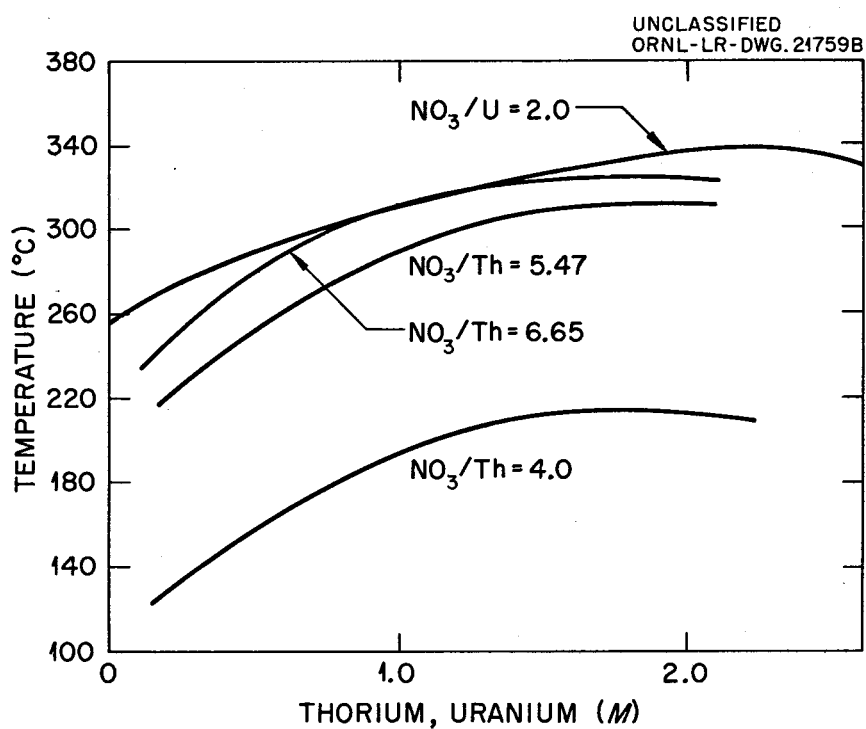
Fig. 5.40. Hydrolytic Stability of Thorium Nitrate—Nitric Acid and Uranyl Nitrate Solutions.

5.41. The System $ThO_2-CrO_3-H_2O$ at 25°C

1. H. T. S. Britton, *J. Chem. Soc.* 123, 1429 (1923).

2. W. L. Marshall, F. J. Loprest, and C. H. Secoy, *HRP Quar. Prog. Rep. Jan. 31, 1955,* ORNL-1853, p 205-6.

The phase diagram at 25° was determined by Britton. Points 1-7 indicate compositions investigated at high temperature by Marshall, Loprest, and Secoy. These solution compositions were phase stable up to 160°C for point 7 and 320°C for point 1.
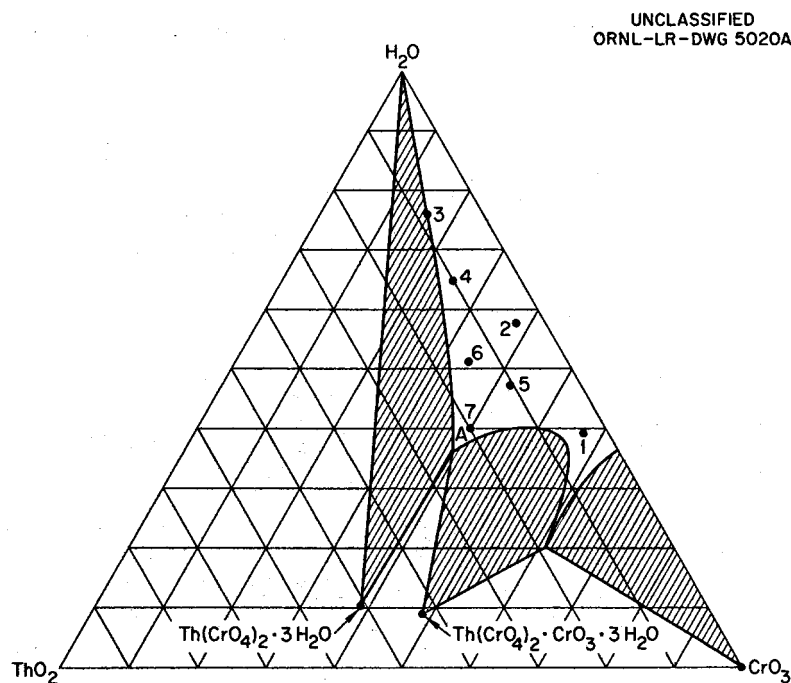
Fig. 5.41. The System $ThO_2-CrO_3-H_2O$ at 25°C. Compositions are in weight per cent.

5.42. Phase Stability of ThO_2–H_3PO_4–H_2O Solutions at High Concentrations of ThO_2

W. L. Marshall, experimental data in ORNL research notebook 2881, p 35 (May 1953).

Solutions of appropriate concentrations were prepared and analyzed. These solutions were sealed in glass tubes and shaken at various temperatures for times varying from 1 hr to several days. In this manner the phase stability boundaries with respect to concentration and temperature were established. At first inspection of the figure it is surprising that more ThO_2 can be dissolved per liter at the lower H_3PO_4/ThO_2 ratio than at the higher ratio. Actually, there is a physical volume limitation due to the high fractional volumes occupied by ThO_2 and H_3PO_4 at these concentrations. As any solution is diluted with H_2O, hydrolysis of thorium in solution occurs. At room temperature, solutions in which the H_3PO_4/ThO_2 ratio is 5:1 are gels, whereas 10:1 ratio solutions are still fluid.

UNCLASSIFIED
ORNL-LR-DWG. 38529
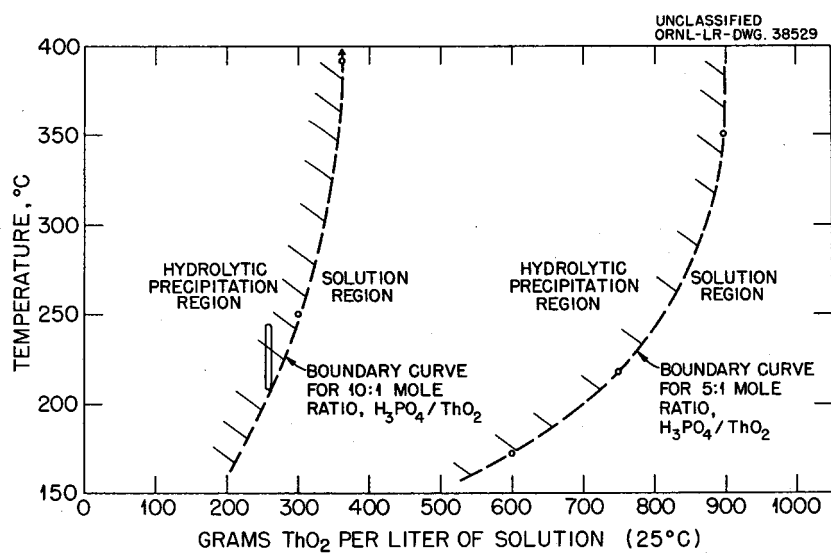
Fig. 5.42. Phase Stability of ThO_2–H_3PO_4–H_2O Solutions at High Concentrations of ThO_2.

## ACKNOWLEDGMENT
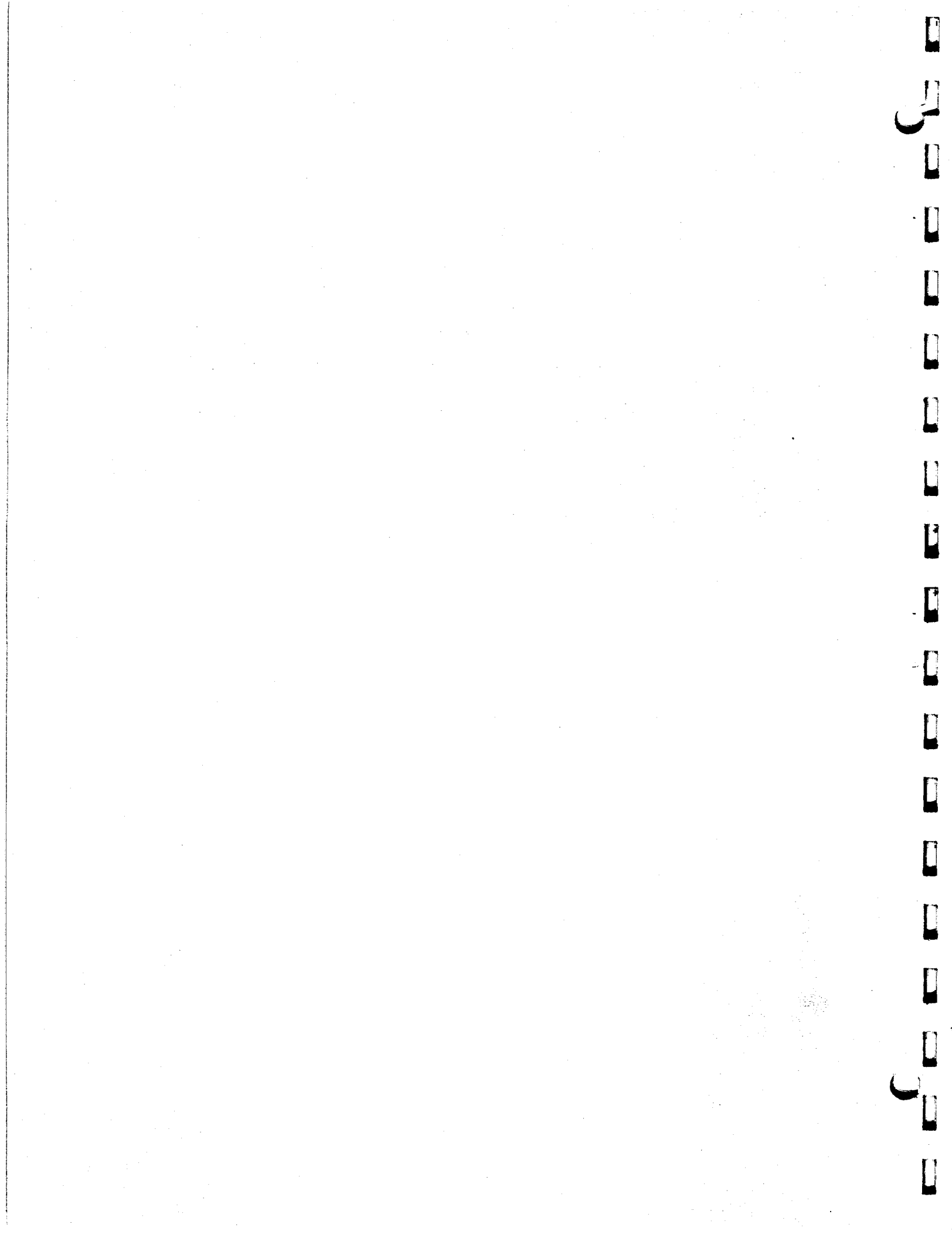
INTERNAL DISTRIBUTION

1. R. D. Ackley
2. R. E. Adams
3. G. M. Adamson
4. L. G. Alexander
5. K. A. Allen
6. C. F. Baes
7-11. C. J. Barton
12. S. E. Beall
13. P. R. Bell
14. J. O. Betterton
15. A. M. Billings
16. D. S. Billington
17. C. A. Blake
18. J. P. Blakely
19. R. E. Blanco
20. F. F. Blankenship
21. M. Blander
22. E. P. Blizard
23. C. M. Blood
24. A. L. Boch
25. E. G. Bohlman
26. S. E. Bolt
27. G. E. Boyd
28. M. A. Bredig
29. J. C. Bresee
30. R. B. Briggs
31. H. R. Bronstein
32. J. R. Brown
33. K. B. Brown
34. W. E. Browning
35. F. R. Bruce
36. W. D. Burch
37. S. R. Buxton
38. S. Cantor
39. W. H. Carr
40. W. L. Carter
41. G. H. Cartledge
42. G. I. Cathers
43. C. E. Center
44. R. H. Chapman
45. R. A. Charpie
46. R. D. Cheverton
47. H. C. Claiborne
48. G. W. Clark
49. C. F. Coleman
50. E. L. Compere
51. J. A. Cox
52. J. H. Crawford
53. C. R. Croft
54. F. L. Culler

55. J. S. Culver
56. D. R. Cuneo
57. J. E. Cunningham
58. D. G. Davis
59. R. J. Davis
60. W. C. Davis
61. J. H. DeVan
62. R. R. Dickison
63. L. M. Doney
64. F. A. Doss
65. J. S. Drury
66. A. S. Dworkin
67. L. B. Emlet (K-25)
68. J. L. English
69. J. E. Eorgan
70. R. B. Evans
71. D. E. Ferguson
72. J. L. Fowler
73. A. P. Fraas
74. H. A. Friedman
75. J. H. Frye, Jr.
76. C. H. Gabbard
77. W. R. Gall
78. J. S. Gill
79. J. H. Gillette
80. L. O. Gilpatrick
81. J. M. Googin (Y-12)
82. R. S. Greeley
93. A. T. Gresky
84. J. C. Griess
85-89. W. R. Grimes
90. E. Guth
91. P. A. Haas
92. P. H. Harley
93. C. S. Harrill
94. L. A. Harris
95. P. N. Haubenreich
96. G. M. Hebert
97. H. L. Hemphill
98. J. W. Hill
99. E. C. Hise
100. E. E. Hoffman
101. H. W. Hoffman
102. A. Hollaender
103. R. W. Horton
104. A. S. Householder
105. H. Insley
106. G. H. Jenks
107. D. T. Jones
108. E. V. Jones

109.	W. H. Jordan	165.	D. Phillips
110.	P. R. Kasten	166.	L. R. Phillips (Y-12)
111.	G. W. Keilholtz	167.	M. L. Picklesimer
112.	C. P. Keim	168.	W. T. Rainey
113.	M. T. Kelley	169.	A. D. Redman
114.	M. J. Kelley	170.	S. A. Reed
115.	B. W. Kinyon	171.	P. M. Reyling
116.	N. A. Krohn	172.	D. M. Richardson
117.	J. A. Lane	173.	R. C. Robertson
118.	S. Langer	174.	A. D. Ryon
119.	C. G. Lawson	175.	H. C. Savage
120.	J. E. Lee, Jr.	176.	H. W. Savage
121.	R. E. Leed	177.	F. A. Schimmel (Y-12)
122.	R. E. Leuze	178.	J. M. Schmitt
123.	W. H. Lewis	179.	J. M. Schreyer (Y-12)
124.	M. H. Lietzke	180.	H. E. Seagren
125.	T. A. Lincoln	181.	C. H. Secoy
126.	S. C. Lind	182.	C. L. Segaser
127.	R. B. Lindauer	183.	J. H. Shaffer
128.	R. S. Livingston	184.	E. M. Shank
129.	J. T. Long	185.	R. J. Sheil
130.	R. A. Lorenz	186.	R. P. Shields
131.	R. E. Lowrie	187.	E. D. Shipley
132.	M. I. Lundin	188.	M. D. Silverman
133.	R. N. Lyon	189.	M. J. Skinner
134.	J. P. McBride	190.	R. Slusher
135.	W. B. McDonald	191.	N. V. Smith
136.	H. F. McDuffie	192.	W. T. Smith, Jr.
137.	H. A. McLain	193.	A. H. Snell
138.	R. A. McNees	194.	B. A. Soldano
139.	H. G. MacPherson	195.	I. Spiewak
140.	T. N. McVay	196.	H. H. Stone
141.	J. R. McWherter	197.	R. A. Strehlow
142.	W. D. Manly	198.	B. J. Sturm
143-147.	W. L. Marshall	199.	C. D. Susano
148.	R. E. Meadows	200.	J. E. Sutherland
149.	R. P. Metcalf	201.	J. A. Swartout
150.	R. P. Milford	202.	A. Taboada
151.	A. J. Miller	203.	E. H. Taylor
152.	J. W. Miller	204-213.	R. E. Thoma
153.	C. S. Morgan	214.	D. G. Thomas
154.	K. Z. Morgan	215.	M. Tobias
155.	R. E. Moore	216.	D. S. Toomb
156.	R. L. Moore	217.	D. B. Trauger
157.	J. P. Murray (Y-12)	218.	J. Truitt
158.	M. L. Nelson	219.	W. E. Unger
159.	G. J. Nessle	220.	R. Van Winkle
160.	R. F. Newton	221.	F. C. VonderLage
161.	L. G. Overholser	222.	W. T. Ward
162.	L. F. Parsly, Jr.	223.	G. M. Watson
163.	R. L. Pearson	224.	B. S. Weaver
164.	F. N. Peebles	225.	C. F. Weaver

226. A. M. Weinberg
227. K. W. West
228. M. E. Whatley
229. G. C. Williams
230. C. E. Winters
231. H. W. Wright
232. J. P. Young
233. F. C. Zapp
234. P. H. Emmett (consultant)
235. H. Eyring (consultant)
236. D. G. Hill (consultant)
237. C. E. Larson (consultant)

238. W. O. Milligan (consultant)
239. J. E. Ricci (consultant)
240. G. T. Seaborg (consultant)
241. E. P. Wigner (consultant)
242. Biology Library
243-244. Central Research Library
245. Health Physics Library
246-265. Laboratory Records Department
266. Laboratory Records, ORNL R.C.
267. Reactor Experimental Engineering Library
268. ORNL – Y-12 Technical Library,
　　　Document Reference Section

EXTERNAL DISTRIBUTION

269-270. Stanford Research Institute, Menlo Park, Calif. (1 copy ea. to D. Cubicciotti and J. W. Johnson)

271-272. National Lead Co., P. O. Box 158, Cincinnati 39, Ohio (1 copy ea. to R. E. DeMarco and K. Notz)

273. Geophysical Laboratory, Carnegie Institution of Washington, 2801 Upton St., Washington 8, D.C. (J. W. Grieg)

274. Mound Laboratory, Miamisburg, Ohio (E. F. Eichelberger)

275-276. Minnesota Mining and Manufacturing Co., Central Research Dept., 2301 Hudson Rd., St. Paul 9, Minn. (1 copy ea. to J. R. Johnson and G. D. White)

277. Chemical Separations and Development Branch, Nuclear Technology, Division of Reactor Development, AEC, Washington 25, D.C. (F. Kerze, Jr.)

278. Dept. of Chemistry, Brown University, Providence 12, R.I. (C. A. Kraus)

279. Mallinckrodt Chemical Works, Uranium Division, P.O. Box 472, St. Charles, Mo. (C. W. Kuhlman)

280. Portland Cement Association Fellowship, National Bureau of Standards, Washington 25, D. C. (E. M. Levin)

281-282. National Carbon Research Laboratories, P.O. Box 6116, Cleveland, Ohio (1 copy ea. to G. W. Mellors and S. Senderoff)

283. College of Mineral Industries, Pennsylvania State University, University Park, Pa. (E. F. Osborn)

284. Los Alamos Scientific Laboratory, P.O. Box 1663, Los Alamos, N. M. (B. J. Thamer)

285. Dept. of Physics, University of Chicago, Chicago, Ill. (W. H. Zachariasen)

286. Reaction Motors Division, Thiokol Chemical Corp., Denville, N.J. (F. L. Loprest)

287. National Bureau of Standards, Washington 25, D. C. (H. F. McMurdie)

288. U.S. Geological Survey, Washington 25, D. C. (G. W. Morey)

289. National Carbon Co., Union Carbide Corporation, Parma, Ohio (F. E. Clark)

290. Division of Research and Development, AEC, Washington

291. Division of Research and Development, AEC, ORO

292. Division of Reactor Development, AEC, Washington

293. Division of Reactor Development, AEC, ORO

294. Oak Ridge Institute of Nuclear Studies, Oak Ridge

295-851. Given distribution as shown in TID-4500 (15th ed.) under Chemistry-General category (75 copies - OTS)